University of Southampton Research Repository

Copyright © and Moral Rights for this thesis and, where applicable, any accompanying data are retained by the author and/or other copyright owners. A copy can be downloaded for personal non-commercial research or study, without prior permission or charge. This thesis and the accompanying data cannot be reproduced or quoted extensively from without first obtaining permission in writing from the copyright holder/s. The content of the thesis and accompanying research data (where applicable) must not be changed in any way or sold commercially in any format or medium without the formal permission of the copyright holder/s.

When referring to this thesis and any accompanying data, full bibliographic details must be given, e.g.

Thesis: Author (Year of Submission) "Full thesis title", University of Southampton, name of the University Faculty or School or Department, PhD Thesis, pagination.

Data: Author (Year) Title. URI [dataset]

University of Southampton

Faculty of Environmental and Life Sciences

Ocean and Earth Science

The impacts of nutrient enrichment and skewed nitrogen: phosphorus (N:P) stoichiometries on the skeletal microstructure and geochemistry of zooxanthellate corals

by Michael Christopher Buckingham

ORCID ID: 0000-0002-8946-9854

Thesis for the degree of Doctor of Philosophy

March 2023

University of Southampton

Abstract

Faculty of Environmental & Life Sciences (School of Ocean & Earth Science).

Thesis for the degree of Doctor of Philosophy

The impacts of nutrient enrichment and skewed nitrogen: phosphorus (N:P) stoichiometries on the skeletal microstructure and geochemistry of zooxanthellate corals

by Michael Christopher Buckingham

The skeletons of zooxanthellate corals provide the foundations of coral reefs, which in turn are biodiverse and productive marine ecosystems of great importance to human populations. They also provide useful environmental proxies, due to the capacity for changes of climatic conditions or seawater chemistry to be recorded as modifications to the skeletal structure and geochemistry. However, studies on the impacts of nutrient enrichment on coral skeletal growth have provided contradictory results, while the impacts of nutrient stress on skeletal growth, microstructure and geochemistry remain relatively understudied. This thesis aimed to investigate the impacts of nutrient enrichment and stress on the skeletons of zooxanthellate corals, and how this might affect the use of microstructural and geochemical features as environmental proxies. First, the published literature relating to the impacts of nutrient enrichment on coral skeletal growth and microstructure was re-evaluated. By considering coral taxonomy and the resultant seawater nitrogen (N): phosphorus (P) stoichiometry some of the major contradictions were resolved. The impacts of four different nutrient treatments on two species, *Acropora polystoma* and *Euphyllia paradivisa* were then assessed using replicate coral colonies cultured in an experimental mesocosm. The nutrient conditions considered were high nitrate: high phosphate (HNHP), low nitrate: low phosphate (LNLP), high nitrate: low phosphate (HNLP) and low nitrate: high phosphate (LNHP). The impacts on zooxanthellae density, photochemical efficiency and skeletal growth were recorded, and the coral skeletons were analysed using micro-computed tomography (µ-CT) and mass spectrometry to determine differences in skeletal micro-structure and geochemistry respectively. HNHP conditions were associated with high zooxanthellae densities in both species, rapid skeletal growth in *A. polystoma* and a corallite shape and structure indicative of large polyp biomass in *E. paradivisa*. The HNLP and LNLP treatments caused bleaching in all corals of both species, with the additional effect of P-starvation in the residual symbionts of HNLP corals. In *A. polystoma* bleaching was associated with reduced skeletal growth and thickened skeletal elements, while in *E. paradivisa* reduced corallite size and shallow endothecal dissepiments indicated substantial polyp tissue loss, this being most severe in HNLP corals. Bleaching susceptibility differed for the two species under the LNHP treatment, but in both species the effects on coral physiology and skeletal structure indicated a much less severe impact of low N:P ratios than for high ratios (the HNLP treatment). All of the isotopic (δ^{13}C and δ^{18}O) and trace element (Li/Ca, Mg/Ca, Sr/Ca and B/Ca) ratios analysed were impacted by the nutrient treatments such that corals from the HNHP, HNLP and LNLP treatments were identifiable from characteristic geochemical responses common to both species. The differences in δ^{18}O, Li/Ca, Mg/Ca and Sr/Ca values between treatments were equivalent to erroneously large proxy-derived temperature differences between treatment tanks. Patterns of trace element and stable isotope differences between treatments indicated that different forms of nutrient stress likely impact coral skeletal geochemistry through variable impacts on calcifying fluid chemistry, Rayleigh fractionation and the degree of isolation of the calcifying fluid. The skeletons of zooxanthellate corals may record the impacts of nutrient stress in their skeletal structure and geochemistry. Such modifications can impact ecosystem processes and present challenges relating to their proxy use.

List of contents

List of figures

List of tables

Accompanying material

Datasets relating to this research are available from the University of Southampton data repository (PURE) via the link below:

https://doi.org/10.5258/SOTON/D2520

Requests for data may need to be authorized by Professor Jörg Wiedenmann.

Research thesis: Declaration of authorship

Name: **Michael Christopher Buckingham**

Title of thesis: **The impacts of nutrient enrichment and skewed nitrogen: phosphorus (N:P) stoichiometries on the skeletal microstructure and geochemistry of zooxanthellate corals**

I declare that this thesis and the work presented in it is my own and has been generated by me as the result of my own original research.

I confirm that:

1. This work was done wholly or mainly while in candidature for a research degree at this University;
2. Where any part of this thesis has previously been submitted for a degree or any other qualification at this University or any other institution, this has been clearly stated;
3. Where I have consulted the published work of others, this is always clearly attributed;
4. Where I have quoted from the work of others, the source is always given. With the exception of such quotations, this thesis is entirely my own work;
5. I have acknowledged all main sources of help;
6. Where the thesis is based on work done by myself jointly with others, I have made clear exactly what was done by others and what I have contributed myself;
7. Chapter 2 of this work has been published as

Buckingham et. al. (2022) Impact of nitrogen (N) and phosphorus (P) enrichment and skewed N:P stoichiometry on the skeletal formation and microstructure of symbiotic reef corals, *Coral Reefs*, [Published online 20/04/2022 as DOI: 10.1007/s00338-022-02223-0]

Signature: *Mike Buckingham*

Date: 03/10/2022

Acknowledgements

Firstly, I would like to thank my supervisors Jörg, Cecilia, Ken and Bastian for their excellent guidance and support during this project. I am very grateful for the invaluable encouragement and insights they have provided throughout the course of my PhD and for the constructive feedback provided in relation to all aspects of this work.

I am especially grateful to Professor Gavin Foster and Dr. Chris Standish who took the time to provide comments on my draft versions of Chapter 4. The document is immeasurably better for your input.

I am also very thankful to my examiners, Professor Tom Bibby and Professor Jens Zinke for agreeing to be my examiners and for providing me with such useful feedback and the benefit of their professional insights.

My panel chair, Paul Wilson also provided valuable feedback during my progression reviews and the confirmation process - thank you.

I must also thank Dr. Tom Chalk, Zoe Connelly, Carolina Olla, Mohammad Saeed, Robbie Robinson, George Clarke for their assistance in the culturing phases of this project.

Megan Wilding, Dr. Clive Trueman, Dan Doran and Matthew Beverley-Smith all assisted with the preparation of coral skeletal samples and the mass spectrometry analysis – thank you very much.

I am also grateful for the support provided to me by the μ-CT teams based at both the Natural History Museum, London and The University of Southampton.

I could not have completed this thesis without the support of my amazing partner Davina. Sorry I missed so many weekends with you and Luke because I was working. I know how hard you had to work so that I could write this thesis. I love you and Luke more than you can imagine. Thank you also to Julie for giving up so many days to look after Luke while Davina and I both had to work. The extra days that this made available to me were crucial to me finishing on time. Finally, thank you to Luke. I might be exhausted by the 5 am starts but you put a smile on my face every day, making it all seem worthwhile.

List of abbreviations

AIC = Akaike Information Criterion

ANOVA = Analysis Of Variance

Ar = aragonite

ATP = adenosine tri-phosphate

B = boron

$B(OH)_4^-$ = borate

C = carbon

CA = carbon anhydrase

Ca = calcium

$CaCO_3$ = calcium carbonate

cf = calcifying fluid

CO_2 = carbon dioxide

CO_3^{2-} = carbonate

DDN = diazotrophically derived nitrogen

DFA = discriminant function analysis

DHW = degree heating week

DIC = dissolved inorganic carbon

DIN = dissolved inorganic nitrogen

DIP = dissolved inorganic phosphorus

DOM = dissolved organic matter

DON = dissolved organic nitrogen

DOP = dissolved organic phosphorus

DNA = deoxyribonucleic acid

El = element

F_{Ca} = Fraction of calcium

Fv/Fm = quantum yield of photochemical efficiency

GBR = Great Barrier Reef

H^+ = hydrogen ion

H_2O = water

H_2O_2 = hydrogen peroxide

HCO_3^- = bicarbonate

HN/AP = high nitrate/ ambient phosphate

HNHP = high nitrate/ high phosphate

HNLP = high nitrate/ low phosphate

HNO_3 = hydrogen nitrate

HRF = host release factor

HSD = honestly significant difference

IAEA = International Atomic Energy Agency

ICP-MS = inductively coupled plasma mass spectrometry

IRMS = isotope ratio mass spectrometry

LA = laser ablation

Li = lithium

LD = linear discriminant

LNHP = low nitrate/ high phosphate

LNLP = low nitrate/ low phosphate

MANOVA = Multivariate Analysis Of Variance

Mg = magnesium

MLR = multiple linear regression

MMM = maximum monthly mean (temperature)

N = nitrogen

NaClO = sodium hypochlorite

$NaNO_3$ = sodium nitrate

$NaPO_4^{3-}$ = sodium phosphate

NGO = Non-Governmental Organisation

NH_3 = ammonia

NH_4^+ = ammonium

NHM = Natural History Museum

NO_2^- = nitrite

NO_3^- = nitrate

O_2^- = super oxide

OM = organic matter

P = phosphorus

PAM = pulse amplitude modulation

PAR = photosynthetically active radiation

PO_4^{3-} = phosphate

PSII = Photosystem 2

p.s.u. = practical salinity units

ROI – region of interest

ROS = reactive oxygen species

RuBisCo = Ribulose-1.5-biphosphate carboxylase-oxygenase

s.dev = standard deviation

SE = standard error

SEM = scanning electron microscope

(nano) SIMS = nanoscale secondary ion mass spectrometry

SOES = School of Ocean and Earth Sciences

SQDG = sulfoquinovosyldiacylglycerol

Sr = strontium

SST = sea surface temperature

SV = skeletal volume

Sw = seawater

TA = total alkalinity

TE = trace element

TV = total volume

UHS = University Hospital of Southampton

VPDB = Vienna Pee Dee Belemnite

$^1O_2$ = singlet oxygen

3D = 3-dimensional

•OH = hydroxyl

$\delta^{11}B$ = boron-11 stable isotope

$\delta^{13}C$ = carbon-13 stable isotope

$\delta^{15}N$ = nitrogen-15 stable isotope

$\delta^{18}O$ = oxygen-18 stable isotope

Ω_{Ar} = saturation state

µ-CT = micro-computed tomography

Chapter 1 - Introduction

1.1. Background

Coral reefs are among the most biodiverse and productive ecosystems on our planet, and it is commonly cited that "despite covering only ~0.2% of the ocean floor they support at least 25% of all marine species" (GCRMN, 2020; UNEP, 2020; EPA, 2021). They provide vital ecosystem services including fisheries, coastal protection and income from tourism and leisure activities, collectively estimated to be worth around US$2.7 trillion a year to the global economy (GCRMN, 2020). The primary architects of coral reefs are reef-building corals, which form the structures of reefs through the calcification of their aragonite skeletons. However, coral reefs are in decline throughout much of their range, primarily because of recurrent mass bleaching events caused by anthropogenic global warming, commonly exacerbated by local stressors such as nutrient pollution (Hughes *et al.*, 2017; Lough, Anderson and Hughes, 2018; GCRMN, 2020). Bleaching events often lead to mass coral mortality which can shift reef carbonate budgets towards net erosion (Lange and Perry, 2019; Perry *et al.*, 2020). Consequently, the 3-dimensional complexity of a reef may be reduced, resulting in decreases to ecosystem biodiversity and productivity and a reduced capacity to protect the adjacent coastline (Sheppard *et al.*, 2005; Purkis, Graham and Riegl, 2008; Graham and Nash, 2013; Couch *et al.*, 2017; Lange and Perry, 2019). Microstructural and geochemical signatures associated with thermal bleaching events have been identified in coral skeletons, and have been used to investigate the extent of bleaching episodes and their impacts on coral physiology (D'Olivo and McCulloch, 2017; DeCarlo and Cohen, 2017; Barkley *et al.*, 2018; Fouke, Trop and Sivaguru, 2021; Schoepf *et al.*, 2021). However, recent studies show that nutrient stress, arising through either imbalanced nutrient enrichment or nutrient limitation can also cause corals to bleach (Wiedenmann *et al.*, 2013; D'Angelo and Wiedenmann, 2014; Rosset *et al.*, 2017). The impacts of nutrient-stress mediated bleaching on the skeletal microstructure and geochemistry of zooxanthellate corals have not yet been properly assessed. Therefore, it is unclear whether newly identified microstructural responses to thermal bleaching are replicated under such circumstances, or whether more established geochemical climate proxies might also be affected.

1.1.1. Reef building corals and the coral reef environment

1.1.1.1. Hermatypic and zooxanthellate corals

Corals form part of the phylum *Cnidaria*, a vast group of aquatic and marine invertebrates that also includes jellyfish and anemones, and which are characterised by specialised stinging cells called 'cnidocytes' which they use to capture prey (WoRMS, 2022). The order *Scleractinia* describes corals with the ability to form calcium carbonate exoskeletons, and contains over 70 families, comprising > 800 species (Veron et. al., 2016; WoRMS, 2022). *Scleractinian* corals are globally distributed throughout the world's oceans and found at all depth ranges, including shallow seas and the deep ocean. Perhaps the most iconic and familiar members of this diverse group of animals are those that build coral reefs in the warm, sunlit waters of the tropics - the so called 'hermatypic' or 'zooxanthellate' corals. The terms hermatypic and zooxanthellate are often used interchangeably. But, whereas 'hermatypic' describes those corals responsible for building reefs, the term 'zooxanthellate' strictly refers to corals that form an endosymbiosis with unicellular dinoflagellates of the family *Symbiodiniaceae* (LaJeunesse *et al.*, 2018), which are commonly referred to as 'zooxanthellae'.

The symbiosis between the coral and its zooxanthellae is mutually beneficial for both partners. The zooxanthellae benefit through access to N excreted by the coral in the form of ammonium (NH^{4+}) (Rahav *et al.*, 1989; Tanaka *et al.*, 2015) and the provision by the host of a favourable environment to sustain high rates of photosynthesis (Furla, Allemand and Orsenigo, 2000; Al-Horani, Al-Moghrabi and De Beer, 2003a; Enríquez, Méndez and Iglesias-Prieto, 2005). Meanwhile the coral can obtain > 90% of its energetic requirements from the zooxanthellae in the form of translocated carbohydrates (Falkowski *et al.*, 1984, 1993) as well as access to additional sources of nitrogen (N) and phosphorus (P) which would otherwise remain unavailable (Miller and Yellowlees, 1989; Godinot, Ferrier-pagès and Grover, 2009; Davy, Allemand and Weis, 2012; Ferrier-Pagès *et al.*, 2016).

The majority of coral species found on coral reefs are both hermatypic and zooxanthellate. Some species of corals live as solitary polyps, but hermatypic corals form large colonies, sometimes comprising of hundreds or thousands of genetically identical polyps. The polyps are connected by a thin layer of live tissue (the coenosarc) overlying a shared

exoskeleton which is attached to the underlying substrate (Madl, Schabetsberger and Lipovnik, 2014). The morphologies of coral colonies vary between, and within genera but the most conspicuous morphologies on many coral reefs are massive (boulder-like), branching or tabular (Tan *et al.*, 2011; Veron, 2013; Madl, Schabetsberger and Lipovnik, 2014). Skeletal morphologies may also vary within species due to specific environmental conditions; for example, branches may become shorter and thicker in corals growing on wave-exposed sections of reefs (Veron, 2013), or surfaces may become flatter in low light environments to enhance light capture *(reviewed in* Roth, 2014).

1.1.1.2. The coral reef environment

Reefs can broadly be defined as large ridges of material that cause the seafloor to rise close to the sea surface. Natural reefs form either because of marine geological processes or biogenically through the skeletal growth of organisms such as corals, bivalves or polychaetes. In the case of coral reefs, the reef structure is largely comprised of the skeletons of both living and dead corals, which are attached to the shallow substrate of the seafloor. The morphologies of the dominant coral species on a particular reef determine the 3-dimensional structural complexity (rugosity) of the reef, and rugosity is highest when levels of live coral cover are high and/or a reef is dominated by coral species with branching morphologies (Graham and Nash, 2013). Biodiversity and biomass are both high on coral reefs, and are positively corelated to rugosity; this is due to the multitude of micro-habitats and opportunities for shelter that more complex, 3-dimensional structures provide to other reef inhabitants (Purkis, Graham and Riegl, 2008; Graham and Nash, 2013). Corals also form the basis of a food chain by excreting organic matter in the form of mucus that provides a food source for planktonic and benthic microbial communities, and are prey for coral-feeding organisms (Cole, Pratchett and Jones, 2008; Haas *et al.*, 2010; Ruppert *et al.*, 2013; McNally *et al.*, 2017). As such, hermatypic corals play a vital role in both establishing and maintaining the healthy functioning of coral reef ecosystems.

Zooxanthellate corals have a much narrower geographic range than *Scleractinia*, and their distribution is primarily controlled by the availability of photosynthetically active radiation (PAR), sea surface temperature (SST), dissolved inorganic nutrient concentrations and the saturation state of seawater with respect to aragonite (Ω_{Ar}) (Kleypas, Mcmanus and Menez, 1999; Couce, Ridgwell and Hendy, 2012; Guan, Hohn and Merico, 2015). They also have

a tolerated range of salinity (23 – 42 p.s.u.), but this is much less important in determining the geographical distribution of coral reefs (Kleypas, Mcmanus and Menez, 1999; Couce, Ridgwell and Hendy, 2012; Guan, Hohn and Merico, 2015).

Light is limiting to zooxanthellate coral growth because corals rely on photosynthesised carbohydrates produced by their endosymbiotic zooxanthellae as their primary food source, and these products can account for > 90% of the coral's energetic requirements (with the rest being sourced heterotrophically) (Falkowski *et al.*, 1984, 1993). The minimum annual mean PAR required to sustain coral reefs has been estimated to be between 250 - 450 μmol m^{-2} s^{-1} (Kleypas, Mcmanus and Menez, 1999; Guan, Hohn and Merico, 2015). Since light intensity varies seasonally and latitudinally, and the depth of light penetration depends on water clarity, the maximal depths of coral reefs may be restricted to < 10 m in some places but extend to almost 100 m in others (Figure 1.1) (Kleypas, Mcmanus and Menez, 1999; Couce, Ridgwell and Hendy, 2012).

Ω_{Ar} indicates the degree of seawater saturation with respect to aragonite, this being the mineral form of calcium carbonate ($CaCO_3$) from which corals build their skeletons through a process called 'calcification'. Ω_{Ar} values < 1 indicate that seawater is undersaturated with respect to aragonite and it is liable to dissolve, while values > 1 indicate that seawater is oversaturated, and aragonite is likely to precipitate. Thus, higher saturation states are associated with more rapid rates of calcification (Zeebe, 2001). The minimum Ω_{Ar} required to sustain coral reef development is thought to be between 2.82 – 3.28 (Kleypas, Mcmanus and Menez, 1999; Guan, Hohn and Merico, 2015). Mean annual SST on coral reefs ranges between 21.0 – 29.6 ℃, although seasonal minima and maxima may fall beyond these values (Kleypas, Mcmanus and Menez, 1999; Guan, Hohn and Merico, 2015). In the global oceans, Ω_{Ar} is, to a large part controlled by a positive correlation with SST (Zeebe, 2001), so the restriction of coral reefs to warm shallow waters is to some extent linked to the relative ease with which they can form their $CaCO_3$ skeletons in these regions (Figure 1.1).

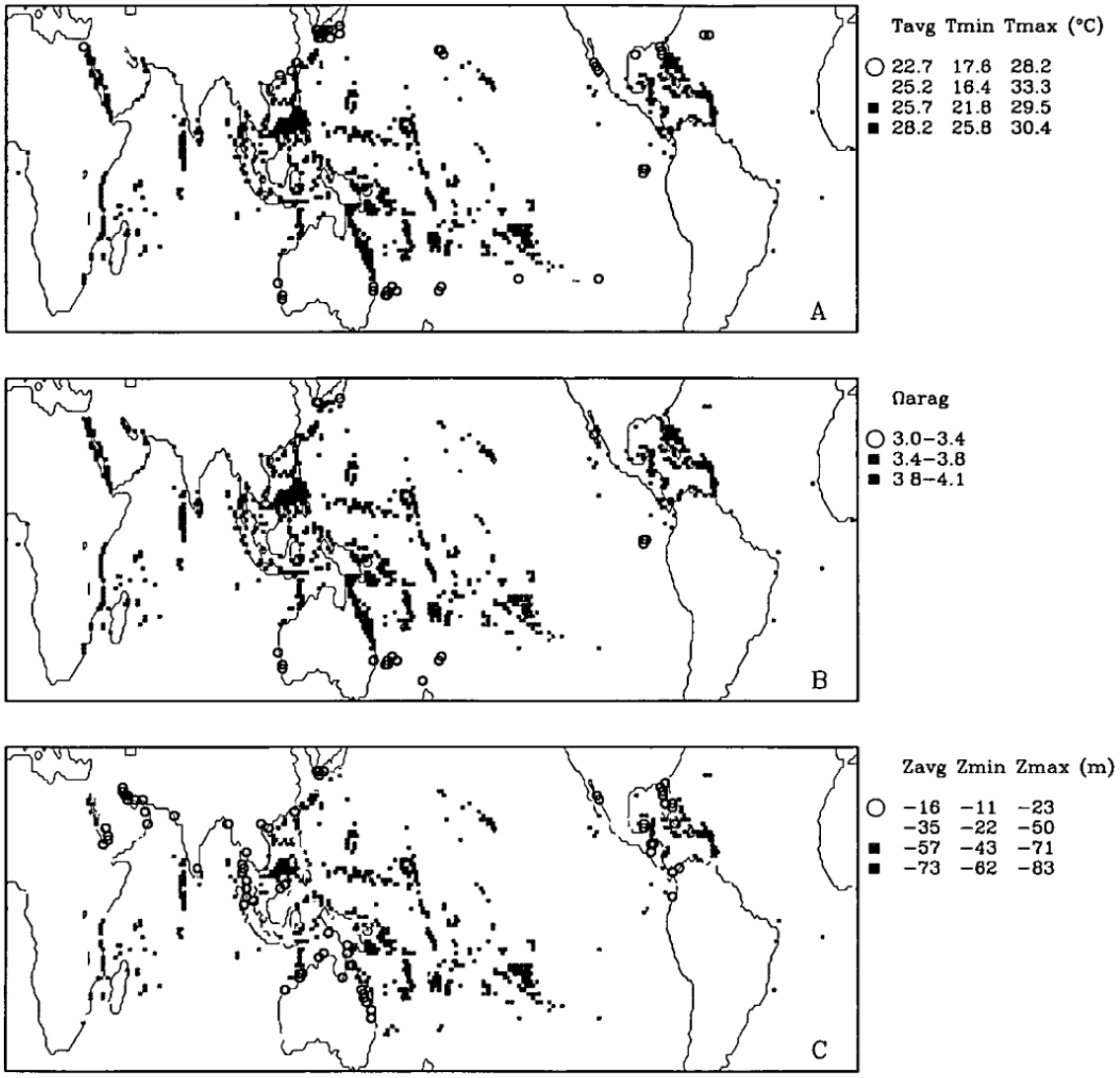

Figure 1.1. Global clustering of coral reefs. Clusters are presented with respect to (A) sea surface temperature Tavg = average temperature, Tmin = minimum, Tmax = maximum); (B) aragonite saturation state (ΩAr); and (C) monthly average depth of noon-day light penetration (Zavg = average depth, Zmin = minimum and Zmax = maximum). Figure sourced from Kleypas, Mcmanus and Menez, (1999).

Kleypas, Mcmanus and Menez (1999) estimated that the maximum average nitrate (NO_3^-) and phosphate (PO_4^{3-}) concentrations on coral reefs were 3.34 μM and 0.54 μM, respectively. More recently, Guan, Hohn and Merico (2015) estimated these values to be NO_3^- = 4.51 μM and PO_4^{3-} = 0.63 μM. These values are relatively low for coastal environments, and the waters of most coral reefs are considered to be oligotrophic. But as with all organisms, corals and their zooxanthellae require nutrients including N and P to support growth and reproduction. Indeed, nutrient enrichment with inorganic forms of N and P can increase symbiont and host growth and even increase the coral's resistance to seasonal bleaching (Fabricius, 2005; D'Angelo and Wiedenmann, 2014). But, at higher

concentrations of dissolved inorganic nutrients coral health is indirectly and negatively affected by factors such as increased competition for light and space from algal competitors, increased susceptibility to bleaching, bio-erosion and disease and even increased predation (Kinsey and Davies, 1979; Edinger *et al.*, 2000; Brodie *et al.*, 2005; Fabricius, 2005; D'Angelo and Wiedenmann, 2014; Thurber *et al.*, 2014). As such, nutrification is commonly associated with increased coral mortality and the degradation of coral reef ecosystems (Fabricius, 2005; D'Angelo and Wiedenmann, 2014).

The environmental conditions that determine the global range of coral reefs reflect the importance of two key characteristics of reef-building corals: - 1) maintenance of a mutually beneficial symbiosis between coral and zooxanthellae is vital for the survival of both partners but relies on favourable light and nutrient conditions, and 2) the geographic extent of reef-building corals is restricted to regions where rapid formation of their calcium carbonate ($CaCO_3$) skeletons is favoured. This thesis investigates how disruption of the coral-zooxanthellae symbiosis, caused by modification of the inorganic nutrient environment affects the growth, structure and chemistry of zooxanthellate coral skeletons.

1.1.2. Nutrients in the coral-zooxanthellae symbiosis

1.1.2.1. Photosynthesis and the translocation of carbohydrates

Zooxanthellae are hosted in the gastrodermis (a layer of the oral endoderm), and in healthy corals there may be millions of algal cells per square centimetre of host tissue (Figure 1.2) (Dubinsky and Stambler, 2011). Individual algal cells are located within specialised vacuoles of host cells known as symbiosomes (Yellowlees, Rees and Leggat, 2008; Dubinsky and Stambler, 2011) which means that all molecules that become available to the zooxanthellae must first pass through host tissue and multiple cellular membranes (Yellowlees, Rees and Leggat, 2008). Carbon dioxide (CO_2) is required for photosynthesis and theoretically may have three possible initial sources:- i) CO_2 respired by the host and its symbionts (Harland and Davies, 1995), ii) CO_2 produced as a by-product of calcification (Ware, Smith and Reaka-Kudla, 1992) and iii) dissolved CO_2 derived from seawater (Furla *et al.*, 2000; Furla, Allemand and Orsenigo, 2000). At the mean seawater pH of ~8.1, less than 1 % of DIC in seawater is comprised of dissolved CO_2 (Zeebe, 2001).

Meanwhile, pH at the site of calcification is upregulated to even higher values which creates a CO_2 concentration gradient causing CO_2 to diffuse from the animal tissue (and away from the symbionts) into the calcifying space, so calcification-derived CO_2 is unlikely to contribute meaningfully to supporting zooxanthellae photosynthesis (Furla *et al.*, 2000; Al-Horani, Al-Moghrabi and De Beer, 2003b, 2003a). In fact, because both photosynthesis and calcification utilise carbon (C) from the animal's internal carbon pool (Furla *et al.*, 2000), CO_2-limitation of photosynthesis is a challenge that the host must help the symbionts to overcome. It is believed that the coral promotes CO_2 uptake from the surrounding seawater and transports it to the symbiosome. This is thought to be facilitated in the same way as has been demonstrated in experiments using *Anemenia viridis,* which uses H^+-ATPases to excrete H^+ ions from its ectodermal cells into the surrounding seawater; this lowers the pH and elevates the CO_2 concentration of the layer of seawater immediately adjacent to the tissue surface, causing CO_2 to passively diffuse into the host tissue down a concentration gradient (Furla, Allemand and Orsenigo, 2000; Davy, Allemand and Weis, 2012). Carbonic anhydrase (CA) facilitates the interconversion between HCO_3^- and CO_2 and has been detected in three localities of host tissue:- the surfaces facing the seawater, inside the coelenteron (gastro-vascular cavity), and also intracellularly (Al-Horani, Al-Moghrabi and De Beer, 2003a). CA probably facilitates the acquisition and transport of CO_2 to the zooxanthellae (and also to the calcifying space) because the experimental use of CA inhibitors causes both photosynthesis and calcification to be suppressed (Al-Horani, Al-Moghrabi and De Beer, 2003a). Photosynthesis is further promoted by the high reflectance and scattering properties of the coral skeleton, which maximises light availability for the symbionts (Enríquez, Méndez and Iglesias-Prieto, 2005).

Having provided favourable conditions for high rates of photosynthesis, corals are believed to induce translocation of carbohydrates from the zooxanthellae by restricting ammonium (NH_4^+) availability in the symbiosome which limits zooxanthellae protein synthesis and thereby restricts the specific growth rate of the symbionts (Muscatine *et al.*, 1989; Falkowski *et al.*, 1993; Yellowlees, Rees and Leggat, 2008). Symbiont photosynthesis and growth thereby become uncoupled, with surplus carbohydrates being produced by the zooxanthellae. These are consequently translocated to the host, and can provide up to 90% of the coral's energetic requirements (Falkowski *et al.*, 1984, 1993). Carbon translocation is also promoted by the production of compounds - collectively referred to as 'host release

factors' (HRF) - that are released by the coral, and which cause the zooxanthellae to excrete greater quantities of carbohydrates (Muscatine, Pool and Cernichiari, 1972; Sutton and Hoegh-Guldberg, 1990). Excreted compounds containing carbon that may be translocated to the host from the zooxanthellae include glycerol, amino acids and various lipids (reviewed in Davy, Allemand and Weis, 2012).

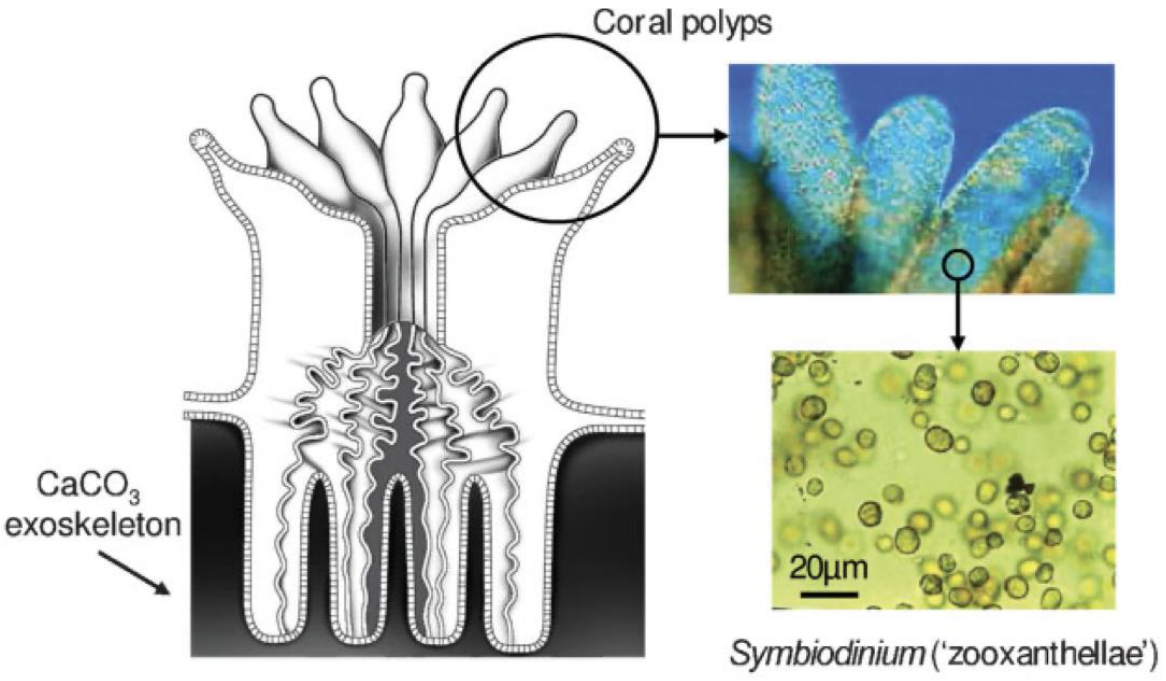

Figure 1.2. Schematic diagram and digital photographs illustrating the distribution of zooxanthellae within the coral tissue. Zooxanthellae are hosted within a layer of the oral endoderm called the gastrodermis and are concentrated in tissues which have higher levels light exposure such as tentacles. Zooxanthellae are microscopic dinoflagellates and can be present in concentrations of millions of cells per square centimetre of animal tissue. Figure sourced from Wooldridge, (2010).

1.1.2.2. Dissolved inorganic nitrogen and phosphorus

Nitrogen (N) is a critically limiting nutrient for all organisms. As a base constituent of amino acids, it is found in most important biomolecules including DNA, ATP, structural proteins and enzymes, and chlorophyll in plants. Dissolved inorganic nitrogen (DIN) is present in three biologically accessible forms in seawater: - ammonium (NH_4^+), nitrate (NO_3^-) and nitrite (NO_2^-) (O'Neil and Capone, 2008; Rädecker *et al.*, 2015). Zooxanthellae may obtain up to 90% of their N uptake through the recycling of NH_4^+, which is excreted as a waste product from the host (Rahav *et al.*, 1989; Tanaka *et al.*, 2015). Ammonium can

be directly assimilated by the coral and the zooxanthellae, and is the preferred form of DIN incorporated into both partners when both NH_4^+ and NO_3^- are available from seawater (Grover *et al.*, 2003; Davy, Allemand and Weis, 2012). NH_4^+ enrichment results in more rapid assimilation and/or translocation of N to the coral host than does NO_3^- enrichment (Kopp *et al.*, 2013), despite most of the N being retained by the symbionts (Pernice *et al.*, 2012). However, rapid ecosystem uptake of NH_4^+ usually leads to its relatively low concentrations on coral reefs (~0.05 – 0.5 μM) (reviewed in O'Neil and Capone, 2008), and seawater NO_3^- concentrations are typically more important to coral survival (Kleypas, Mcmanus and Menez, 1999; Guan, Hohn and Merico, 2015). Indeed, despite its relatively low concentrations on most reefs nitrate has been estimated to account for about 1/3rd of the total N uptake by zooxanthellate corals (Grover *et al.*, 2008).

Unlike their coral host, zooxanthellae have the nitrate and nitrite reductases necessary to facilitate the assimilation of N derived from seawater NO_3^- and NO^{2-} respectively, and both molecules are believed to be assimilated along similar pathways (Miller and Yellowlees, 1989; Davy, Allemand and Weis, 2012). NO^{2-} is often considered an intermediary product produced during nitrification and denitrification reactions, and is present in seawater at lower concentrations than NO_3^- (O'Neil and Capone, 2008). Consequently, many published studies neglect to report NO_2^- concentrations when investigating the nutrient environment, while others present combined $NO_3^- + NO_2^-$ concentrations in their data (Tomascik and Sander, 1985; Fabricius *et al.*, 2013). Within chapters 2-4 of this thesis, the importance of NO_3^- is discussed with only minor references being made to NO_2^-. This is done on the basis that NO_2^- constitutes a relatively minor, but consistent proportion (~10 %) of total DIN in the experimental mesocosm used for this research when compared to NO_3^- (~90 %) (Wiedenmann *et al.*, 2013), and also because it is NO_3^- which is generally considered critically important to zooxanthellate coral survival (Kleypas, Mcmanus and Menez, 1999; Guan, Hohn and Merico, 2015). However, this should not be interpreted to mean that the lesser - but still important – contribution of nitrite to coral nutrition is not recognised. Zooxanthellae densities often increase following nitrate enrichment (Marubini and Davies, 1996; Koop *et al.*, 2001; Wiedenmann *et al.*, 2013; Shantz and Burkepile, 2014) even though nitrate and nitrite are both charged ions which cannot passively diffuse through coral cell membranes. The mechanisms by which these forms of DIN reach and enter the symbiosome remain unclear, but are likely to involve transporter enzymes with a high affinity for nitrate and/or nitrite. However to date, such enzymes have only been identified

in zooxanthellae (Sproles *et al.*, 2018). The capacity for zooxanthellae to translocate N obtained from seawater NO_3^- has been demonstrated by ^{15}N-labelling experiments. $^{15}NO_3^-$ enrichment of the culture medium leads to ^{15}N enrichment of both zooxanthellae and coral tissue, although the $\%^{15}N$ increase in the symbiont can be ~10 times higher than for the host tissue (Grover *et al.*, 2003; Tanaka *et al.*, 2006; Pernice *et al.*, 2012). Nitrogen incorporated by the zooxanthellae is believed to be translocated to the host in the form of free amino acids and proteinaceous glycoconjugates (Davy, Allemand and Weis, 2012; Rädecker *et al.*, 2015). Nitrate enrichment may result in increases to cellular N and C content in both the symbiont and the host (Grover *et al.*, 2003), but proportionally less photosynthetically derived carbohydrates per cell are translocated to the coral under such conditions (Falkowski *et al.*, 1993). When the limitation of symbiont primary production is relieved through nitrate enrichment corals have little capacity to restrict the proliferation of zooxanthellae (Marubini and Davies, 1996; Koop *et al.*, 2001; Wiedenmann *et al.*, 2013; D'Angelo and Wiedenmann, 2014; Shantz and Burkepile, 2014). This loss of control over the zooxanthellae population means that the coral derives less benefit from the symbiosis due to the partitioning of nutrients and carbohydrates into the symbiont population (Falkowski *et al.*, 1993; Grover *et al.*, 2003; Tanaka *et al.*, 2006; Pernice *et al.*, 2012). In some cases, this effect can be so severe that the zooxanthellae might be considered parasites (Baker *et al.*, 2018). It is believed that to control zooxanthellae populations, and potentially also to access the partitioned nutrients corals continuously degrade and expel excess algal cells (Titlyanov *et al.*, 1996). Degradation takes place in the gastrodermis (as well as in tentacles and mesenteries) and expelled algal pellets are depleted in DNA, protein and lipids (Titlyanov *et al.*, 1996), suggesting that the zooxanthellae are digested to provide the coral with access to the nutrients partitioned within these biomolecules.

Phosphorus (P) has been termed the "ultimate limiting nutrient" to total oceanic productivity (Tyrrell, 1999), and is crucial for all living organisms due to its use in the synthesis of DNA, ATP and cell membranes, as well as in protein phosphorylation. The uptake of PO_4^{3-} - which does not occur in azooxanthellate or aposymbiotic corals - increases with photosynthesis, or under high light conditions in zooxanthellate corals, suggesting an active role of the symbionts in phosphorus acquisition (Godinot, Ferrier-pagès and Grover, 2009; Davy, Allemand and Weis, 2012). Similar to NO_3^- and NO_2^-, phosphate forms a negatively charged ion which cannot pass through cellular membranes by diffusion. However, active phosphate carriers have been detected in both zooxanthellae

and the coral during enrichment experiments on *Stylophora pistillata* (Godinot, Ferrier-pagès and Grover, 2009), providing a mechanism by which PO_4^{3-} could be supplied to the zooxanthellae within the symbiosome. Phosphate enrichment has been shown to increase both zooxanthellae density and coral growth in some experiments but not others (Muscatine *et al.*, 1989; Stambler *et al.*, 1991; Koop *et al.*, 2001), implying that phosphorus acquired by zooxanthellae from PO_4^{3-} can (at least in some circumstances) be translocated to the host (Ferrier-Pagès *et al.*, 2016). PO_4^{3-} enrichment results in a greater proportion of assimilated P being retained by the zooxanthellae, and the symbionts are considered to be a sink for P in the symbiosis (Godinot, Ferrier-pagès and Grover, 2009). P uptake rates increase when corals are starved, suggesting that heterotrophically acquired P is important to both corals and their zooxanthellae under conditions of normal prey availability (Godinot, Ferrier-pagès and Grover, 2009). Phosphorus cycling in zooxanthellate corals is poorly understood and the P-bearing molecules translocated to the host have not been conclusively identified. However, polyphosphate esters and phosphonates are both potential candidates and have been found in both the zooxanthellae and host (Ferrier-Pagès *et al.*, 2016).

1.1.2.3. Dissolved organic nitrogen and phosphorus

Dissolved organic matter (DOM) enters seawater through the excretion, defecation or decomposition of other organisms and also provides a vital source of N and P to sustain coral growth (Meyer, Schultz and Helfman, 1983; Meyer and Schultz, 1985; Goldberg, 2018; Savage, 2019). Dissolved urea is a source of N, and when available it is preferentially incorporated ahead of nitrate, accumulating in the host more rapidly than the zooxanthellae (Grover *et al.*, 2006). Dissolved free amino acids are also present in seawater and also accumulate in the host at faster rates than the zooxanthellae when available (Grover *et al.*, 2008). Both urea and free amino acids are actively taken up by corals even when available only at very low concentrations, reflecting an effective adaption by the host to maximise the use of organic sources of N that can be effectively partitioned from the symbionts (Grover *et al.*, 2006, 2008). It has been estimated that collectively, urea and free amino acids may provide ~24% of a coral's N requirement, while combined DIN and DON uptake may be sufficient to supply almost 100% of the coral's nitrogen needs for tissue growth (Grover *et al.*, 2008). The importance of dissolved organic phosphorus (DOP) to coral nutrition is poorly understood and mechanisms for its

sequestration and assimilation have yet to be identified (Ferrier-Pagès *et al.*, 2016; Goldberg, 2018). However, phosphatases associated with the hydrolysation of DOP to dissolved inorganic phosphorus (DIP) have been identified in both the zooxanthellae and host, and their activity is upregulated during periods of phosphorus deficiency suggesting a role in accessing phosphorus from dissolved organics (Wiedenmann *et al.*, 2013; Ferrier-Pagès *et al.*, 2016).

Different forms of nutrient stress

Nutrient stress is the physiological response to a nutrient shortage (Moore et al., 2003).

Nutrient limitation is the limitation of growth of individual cells due to low nutrient concentrations. The availability of a nutrient may ultimately restrict the amount of total biomass that can form (Moore et al., 2003)

Nutrient deficiency is the stoichiometric lack of one element relative to another (Moore et al., 2003). **Phosphorus-starvation** is a form of nutrient deficiency that can occur in the zooxanthellae of corals as a consequence of over-supply of inorganic nitrogen (Wiedenmann et. al. 2013).

Nutrient co-limitation is considered to occur when two (or more) nutrients have been depleted to such an extent that addition of both (or all) limiting nutrients is required to stimulate growth. This may occur because a) because both nutrients have been drawn down to equally limiting levels, such that both must be added to support growth, b) an organism may have substituted a limiting nutrient within a cellular molecule for another nutrient, or substituted molecules containing nutrients within the cell, c) one nutrient may be required to facilitate the uptake of another or 4) in biological communities, where different species respond to the addition of different nutrients (Moore et. al., 2003).

1.1.2.4 Heterotrophy

All corals are predators, and are characterised by stinging cells known as cnidocytes which are used to subdue zooplankton prey (WoRMS, 2022). Many species also feed on phytoplankton, microbial organisms and particulate organic matter (POM), and the capture of these smaller particles of food is facilitated by a 'mucus net' cast around the mouth and mesenterial filaments (reviewed in Goldberg, 2018). The digestion of planktonic prey provides a vital source of organic carbon, nitrogen and phosphorus (Wijgerde *et al.*, 2011); indeed in deep sea or cold water corals - which lack zooxanthellae - all essential nutrients must be obtained heterotrophically. Nutrient and energy acquisition via heterotrophy becomes more important in zooxanthellate corals following bleaching when the

translocation of nutrients from the symbionts is compromised, and can be vital to determining whether corals survive such events (Grottoli, Rodrigues and Palardy, 2006; Hughes and Grottoli, 2013). Heterotrophy may also provide a benefit to the symbionts, and feeding typically leads to an increase in zooxanthellae density (reviewed by Houlbrèque and Ferrier-Pagès, 2009, but see Rosset, D'Angelo and Wiedenmann, 2015) probably due to resultant higher NH_4^+ excretion rates by the host.

1.1.2.5. Nitrogen fixation

The coral microbiome contains a diverse community of bacteria, cyanobacteria and archaea which have been proposed to provide various services to the coral, such as enhanced immunological responses and the fixation of nitrogen (Reshef *et al.*, 2006; Rädecker *et al.*, 2015; Bednarz *et al.*, 2017). Diazotrophic (nitrogen-fixing) bacteria have been detected in coral tissue and mucus, and the majority of diazotrophs associated with corals are those of the bacterial group *Rhizobia* (Lema, Willis and Bourneb, 2012; Goldberg, 2018). *Rhizobia* are common in terrestrial ecosystems where they form mutualistic symbioses with leguminous plants and supply their hosts with a vital source of N. In reef building corals, two mechanisms for host assimilation of diazotrophically derived nitrogen (DDN) have been proposed but not confirmed, these being the uptake of NH_4^+ excreted by the diazotrophs or by direct ingestion of the diazotrophs (reviewed by Benavides, Bednarz and Ferrier-Pagès, 2017). The importance of DDN assimilation varies depending on environmental conditions and the metabolic status of the coral (Bednarz *et al.*, 2017); shallow water corals assimilate very little DDN (~1 %) unless PO_4^{3-} concentrations are enriched ($\geq$3 μM), meanwhile deep sea corals may obtain up to ~15% of their N through DDN assimilation but this is primarily through heterotrophy of diazotrophic plankton (Bednarz *et al.*, 2017).

1.1.3. The coral skeleton

1.1.3.1 Calcification – reactants and favourable conditions

Coral skeletons are formed primarily from aragonite, a crystal form of calcium carbonate ($CaCO_3$) which precipitates through the reversible reaction $Ca^{2+} + CO_3^{2-} \leftrightarrow CaCO_3$ using

calcium (Ca^{2+}) and carbonate (CO_3^{2-}) ions obtained directly and indirectly from the seawater. From here onwards, this reaction will be interchangeably referred to as calcification or $CaCO_3$ precipitation. Calcium availability is not typically limiting to calcification in seawater, with mean oceanic concentrations being 10.3 mmol kg^{-1} (Millero *et al.*, 2008). CO_3^{2-} is one of four species of dissolved inorganic carbon (DIC) found in seawater, and although [DIC] in seawater ($[DIC]_{sw}$) typically ranges between ~1.8 - 2.1 mmol kg^{-1} (Uthicke, Furnas and Lønborg, 2014; Guan, Hohn and Merico, 2015; Ross *et al.*, 2018; Zeebe, 2001), the concentration of CO_3^{2-} ions is much lower. This is due to the pH dependence of DIC speciation in seawater (with seawater $[CO_3^{2-}]$ being positively correlated to pH). At the mean seawater pH of ~8.1 only ~13 % of DIC is present as CO_3^{2-} ions with ~86.6 % present as bicarbonate ions (HCO_3^-) and the remainder available as carbonic acid (H_2CO_3) and dissolved carbon dioxide (CO_2). Consequently - and merely as an example - at SST = 25 ℃, $[DIC]_{sw}$ = 2.1 mmol kg^{-1} and ${}_pCO_2$ = 365 µatm, the concentration of carbonate ions would only be 272 µmol kg^{-1} (Zeebe, 2001). Therefore, given that $CaCO_3$ incorporates Ca^{2+} and CO_3^{2-} ions at the same ratio, it is the availability of CO_3^{2-} that limits calcification in oceanic settings. Furthermore, the partitioning of DIC species in seawater is determined by a series of reactions summarised by the following equilibrium equation:- $CO_2(aq) + H_2O \leftrightarrow H_2CO_3 \leftrightarrow HCO_3^- + H^+ \leftrightarrow CO_3^{2-} + 2H^+$. This means that the net reaction of calcification produces H^+ ions by promoting the reactions to the left of the equation. It therefore causes the pH of the precipitating fluid to decrease and reduces the proportion of DIC remaining in the fluid as CO_3^{2-} ions. In other words, the process of calcification alters the chemistry of the precipitating fluid such that conditions become less favourable to support further calcification.

The readiness for $CaCO_3$ to precipitate from seawater is described by the saturation state of seawater (Ω_{sw}), which is calculated from the equation:- $\Omega_{sw} = [Ca^{2+}]_{sw} * [CO_3^{2-}]_{sw} / K_{sp}$, where $[Ca^{2+}]_{sw}$ and $[CO_3^{2-}]_{sw}$ are the concentrations of calcium and carbonate ions in seawater respectively, and K_{sp} is the equilibrium constant for the reaction at specific temperature, salinity and pressure conditions (e.g. at SST = 25 ℃, salinity = 35 p.s.u., and pressure = 1 atmosphere the K_{sp} of aragonite = $10^{-6.19}$) (Zeebe, 2001). When $\Omega > 1$ $CaCO_3$ precipitates and calcification rates increase at higher values of Ω; meanwhile, when $\Omega < 1$ $CaCO_3$ dissolves. The temperature dependence of K_{sp} means that Ω_{sw} is positively correlated to SST and, as previously discussed the geographic range of hermatypic corals

coincides with high values of both temperature and Ω (Kleypas, Mcmanus and Menez, 1999; Guan, Hohn and Merico, 2015; Zeebe, 2001).

Coral skeletons and the reefs they form are continuously being eroded through a variety of mechanical and biological processes (Lange, Perry and Alvarez-Filip, 2020). Furthermore, the equilibration reactions that occur during calcification are responsible for increasing $[H^+]$ and lowering pH of the precipitating medium, which reduces Ω at the site of calcification. For skeletal growth to be maintained, DIC and/or pH at the site of calcification must be upregulated to increase the saturation state at the site of calcification to values higher than that of the surrounding seawater (McConnaughey, 1989a, 1989b; Adkins *et al.*, 2003; Al-Horani, Al-Moghrabi and De Beer, 2003b; Ross *et al.*, 2018). This is achieved by modifying the chemistry of the calcifying fluid.

1.1.3.2. The calcifying fluid

Calcification occurs in a semi-isolated, sub-micrometre space between the aboral ectoderm and the underlying skeleton and/or substrate (Dubinsky and Stambler, 2011; S. Tambutté *et al.*, 2011). This space is filled with modified seawater which throughout this thesis will be termed the calcifying fluid (cf). Unmodified seawater of ambient pH leaks into the calcifying space via paracellular channels, bringing with it a supply of Ca^{2+} ions and DIC (Dubinsky and Stambler, 2011; S. Tambutté *et al.*, 2011; Venn *et al.*, 2020), but as previously discussed an additional supply of both is required to sustain skeletal growth. Ca^{2+} ion concentrations are lower on the surface of the coral polyp than in the surrounding seawater, and even lower inside the coelenteron which allows Ca^{2+} ions to passively diffuse from the seawater into the coral's internal tissues (Al-Horani, Al-Moghrabi and De Beer, 2003b). The enzyme Ca-ATPase - which is present in the calicoblastic cells – then actively transports Ca^{2+} ions from the animal cells into the calcifying fluid and, for every Ca^{2+} ion transported it transfers two H^+ ions in the opposite direction. Ca-ATPase thereby performs the dual role of increasing $[Ca^{2+}]_{cf}$ and pH_{cf} to values that are higher than that of the surrounding seawater (McConnaughey, 1989a, 1989b; Adkins *et al.*, 2003; Al-Horani, Al-Moghrabi and De Beer, 2003b). The increased pH_{cf} increases the proportion of DIC_{cf} present as carbonate ions, but does not replenish the DIC used by calcification. This means that a further source of DIC is required to maintain high Ω_{cf} and calcification rates.

About 70-75 % of the DIC incorporated into coral skeletons is derived from CO_2 respired by the coral and its symbionts, and enters the calcifying fluid by passive diffusion down a diffusion gradient created by the elevated pH_{cf} conditions (McConnaughey, 1989a, 1989b; Furla *et al.*, 2000; Adkins *et al.*, 2003). This supply of DIC may be supplemented by active bicarbonate transporters present in the calicoblastic cells, but the other 25-30 % of C incorporated into skeletons is believed to be mostly derived from DIC obtained through seawater leakage (Furla *et al.*, 2000; Zoccola *et al.*, 2015). It is also believed that CA plays a role in supplying DIC to the calcifying fluid because calcification rates are reduced when corals are exposed to inhibitors of CA activity (Al-Horani, Al-Moghrabi and De Beer, 2003a). Figure 1.3 provides an overview of the different processes influencing calcifying fluid chemistry in zooxanthellate corals. The chemistry of the calcifying fluid changes both diurnally and seasonally due to changes in photosynthesis rates and this impacts calcification rates at the same temporal scales (Al-Horani, Al-Moghrabi and De Beer, 2003a, 2003b; McCulloch *et al.*, 2017; Ross *et al.*, 2018). In a series of experiments, Al-Horani, Al-Moghrabi and De Beer (2003b, 2003a) used micro-sensors inserted underneath the calicoblastic layer to demonstrate that both $[Ca^{2+}]_{cf}$ and $pH_{cf,}$ are elevated above that of the surrounding seawater and that their values are highest during daylight hours when photosynthesis is occurring (Al-Horani, Al-Moghrabi and De Beer, 2003b). Moreover, they demonstrated that – at the colony level – when photosynthesis is elevated during high light conditions respiration, ATP production and calcification all increase. The subsequent experimental use of CA, Ca-ATPase and photosynthesis inhibitors indicated that zooxanthellae photosynthesis provides much of the energy the coral the requires to modify the calcifying fluid and that this is done by producing ATP which in turn is used to power Ca-ATPase activity (although calcification itself is probably triggered by light) (Al-Horani, Al-Moghrabi and De Beer, 2003b).

Seasonal changes to calcifying fluid chemistry and calcification rates were found to differ in two studies on corals from typical and marginal reef locations in Australia (McCulloch *et al.*, 2017; Ross *et al.*, 2018). The boron chemistry of cores from *Porites spp.* taken from two locations on the Great Barrier Reef showed that $[DIC]_{cf}$ is highest (~3.2 x seawater values) in the summer and lowest in winter (~2 x seawater values) which is consistent with photosynthesis (and the supply of respired CO_2) being enhanced by high light levels/ higher temperatures in the summer. Furthermore, pH_{cf} was lowest during summer (when $[DIC]_{cf}$ was highest) and reached its highest values during winter, such that Ω_{cf} was

maintained at around 5 x the value of the surrounding seawater, thus minimising seasonal variability in calcification rates (McCulloch *et al.*, 2017). Contrastingly, in *Turbinara reniformis* from the marginal reefs of Southern Australia, calcification was highest in winter when $[DIC]_{cf}$ was lowest and pH_{cf} was at its highest annual values, and the inverse relationship between the pH_{cf} and $[DIC]_{cf}$ had a similar effect in stabilising Ω_{cf} throughout the year (Ross *et al.*, 2018). In the case of *T. reniformis,* elevated seawater *chl a* concentrations during the winter suggested that the corals likely upregulated the proportion of nutrition derived through heterotrophy during winter at this marginal location and that this, alongside the increase in pH_{cf} explained the enhanced winter skeletal growth rates (Ross *et al.*, 2018). Regardless of the contrasting seasonal patterns of growth reported from these two studies, together they demonstrate that in zooxanthellate corals Ω_{cf} is maintained at values higher than that of the surrounding water, and that although both pH_{cf} and $[DIC]_{cf}$ vary on a seasonal basis Ω_{cf} remains relatively stable due to a dynamic antithetical relationship between pH_{cf} and $[DIC]_{cf}$ (McCulloch *et al.*, 2017; Ross *et al.*, 2018). It has been suggested that the negative correlation between pH_{cf} and $[DIC]_{cf}$ may arise due to active and dynamic upregulation of pH_{cf} by the coral by increasing Ca-ATPase activity when the rate of metabolically-derived CO_2 diffusion is decreased (McCulloch *et al.*, 2017; Ross *et al.*, 2018). However, the results of the modelling study of Guo (2019) indicate that SST and buffering capacity are the primary controls on pH_{cf} elevation, while physiological responses affecting the dynamics between proton pumping, CO_2 diffusion and mixing with external seawater play a less important role.

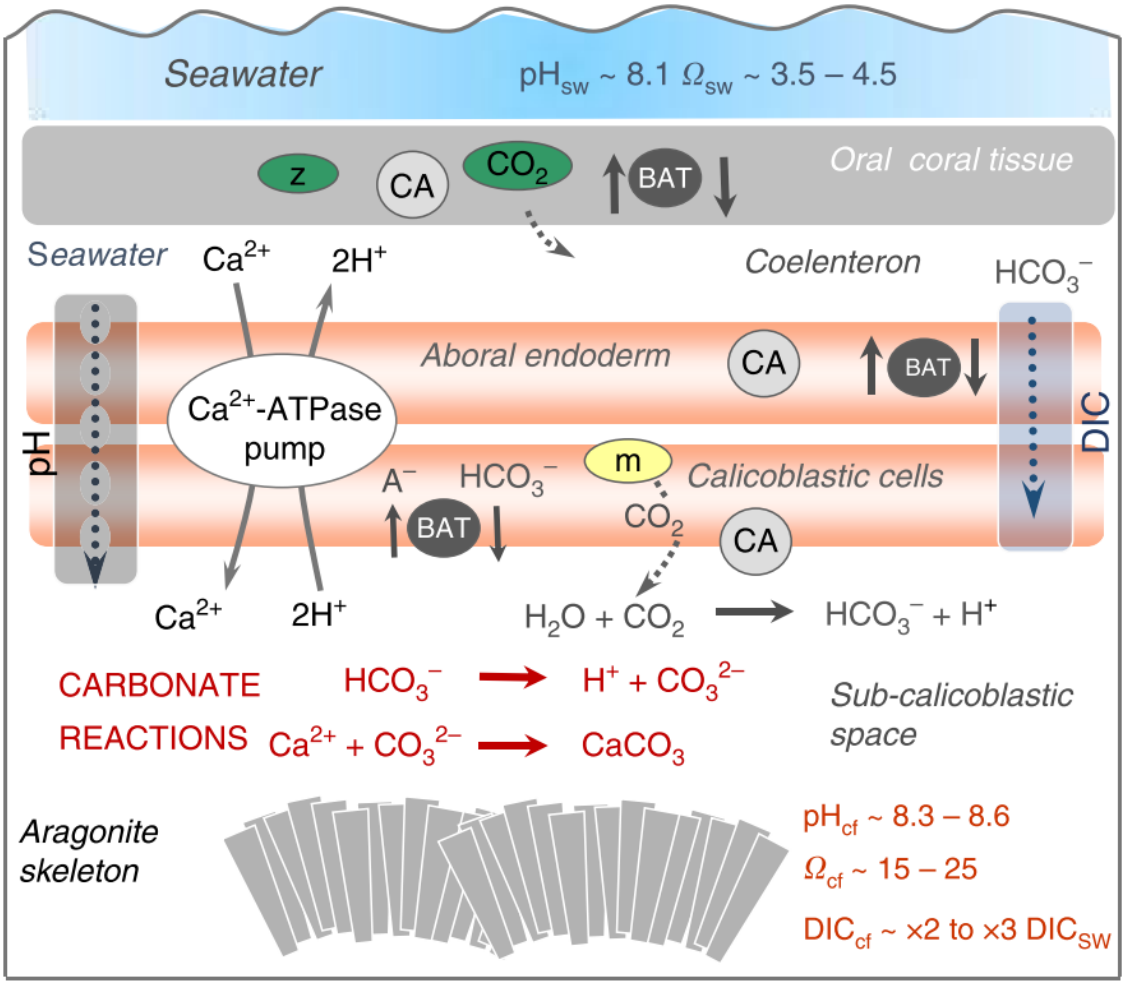

Figure 1.3. Mechanisms involved in coral calcification. Calcification occurs within the subcalicoblasic space from an initial seawater derived calcifying fluid with additional metabolic sourced supply of DIC. Elevation of pHcf occurs via removal of protons from the calcifying site by Ca-ATPase pumping. Carbonic anhydrases (CA) catalyse the forward reactions converting CO2 into HCO_3^- ions. Transfer of DIC into the subcalicoblastic space (which contains the calcifying fluid) occurs via diffusion of metabolic CO_2 and by HCO_3^- pumping via bicarbonate anion transporters (BAT). Figure sourced from (McCulloch *et al.*, 2017).

In contrast to the seasonal patterns described above, when $[DIC]_{cf}$ decreases during thermal-stress bleaching the pH_{cf} may remain unchanged, or may even be marginally reduced causing calcification rates to decrease (Rodrigues and Grottoli, 2006; D'Olivo and McCulloch, 2017; Schoepf *et al.*, 2021). This failure of pH_{cf} to increase in response to reduced $[DIC]_{cf}$ likely arises due to reduced energy availability to power Ca-ATPase activity when photosynthesis and respiration rates are reduced (Al-Horani, Al-Moghrabi and De Beer, 2003b). However, it should be noted that the energy required for Ca-ATPase pumping to maintain calcification typically constitutes < 1 % of that produced by

photosynthesis in healthy corals, and is considered an energetically inexpensive process (McCulloch *et al.*, 2012).

1.1.3.3. The physical interface between coral tissue and skeleton

The distance between the basal coral tissue and adjacent skeleton may vary between species, regions of the skeleton and also on a diurnal basis, but it is not believed to exceed 1 µm (reviewed in S. Tambutté *et al.* (2011). The calicoblastic ectoderm (the basal tissue layer containing the calicoblastic cells) is attached to the skeleton by anchoring cells known as desmocytes, and this intimate attachment serves to preserve a perfect correspondence between the surface features of the tissue and skeleton (Muscatine, Tambutte and Allemand, 1997; Tambutté *et al.*, 2007; Li *et al.*, 2020). Cup-like structures in the coral skeleton called corallites form beneath and around individual polyps. Common to all corallites are two skeletal elements: - i) walls known as theca that delineate the corallite from the rest of the skeleton and ii) septa, which are vertically oriented plate-like elements that radiate inwards towards the centre of the corallite from the theca (Veron, 2000). The size and shape of corallites vary between species as do the abundance of septa, while additional skeletal elements such as columella may be present within the corallites of some species but not others. As such, differences in corallite morphology are commonly used to aid taxonomic classifications (Veron, 2013; Madl, Schabetsberger and Lipovnik, 2014; Luzon *et al.*, 2017). The perfect correspondence between the tissue and skeletal surfaces means that morphological characteristics of coral skeletons can be used to infer patterns of soft tissue growth; for example, the size and shape of a corallite indicates the size and shape of the corresponding polyp (Tambutté *et al.*, 2007). Another example is that of endo-thecal dissepiments (skeletal elements that form at the base of polyps) which provide a reliable proxy for polyp tissue thickness when the distance between the apex of the theca and the uppermost dissepiment is measured (Barnes and Lough, 1992; Barkley *et al.*, 2018; Precoda *et al.*, 2020). Finally, because changes in polyp shape during asexual reproduction can also be recorded in the shape of corallites, examination of corallites from *Galaxea fascicularis* revealed that in this species budding apparently occurs only once a critical canalised ratio between the corallite perimeter and surface area is attained (Gateño and Rinkevich, 2003).

1.1.3.4. The crystal structure and organic matrix

The crystalline structures of coral skeletons are heterogenous and consist of regions of sub-micron granular material and elongated fibrous crystals (Holcomb *et al.*, 2009; Case *et al.*, 2010; Montagna *et al.*, 2014). The granular crystals are concentrated in regions called 'centres of calcification' and their higher contents of lithium (Li) and magnesium (Mg), along with their amorphous shapes are indicative of more rapid rates of calcification in these regions (Holcomb *et al.*, 2009; Case *et al.*, 2010; Montagna *et al.*, 2014). Fast calcification rates reflect high Ω_{cf} values, which in part are controlled by the Ca-ATPase activity of the calicoblastic cells (Al-Horani, Al-Moghrabi and De Beer, 2003b). The calicoblastic cells have also been identified as being responsible for the synthesis of an organic matrix (OM) that pervades the entire coral skeleton and is composed of excreted proteins, lipids and sugars (reviewed in Dubinsky and Stambler, 2011 and Tambutté *et al.*, 2011). As discussed, coral skeletal morphology can be used for taxonomic classifications (Veron, 2013; Madl, Schabetsberger and Lipovnik, 2014; Luzon *et al.*, 2017) indicating that skeletal formation is genetically controlled to some extent. The OM is believed to be implicated in the processes by which corals control the morphology of their skeletons, although different theories exist regarding how such a control may be exerted. These include (but are not limited to) the OM acting as a structural skeletal template upon which $CaCO_3$ can be precipitated or, that the release of organics into the calcifying fluid modifies the Ω_{cf} to either increase or decrease calcification rates, and that the organics are subsequently trapped as by-product in the resultant skeletal structure (reviewed in Dubinsky and Stambler, 2011; S. Tambutté *et al.*, 2011). Regardless of the role played by the OM, its synthesis is considered a prerequisite for skeletal growth (reviewed in Dubinsky and Stambler, 2011) and the excretion of N, P and C in the form of proteins, lipids and sugars requires that the animal replenishes these nutrients to sustain its growth.

1.1.3.5. Measuring coral skeletal growth and morphological properties

Coral skeletal growth rates vary between species, genera and morphological type and can be measured either as linear extension or calcification (skeletal weight gain). As an example, a study of 12 species across 6 genera in the Indian Ocean recorded mean linear extension rates ranging between 1.8 – 59 mm y^{-1} and mean calcification rates ranging

between 0.31 to 2.40 g cm^{-2} y^{-1}, with the highest growth rates being reported for branching species of the *Acropora* genus (Morgan and Kench, 2012). However, individual colonies may survive for hundreds of years during which their incremental growth can produce enormous structures. Recently, a massive *Porites spp.* colony was discovered on The Great Barrier Reef which had a basal diameter of 10.4 m and a circumference of 31 m; to date this is the largest coral colony discovered and is estimated to be 421-438 years old (Smith *et al.*, 2021). Coral growth rates vary on a seasonal and annual basis as consequence of variability in environmental conditions such as the availability of light and/or nutrients and this results in alternating bands of high/low density skeleton that can be dated and used to reconstruct growth rate histories from samples of skeletal cores (Barkley *et al.*, 2018; Benson *et al.*, 2018; Rippe *et al.*, 2018).

Linear extension refers to increases in the length of branches or tabular structures, or increases in the diameter or circumference of massive species. Linear extension can be measured in a number of ways including the use of tape measures, photogrammetry, skeletal staining and the coring of massive species (Morgan and Kench, 2012; Barkley *et al.*, 2018; Lange and Perry, 2020; Smith *et al.*, 2021). Linear extension is often the preferred method for measuring growth used in field settings because the determination of skeletal mass is often impractical. Measurements using tapes or photogrammetry are non-invasive and non-destructive to colony structures and repeated measurements allow extension rates to be calculated with relative ease (Koop *et al.*, 2001; Lange and Perry, 2020). Skeletal staining, normally using calcein or alizarin is used in both field and laboratory settings (Allison *et al.*, 2011; Morgan and Kench, 2012) and although the skeletons of live corals can be effectively stained without significantly disrupting coral physiology, the need to subsequently analyse extracted skeletal cores or sections mean that ultimately such techniques are destructive (Holcomb, Cohen and McCorkle, 2013).

Calcification is most easily measured through the change in skeletal mass. In laboratory settings this is typically achieved through repeated measures of buoyant weight (Jokiel, Maragos and Franzisket, 1978; Davies, 1989). This method disregards the contribution of coral tissue growth which typically only accounts for between 1-5 % of total buoyant weight (Jokiel, Maragos and Franzisket, 1978; Davies, 1989). Corals are measured in the culture water which has two advantages over measuring corals by removing them from experimental tanks:- i) it does not allow differential rates of water drainage from skeletal

pores to influence measurements and ii) any stress placed on the coral during measurement is minimised (Jokiel, Maragos and Franzisket, 1978). Calcification can also be measured using the 'alkalinity anomaly method' (Chisholm and Gattuso, 1991). This method relies on the fact that the total alkalinity (TA) of seawater (it's capacity to neutralise H^+ ions) is reduced by 2 moles for every mole of $CaCO_3$ precipitated, but is unaffected by photosynthesis or respiration (Chisholm and Gattuso, 1991). The TA of the culture medium/seawater is measured by titration repeatedly to measure changes over time and this method has been successfully employed to determine long-term changes to coral growth rates in field conditions as well as laboratory settings (Chisholm and Gattuso, 1991; Koop *et al.*, 2001).

Skeletal density varies both between and within coral skeletons, and is derived through a combination of two properties. 'Micro-density' refers to the specific gravity of the material of which the skeleton is made (Barnes and Devereux, 1988; Bucher, Harriott and Roberts, 1998). Pure aragonite has a micro-density estimated to be between 2.92 and 2.95 g cm^{-3}, but in corals micro-density can range between 2.62 and 2.82 g cm^{-3} (reviewed in Bucher, Harriott and Roberts, 1998). Differences in micro-density presumably arise due to the entrapment or substitution of trace elements which alters the molar mass of $CaCO_3$ crystals. 'Bulk density' refers to the mass of skeleton for a given volume and effectively gives an indication of the amount of void spaces in the skeleton (its porosity) (Barnes and Devereux, 1988; Bucher, Harriott and Roberts, 1998). Bulk density is partly determined by micro-density but is mostly influenced by the spacing between skeletal elements and potentially also by the arrangement of aragonite crystals within the skeletal structure (Buddemeier and Maragos, 1974; Barnes and Devereux, 1988; Bucher, Harriott and Roberts, 1998). Methods for measuring skeletal density include the use of X-radiography (Buddemeier and Maragos, 1974), the analysis of transmitted light photonegatives and cross polarised light images (Adkins *et al.*, 2003), buoyant weight analysis when the volume of the skeleton can also be determined (Bucher, Harriott and Roberts, 1998; Dunn, Sammarco and LaFleur, 2012; Rocker *et al.*, 2017) or the determination of skeletal porosity using micro-computed tomography (μ-CT) (Roche *et al.*, 2010, 2011). This final method relies on the observation that skeletal porosity (a measure of the void spaces within the skeleton) is strongly negatively correlated with skeletal bulk density (Koop *et al.*, 2001; Caroselli *et al.*, 2011).

1.1.3.6. Skeletal density and its use as an environmental proxy

Skeletal density can be highly variable within a single coral skeleton. Alternating bands of high- and low-density form in the skeletons of many massive coral species in response to seasonal fluctuations in SST and/or nutrient availability, and high density 'stress bands' may also form during periods of thermal stress (Dávalos-Dehullu, Hernández-Arana and Carricart-Ganivet, 2008; DeCarlo and Cohen, 2017; Barkley *et al.*, 2018; Fouke, Trop and Sivaguru, 2021). Intra-colonial differences in skeletal density have been shown to arise through the thickening of skeletal elements and/or a reduction in the spacing between them (Barnes and Devereux, 1988; Dávalos-Dehullu, Hernández-Arana and Carricart-Ganivet, 2008; DeCarlo and Cohen, 2017; Fouke, Trop and Sivaguru, 2021). Elements may thicken on the inside and outside of corallites, but not all skeletal elements are prone to thickening. Exo-thecal dissepiments, costae and theca have all been reported to contribute towards the formation of high-density skeletal regions through thickening, while septa, columella and endo-thecal dissepiments have not (Dávalos-Dehullu, Hernández-Arana and Carricart-Ganivet, 2008; Fouke, Trop and Sivaguru, 2021). The thickness of skeletal elements in a particular region of a coral skeleton relies on several factors. 1) Calcification occurs throughout the depth of the tissue layer, the thickness of which varies between species and genera, and is also as a reflection of nutritional status (Barnes and Lough, 2001; Qin *et al.*, 2020). Tissue thickness values are typically highest in massive species, especially those of *Porites spp.* for which it may exceed 10 mm, and are lowest in branching species, particularly those of *Acropora spp.* for which values may be < 2 mm (Barnes and Lough, 1992; Qin *et al.*, 2020). Tissue thickness can be heterogeneous throughout a colony and may vary seasonally, reflecting the current and/or localised nutritional status of the coral (Meyer and Schultz, 1985a; Barnes and Lough, 1992; Cohen *et al.*, 2004; Barkley *et al.*, 2018; Qin *et al.*, 2020). 2) The lowermost surface of the tissue is periodically stretched or uplifted, which results in the formation of new dissepiments and vacation of the underlying skeleton, thus terminating the term of thickening for the vacated skeleton (Barnes and Lough, 2001; Dávalos-Dehullu, Hernández-Arana and Carricart-Ganivet, 2008; DeCarlo and Cohen, 2017). 3) Lateral variations in skeletal density within the tissue layer arise as a consequence of differential rates of calcification (Barnes and Lough, 2001). Lateral heterogeneity in intra-colonial calcification rates have been demonstrated by lateral variability in skeletal geochemistry and the structures of aragonite crystals (Holcomb *et al.*, 2009; Case *et al.*, 2010; Montagna *et al.*, 2014). Taken together, it can be seen that a

combination of the tissue layer thickness and the rate at which the skeleton is vacated by live tissue determines the duration of thickening that any particular skeletal element undergoes. This, along with the localised calcification rate determines the skeletal element thickness, which in turn determines skeletal density for a particular region of the skeleton (Barnes and Lough, 2001). Tissue thickness, linear extension and calcification rates all decrease as a result of thermal-stress mediated bleaching (Mendes and Woodley, 2002; Rodrigues and Grottoli, 2006). The impact this has on the duration of contact between tissue and skeleton is unclear but high-density bands are associated with thermal stress bleaching events in massive corals such as *Porites spp.* (Barkley and Cohen, 2016; DeCarlo and Cohen, 2017; Barkley *et al.*, 2018). Although changes to skeletal density due to environmental change are primarily studied in massive coral species, similar responses have been reported for the phaceloid *Cladocora caespitosa* (Peirano *et al.*, 2005) and branching *Acropora spp.* (Koop *et al.*, 2001; Dunn, Sammarco and LaFleur, 2012; Rocker *et al.*, 2017).

1.1.3.7. Corallite size as an environmental proxy

There is indirect evidence that corallite size may also reflect environmental conditions. A recent study demonstrated that corallite size in a number of species of different genera varies throughout different regions of the Red Sea (Sadek *et al.*, 2018) Although the authors of the study did not comment on the likely causes of this variability, it is possible that corallite size may be a plastic response to environmental conditions. Two studies have produced findings that suggest corallite size may be indicative of a coral's nutritional status. Firstly, Foster (1979) reported that transplantation of *Montastraea annularis* and *Siderastrea siderea* from sand channels to reef lagoons which were characterised by higher concentrations of zooplankton, bacteria and dissolved organic matter resulted in larger corallite sizes. Secondly, the corallites of *Montrastraea cavernosa* collected from mesophotic environments are smaller than those collected from shallower depths, potentially a reflection of light-limitation of photosynthesis and lower rates carbohydrate translocation which was indicated by reduced zooxanthellae density and chlorophyll contents (Studivan, Milstein and Voss, 2019). However, a recent study suggested that polyp size (which corresponds with corallite size) is a poor indicator of tissue biomass (and therefore nutritional status) which is more reliably inferred from tissue thickness (Meyer and Schultz, 1985a; Barnes and Lough, 1992; Cohen *et al.*, 2004; Tambutté *et al.*, 2007;

Barkley *et al.*, 2018; Precoda *et al.*, 2020; Qin *et al.*, 2020). The correspondence between the maximal penetration of tissue within the coral skeleton and the depth of the uppermost dissepiment consequently allows the tentative use of coral skeletons as a gauge for nutritional status (Barnes and Lough, 1992; DeCarlo and Cohen, 2017).

1.1.3.8. Trace element and stable isotope ratios as records of environmental change and coral physiology

The trace element (TE) and stable isotope contents of coral skeletons are also commonly used as proxies to investigate environmental conditions and/or coral physiology. TE contents are normally reported as a molar ratio relative to skeletal Ca content (TE/Ca). Meanwhile, stable isotope values are typically given as positive or negative values relative to a standard reference material, using the prefix δ. Of particular interest – especially at a time when urgent research into climate change and its impacts is required - are those geochemical markers that have been identified as potential paleo-thermometers, which include (but are not limited to) Sr/Ca (Beck *et al.*, 1992), Mg/Ca (Mitsuguchi *et al.*, 1996), Li/Ca (Marriott, Henderson, Belshaw, *et al.*, 2004; Marriott, Henderson, Crompton, *et al.*, 2004) and $\delta^{18}O$ (Weber and Woodhead, 1972). From this point onwards, this thesis will focus the discussion of coral skeletal geochemistry on these geochemical markers, along with B/Ca (which is used to infer calcifying fluid carbonate chemistry) and $\delta^{13}C$ (which can be used to infer the role of photosynthesis in corals and/or seawater ^{13}C values) (Swart, 1983; McConnaughey, 1989a, 1989b; Swart *et al.*, 2010). It is recognised that other geochemical markers in coral skeletons have been identified as useful environmental and physiological proxies, but for the purposes of brevity and clarity they remain outside the scope of this work.

Li^+, Mg^{2+} and Sr^{2+} ions may become incorporated into coral skeletons during crystal formation by the process of surface entrapment (Gaetani and Cohen, 2006; Montagna *et al.*, 2014; Rollion-Bard and Blamart, 2015). However, the substitution of Li^+ ions for Ca^{2+} ions within the $CaCO_3$ crystal lattice has also been proposed as an alternative method for the inclusion of lithium (Marriott, Henderson, Crompton, *et al.*, 2004). The methods of Mg incorporation are also controversial, and high Mg/Ca values have been interpreted to indicate high concentrations of residual organic matter within the skeleton (Inoue *et al.*, 2018). This is based on strong correlations within the skeletal microstructure between high

Mg/Ca values, amorphous granular crystals associated with 'centres of calcification' and Mg-bearing organic molecules capable of binding to calcium (Meibom *et al.*, 2004; Holcomb *et al.*, 2009; Case *et al.*, 2010; Montagna *et al.*, 2014).

Regardless of the means by which TE's are included into skeletal structures, the abundance of a given TE in an isolated precipitating medium is finite, and the distribution of that element between the two phases (liquid and solid) depends on the distribution coefficient specific to that element under the ambient conditions (D_{El}). In the case of Li/Ca, Mg/Ca and Sr/Ca, the respective D_{El} values are all temperature dependent (Marriott, Henderson, Belshaw, *et al.*, 2004; Marriott, Henderson, Crompton, *et al.*, 2004; Gaetani and Cohen, 2006) which is the characteristic that distinguishes these elemental ratios as potential paleothermometers. However, Li/Ca and Mg/Ca values are also positively correlated to calcification rate (Gabitov *et al.*, 2008, 2011). As previously discussed, calcification rates are ultimately controlled by Ω which – in addition to also being temperature-dependent – is a function of Ca^{2+} and CO_3^{2-} ion concentrations. In corals, Ω_{cf} is biologically mediated through Ca-ATPase activity, the supply of metabolic CO_2 and the active transport of HCO_3^- ions (Furla *et al.*, 2000; Al-Horani, Al-Moghrabi and De Beer, 2003b; Zoccola *et al.*, 2015). This means that coral physiology also impacts calcification rates, and can affect skeletal TE/Ca ratios without any modification of temperature being required. In zooxanthellate corals, skeletal Li/Ca and Mg/Ca values are both enriched in rapidly precipitated 'centres of calcification' where pH_{cf} values and calcification rates are highest (Holcomb *et al.*, 2009; Case *et al.*, 2010; Montagna *et al.*, 2014). Montagna *et al.* (2014) found that in zooxanthellate corals, Mg/Ca is less sensitive to temperature changes than Li/Ca and, whereas Mg/Ca values are positively correlated with temperature (Reynaud *et al.*, 2007; Rollion-Bard and Blamart, 2015; Marchitto *et al.*, 2018), the relationship between Li/Ca and temperature is negatively correlated (Reynaud *et al.*, 2007; Rollion-Bard and Blamart, 2015; Marchitto *et al.*, 2018). This has led to the conclusion that in zooxanthellate corals 1) Li/Ca and Mg/Ca are likely to be primarily controlled by kinetics relating to calcification rate rather than temperature and consequently, 2) that skeletal Li/Mg ratios provide a more reliable proxy for determining SST because they are apparently unaffected by biological influences (Raddatz *et al.*, 2013; Montagna *et al.*, 2014; Marchitto *et al.*, 2018). Skeletal Sr/Ca ratios (which are negatively correlated to SST) (Reynaud *et al.*, 2007; Marchitto *et al.*, 2018) are also influenced by additional factors relating to the calcification process. However, this likely relates to the variable H^+

ion buffering capacity of the calcifying fluid at different values for $[DIC]_{cf}$ and Sr/Ca values are not directly correlated to either $[DIC]_{cf}$ or pH_{cf} in a way that results in a correlation with calcification rate (Allison and Finch, 2010b; Brahmi *et al.*, 2012).

Biological influences that override, or are imprinted on environmentally derived geochemical signatures are commonly referred to as 'vital effects' (Gagnon *et al.*, 2007; Pérez-Huerta *et al.*, 2010; Juillet-Leclerc *et al.*, 2014; Robinson *et al.*, 2014). While 'vital effects' do not necessarily invalidate the use of geochemical markers as environmental proxies they do complicate their use, and often require careful calibration according to the species or genus being studied (Montagna *et al.*, 2014; Ross, DeCarlo and McCulloch, 2019).

Another process that must be taken into consideration when considering skeletal TE/Ca ratios is that of Rayleigh fractionation. Trace elements with (D_{El}) > 1 (such as Sr) are preferentially incorporated into the skeleton, while those with a distribution coefficient < 1 (e.g. Li, Mg and B) are discriminated against. This means that as calcification proceeds from an isolated precipitating medium, the calcifying fluid concentration of elements such as Sr decreases relative to $[Ca^{2+}]_{cf}$, while elements such as Li, Mg and B increase. Because calcification is an incremental process, the skeleton's TE content changes as a greater proportion of the calcifying fluid is utilised. When D_{El} is known, TE/Ca ratios can therefore be used to interpret the proportion of calcium ions from the starting fluid composition that remain in the calcifying fluid (F_{Ca}). However, the calcifying space of corals is not fully isolated. Seawater leaks into the calcifying space via paracellular channels, thus returning calcifying fluid TE concentrations to values that are closer to that of unmodified seawater (E. Tambutté *et al.*, 2011; Venn *et al.*, 2020). This has led to the use of F_{Ca} to investigate the extent of isolation of the calcifying fluid (D'Olivo and McCulloch, 2017; Venn *et al.*, 2020; Ram and Erez, 2021). Resultantly, it has been shown that changes to seawater pH and/or temperature can alter seawater paracellular transport rates (Venn *et al.*, 2020) and that the degree to which the calcifying fluid is isolated from the external medium differs between coral genera (Ram and Erez, 2021). Thermal-stress bleaching has also been found to increase F_{Ca} and is indicative of a 'loss of precipitation efficiency', although this could be ascribed to either increased paracellular leakage and/or decreased precipitation rate (D'Olivo and McCulloch, 2017).

The ^{18}O:^{16}O ratio ($\delta^{18}O$) of biological carbonates was initially identified as a potential paleothermometer by Epstein and Mayeda (1953), following recognition that the isotopic fractionation of oxygen between $CaCO_3$ and H_2O is temperature dependent (Urey, 1947; McCrea, 1950). However, more recent work has established that the fractionation of oxygen isotopes differs between DIC species in seawater (Usdowski and Hoefs, 1993). Therefore, because seawater DIC speciation is determined by pH_{sw}, the $\delta^{18}O$ values of marine biological carbonates also reflect the pH of the precipitating fluid at the time of calcification (Usdowski and Hoefs, 1993). This effect can predominate in corals because high rates of metabolic CO_2 diffusion into the calcifying fluid ensure high Ω_{cf} values. Consequently, calcification may occur too quickly for temperature-dependent equilibration to be attained between the solid ($CaCO_3$) and liquid (H_2O) phases. This means that the $\delta^{18}O$ value of coral skeletons often more strongly reflects pH_{cf} than temperature (Adkins *et al.*, 2003; Rollion-Bard, Chaussidon and France-Lanord, 2003; Devriendt, Watkins and McGregor, 2017).

Similar to the fractionation of oxygen isotopes, skeletal $\delta^{13}C$ values are also influenced during the calcification process by fractionation between the aqueous species of DIC and by fractionation between the solid (aragonite) and liquid phases (seawater) (Faure & Mensing, 2005). In deep sea corals - which lack zooxanthellae - skeletal $\delta^{18}O$ and $\delta^{13}C$ values form a linear relationship that is positively correlated and which passes through seawater equilibrium (McConnaughey, 1989a, 1989b; Adkins *et al.*, 2003). Skeletal $\delta^{13}C$ is therefore shown to be influenced by temperature and pH_{cf}, and if temperature conditions remain constant (which is typically the case for deep sea corals) can be considered to reflect the speciation of DIC species in the calcifying fluid, thus pH_{cf} (Adkins *et al.*, 2003; Faure & Mensing, 2005). However, in zooxanthellate corals, skeletal $\delta^{13}C$ values are enriched relative to $\delta^{18}O$. Skeletal ^{13}C enrichment occurs as a consequence of photosynthesis by the zooxanthellae, which preferentially take up $^{12}CO_2$ resulting in enrichment of the surrounding animal tissue with $^{13}CO_2$ (Swart, 1983). As previously discussed, about 70-75 % of C incorporated into the skeletons of zooxanthellate corals is derived from metabolic CO_2 which diffuses into the calcifying space from the animal tissue (Furla *et al.*, 2000), and when photosynthesis rates are high, the proportion of ^{13}C incorporated into the skeleton increases (Swart, 1983; McConnaughey, 1989a, 1989b; Reynaud-Vaganay *et al.*, 2001). Another potential physiological control on skeletal $\delta^{13}C$

values is the degree of isolation of the calcifying fluid, but this should be considered an indirect control through pH because enhanced seawater leakage returns pH_{cf} to values closer to that of the surrounding seawater (McConnaughey, 1989a, 1989b; Adkins *et al.*, 2003). Although the skeletal $\delta^{13}C$ values of zooxanthellate corals are therefore primarily the consequence of 'vital effects', they are also impacted by climate change. The 'Suess effect' refers to the enrichment of atmospheric $^{12}CO_2$ from the burning of fossil fuels which has the opposite effect to photosynthesis (Baker, Webster and Kim, 2010; Swart *et al.*, 2010; Dean, Leng and Mackay, 2014). CO_2 is constantly being exchanged across the atmosphere-ocean interface and progressive decreases in coral skeletal $^{13}CO_2$ values since the start of the industrial revolution in the 1800's have been detected in a number of studies (Baker, Webster and Kim, 2010; Swart *et al.*, 2010; Dean, Leng and Mackay, 2014).

B/Ca is controlled by the ratio between borate and carbonate ions in the calcifying fluid $[B(OH)_4^-]/[CO_3^{2-}]_{cf}$ (Holcomb *et al.*, 2016). B/Ca cannot, on its own be used to determine $[CO_3^{2-}]_{cf}$ in corals because $[CO_3^{2-}]_{cf}$ is dependent on both $[DIC]_{cf}$ and pH_{cf}, and as previously discussed $[CO_3^{2-}]_{cf}$ and $[DIC]_{cf}$ can vary independently of each other in the calcifying fluid of corals. However, coral skeletal B/Ca has recently been recognised as a valuable tool when used alongside measurements of skeletal $\delta^{11}B$, which is an established proxy for pH. When used together, these two geochemical markers can be used to fully constrain calcifying fluid chemistry, first by determining pH_{cf} and then by calculating $[DIC]_{cf}$ using knowledge of the pH-dependent speciation of DIC species (Zeebe, 2001; Holcomb *et al.*, 2016; McCulloch *et al.*, 2017; Decarlo, Holcomb and McCulloch, 2018).

1.1.4. Coral bleaching and nutrient enrichment

1.1.4.1. The impacts of coral bleaching

Coral reef ecosystems are in decline globally, and a recent report concluded that between 2009 and 2018 about 14 % of the world's live coral cover was lost, primarily as a result of large-scale coral bleaching events, but also due to local stressors including pollution, overfishing, coastal development and tropical storms (GCRMN, 2020). Global-scale mass bleaching events are a modern phenomenon, and are the result of a trend of increasing thermal stress that begun in the 1800's, and which has been unequivocally linked to

anthropogenic emissions of CO_2 (Hoegh-Guldberg *et al.*, 2007; Hughes *et al.*, 2017a; Hughes, Anderson, *et al.*, 2018; Lough, Anderson and Hughes, 2018). Widespread bleaching on reefs occurs as a result of accumulated thermal stress, and can be reliably predicted by calculating the 'Degree Heating Weeks' (DHW) value over a rolling 12-week period (Liu, Strong and Skirving, 2003). The DHW value is a measure of the temperature anomaly above the maximum mean monthly temperature (MMM) such that, if the temperature is 1 ℃ above the MMM for 1 week then a DHW value of 1 is given. Bleaching occurs when DHW values of ~4 are reached across a 12-week period, and is widespread at values ≥ 8 (Liu, Strong and Skirving, 2003). Three major global mass bleaching events have occurred in the last 25 years (1998, 2002 and 2016), but numerous other more localised mass bleaching events have occurred around the world during this period. The increasing frequency and severity of thermal stress episodes is now commonly preventing corals from recovering sufficiently before bleaching re-occurs, and is driving the rapid decline of coral reef ecosystems globally (Hughes *et al.*, 2017a; Hughes *et al.*, 2017; Lough, Anderson and Hughes, 2018; GCRMN, 2020).

Thermal-stress induced bleaching involves the loss of zooxanthellae, and is so called because the loss of algal pigment leaves the coral tissue transparent thereby making the underlying white skeleton visible and gives the coral a whitish appearance. Elevated temperature and irradiance conditions are believed to cause damage to multiple locations of zooxanthellae photosynthetic apparatus. These include the D1 protein of photosystem II (PSII) reaction centres, the enzyme ribulose biphosphate carboxylase oxygenase (RuBisCo) and thylakoid membranes (Lesser, 1997; Warner, Fittt and Schmidt, 1999; Tchernov *et al.*, 2004; Weis, 2008). Damage to each of these components results in an excess of electrons being released through the disruption of photosynthetic electron transfer pathways. This leads to O_2 molecules being reduced and a series of reactions that increase the production of reactive oxygen species (ROS) including singlet oxygen ($^1O_2$), superoxide (O_2^-), hydrogen peroxide (H_2O_2) and hydroxyl radical ($\cdot OH$) (reviewed in Weis, 2008). ROS are common but harmful by-products of photosynthesis and zooxanthellae routinely defend against their damaging effects using antioxidants. However, if concentrations of ROS become too high the symbiont's defences can be overwhelmed and further damage is caused to the zooxanthellae's photosynthetic membranes which exacerbates the situation and reduces photochemical efficiency (Fv/Fm) (Lesser, 1996, 1997; Warner, Fittt and Schmidt, 1999; Tchernov *et al.*, 2004; Weis, 2008;

Rehman *et al.*, 2016). Elevated concentrations of ROS have also been detected in host tissues during thermal stress, the source of which may be excretion by zooxanthellae, and/or increased cellular ROS production by the host (Lesser and Farrell, 2004; Weis, 2008; Tchernov *et al.*, 2011; Rehman *et al.*, 2016). Elevated host tissue ROS concentrations cause damage to host cells and trigger apoptosis (programmed cell death) which has, in turn been linked to the expulsion of the symbionts probably as a defensive mechanism (Lesser and Farrell, 2004; Weis, 2008; Tchernov *et al.*, 2011; Rehman *et al.*, 2016).

Although bleaching is not necessarily fatal for the host, it does represent the loss of the coral's primary energy source, and an important means of obtaining inorganic nutrients from the environment. (Falkowski *et al.*, 1984, 1993; Grover *et al.*, 2002, 2003, 2008; Godinot, Ferrier-pagès and Grover, 2009; Davy, Allemand and Weis, 2012). To survive, bleached corals must use stored energy and nutrient reserves by catabolising carbohydrates, lipids and proteins (Rodrigues and Grottoli, 2007; Rodrigues, Grottoli and Pease, 2008; Wall *et al.*, 2019) or upregulate heterotrophic feeding (Grottoli, Rodrigues and Palardy, 2006; Hughes and Grottoli, 2013). Loss of biomass is a typical consequence of coral bleaching (Rodrigues and Grottoli, 2007; Wall *et al.*, 2019) and genera characterised by greater tissue thickness/ biomass or a better capacity to upregulate heterotrophic feeding have been shown to have greater ability to recover from bleaching events (Grottoli, Rodrigues and Palardy, 2006; Hughes and Grottoli, 2013; Qin *et al.*, 2019, 2020). However, stored energy reserves are finite and the availability of planktonic prey on coral reefs is often unreliable so, if stress conditions persist or if corals are unable to replace their lost symbionts, they are likely to die (Baird and Marshall, 2002; Baker, Glynn and Riegl, 2008).

Coral mortality during mass bleaching events is highest among species with branching and tabular morphologies which are characterised by lower tissue thickness than more resilient species (which often have more compact morphologies) (Marshall and Baird, 2000; Hughes, Kerry, *et al.*, 2018; Qin *et al.*, 2019, 2020). The reduced community calcification rates associated with losses of coral live cover may result in the reef accretion/ erosion balance being shifted towards net erosion (Lange and Perry, 2019; Perry *et al.*, 2020). Both reef biodiversity and productivity are positively correlated to rugosity which is highest when live coral cover is high and there is a high proportion of branching species present

(Purkis, Graham and Riegl, 2008; Graham and Nash, 2013). Since both coral cover and the %age cover of branching species are reduced during bleaching, there is commonly a consequent negative impact on ecosystem functioning (Hughes, Kerry, *et al.*, 2018). Furthermore, erosion of the reef structure can result in 'pseudo sea level rises' which increase the wave energy that reaches the shoreline and reduce the level of coastal protection that is afforded by the reef (Sheppard *et al.*, 2005).

1.1.4.2. The impacts of nutrient enrichment

As previously discussed, coral reefs are typically confined to regions where nutrient concentrations are relatively low (with mean concentrations of NO_3^- ~0.25 μM and PO_4^{3-} ~ 0.13 μM) although NO_3^- concentrations as high as ~4.5 μM can support functioning reef ecosystems (Kleypas, Mcmanus and Menez, 1999; Guan, Hohn and Merico, 2015). However, the restriction of coral reefs to shallow waters also means that many reefs are found in close proximity to human population centres and are consequently exposed to nutrient pollution that may elevate nutrients above optimal concentrations. Examples of nutrient pollution include terrestrial run-off of agricultural DIN and DIP, high production rates of DIN and DON from fish farms, the direct input and groundwater seepage of untreated sewage containing organic nutrients, the settling of phosphate dust onto surface waters and the stirring up of benthic nutrients by dredging activity (reviewed by Fabricius, 2005). The nutrification of coral reefs can have positive (Koop *et al.*, 2001; Bongiorni *et al.*, 2003; Dunn, Sammarco and LaFleur, 2012; Rocker *et al.*, 2017) or negative (Tomascik and Sander, 1985; Brodie *et al.*, 2005; Duprey, Yasuhara and Baker, 2016; Cybulski *et al.*, 2020) impacts on coral health and survival which in the past has made it hard to reach a consensus on approaches to tackle the problem of nutrient pollution. However, it is important to recognise that nutrient enrichment can have a range of direct and indirect impacts on zooxanthellate corals, and that it is the combinations of these different impacts that ultimately determines reef survival capacity (D'Angelo and Wiedenmann, 2014).

Modest and balanced seawater enrichment of both DIN and DIP can increase zooxanthellae densities, chlorophyll *a* content and protein content (Muscatine *et al.*, 1989; Stambler *et al.*, 1991; Falkowski *et al.*, 1993), and promote coral growth and health (Koop *et al.*, 2001; Bongiorni *et al.*, 2003; Dunn, Sammarco and LaFleur, 2012; Rocker *et al.*, 2017). However, the nature and context of nutrient pollution is important. The meta-

analysis of Shantz and Burkepile (2014) demonstrated that different coral taxa have varying capacities to respond positively to nutrient enrichment, and also that negative responses are more likely when nutrification occurs as a result of anthropogenic pollution rather than via a natural source. Furthermore, they showed that N enrichment often enhances zooxanthellae density and/or chlorophyll content while reducing coral growth, suggesting that under some nutrient enrichment scenarios the coral-zooxanthellae symbiosis is disturbed (Shantz and Burkepile, 2014). Such a situation may arise when nutrient enrichment results in skewed N:P ratios and causes the relative undersupply of another essential nutrient (Wiedenmann *et al.*, 2013; Rosset *et al.*, 2017).

When nutrient enrichment is sustained and represents a significant modification of the nutrient environment, the cumulative indirect impacts are typically negative and tend to negate or overwhelm any positive direct impacts that corals may derive (Tomascik and Sander, 1985; Fabricius, 2005; D'Angelo and Wiedenmann, 2014; Duprey, Yasuhara and Baker, 2016). Increased nutrient concentrations result in rapid increases in phytoplankton densities in the water column (Furnas *et al.*, 2005). While this may increase the availability of particulate food, it reduces light availability which is required to support zooxanthellae photosynthesis (although this in turn, may alleviate light stress during periods of thermal stress) (reviewed in Fabricius, 2005). Macro-algae also benefit from enhanced growth under high nutrient concentrations, and nutrification enhances competition for both light and space on the seafloor which leads to increased macro-algae coverage at the expense of live coral cover (Kinsey and Davies, 1979; Lapointe, Tewfik and Phillips, 2021). The increased availability of particulate food may also benefit other species, including the larvae of species which prey on corals as adults, e.g. *Acanthaster planci* (Crown of Thorns starfish) (Brodie *et al.*, 2005). Finally, nutrient enrichment has also been shown to increase the abundance of macro-bioeroders (presumably also by indirectly providing a food source to their larvae) (Cooper *et al.*, 2008) and the susceptibility of corals to disease (Voss and Richardson, 2006; Thurber *et al.*, 2014). Despite this array of known indirect impacts from nutrient enrichment, high nutrient reefs can be found in locations such as the Galápagos Islands and off the Brazilian coast (Kleypas, Mcmanus and Menez, 1999) and high nutrient concentrations are not necessarily always detrimental to coral health (Szmant, 2002). However, the observation that high nitrogen concentrations lead to increased bleaching susceptibility (Wooldridge, 2009) prompted a series of studies that subsequently identified

skewed seawater N:P stoichiometries as a direct threat to coral survival (Wiedenmann *et al.*, 2013; D'Angelo and Wiedenmann, 2014; Rosset *et al.*, 2017).

1.1.4.3. The impacts of skewed nitrogen: phosphorus stoichiometries

Wooldridge (2009) identified that corals in regions of the Great Barrier Reef that were exposed to high concentrations of DIN derived from terrestrial run-off had reduced bleaching thresholds (bleached at lower temperatures). A mechanism capable of explaining this phenomenon was subsequently identified, this being not a direct response to high concentrations of DIN, but instead due to the relative undersupply of phosphorus (Wiedenmann *et al.*, 2013). A series of experiments using multiple coral species demonstrated that following DIN enrichment ($NO_3^- + NO_2^- > 3$ µM) while PO_4^{3-} concentrations were kept low (~ 0.07 µM), the zooxanthellae became phosphorus-starved (Wiedenmann *et al.*, 2013). The upregulation of alkaline phosphatase activity, reduced photochemical efficiency (Fv/Fm) and the substitution of sulpholipids for phospholipids in thylakoid membranes have all previously been identified as markers of P-starvation in unicellular photosynthetic organisms (Parkhill, Maillet and Cullen, 2001; Annis and Cook, 2002; Frentzen, 2004). All of these responses were detected in the zooxanthellae of corals cultured under high nitrate: low phosphate (HNLP) conditions, but were absent in corals cultured under nutrient replete or nutrient-limited conditions (Wiedenmann *et al.*, 2013). Subsequent exposure of corals from each of the treatments to light and thermal stress confirmed that those with P-starved symbionts were indeed more susceptible to bleaching, and that bleaching was associated with drastic reductions in Fv/Fm (Wiedenmann *et al.*, 2013). As previously discussed, bleaching is associated with reductions in Fv/Fm and increased cellular production of ROS (Lesser, 1996, 1997; Warner, Fittt and Schmidt, 1999; Tchernov *et al.*, 2004; Rehman *et al.*, 2016). Tchernov *et al.* (2004) showed that ROS production increases when the structural integrity of thylakoid membranes is compromised, and that this is more likely to occur when the saturation of membrane lipids is reduced. Meanwhile, Frentzen (2004) demonstrated that in photosynthetic membranes, sulfoquinovosyldiacylglycerol (SQDG) can be substituted to replace phosphatidylglycerol during periods of P-limitation, but that a certain amount of phosphatidylglycerol must be retained to maintain correct photosynthetic functioning. The high levels of SQDG's measured in zooxanthellae from the HNLP treatment suggest that the structural integrity of thylakoid membranes had been compromised, and therefore provides evidence of a

mechanism explaining how P-starvation of zooxanthellae increases the susceptibility of corals to bleaching (Wiedenmann *et al.*, 2013). The fact that this response was not observed when N and P were both replete or limited indicated that it was the stoichiometric imbalance between N and P that caused the detrimental response, rather than elevated N or depleted P concentrations *per se* (Wiedenmann *et al.*, 2013). Additionally, the concentrations of nutrients used in the replete and limited treatments indicated that the effect of seawater N:P stoichiometry was less important if NO_3- (< 0.7 µM) or PO_4^{3-} (> 0.3 µM) concentrations were sufficiently low or high, respectively (Wiedenmann *et al.*, 2013).

Following on from this study, the impacts of chronic exposure to skewed N:P stoichiometries were tested in the absence of light and thermal stress using *Euphyllia paradivisa* (Rosset, D'Angelo and Wiedenmann, 2015; Rosset *et al.*, 2017). In these studies, corals were exposed to four different nutrient treatments for ≥ 6 months:- high nitrate : high phosphate (HNHP), high nitrate: low phosphate (HNLP), low nitrate: high phosphate (LNHP) and low nitrate: low phosphate (LNLP) allowing the effect of N-starvation to also be assessed (Rosset, D'Angelo and Wiedenmann, 2015; Rosset *et al.*, 2017). Interestingly, two distinct coral responses were observed. HNHP and LNHP corals retained high zooxanthellae densities and a healthy appearance, and were characterised by large polyp sizes. Meanwhile, HNLP and LNLP corals had reduced zooxanthellae densities consistent with their bleached appearance and significantly smaller polyps (Rosset, D'Angelo and Wiedenmann, 2015; Rosset *et al.*, 2017). The zooxanthellae from the HNLP and LNLP treatments also differed from those of the HNHP and LNHP treatments. HNLP and LNLP symbionts had increased cell size and increased concentrations of carbon-rich storage compounds (lipid bodies and starch granules), indicating that photosynthesis had become uncoupled from algal growth (Rosset *et al.*, 2017). As before, the HNLP zooxanthellae also had reduced Fv/Fm indicative of P-starvation (Parkhill, Maillet and Cullen, 2001; Wiedenmann *et al.*, 2013), and were characterised by the accumulation of uric crystals (which are used as N-storage compounds) (Kopp *et al.*, 2013). The smaller cell size and higher density of zooxanthellae after exposure to LNHP conditions indicated that the zooxanthellae were better adapted to withstand N-starvation than P-starvation and this was reflected by healthier corals which had a greater capacity to retain biomass (Rosset, D'Angelo and Wiedenmann, 2015; Rosset *et al.*, 2017).

Seawater N:P ratios on coral reefs are typically ≤ 12:1 (Kleypas, Mcmanus and Menez, 1999), but elevated ratios (in some cases as high as high as 74:1) arising through anthropogenic nutrient pollution have historically been reported in Barbados (Spencer Davies, 1990), Jamaica (Lapointe, 1997) and Brazil (Szmant, 2002). In all three cases nutrient pollution was identified as a driver of reef decline, albeit that the role of nutrient stoichiometry was not considered (Spencer Davies, 1990; Lapointe, 1997; Szmant, 2002). A more recent study also found that an increase in the N:P ratio from ~30:1 to ~70:1 on the Belize Barrier Reef coincided with a drastic reduction in live coral cover (Lapointe, Tewfik and Phillips, 2021). But, very high N:P ratios may not necessarily be required for corals to be detrimentally affected by skewed N:P stoichiometries because a further study found that a modest increase in the N:P ratio from 9.5 to just 26.5 also led to the decline of zooxanthellate corals on a reef in Florida, USA (Lapointe *et al.*, 2019). Consequently, it has been highlighted that water quality management plans must include strategies for minimising the impacts that nutrient pollution has on coral reef seawater N:P ratios, and that such actions may allow a level of mitigation to be achieved against the negative effects of global warming (D'Angelo and Wiedenmann, 2014; Lapointe *et al.*, 2019; Lapointe, Tewfik and Phillips, 2021).

1.2. Knowledge gaps and aims of the thesis

Nutrient pollution that leads to high seawater N:P ratios has been shown to increase the susceptibility of reef corals to bleaching during thermal stress (Wiedenmann *et al.*, 2013) and can also cause bleaching to occur at ambient SST's (Rosset *et al.*, 2017). Consequently, water quality management strategies that consider seawater N:P stoichiometries as well as nutrient concentrations have been identified as a potentially effective method for mitigating the harmful effects of climate change (D'Angelo and Wiedenmann, 2014; Lapointe *et al.*, 2019; Lapointe, Tewfik and Phillips, 2021). Skeletal growth rates are reduced, and net reef erosion rates increase following episodes of thermal stress and bleaching (Lange and Perry, 2019; Perry *et al.*, 2020), and this can negatively impact ecosystem functioning and the provision of ecosystem services (Sheppard *et al.*, 2005; Purkis, Graham and Riegl, 2008; Graham and Nash, 2013). However, divergent responses have been reported in the scientific literature regarding the impacts of nutrient enrichment on coral skeletal growth and microstructural properties such as density or

porosity. This is problematic because the growth rates and microstructural properties of coral skeletons are important determinants of reef erosion rates (Chamberlain, 1978; Marshall, 2000; Lange and Perry, 2019; Perry *et al.*, 2020), and a more complete understanding of how they are impacted by nutrient pollution could improve the evidence-based management of reef ecosystems. Coral taxonomy and different sources of nutrient pollution have previously been identified as potential causes for the differential coral skeletal responses to nutrient enrichment, but the evidence for a role of skewed N:P ratios is equivocal (Shantz and Burkepile, 2014).

Therefore, the first aim of this thesis is to investigate whether skewed seawater N:P ratios, brought about by imbalanced nutrient enrichment can explain the different impacts that nutrient enrichment is reported to have on the growth and microstructural properties of zooxanthellate coral skeletons.

The macro- and micro-scale morphological features of coral skeletons have utility as environmental proxies. Seasonal fluctuations in SST and/or nutrient availability cause alternating bands of high- and low-density to form in coral skeletons, while periods of thermal stress give rise to high-density 'stress bands' (Barnes and Devereux, 1988; Dávalos-Dehullu, Hernández-Arana and Carricart-Ganivet, 2008; DeCarlo and Cohen, 2017; Fouke, Trop and Sivaguru, 2021). Intra-colonial increases in skeletal density have been attributed to enhanced thickening of, and/or a reduction to the spacing between skeletal elements, with some skeletal elements being more prone to modification than others (Barnes and Devereux, 1988; Dávalos-Dehullu, Hernández-Arana and Carricart-Ganivet, 2008; DeCarlo and Cohen, 2017; Fouke, Trop and Sivaguru, 2021). Meanwhile, corallite size and the depth of dissepiments reflect polyp size and tissue depth respectively, thus indicating the nutritional status of the associated polyp (Barnes and Lough, 1992; Barkley *et al.*, 2018; Precoda *et al.*, 2020). However, previous research into the impacts of environmental disturbances on the micro-scale structures of coral skeletons has primarily focussed at the colony level in species with massive morphologies. Little attention has been paid to impacts at the level of the corallite, or to species with different morphologies. Colonies of *E. paradivisa* have a phaceloid morphology which is characterised by isolated polyps accommodated in distinct corallites. A recent study showed that chronic exposure to high N:P ratios caused *E. paradivisa* corals to bleach, and polyp volume was reduced (Rosset *et al.*, 2017). However, the impacts on the coral skeleton were not assessed. It is

unclear whether the reduction in polyp volume was mirrored by modification of the corallite, or whether the thickness or spacing of skeletal elements are affected. Furthermore, there are no studies in the literature that report the impacts of skewed N:P stoichiometries on the structure of the corallite for corals of any morphology. This knowledge gap could represent a potential complication for researchers seeking to use features of the skeletal microstructure as proxies for bleaching events. This is especially true because high seawater N:P stoichiometries have been reported in a number of regions where corals are in decline (Spencer Davies, 1990; Lapointe, 1997; Szmant, 2002; Lapointe *et al.*, 2019; Lapointe, Tewfik and Phillips, 2021). Therefore, the second aim of this thesis is to investigate how nutrient enrichment, limitation and skewed N:P ratios can impact the size and morphology of corallites in zooxanthellate corals.

Coral skeletal geochemistry is more established than skeletal morphology in its use as an environmental proxy, and geochemical signals associated with thermal-stress mediated bleaching have been identified. Changes to skeletal B/Ca ratios and $\delta^{11}B$ values have revealed that thermal-stress mediated bleaching modifies calcifying fluid chemistry by decreasing $[CO_3^{2-}]_{cf}$ and Ω_{cf} (McCulloch *et al.*, 2017; Schoepf *et al.*, 2021). This is potentially due to reduced metabolic CO_2 diffusion into the calcifying space. Theoretically, this should be accompanied by a decrease in the skeletal $\delta^{13}C$ value, due to reduced isotopic fractionation by photosynthesis when the coral loses its symbionts (Swart, 1983; McConnaughey, 1989b, 1989a; Furla *et al.*, 2000; Inoue *et al.*, 2018). Meanwhile, changes to SST and bleaching can also modify the rate of seawater leakage into the calcifying space, an effect that has the potential to modify skeletal TE/Ca ratios through changes impacting Rayleigh fractionation (D'Olivo and McCulloch, 2017; Venn *et al.*, 2020; Ram and Erez, 2021). All of these observed and expected changes to TE and stable isotope ratios are considered 'vital effects' (Pérez-Huerta *et al.*, 2010) and reflect a coral's physiological response to thermal-stress bleaching. However as previously discussed, bleaching can also occur as a consequence of severe nutrient limitation or due to chronic exposure to high N:P ratios (Rosset, D'Angelo and Wiedenmann, 2015; Rosset *et al.*, 2017). Beyond bleaching and a loss of polyp biomass, little is known about the physiological response of the coral to these different forms of nutrient stress, despite the impacts on zooxanthellae being well characterised (Rosset, D'Angelo and Wiedenmann, 2015; Rosset *et al.*, 2017). The final aim of this thesis is to establish the impacts of nutrient

enrichment, limitation and skewed N:P ratios on the skeletal geochemistry of zooxanthellate corals, and where possible to speculate on the coral's physiological responses to these different forms of nutrient stress.

The major research questions of this thesis are:-

1. Can the divergent responses that have been reported for skeletal growth and modification of the skeletal microstructure following nutrient enrichment be explained by the resultant N:P stoichiometry of seawater?

2. What impacts do severe nutrient limitation and skewed seawater N:P stoichiometries have on the micro- and macro-scale structural morphologies of corals at the level of the corallite?

3. What impacts do severe nutrient limitation and skewed seawater N:P stoichiometries have on the trace element and stable isotope ratios of zooxanthellate coral skeletons, and how might this impact the reliability of these geochemical markers as environmental proxies?

1.3. Approach and thesis outline

The remainder of this thesis comprises of three data chapters (chapters 2-4), presented in the style of published scientific research papers, plus a synthesis chapter (Chapter 5). Each data chapter deals with a single research question in the sequential order they have been posed above. As with most scientific publications, the data chapters each consist of 5 parts: - Abstract, Introduction, Methods, Results and Discussion. Chapter 2 has recently been published in the journal *Coral Reefs* (DOI: 10.1007/s00338-022-02223-0), and the co-author contributions are detailed within. Chapter 5 starts with a critique of the strengths and weaknesses for each data chapter, before synthesising the three data chapters and discussing the broader implications of the research findings. Chapter 5 then concludes with proposals for future research questions that could further our understanding in this field of study.

The studies described in this thesis relate to experiments conducted on two model species of zooxanthellate corals, *Acropora polystoma* and *Euphyllia paradivisa*. Both species were exposed to the same suite of nutrient treatments in the experimental mesocosm of The Coral Reef Laboratory, University of Southampton, UK which is located at The National Oceanography Centre, Southampton (Waterfront campus). The design features of this multi-compartment facility allow all other environmental conditions to be tightly controlled, thereby allowing the treatment effect to be assessed with minimal additional effect caused by any confounding variables. The experimental nutrient treatments used during the three studies have been defined as follows: - high nitrate: high phosphate (HNHP), high nitrate: low phosphate (HNLP), low nitrate: high phosphate (LNHP) and low nitrate: low phosphate (LNLP). Chapter 2 relates to the exposure of *A. polystoma* to this suite of nutrient treatments in a series of experiments lasting 10-20 weeks, and no information regarding experimentation on these corals has previously been published. Chapter 3 refers to fragments of *E. paradivisa* exposed to the same suite of nutrient conditions for ≥ 1 year. Data relating to these corals has previously been published (Rosset, D'Angelo and Wiedenmann, 2015; Rosset *et al.*, 2017) but the effects on the coral skeleton were not considered. Chapters 2 and 3 describe the impacts of the four nutrient treatments on coral skeletal morphology as determined using micro-computed tomography (µ-CT), this being work that has not previously been conducted on these specimens. µ-CT imaging of the coral skeletons was conducted at two locations, these being The University Hospital Southampton, UK and The Natural History Museum, London, UK. Chapter 4 deals with geochemical analysis of the skeletons from these two experiments and covers the effects of the nutrient treatments on the skeletons of both species. The geochemical analysis was conducted in two parts. Stable isotope analysis of skeletal $\delta^{18}O$ and $\delta^{13}C$ was conducted at The Ocean and Earth Science department's Stable Isotope Laboratory at the University of Southampton using a Thermo Finnigan Kiel-IV Carbonate Device coupled to a isotope ratio mass spectrometer (IRMS). Trace element ratios were analysed at The University of Southampton (National Oceanography Centre), UK using an ICP-MS Triple Quad ICP mass spectrometer coupled to a laser ablation system. The working hypothesis and approach for each chapter are as follows:-

Chapter 2 - Impact of nitrogen (N) and phosphorus (P) enrichment and skewed N:P stoichiometry on the skeletal formation and microstructure of symbiotic reef corals

H_1 – Divergent responses in skeletal growth and microstructural properties reported following nutrient enrichment can be explained by differences in the coral response that occur when imbalanced nutrient enrichment causes seawater N:P stoichiometries to become skewed.

This study comprises two parts. The first section revisits the results of published studies that investigated the effects of nutrient enrichment on the linear extension, calcification and skeletal density of zooxanthellate corals. These published studies included laboratory and field studies of the effects of both anthropogenic and natural sources of nutrient enrichment. 92 responses from 25 published studies were categorised according to the resultant N:P stoichiometries and also the taxonomy of the coral genus being that had been studied. This categorisation revealed that the skeletal growth response of corals from the genus *Acropora* was particularly sensitive to skewed seawater N:P stoichiometries following imbalanced nutrient enrichment. Consequently, fragments of *A. polystoma* were exposed to the previously described suite of nutrient treatments to test the impacts of medium-term exposure to enriched nutrient replete conditions, severe nutrient limitation and skewed (high and low) N:P stoichiometries. During the culture phase, the impacts on the coral-zooxanthellae symbiosis were measured through changes to zooxanthellae density and photochemical efficiency (Fv/Fm), while the skeletal growth response was quantified through measurements of linear extension and calcification. 3-dimensional images of the coral skeletons were subsequently obtained by use of micro-computed tomography. The skeletal element thickness and skeletal porosity were then measured using the open source software, ImageJ. Finally, the statistical significance of differences between the treatments were assessed using univariate statistical analysis methods (ANOVA and Tukey HSD test or Kruskal-Wallis and Dunn's test).

Figure 1.4. A small colony of *Acropora polystoma* on a coral reef in Papua New Guinea. Photo by Charlie Veron. Image sourced from *Corals of the World* website.

Chapter 3 - Chronic nutrient limitation and skewed nitrogen: phosphorus (N:P) stoichiometries modify corallite size and structure in the zooxanthellate coral Euphyllia paradivisa

H_2 – Reductions to coral polyp volume and biomass in *E. paradivisa* that have been reported to occur following chronic exposure to severe nutrient limitation or high N:P ratios are associated with changes to the size and structural morphology of the corallite.

Two published studies have previously reported the impacts of chronic exposure to severe nutrient limitation and skewed N:P ratios on the coral-zooxanthellae symbiosis of *E. paradivisa* (Rosset, D'Angelo and Wiedenmann, 2015; Rosset *et al.*, 2017). During these studies, coral polyp volume and biomass were both significantly reduced in corals exposed to severe nutrient limitation and high N:P ratios (Rosset, D'Angelo and Wiedenmann, 2015; Rosset *et al.*, 2017). The intimate contact between coral tissue and skeleton means that there is a perfect correspondence between the surface features of coral tissue and skeleton in zooxanthellate corals (Muscatine, Tambutte and Allemand, 1997; Tambutté *et al.*, 2007; Li *et al.*, 2020). This led to formulation of the hypothesis that the size and structure of the *E. paradivisa* corallites from these published studies (Rosset, D'Angelo

and Wiedenmann, 2015; Rosset *et al.*, 2017) would have been similarly impacted. The coral skeletons from the previously published studies were made available for the purpose of this study. The size and macro-scale morphological features of these corallites were measured using digital photographs analysed using the open source image analysis software, ImageJ. A sub-set of representative corallites were then imaged using µ-CT, and analysed using ImageJ. Differences in corallite area, theca length, extension rate, circularity, the number of septa and the mean thickness of theca, septa and dissepiments were determined using univariate statistical analysis methods (ANOVA and Tukey HSD test or Kruskal-Wallis and Dunn's test). Multi-level linear regression models and regression analysis were then used to assess how the different nutrient treatments impacted the relationships between corallite size and shape, skeletal element thickness and the abundance of internal skeletal structures (septa and dissepiments).

Figure 1.5. Colony of *Euphyllia paradivisa* with tentacles retracted showing underlying colony structure (Philippines). Photograph by Charlie Veron. Image sourced from Corals of the World website.

Chapter 4 - Imbalanced nutrient enrichment and severe nutrient limitation alter stable isotope ratios and trace element contents in the skeletons of Acropora polystoma and Euphyllia paradivisa

H3 – The stable isotope and TE/Ca ratios of corals exposed to severe nutrient limitation and skewed N:P ratios differ from those of corals exposed to nutrient replete conditions.

The null hypotheses relating to chapters 2 and 3 were rejected in both cases. This led to the further working hypothesis that geochemical signatures specific to each of the nutrient treatments would be detectable for both species. Therefore, a representative sub-set of the skeletons of both species were analysed to determine their stable isotope ($\delta^{13}C$ and $\delta^{18}O$) and trace element (Li/Ca, Mg/Ca, Sr/Ca and B/Ca) ratios. Stable isotope and TE contents were determined using an isotope ratio mass spectrometer (IRMS) and an ICP-MS Triple Quad ICP mass spectrometer coupled to a laser ablation system, respectively. Differences in the stable isotope contents between species and treatments were assessed using two-way ANOVA tests. The differences in TE/Ca contents between the different nutrient treatments were assessed for both species using a non-parametric multivariate statistical method (Robust MANOVA) followed up by linear discriminant function analyses to explain the observed differences between the nutrient treatments. Simple linear regression and multiple linear regression models were subsequently used to explore the relationships between the TE/Ca ratios and stable isotope contents. The impacts on skeletal Li/Ca, Mg/Ca, Sr/Ca and $\delta^{18}O$ values were compared against the published thermal sensitivities for each proxy. The chapter concludes with a speculative interpretation of the physiological responses of both coral species to each of the different nutrient treatments.

Chapter 2 - Impact of nitrogen (N) and phosphorus (P) enrichment and skewed N:P stoichiometry on the skeletal formation and microstructure of symbiotic reef corals

M. C. Buckingham, C. D'Angelo, T. B. Chalk, G. L. Foster, K. G. Johnson, Z. Connelly, C. Olla, M. Saeed & J. Wiedenmann

[Published online on 20/04/2022 as Buckingham et. al. (2022) Impact of nitrogen (N) and phosphorus (P) enrichment and skewed N:P stoichiometry on the skeletal formation and microstructure of symbiotic reef corals, *Coral Reefs*, DOI: 10.1007/s00338-022-02223-0]

Author contributions - Zoe Connelly, Carolina Olla, and Muhammad Saeed contributed to the experiments by culturing corals as part of their undergraduate research projects at SOES which were supervised by Cecilia D'Angelo, Gavin Foster, Tom Chalk and Joerg Wiedenmann. Ken Johnson provided technical advice regarding the analysis of coral skeletons using µ-CT techniques and specialist insights into the nature of skeletal morphology. Michael Buckingham undertook all µ-CT and statistical analyses. The final report was prepared by Michael Buckingham and Joerg Wiedenmann.

Acknowledgements - We thank Robbie Robinson and George Clarke for their assistance with coral husbandry and their continued support in maintaining the experimental mesocosm during challenging times. We also acknowledge the technical staff of the µ-CT imaging laboratories at UHS and NHM, and Dan Doran and Matthew Beverley-Smith of the SOES Rock Preparation and Thin- Sectioning Facility for their assistance. This work was supported by the Natural Environmental Research Council [grant numbers NE/L002531/1 and NE/T001364/1 "Defining Nutritional Bottlenecks of Reef Coral Growth and Stress Tolerance"] and the European Research Council (ERC) H2020-EU.1.1 (ERC-2019-ADG Grant agreement ID: 884650, Microns2Reefs)

2.1. Abstract

Reported divergent responses of coral growth and skeletal microstructure to the nutrient environment complicate knowledge-based management of water quality in coral reefs. By re-evaluating published results considering the taxonomy of the studied corals and the N:P stoichiometry of their nutrient environment, we could resolve some of the major apparent contradictions. Our analysis suggests that *Acroporids* behave differently to several other common genera and show distinct responses to specific nutrient treatments. We hypothesised that both the concentrations of dissolved inorganic N and P in the water and their stoichiometry shape skeletal growth and microstructure. We tested this hypothesis by exposing *Acropora polystoma* fragments to four nutrient treatments for > 10 weeks: high nitrate/high phosphate (HNHP), high nitrate/low phosphate (HNLP), low nitrate/high phosphate (LNHP) and low nitrate/low phosphate (LNLP). HNHP corals retained high zooxanthellae densities and their linear extension and calcification rates were up to ten times higher than in the other treatments. HNLP and LNLP corals bleached through loss of symbionts. The photochemical efficiency (Fv/Fm) of residual symbionts in HNLP corals was significantly reduced, indicating P-starvation. Micro-computed tomography (µ-CT) of the skeletal microstructure revealed that reduced linear extension in nutrient limited or nutrient starved conditions (HNLP, LNHP, LNLP) was associated with significant thickening of skeletal elements and reduced porosity. These changes can be explained by the strongly reduced linear extension rate in combination with a smaller reduction in the calcification rate. Studies using increased skeletal density as a proxy for past thermal bleaching events should consider that such an increase in density may also be associated with temperature-independent response to the nutrient environment. Furthermore, the taxonomy of corals and seawater N:P stoichiometry should be considered when analysing and managing the impacts of nutrient pollution.

2.2. Introduction

Nutrient enrichment through the introduction of excess nitrogen and/or phosphorus in reef environments typically promotes an array of direct and indirect negative effects leading to the decline of zooxanthellate coral cover. Impacts include increased susceptibility of corals to bleaching, disease and bio-erosion, greater competition for light and space from algal

competitors and the increased abundance of corallivores (Kinsey and Davies, 1979; Edinger *et al.*, 2000; Brodie *et al.*, 2005; Fabricius, 2005; D'Angelo and Wiedenmann, 2014; Thurber *et al.*, 2014). Nutrient enrichment can also impact coral skeletal growth and structure. However, different studies report contradictory results regarding how changes in the nutrient environment affect linear extension, calcification and skeletal structure (Tomascik and Sander, 1985; Marubini and Davies, 1996; Koop *et al.*, 2001; Szmant, 2002; Fabricius, 2005; Dunn, Sammarco and LaFleur, 2012; Shantz and Burkepile, 2014; Rocker *et al.*, 2017). This uncertainty is of concern as the nutrient environments in coral reefs are likely to undergo continued change due to direct anthropogenic impact and climate change. Such changes may occur in the form of nutrient enrichment (Elizalde-Rendón *et al.*, 2010; Browne *et al.*, 2015), skewed N:P stoichiometries (D'Angelo and Wiedenmann, 2014; Lapointe *et al.*, 2019) or nutrient depletion (Sun *et al.*, 2008; Rosset *et al.*, 2017). Accordingly, varied effects on coral skeletons can be expected, which may influence the formation of the 3-dimensional reef framework that is critically important for reef biodiversity and productivity (Purkis, Graham and Riegl, 2008; Graham and Nash, 2013), and coastal protection (Sheppard *et al.*, 2005). Furthermore, impaired coral growth and changes in skeletal structures may shift the reef accretion/erosion balance towards net erosion (Lange and Perry, 2019; Perry *et al.*, 2020) and the consequent loss of rugosity may negatively affect ecosystem services such as fisheries, tourism income and coastal protection. Paradoxically, even when nutrient enrichment may promote coral growth, this can occur alongside reliable indicators of reef degradation such as reduced live coral cover and increased rates of bio-erosion (Edinger *et al.*, 2000). This incomplete understanding impairs knowledge-based management of the nutrient environment in coral reefs and may prevent stakeholder support for required coastal zone and catchment management projects (Bell, Lapointe and Elmetri, 2007). Therefore, a better understanding of the impacts of changes in the nutrient environment on skeletal growth and structure is needed to forecast, and potentially mitigate, effects of environmental change on reef ecosystems.

Coral skeletal growth is commonly quantified using three metrics: linear extension, calcification rates and skeletal density. Linear extension describes the change in length of branches or foliose skeletons, or the increase in diameter of massive species. Calcification refers to the precipitation of the aragonite ($CaCO_3$) skeleton. In many experiments, calcification is commonly presumed to be reflected mostly in a mass change as the contribution of the soft tissue to the overall weight is relatively small. Skeletal density is

often measured alongside growth and is ultimately a property of the skeletal microstructure. Skeletal density comprises two components: micro-density and bulk density. Micro-density refers to the specific gravity of the material from which the skeleton is formed and is affected by the inclusion of trace elements, non-$CaCO_3$ compounds and organic content; bulk density is the mass divided by the total volume and takes into account the micro-density and the porosity of the skeletal structure (Bucher, Harriott and Roberts, 1998; Caroselli *et al.*, 2011). Porosity is the primary control on bulk density (to which it is negatively correlated) and is important ecologically because high skeletal porosity is associated with reduced mechanical strength and greater susceptibility to breakage and erosion caused by biotic and abiotic factors (Chamberlain, 1978; Bucher, Harriott and Roberts, 1998; Marshall, 2000).

Coral growth is limited by the availability of energy and nutrients, mostly in the form of carbon, nitrogen and phosphorus (Dubinsky and Jokiel, 1994; Davy, Allemand and Weis, 2012; D'Angelo and Wiedenmann, 2014; Rädecker *et al.*, 2015; Ferrier-Pagès *et al.*, 2016). At a global scale, mean concentrations of dissolved nitrate (NO_3^-) (0.25 ±0.28 μM) and phosphate (PO_4^{3-}) (0.13 ±0.08 μM) in coral reef waters are relatively low (Kleypas, Mcmanus and Menez, 1999). Nitrogen is most commonly the limiting nutrient on coral reefs (Kleypas, Mcmanus and Menez, 1999; Furnas *et al.*, 2005; D'Angelo and Wiedenmann, 2014). These low nutrient concentrations limit water column productivity and, subsequently, the availability of coral food. Consequently, reef-forming corals rely on a mutually beneficial symbiosis with microscopic dinoflagellates of the family *Symbiodiniaceae* (LaJeunesse *et al.*, 2018) (commonly referred to as zooxanthellae) to access nutrients in their dissolved inorganic forms that are otherwise not accessible to the coral animals (Falkowski *et al.*, 1984, 1993; Davy, Allemand and Weis, 2012; Rädecker *et al.*, 2015; Ferrier-Pagès *et al.*, 2016). The photosynthetic symbionts—which reside in the coral gastrodermis—translocate excess carbohydrates to the coral, in some cases providing > 90% of the host's energetic requirements (Falkowski *et al.*, 1984, 1993). ^{15}N tracer studies have demonstrated the capacity of the symbionts to incorporate NO_3^- and subsequently translocate the labelled N (Grover *et al.*, 2003; Tanaka *et al.*, 2006). Aposymbiotic and non-symbiotic corals are incapable of incorporating dissolved PO_4^{3-}, while in species harbouring zooxanthellae, PO_4^{3-} uptake increases in the light presumably in association with photosynthesis (reviewed in Davy, Allemand and Weis, 2012; Ferrier-Pagès *et al.*, 2016).

The importance of the symbiosis for coral growth is demonstrated by the fact that calcification rates may be up to 4 times higher in the light compared to the dark and these increases coincide with elevated symbiont photosynthesis and host respiration (Furla *et al.*, 2000). However, enhanced zooxanthellae density and photosynthesis associated with nutrient enrichment may occur alongside increases (Koop *et al.*, 2001; Dunn, Sammarco and LaFleur, 2012) or decreases (Fabricius, 2005; Shantz and Burkepile, 2014) in skeletal growth. Nutrient enrichment at skewed N:P ratios can have a detrimental effect on symbiotic corals as the relative oversupply of one nutrient leads to nutrient starvation of zooxanthellae with respect to another (Wiedenmann *et al.*, 2013; Rosset *et al.*, 2017). In particular, N-enrichment without sufficient supply with phosphorus stimulates the unsustainable proliferation of zooxanthellae facilitated by the reallocation of cellular P resources by the symbionts to support vital metabolic processes. This ultimately causes P-starvation of the zooxanthellae, reduces the host's resistance to heat and light induced bleaching and decreases coral biomass (Wiedenmann *et al.*, 2013; Rosset *et al.*, 2017). Contrastingly, the experimental addition of P, along with N, can ameliorate the negative effects of N enrichment alone (Shantz and Burkepile, 2014).

The impact of skewed N:P ratios on polyp size and biomass (Rosset *et al.*, 2017) suggests that skeletal growth may be similarly impacted. We therefore categorised published studies on skeletal growth and structure with a consideration of the N:P stoichiometry experienced by the corals. With this approach, we could resolve some of the major apparent contradictions of previous studies. Notably, the taxonomy of the corals under study seems to be an important determinant in shaping the effect of the nutrient environment on skeletal parameters, with members of the genus *Acropora* responding often differently compared to representatives of several other genera. To test the resulting hypothesis that skewed N:P ratios can alter skeletal growth and micro-structure, we cultured replicate colonies of *Acropora polystoma* associated with *Cladocopium sp.* symbionts under a suite of different nutrient regimes comparing the effects of skewed N:P stoichiometries, nutrient replete and nutrient-limited conditions. The effects on coral growth and symbiont physiology were assessed along with differences in the skeletal microstructure determined by micro-computed tomography (µ-CT).

2.3. Methods and materials

2.3.1. Analysis of published studies

We collated 92 coral responses from 25 papers (Appendix 1) which reported the impacts of seawater nutrient concentrations on the most commonly used skeletal growth metrics: linear extension, calcification and skeletal density. We categorised nutrient enrichment scenarios into three regimes, solely according to the relative molar concentrations of N and P: high nitrogen: low phosphorus (HNLP) where N:P > 35 and low nitrogen: high phosphorus (LNHP) where N:P < 0.5. The corals were considered to be exposed to HNHP or nutrient replete conditions when concentrations of both N and P were higher than the global average (~0.25 ±0.28 µM NO_3^-, ~0.13 ±0.08 µM PO_4^{3-}) (Kleypas, Mcmanus and Menez, 1999) and available at N:P ratios between 0.5 and 35. Importantly, our categorisation of nutrient environments included all species of DIN reported by the original authors. Consequently, where concentrations of NH_3/NH_4^+ were available our quantification of N:P ratios typically exceed the "global average" of Kleypas, Mcmanus and Menez, (1999) who-only considered NO_3^- and PO_4^{3-}. To ensure the most reliable assessment of the literature, all non-significant effects reported by the original authors were categorised alongside reports of no effect as 'No effect'. Thus, any 'Increase' or 'Decrease' reported in our review refers only to statistically significant effects as reported by the authors of the original publication.

2.3.2. Coral husbandry

Coral colonies were cultured in the experimental mesocosm at the National Oceanography Centre, Southampton, UK, which is described in detail in D'Angelo and Wiedenmann, (2012). Temperature (~27 °C) and salinity (~33psu) were maintained at constant levels and a 12-h light/dark cycle at a surface light intensity of ~125 mol m^{-2} s^{-1} was provided by metal halide lamps (Aqualine 10,000, Aqua Medic, Germany). Each experiment used genetically identical replicate colonies (~20–25 mm) from a single parent colony of *A. polystoma* attached to ceramic tiles using epoxy resin. Following fragmentation, corals were allowed to recover for > 3 weeks before being exposed to four dissolved inorganic nutrient treatments that were previously used to simulate nutrient replete and strongly nutrient limited conditions as well as skewed N:P stoichiometry (Rosset *et al.*, 2017). Specifically, the long-term nutrient regimes over the duration of the experiment in the

different experimental system were as follows: high nitrate/high phosphate (HNHP, NO_3^- ~4.5 µM, PO $_4^{3-}$ ~0.6 µM, N:P ~8:1), high nitrate/low phosphate (HNLP, NO-$_3^-$ ~0.073 mM, PO_4^{3-} not detectable (method detection limit = 0.21 µM)), low nitrate/high phosphate (LNHP, NO-$_3^-$ ~0.06 µM PO_4^{3-} ~5.7 µM, N:P ~0.01) and low nitrate/low phosphate (LNLP, NO-$_3^-$ not detectable PO_4^{3-} not detectable).

The terms 'high' and 'low' describe the relative concentrations of NO-$_3^-$ and PO-$_4^{3-}$ in our treatments as detailed previously (Wiedenmann *et al.*, 2013; Rosset *et al.*, 2017). The N and P concentrations of our HNHP treatment are in the range of those found on high nutrient reefs environments at the Galápagos Islands and off the Brazilian coast or in reefs subject to internal wave-driven upwelling (Aston et. al., 2019; Kleypas, Mcmanus and Menez, 1999; Szmant, 2002). Meanwhile, the respective N and P concentrations of the HNLP and LNHP treatments exceed levels observed on unpolluted reefs. The experiment was repeated three times. Corals were not fed during the experiments. Nutrient concentrations were adjusted by the addition of $NaNO_3$ and $NaPO_4^{3-}$ solutions if required, ammonium levels in these systems are constantly low (Wiedenmann *et al.*, 2013). Nitrate in the LNLP conditions was removed continuously from the systems by use of Nitrate reactors (Aqua Medic, Germany). Phosphate in the HNLP and LNLP treatments was removed by filtering the water through RowaPhos Matrix (D-D The Aquarium Solution Ltd, UK). Nutrient concentrations were monitored weekly using the colourimetric detection methods with HACH DR900 Colourimeter (Hach, USA) described in detail in Rosset *et al.* (2017). The positions of corals were regularly alternated in the tanks to minimise any random effects due to light and/or water flow.

2.3.3. Measuring skeletal growth, photosynthetic efficiency, zooxanthellae density and bleaching

Linear extension of the corals along the main axis and side branches was measured using calipers (accuracy ±0.1 mm). The position of the main axial corallite at the start of the experiment was subsequently used to determine the boundary between 'old' and 'new' skeleton. Mass change was determined from wet weight after a defined drip-off period and removal of any non-coral growth from the attachment tile as described in Rosset *et al.* (2017). Since mass gain in *Acroporids* is dominated by the deposition of skeletal material, the terms calcification and mass gain are used inter-changeably hereafter. The maximum

quantum efficiency of PSII photochemistry (Fv/Fm) of zooxanthellae was measured using a submersible pulse amplitude modulated fluorometer (Diving-PAM, Walz, Germany) after > 10 h dark acclimation at minimal background light levels. Zooxanthellae density was determined using a haemocytometer following the removal of the host tissue with a Waterpick® and subsequent separation of host and symbiont fraction by differential centrifugation (Rosset *et al.*, 2017). The visual bleaching response of corals over time was recorded by a single observer using a CoralWatch© colour card, with a decrease in colour score ≥ 2 being considered a bleaching response (Siebeck *et al.*, 2006).

2.3.4. Analysis of skeletal growth using calcein staining

Prior to the 73-d culture, corals were incubated under HNHP conditions in seawater containing calcein (Sigma-Aldrich, Germany) solution at a concentration of ~100 µM for 72 h according to the staining protocols detailed in (E. Tambutté *et al.*, 2011) and Ohno *et al.* (2017). Corals were then soaked twice for 30 min in clean seawater to rinse calcein from the tissue surface and prevent contamination of the experimental mesocosm before being placed into their respective treatment compartments. On completion of the experimental exposure, fragments were first frozen before the tissue was removed using a Waterpick®. Subsequently, the skeletons were washed twice in 10% NaClO (Sigma-Aldrich, Germany) solution for 30 min to remove any residual organic matter before being thoroughly rinsed in MilliQ water (18.2 M ohm cm) and then oven dried. Fragments were then embedded in epoxy resin, cut into 50 µM thick cross-sectional slabs using a slow speed saw and polished using silicon carbide paper. Calcein staining patterns were documented by photographing the thin section under a MZ10 Fluorescent Stereo Micro-scope (LEICA Microsystems, UK), using a Green Fluorescent Protein longpass filter. The fluorescence micrographs were stitched together to cover the full region of interest (ROI). Staining patterns were emphasised by enhancing the red image channel (showing unstained skeleton) and green image channel (showing stained skeleton) using Adobe Photoshop. The blue image channel was set to black.

2.3.5. Micro-CT scanning

Skeletons were cleaned and dried as described above. Scanning was conducted at The University Hospital Southampton, UK (UHS), using the Nikon Med- X (alpha) prototype

(Nikon X-Tek Systems Ltd, UK) and at The Natural History Museum, London, UK (NHM), using a Nikon Metrology HMX ST225 (Nikon Metrology, Tring, UK). Fragments were analysed at UHS using a beam with voltage of 95 kV and 116 A current was generated using a Tungsten reflection target and a 0.25 mm aluminium filter. At the NHM fragments were scanned using a beam with voltage of 100 kV. A 100 A current was generated with a Tungsten reflection target and a 0.5 mm aluminium filter. In both cases, projections were obtained for each sample during a single 360° rotation and each set of radial projections was subsequently reconstructed into a 3-dimensional matrix of isotropic voxels (at a resolution of 11.5 µM for UHS samples and 12.5 µM for NHM samples) using CT Pro 3D v5.

2.3.6. Thickness and porosity of skeletal elements

When analysing differences in skeletal microstructure, we distinguished between 'old' skeleton grown prior to the start of the experimental treatment and 'new' skeleton that grew under controlled treatment conditions. The position of the axial polyp in relation to the base was recorded at the start of each experiment. 'Old skeleton' was defined as the skeleton present below this point at the conclusion of the growth experiment; 'new skeleton' was defined as the skeleton which had formed during the experiment above the original tip of the axial corallite. The skeletal microstructure of *A. polystoma* comprises an axial corallite from which numerous radial corallites diverge. The coenosteum (the skeleton between corallites) is formed from a lattice of interconnected synapticular 'bars" and trabecular "rods" (Gladfelter, 2007; Humblet, Hongo and Sugihara, 2015). The axial and radial corallites comprise a central cavity that contains diminutive septae. When characterising the thickness of the skeletal element, we have not distinguished between these different components in our analysis and from hereon we refer to all skeletal components collectively as 'skeletal elements'.

µ-CT images were analysed using ImageJ (Fiji) version 2.0.0. For each fragment, regions of interest (ROI's) were selected for analysis. ROI's comprised a 0.25 mm thick planar cross section perpendicular to the direction of axial growth. 'Old skeleton' and 'new skeleton' ROI's were located ~0.75 to ~0.50 mm below, and ~0.50 to ~0.75 mm above the original axial corallite tip, respectively (Figure 2.4a). Measurements of mean skeletal thickness, skeletal volume (SV) and total skeletal volume (TV) were obtained using the

BoneJ plugin. Porosity was subsequently calculated as: Porosity (%) = 1- $\frac{SV}{TV}$ × 100. All slices within selected ROI's were measured individually to ensure that an identified artefact of bulk measurement did not influence the absolute measured values. Changes in mean skeletal element thickness and porosity with distance from the corallite tip were determined from measurements of 1-voxel thick slices at 0.25 mm intervals in the upper 9 mm of the fragments from the 100-d culture only. A macro was used to ensure faithful replication of the method for each set of measurements which is available in Appendix 1.

2.3.7. Statistical analysis

Statistical analysis was conducted using R (version 4.0.3). One-way ANOVA and Tukey Honestly Significant Difference tests were used to determine differences between treatments. Where the underlying assumptions regarding equality of variability and normality of distribution were not met, Kruskal–Wallis test was favoured and Dunn's test was employed to determine differences between treatments. Corals analysed using μ-CT images were selected from the 100 and 140 d cultures, respectively. No significant differences were detected between the two datasets (stepwise Welch's t-tests) so data were pooled. The relationship between skeletal element thickness and porosity to distance from the corallite tip were assessed using Pearson's correlation coefficient.

2.4. Results

2.4.1. Analysis of published studies

The reviewed studies encompassed seven different coral genera and a range of nutrient enrichment scenarios including both field and laboratory settings (see Appendix 1). When the responses are grouped disregarding the taxonomy of the studied corals and the type of nutrient enrichment, the only clear trend is a decrease in skeletal density (Figures 2.1a-c). Regarding linear extension and calcification rates, more studies showed no effects or increases than decreased rates. However, when the results of these studies were categorised according to the N:P stoichiometry and coral taxonomy (*Acropora* v other genera), responses of *Acropora* spp. were clearly different (Figures 2.1d-f). Across a range of different settings, nutrient enrichment caused linear extension in *Acropora* spp. to increase

under HNHP conditions but resulted in a decrease or 'no effect' under HNLP conditions. In *Acropora* spp., the impact on calcification was more variable but increases were commonly reported under HNHP conditions. Skewed nutrient ratios were generally associated with 'no effect' or decreases. Under HNHP conditions, the skeletal density of *Acropora* spp. decreased. In contrast, for other genera, linear extension and calcification commonly decreased following nutrient enrichment regardless of N:P stoichiometry, but there was no consistent impact on skeletal density (Figures 2.1g-i). The high number of studies reporting increased linear extension and/or calcification in *Acropora* spp. under HNHP conditions suggests that when the availability of both N and P is elevated, skeletal growth in this genus is enhanced. In contrast, whenever N:P ratios exceed ~72:1, the linear extension and calcification of *Acropora* spp. are more likely to be reduced, suggesting that the relative undersupply of P inhibits skeletal growth.

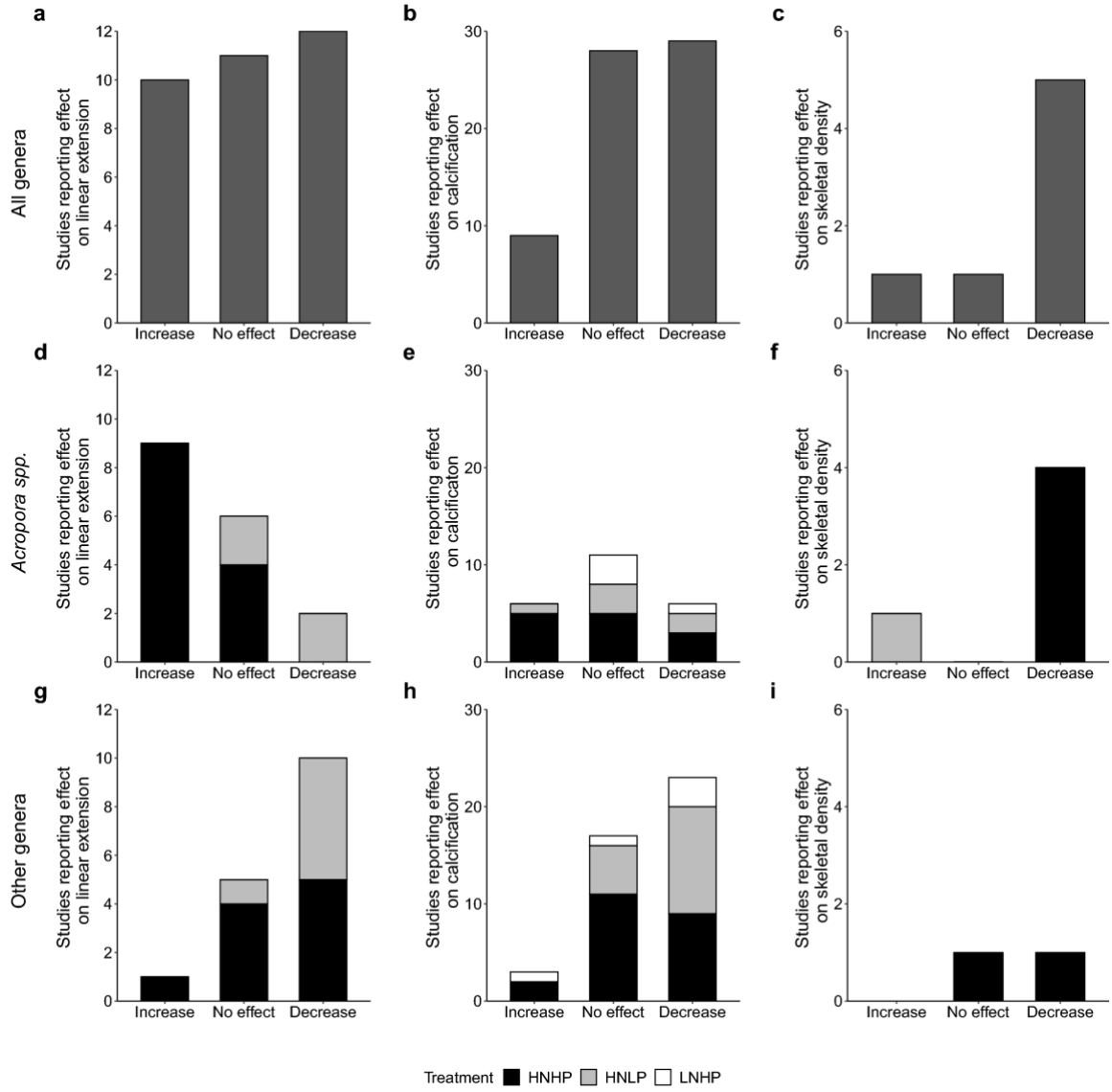

Figure 2.1. Analysis of 25 published research papers covering 92 comparisons (studies) of changes in linear extension, calcification and skeletal density to changes in the dissolved inorganic nutrient environment. a–c) Reported effects from all studies with no distinction between the genus of the studied coral species or the stoichiometry of the nutrient environment. d–f) Reported effects from 33 studies from 8 publications involving 10 species of *Acroporids*. g–i) Reported effects of 6 genera of non-Acropora genera from 59 studies in 23 papers. "Other genera" include *Porites spp., Stylophora spp., Pocillopora spp., Montastrea spp., Montipora spp.* and *Merulina spp.* HNHP = high nitrate: high phosphate (N:P = 0.5–35), HNLP = high nitrate: low phosphate (N:P > 35), LNHP = low nitrate: high phosphate (N:P < 0.5). All increases and decreases to skeletal parameters refer to statistically significant ($p < 0.05$) findings, whereas "no effect" results include increases and decreases deemed non-significant *($p > 0.05$).*

2.4.2. Nutrient effects on *Acropora polystoma* determined in controlled laboratory experiments

2.4.2.1 Effects of nutrient treatments on zooxanthellae density and photosynthetic efficiency

All replicate colonies of *A. polystoma* cultured in the HNHP treatments remained unbleached, while all corals cultured in the HNLP and LNLP treatments bleached. At the conclusion of the 140-d culture experiment, the zooxanthellae density in HNHP corals was ~3 times higher (~1.2 × 10^6cm $^{-2}$) than in those from the LNHP treatment (~0.4 × 10^6cm $^{-2}$) and ~six-fold higher than in corals from the HNLP and LNLP treatments (~0.2 × 10^6 cm^{-2}) *(ANOVA, $F_3 = 100.8$, $p = 0.0003$)* (Figure 2.2a). Fv/Fm was significantly reduced in corals from the HNLP treatment when cultured for 140 *d (ANOVA, $F_{3,8} = 15.4$, $p = 0.001$)* (Figure 2.2b), but corals retained high values of Fv/Fm in the other nutrient treatments.

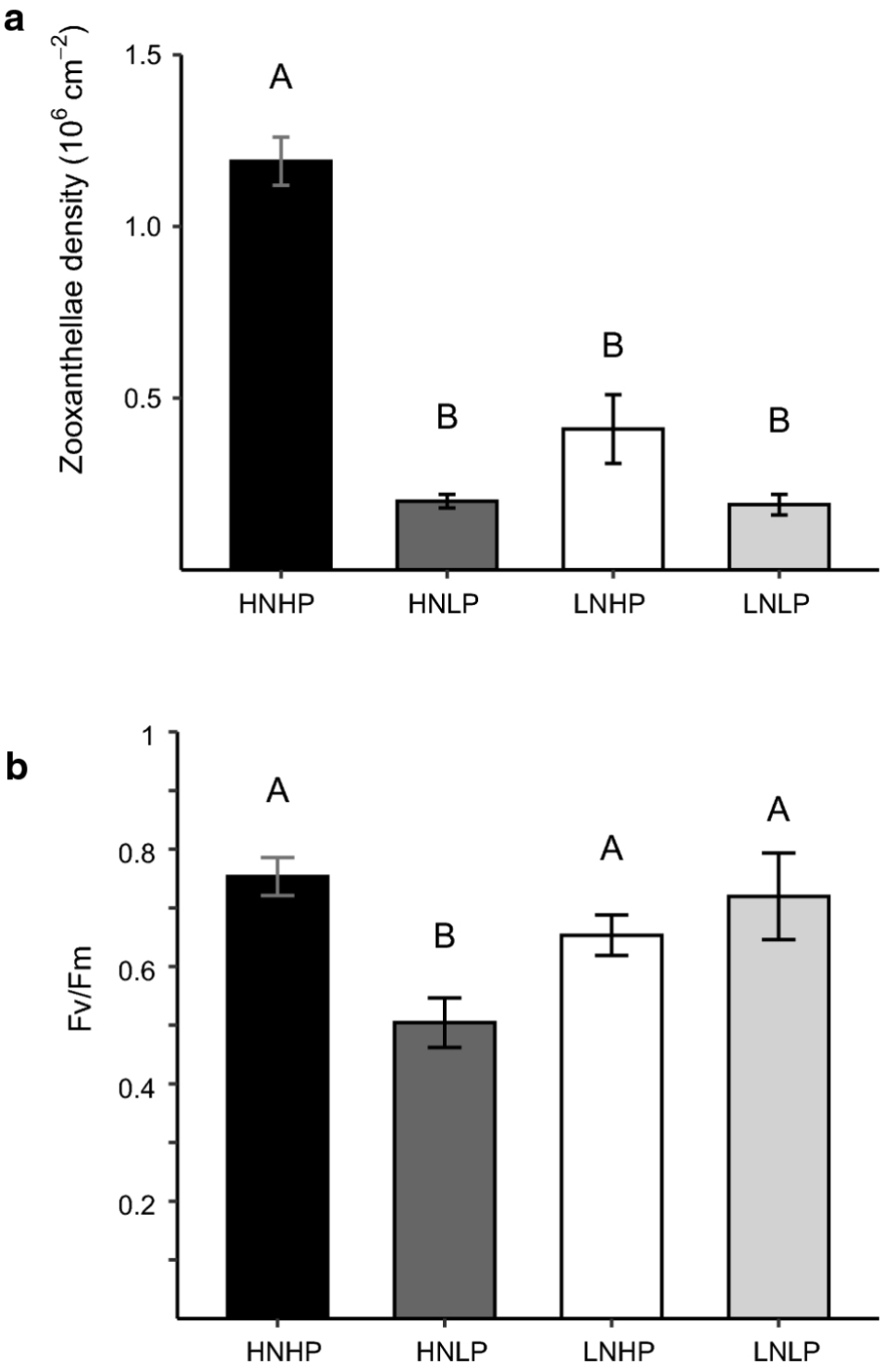

Figure 2.2. Symbiont densities and their photosynthetic efficiency in *A. polystoma* after exposure to different nutrient treatments for 140 days. a) Mean zooxanthellae densities of *A. polystoma* fragments (*ANOVA, p = 0.0003, n = 2*). b) Quantum efficiency of Photosystem II (Fv/Fm) of *A. polystoma* (*ANOVA, p = 0.001, n = 4*). HNHP = high nitrate: high phosphate, HNLP = high nitrate: low phosphate, LNHP = low nitrate: high phosphate and LNLP = low nitrate: low phosphate. Letters above bars indicate significant differences between treatments.

2.4.2.2 Effects of nutrient treatments on skeletal growth

After 140 d, corals cultured in the HNHP treatment extended ~5-times more than those under the other treatments *(ANOVA, $F_{3,12} = 12.18$, $p = 0.0006$)* (Figure 2.3a). Analysis of the calcein stained skeletons confirmed the differences in the skeletal growth between treatments; the extensive formation of 'new' (unstained) skeleton at the tips of the HNHP corallites was largely absent from corals cultured in the HNLP and LNLP treatments (Figure 2.3b). The relationship between linear extension and mass gain was further investigated in a 73-d culture experiment. Linear extension and mass gain of HNHP corals were ~ tenfold and ~ threefold higher, respectively, compared to their counterparts from HNLP and LNLP treatments *(Kruskal–Wallis: linear extension $p = 0.006$, mass gain $p = 0.01$).* Notably, the greater extent to which linear extension was affected relative to mass gain in the HNHP corals can be explained by the fact that linear extension increased at an exponential rate, whereas the mass showed an approximately linear increase (Figures 2.3c and d).

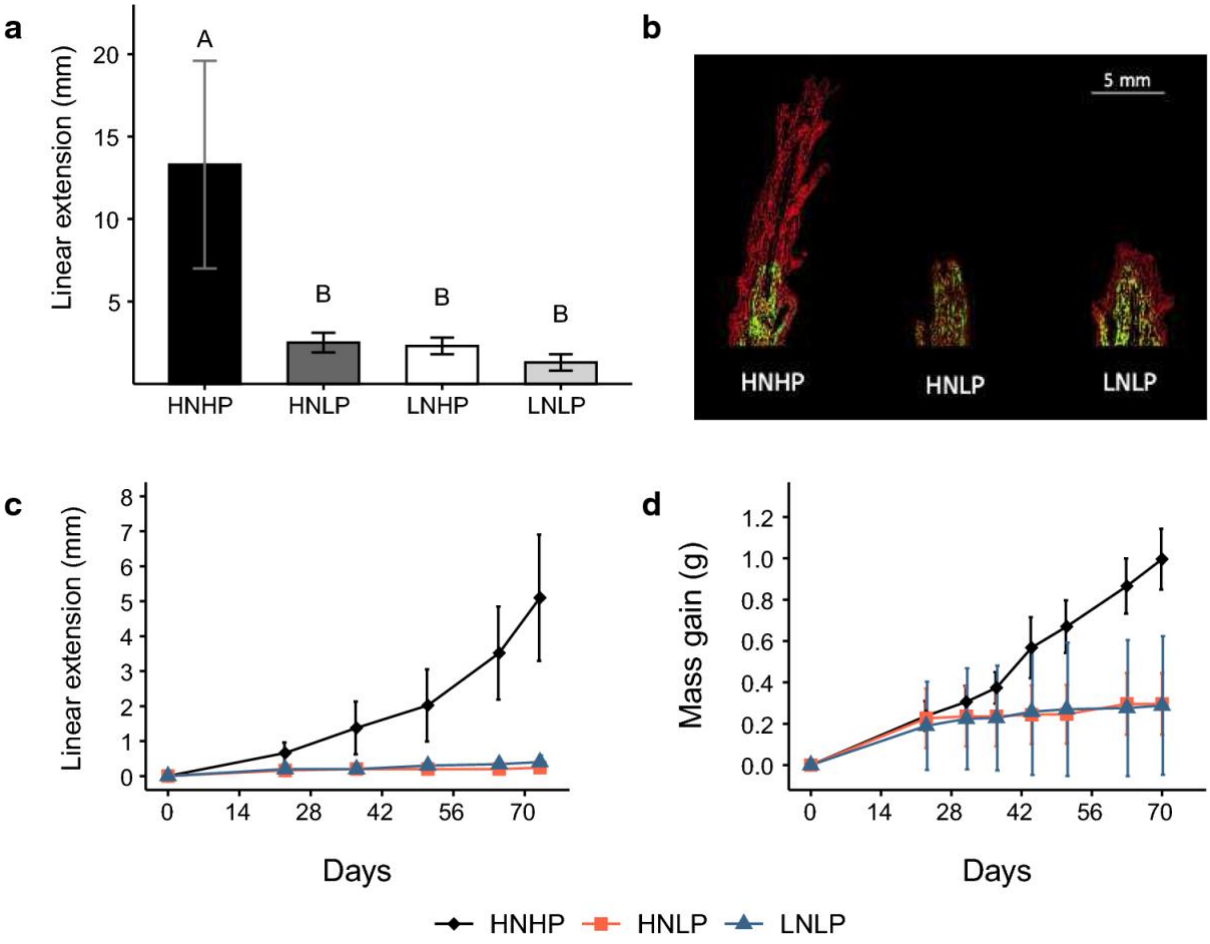

Figure 2.3. Skeletal growth of *A. polystoma* in different nutrient environments. a) Linear extension of *A. polystoma* after 140-d culture *(ANOVA, p = 0.0006, n = 4*). Letters indicate significant differences between treatments. b) Fluorescence micrographs of longitudinal cross sections of calcein-stained *A. polystoma* skeletons imaged with a digital camera fitted to a Leica Mz10 Fluorescent Stereo Microscope using a GFP longpass filter. Calcein stained skeleton highlighted by the green fluorescence. Newly deposited skeleton appears in red. Time course measurements of c) Linear extension (mean ± s.dev.) and d) mass gain (mean ± s.dev.) of *A. polystoma* over 73-d culture in different nutrient environments (*n* = 5). HNHP = high nitrate: high phosphate, HNLP = high nitrate: low phosphate, LNHP = low nitrate: high phosphate and LNLP = low nitrate: low phosphate.

2.4.2.3. Effects of nutrient treatments on skeletal microstructure

The characterisation of the skeletal microstructure by X-ray micro-tomography and subsequent analysis of the resultant reconstructed 3D image files revealed a mean thickness of skeletal elements which ranged from ~30 to ~90 µm between treatments. There were statistically significant differences in mean skeletal element thickness between treatments in both 'old' *(ANOVA, $F_{3,36} = 4.627$, $p = 0.008$)* and 'new' skeleton *(Kruskal–Wallis, $p = 0.006$)* (Figures 2.4b, 2.5a and 2.5b) The thinnest skeletal elements were observed in HNHP corals while significant thickening was observed in both the 'old' and

'new' skeleton of nutrient-limited (LNLP) corals. There was also significant thickening in the 'old' skeleton of HNLP corals while those cultured in the LNHP treatment had skeletal elements of intermediate thickness. Significant differences were also found for porosity in both 'old' *(ANOVA, $F_{3,36} = 12.4$, $p << 0.01$)* and 'new' skeleton *(ANOVA, $F_{3,28} = 5.175$, $p = 0.006$)*. Porosity ranged between 41 and 67% across the treatments, being highest in HNHP corals and lowest in those from the LNLP treatment (Figures 2.5c and d). Porosity was significantly reduced in the 'old' skeleton of HNLP corals and took intermediate values in LNHP skeletons. Across treatments, skeletal element thickness and porosity were found to be inversely related in both the 'old' *($r^2 = 0.39$, $p << 0.001$)* and 'new' skeleton *($r^2 = 0.46$, $p << 0.001$)* (Appendix 1, SM Fig 1). In corals from the HNHP treatment, mean skeletal element thickness was found to be positively correlated *($r^2 = 0.43$, $p << 0.0001$)* to distance from the tip of the axial corallite while in corals from the other treatments, this positive correlation was absent. Under HNHP conditions, corals showed linear extension and associated mass gain at all time points of the experiments (Figure 2.6). The exponential fit of the data points suggests that relatively less mass was gained for a given unit of extension when linear extension rates were high. Contrarily, under HNLP and LNLP conditions, mass gain became largely decoupled from linear extension at later stages of the experiment.

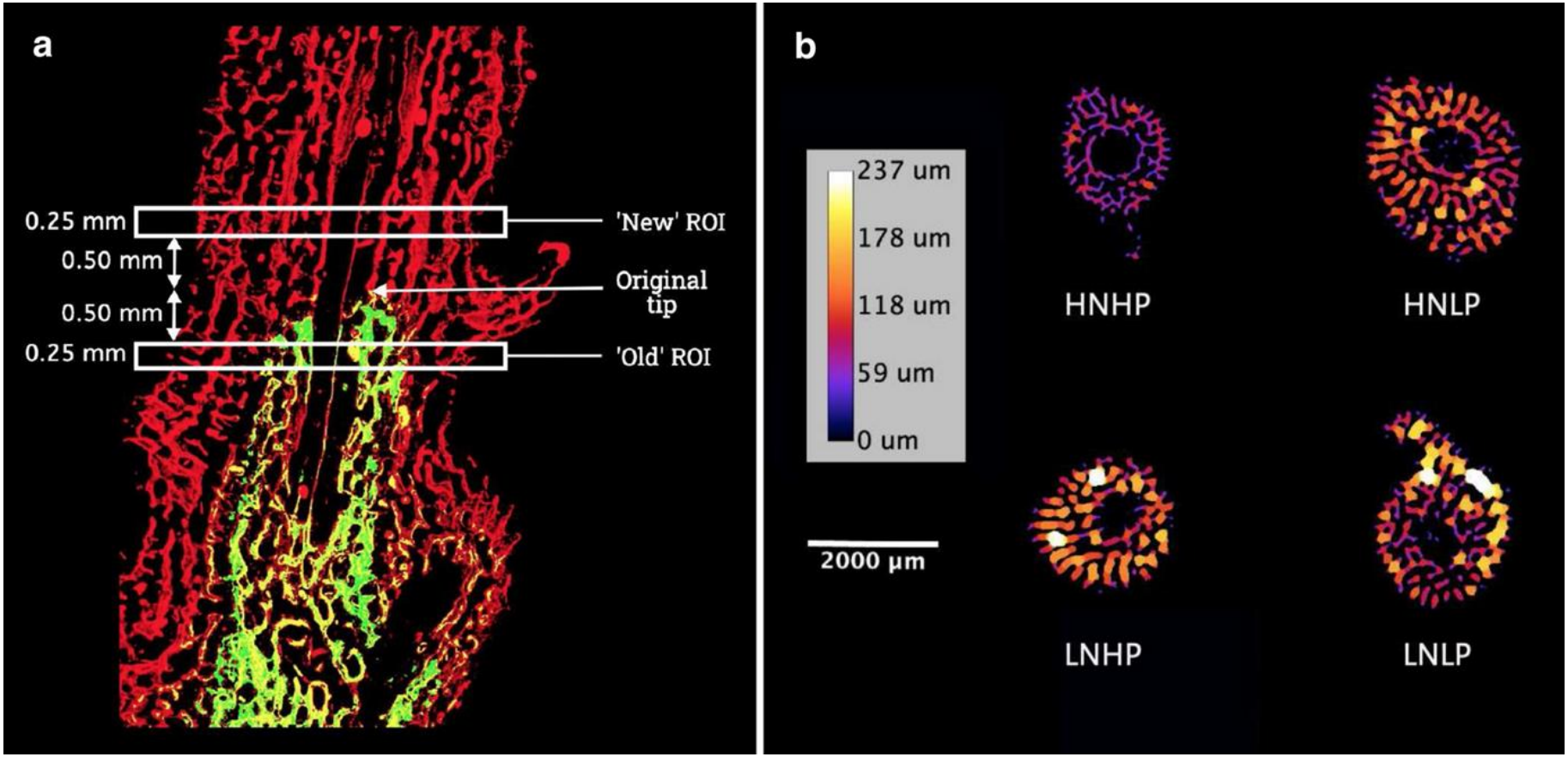

Figure 2.4. Skeletal microstructure of *A. polystoma* from different nutrient environments. a) Fluorescence micrograph of longitudinal cross sections of calcein stained *A. polystoma* skeletons imaged with a digital camera fitted to a Leica Mz10 Fluorescent Stereo Microscope using a GFP longpass filter. Calcein stained skeleton appears green and newly deposited skeleton appears red. The selection of regions of interest (ROI's) with respect to the original tip of the corallite is indicated. B) Heatmaps generated from representative latitudinal cross-sectional µ-CT scan images of *A. polystoma.* Differences in colour represent variation in the skeletal element thickness. HNHP = high nitrate: high phosphate, HNLP = high nitrate: low phosphate, LNHP = low nitrate: high phosphate and LNLP = low nitrate: low phosphate.

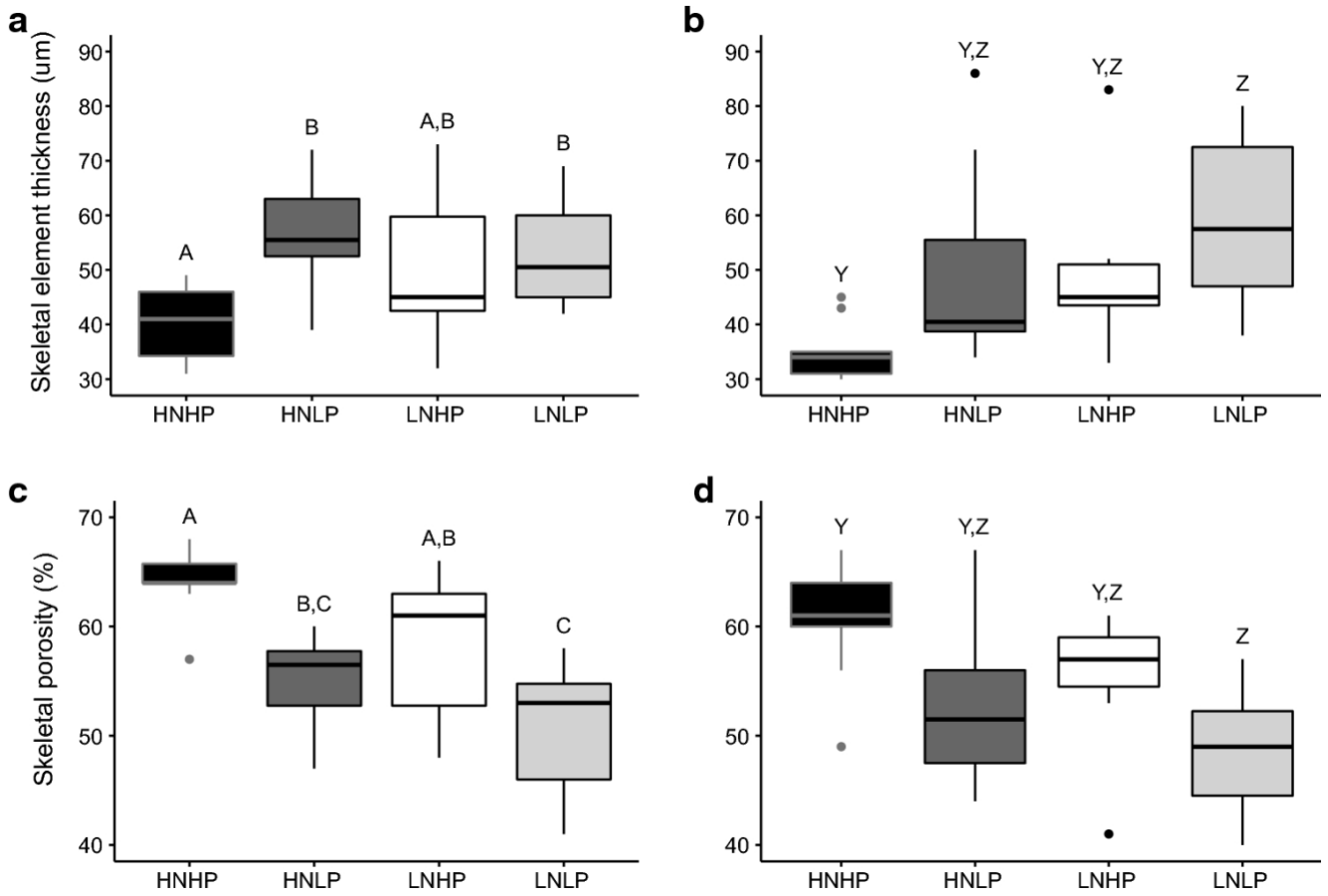

Figure 2.5. Quantitative analysis of skeletal microstructure of *A. polystoma* after culture in different nutrient environments. Mean skeletal element thickness of a) 'old' skeleton *(ANOVA, p = 0.008, n = 10)* and b) 'new' skeleton *(Kruskal–Wallis, p = 0.006, n = 10).* Mean skeletal porosity for c) 'old' *(ANOVA, p < < 0.01, n = 10)* and d) 'new' *(ANOVA, p = 0.006, n = 10)* skeleton. Measurements cover ~0.25 mm thick regions of interest perpendicular to the skeletal axis. In 'old' skeleton, the ROI is located 0.75 to 0.50 mm below the top end of the original axial corallite, and in 'new' skeleton, it is located ~0.50 to 0.75 mm above the top end of the original axial corallite. Letters indicate significant differences between treatments. HNHP = high nitrate: high phosphate, HNLP = high nitrate: low phosphate and LNLP = low nitrate: low phosphate

2.5. Discussion

Recent studies have demonstrated the sensitivity of zooxanthellate corals to skewed stoichiometries of dissolved inorganic nitrogen and phosphorus (Wiedenmann *et al.*, 2013; D'Angelo and Wiedenmann, 2014; Rosset *et al.*, 2017). When nutrient availability remains replete with respect to both N and P, corals can sustain high symbiont densities that show high Fv/Fm values and support an increased coral tissue biomass. Some corals can withstand strong nitrogen limitation that results from phosphate enrichment with low N:P ratios, exhibiting minimal loss of symbionts, Fv/Fm and tissue mass (Rosset *et al.*, 2017). In contrast, at high N:P ratios, the relative undersupply of phosphate leads to P-starvation of the symbionts, resulting in malfunctioning of the photosynthetic apparatus, reduced Fv/Fm and bleaching even under moderate temperature/light conditions. In their bleached appearance and reduced polyp biomass, these P-starved corals resemble those exposed to conditions in which both N and P are strongly limiting. However, in the latter case, the photosynthetic machinery of the symbionts is usually less affected and Fv/Fm values tend to stay high (Wiedenmann *et al.*, 2013; D'Angelo and Wiedenmann, 2014; Rosset *et al.*, 2017).

The observations that corals can either respond by increasing or decreasing rates of linear extension and calcification in response to elevated concentrations of dissolved inorganic nutrients led to the notion that effects of nutrient enrichment are largely unpredictable and the involved physiological mechanisms are poorly understood (Szmant, 2002). We show that it is possible to resolve some of the apparent contradictions among published studies by categorising the findings of previous studies according to the taxonomic background of the experimental corals and the N:P stoichiometry of the treatment. When the published results are grouped under these constraints, *Acropora spp.* show a clear trend to respond with increased linear growth and reduced skeletal density to replete supply with N and P. In contrast, under skewed nutrient stoichiometries with high N:P ratios, growth is inhibited and skeletal density is increased. In the other genera analysed in the published studies (*Porites* spp., *Stylophora* spp., *Pocillopora* spp., *Montastrea* spp., *Montipora* spp. *Merulina* spp.), growth tends to be also inhibited by nutrient enrichment at high N:P ratios, but also combined nitrogen and phosphate enrichment caused a lower linear extension and calcification rates in a comparable number of cases. To verify the effects of skewed N:P stoichiometries on the growth and skeletal structure of *Acropora* spp., we assessed the

response of *A. polystoma* to nutrient replete conditions (HNHP), strong nutrient limitation (LNLP) and the oversupply of nitrate (HNLP) and phosphate (LNHP).

Replicate fragments of *A. polystoma* exposed to HNHP conditions maintained high zooxanthellae densities with high Fv/Fm values. In contrast, corals exposed to HNLP conditions showed the distinctive symptoms of P-starvation, namely a bleached appearance associated with decreased zooxanthellae density and reduced Fv/Fm (Wiedenmann *et al.*, 2013; Rosset *et al.*, 2017). LNLP conditions also caused a reduction in symbiont numbers, but their Fv/Fm values were not affected, suggesting that symbiont photosynthesis remained functional despite the strong nutrient limitation (D'Angelo and Wiedenmann, 2014). Corals from the LNHP treatment lost less symbionts whilst retaining high Fv/Fm values, suggesting that *A. polystoma* and its symbionts are better adapted to withstand low, rather than high N:P ratios.

The results of the present study show that nitrogen enrichment at low phosphate concentrations (HNLP treatment) and the resulting phosphate starvation (Wiedenmann *et al.*, 2013; Rosset *et al.*, 2017) also has profound impacts on the skeletal growth and microstructure of *A. polystoma.* Notably, nutrient enrichment at high N:P ratios has comparable effects on the skeleton as strong nutrient limitation (LNLP treatment). Specifically, linear extension and calcification are inhibited and skeletal elements thicken, leading to reduced porosity and increased density of the skeletal microstructure. The contrasted responses between the HNHP and LNLP treatments demonstrate that enrichment of both NO_3^- and PO_4^{3-} stimulates linear extension and, accordingly, calcification if both N and P are provided in sufficient amounts and in a balanced stoichiometry that does neither result in N nor P limitation or starvation. At the same time, this type of nutrient enrichment results in the formation of thinner skeletal elements and increases skeletal porosity while strong nutrient limitation has the opposite effect. An inverse correlation between extension rate and skeletal density is considered a general relationship also in several other coral species (for review see Szmant, 2002). The less pronounced modification of the skeletal microstructure observed under LNHP conditions corresponds with a less severe impact of this nutrient treatment on the coral-zooxanthellae symbiosis. This observation suggests that changes to the skeletal growth and microstructure reflect the functioning of the symbiosis. The findings of the experimental study are consistent with our evaluation of the literature and the most parsimonious

explanation is that *Acropora* spp. are adapted to exploit modest, and balanced N and P enrichment by increasing linear extension rates with the trade-off of a more porous skeleton. In contrast, under high N:P ratios, the zooxanthellae are affected by P -starvation, the coral becomes susceptible to bleaching and growth rates are reduced. The calcification rate seems less affected as deduced from the continued gain in coral weight (Figure 2.6) so skeletal elements thicken even under these conditions. This differential response of growth and calcification to nutrient limitation can also explain the thickening of the skeletal elements under the LNHP and LNLP conditions. The greater resistance to symbiont loss under low N:P ratios likely reflects the fact that nitrogen is most commonly the limiting nutrient on coral reefs (Kleypas, Mcmanus and Menez, 1999; Furnas *et al.*, 2005; D'Angelo and Wiedenmann, 2014) and that *Acropora* spp. and their symbionts have evolved to cope with these conditions. Natural nitrate: phosphate ratios in coral reef waters are typically ≤12:1, although this encompasses considerable spatial and temporal variability. Amongst the reviewed literature, a maximum "natural" N:P ratio of ~33:1, for instance, was recorded due to nutrient enrichment through seabird guano (Savage, 2019). HNLP conditions with a N:P ratio of up to 74:1 have been reported for anthropogenically disturbed reefs, for instance in Brazil (Szmant, 2002), Jamaica (Lapointe, 1997) and Barbados and have been linked to the inhibition of skeletal growth in some non-*Acroporid* species (Spencer Davies, 1990). The importance of considering all dissolved inorganic nitrogen species was demonstrated during the ENCORE experiments when the experimental addition of NH_4^+, resulting in N:P ratios > 70, suppressed the skeletal growth of *Acroporids*, while enrichment at more balanced ratios promoted linear extension (Koop *et al.*, 2001). Critically, a recent study shows that N:P ratios of macroalgae in the Belize Barrier Reef increased from ~30:1 in the 1980s to 70:1, indicating that a skewed N:P stoichiometry coincided with dramatic reductions in live coral cover (Lapointe, Tewfik and Phillips, 2021). Also, Lapointe *et al.* (2019) linked coral reef decline at Looe Key, Florida to an increase in N:P from 9.5 to 26.5. Our findings, alongside those of previous studies (Wiedenmann *et al.*, 2013; Rosset *et al.*, 2017), have identified a physiological mechanism to explain such detrimental effects on reef building corals. While the N:P stoichiometry undoubtedly plays a critical role in the nutrient physiology of symbiotic reef corals, it is important to consider also the absolute concentrations. When phosphate values in the water range around 0.3 μM, the N:P ratio seems to become less critical and the corals are likely to respond in the same way as to nutrient replete (HNHP) conditions (Rosset *et al.*, 2017). Also, at low N concentrations < 0.7 μM in water, the impact of high N:P ratio becomes

less pronounced and corals are more likely to show a strongly nutrient-limited than a phosphorus-starved phenotype (Rosset *et al.*, 2017). Accordingly, there is a continued need for long- term data series of nutrient values in reef environments measured at sufficient frequency using suitable analytical methods with appropriate minimum detection limits (Lapointe, Tewfik and Phillips, 2021).

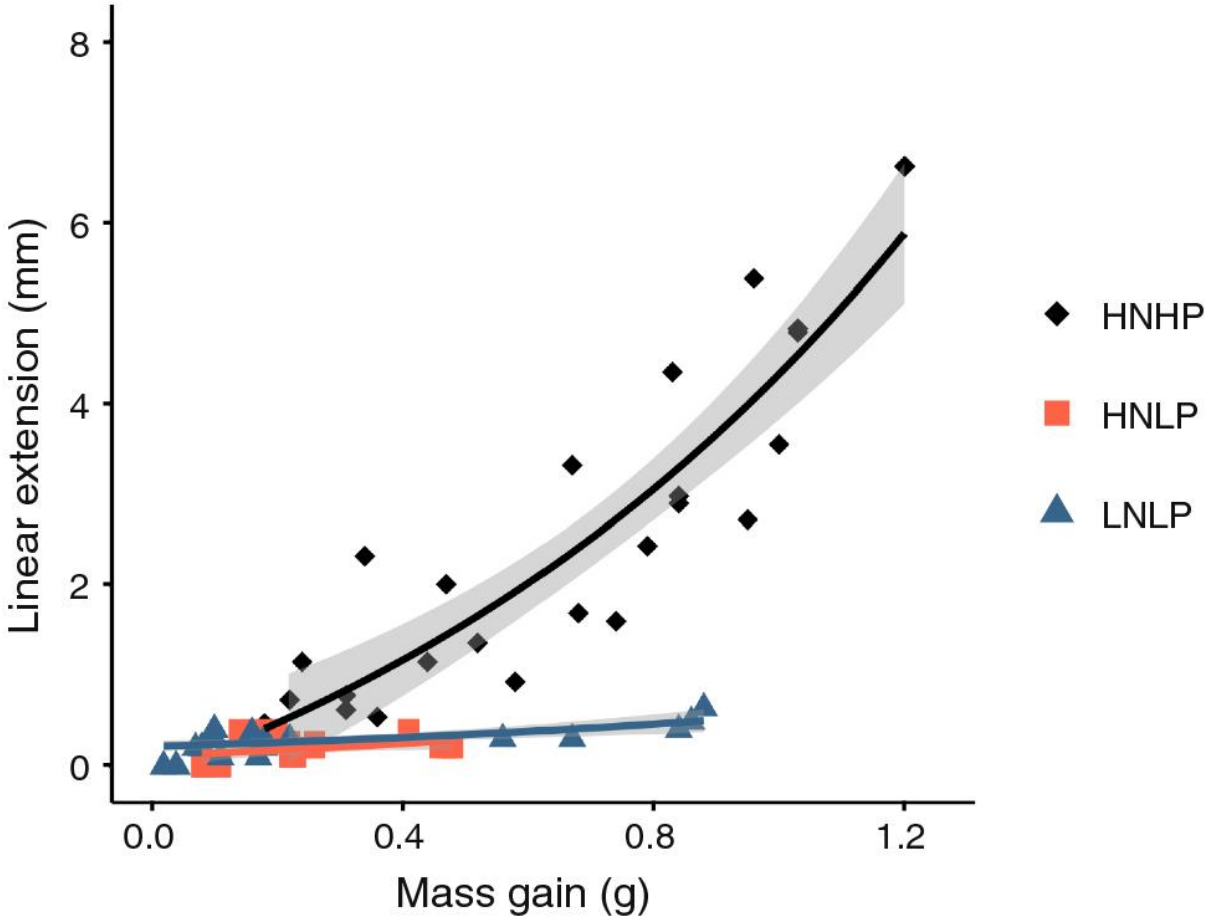

Figure 2.6. The relationship between mass gain and linear extension for *A. polystoma* cultured under three nutrient environments for a total of 73 d *(n = 5).* Each data point represents the linear extension and mass gain of an individual fragment at a particular time point during the culture. Data were fitted using an exponential function. The grey shading represents the 95% confidence interval for each nutrient environment. HNHP = high nitrate: high phosphate, HNLP = high nitrate: low phosphate and LNLP = low nitrate: low phosphate.

Acroporids are important framework builders and enhance the 3-dimensional complexity of reefs, thereby supporting high levels of biodiversity and productivity. Enhanced growth rates, as observed under HNHP nutrient enrichment, may enhance the rugosity of the reef. However, since *Acroporids* are particularly prone to breakage (Bright *et al.*, 2016;

Puotinen *et al.*, 2020), the high skeletal porosity associated with nutrient-fuelled fast growth will likely increase their fragmentation potential (Chamberlain, 1978; Marshall, 2000). While this may promote asexual propagation through resettled fragments and promote the rapid regeneration of parent colonies (Shinn, 1976; Lirman, 2000), frequent fragmentation may lead to a loss of genetic diversity in the population while increasing the susceptibility to specific types of predation, disease and subsequent mortality (Wallace, 1985; Lirman, 2000; Bright *et al.*, 2016). Taken together, chronic nutrient enrichment, specifically with high N:P ratios, may shift the accretion/erosion balance of reefs towards net erosion, similar to the bleaching-induced inhibition of coral growth (Lange and Perry, 2019; Perry *et al.*, 2020). The consequent loss of rugosity may negatively affect ecosystem services such as fisheries, tourism income and coastal protection.

Finally, diagnostic features in the skeletal microstructure of *Acroporids* may be useful for interpreting the nutrient environment under which skeletons formed. Spatial variability in the density of massive coral skeletons is commonly used to identify patterns of seasonal growth and to date stress events (Fowell *et al.*, 2016; DeCarlo and Cohen, 2017) but is yet to be employed as a reliable environmental proxy in *Acroporids*. Positive correlations between skeletal thickness and porosity and distance from the axial corallite have previously been reported for other *Acropora spp.* (Gladfelter, 1982; Roche *et al.*, 2011). In fragments from the HNHP treatment, mean skeletal element thickness was positively correlated with distance from the axial corallite tip but this relationship was absent in fragments from the other treatments. Therefore, longitudinal density profiles may prove useful as indicators of elevated nutrient concentrations, especially if used in combination with biogeochemical markers such as skeletal $\delta^{13}C$:$\delta^{18}O$ and/or P/Ca ratios which can be used to infer photosynthesis rates and seawater phosphate concentrations, respectively (McConnaughey, 1989b; LaVigne *et al.*, 2010).

In summary, we show that the taxonomy of the corals, the N:P ratio of their dissolved inorganic nutrient environment and the P-starvation concept should be considered to resolve apparent contradictions among the published scientific literature. Underpinned by experimental evidence, our findings contribute to an improved understanding of the responses of symbiotic reef corals to changes in their nutrient environment, paving the way towards knowledge-based management of the nutrient environment in coral reefs. Specifically, our results suggest that the reef community structure and the nature of

nutrient enrichment should both be considered when managing regional water quality to promote the resilience of corals to the impact of global climate change.

Chapter 3 - Chronic nutrient limitation and skewed nitrogen: phosphorus (N:P) stoichiometries modify corallite size and structure in the zooxanthellate coral *Euphyllia paradivisa*

3.1. Abstract

Nutrient stress arising from severe nutrient limitation or skewed nitrogen (N): phosphorus (P) ratios may cause bleaching in zooxanthellate corals, resulting in thickening of skeletal elements and reduced skeletal porosity. Skeletal elements within, and peripheral to corallites may also thicken during thermal-stress bleaching episodes or periods of seasonally reduced growth rates, but it is unclear whether nutrient stress has a similar impact on these skeletal elements. Replicates of *Euphyllia paradivisa* have previously been subjected to long-term exposure (≥ 6 months or ≥ 1.5 years) to four nutrient treatments as part of two published projects (Rosset, D'Angelo and Wiedenmann, 2015; Rosset *et al.*, 2017) - high nitrate: high phosphate (HNHP), high nitrate: low phosphate (HNLP), low nitrate: high phosphate (LNHP) and low nitrate: low phosphate (LNLP). Two host responses were observed; HNHP and LNHP corals retained an unbleached appearance and large polyp volumes, while HNLP and LNLP corals bleached and had decreased polyp volume. In corals cultured under HNLP conditions the zooxanthellae showed distinctive symptoms of P-starvation. However, the impacts of the different nutrient treatments on the coral skeletons were not studied. Therefore, the macro- and micro-scale features of the corallites from these corals were analysed using image analysis software and micro-computed tomography (μ-CT). HNHP and LNHP corallites were similar in size but LNHP corallites could be distinguished by their reduced circularity and uniformly thickened theca and septa that retained a normal thickness versus depth profile. Contrastingly, in HNLP and LNLP corals polyp volume loss led to smaller corallite sizes, the formation of shallower endo-thecal dissepiments and the homogenisation of skeletal element thickness throughout the depth of the corallite. These responses were strongest in HNLP corallites, which also had thinner skeletal elements and were characterised by a discontinuity between the corallite and the supporting branch that accommodated an abrupt decrease in corallite size. Improved knowledge of structural modifications to the corallite that occur during nutrient-stress may inform the proxy use of skeletal microstructure for investigating seasonal and episodic environmental conditions.

3.2. Introduction

The partial reliance of hermatypic corals on their algal symbionts (zooxanthellae) to access dissolved inorganic nutrients can make them sensitive to changes to seawater nitrogen (N) and phosphorus (P) concentrations. Modest increases in N and P may have some positive direct impacts on corals, including higher zooxanthellae densities, higher rates of coral growth and increased resistance to seasonal bleaching (Fabricius, 2005; D'Angelo and Wiedenmann, 2014). However, at higher concentrations these benefits are commonly outweighed by indirect impacts such as increased competition from macro-algae, and increased prevalence of disease and corallivores that threaten the survival of reef communities in their original states (Jompa and McCook, 2002; Brodie *et al.*, 2005; D'Angelo and Wiedenmann, 2014; Thurber *et al.*, 2014). Furthermore, if the nutrient environment becomes stoichiometrically imbalanced and results in the relative undersupply of an essential nutrient, it can have direct negative impacts on the coral holobiont (Shick *et al.*, 2011; Wiedenmann *et al.*, 2013; D'Angelo and Wiedenmann, 2014). In particular, P-starvation of zooxanthellae arising from high seawater N:P ratios may lead to breakdown of the symbiosis, enhanced bleaching susceptibility and polyps with reduced biomass (Wiedenmann *et al.*, 2013; D'Angelo and Wiedenmann, 2014; Rosset *et al.*, 2017). A number of studies have shown that changes to seawater nutrient concentrations and skewed N:P ratios can also impact skeletal growth rates and alter the density and/or thickness of coral skeletons (Koop *et al.*, 2001; Shantz and Burkepile, 2014; Buckingham *et al.*, 2022). However, studies examining the impacts of nutrients on coral skeletons tend to focus at the colony level on massive and arborescent branching species, and the impact of nutrient conditions at the level of individual corallites has been neglected. This is important because the formation and thickness of skeletal elements associated with the corallite are also known to vary with environmental conditions, and this has led to the recognition of the coral skeletal microstructure as a potential proxy for investigating climate. For example, thickened dissepiments and theca, as well as more tightly spaced dissepiments have been shown to contribute to bands of high density in the skeletons of massive corals (DeCarlo and Cohen, 2017; Fouke, Trop and Sivaguru, 2021). Alternating bands of high- and low-density in coral skeletons form during alternating periods of slow and fast extension rates respectively, and have been identified as proxies for seasonal fluctuations in sea surface temperature (SST) and/or nutrient availability; meanwhile high density 'stress bands' may form during thermal-stress mediated bleaching

events (Peirano *et al.*, 2005; Dávalos-Dehullu, Hernández-Arana and Carricart-Ganivet, 2008; DeCarlo and Cohen, 2017; Barkley *et al.*, 2018; Fouke, Trop and Sivaguru, 2021). Despite the fact that both thermal and nutrient-stress can impact the structural properties and growth of coral skeletons, there are no studies in the literature that specifically report the impacts of nutrient-stress on skeletal elements associated with the corallite. Furthermore, it is unclear to what extent the impacts of thermal-stress bleaching on skeletal element thickness might be replicated by nutrient-stress mediated bleaching. A more complete understanding of how corallite structures can be impacted by changes to the seawater nutrient environment is required to better constrain or calibrate the proxy use of coral skeletons. This is especially important given the predominant roles played by both global warming and nutrient pollution in driving the decline of coral reef ecosystems.

The sensitivity of hermatypic corals to seawater nutrient concentrations derives from their symbiosis with algal dinoflagellates of the family *Symbiodiniaceae* (LaJeunesse *et al.*, 2018) – commonly referred to as zooxanthellae – which are hosted in the coral's gastrodermis. The mean global concentrations of nitrate (NO_3^- ~ 0.25 $\pm$ 0.28 μM) and phosphate (PO_4^{3-} ~ 0.13 $\pm$ 0.08 μM) on coral reefs are sufficiently low that most coral reefs are considered oligotrophic and N-limited (Kleypas, Mcmanus and Menez, 1999; D'Angelo and Wiedenmann, 2014). Consequently, seawater primary production and the availability of zooplankton prey is low, a problem that zooxanthellate corals overcome by exploiting the plant-like characteristics of their photosynthetic endosymbionts. Unlike their animal hosts, zooxanthellae have the necessary cellular toolkit required to isolate and assimilate N from NO_3^- and nitrite (NO_2^-). But, the endosymbionts reside in specialised compartments called symbiosomes and all nutrients they have access to must first pass through host tissue (Yellowlees, Rees and Leggat, 2008). It has been suggested that the coral limits ammonium (NH_4^+) availability in the symbiosome to exert N-limitation on the zooxanthellae; this limits zooxanthellae protein synthesis thereby restricting the specific growth rate of the symbionts (Muscatine *et al.*, 1989; Falkowski *et al.*, 1993; Yellowlees, Rees and Leggat, 2008). Under such conditions, the photosynthesising zooxanthellae produce carbohydrates in excess of their own cellular requirements and much of this surplus is translocated to the coral, providing up to 90% of the host's energetic requirements (Falkowski *et al.*, 1984, 1993). This process is further promoted by the host which produces compounds collectively referred to as 'host release factors' that increase the rate of carbohydrate excretion by the zooxanthellae (Muscatine, Pool and Cernichiari,

1972; Sutton and Hoegh-Guldberg, 1990). The zooxanthellae also provide a means by which the host can access N from dissolved NO_3^- and NO_2^-, but the symbionts typically derive a greater benefit than the host at higher concentrations of these dissolved inorganic nitrogen (DIN) species (Grover *et al.*, 2003). Studies using labelled stable isotopes have demonstrated that zooxanthellae translocate ^{15}N to the host following $^{15}NO_3^-$ enrichment of the culture medium, but that the $\%^{15}N$ increase in the symbiont is ~10 times higher than it is in host tissue (Grover *et al.*, 2003; Tanaka *et al.*, 2006). Zooxanthellae density often increases following nitrate enrichment suggesting that the host is unable to control N-availability and symbiont growth under higher seawater NO_3^- concentrations (Marubini and Davies, 1996; Koop *et al.*, 2001; Wiedenmann *et al.*, 2013; Shantz and Burkepile, 2014). Although this can result in increases to cellular N and carbon (C) content in both the symbiont and the host (Grover *et al.*, 2003), proportionally less photosynthetically derived carbohydrates per cell are translocated to the coral under such conditions (Falkowski *et al.*, 1993). Meanwhile, the uptake of PO_4^{3-} - which does not occur in azooxanthellate or aposymbiotic corals - increases with photosynthesis under high light conditions in zooxanthellate corals, suggesting an active role of the symbionts in phosphorus acquisition (reviewed in Davy, Allemand and Weis, 2012). Phosphate enrichment has been shown to increase zooxanthellae density and coral growth in some experiments but not others (Muscatine *et al.*, 1989; Stambler *et al.*, 1991; Koop *et al.*, 2001) implying that phosphate acquired by zooxanthellae can be translocated to the host, although the mechanism by which PO_4^{3-} uptake occurs is poorly understood (Ferrier-Pagès *et al.*, 2016).

The sensitivity of zooxanthellate corals to environmental change extends to their skeletal structures, allowing their proxy use to aid climate reconstructions. For example, high density stress bands in *Porites spp.* from the central equatorial Pacific have been temporally resolved against the region's thermally induced mass bleaching events (Barkley *et al.*, 2018). But, bleaching in corals can also occur as a consequence of nutrient stress (Wiedenmann *et al.*, 2013; Rosset *et al.*, 2017), and may be recorded in the skeleton as changes to extension rates, skeletal element thickness and porosity (Buckingham *et al.*, 2022). Meanwhile, nutrient enrichment may lead to increases (Koop *et al.*, 2001; Dunn, Sammarco and LaFleur, 2012) or decreases (Fabricius, 2005; Shantz and Burkepile, 2014) in coral skeletal growth rates. A recent review of previous studies, supported by experimental findings showed that in *Acropora spp.* the skeletal growth response to nutrient enrichment depends on the resultant stoichiometry of seawater with respect to N

and P (Buckingham *et al.*, 2022). When nutrient enrichment occurs such that seawater N:P ratios are balanced (between 0.5:1 and 35:1), linear extension and calcification rates increase and skeletal element thickness is reduced. Conversely, when N:P ratios exceed 35:1 or when nutrient limitation is severe (N and P concentrations are both lower than the experimental limit of detection), linear extension and calcification rates decrease and skeletal element thickness increases. At N:P ratios < 0.5:1 linear extension decreases but skeletal density is not significantly impacted. This less severe response is attributable to the retention of high zooxanthellae densities in some corals under low nitrate: high phosphate conditions, a response shared with the corals exposed to balanced N:P ratios (Buckingham *et al.*, 2022). The skeletal growth response in *Acroporids* to nutrient enrichment is apparently more sensitive to N:P stoichiometry than other coral genera (Buckingham *et al.*, 2022). But, negative physiological impacts have also been reported in non-*Acroporid* species in response to high N:P ratios (Wiedenmann *et al.*, 2013; Rosset *et al.*, 2017).

The importance of seawater N:P stoichiometry to zooxanthellate corals has previously been highlighted by a series of experiments conducted in the experimental mesocosm at The National Oceanography Centre, University of Southampton (Wiedenmann *et al.*, 2013; Rosset, D'Angelo and Wiedenmann, 2015; Rosset *et al.*, 2017). After 5 weeks of exposure to high nitrate/ ambient phosphate (HN/AP) conditions, the zooxanthellae density in fragments of *Montipora foliosa* increased significantly; but, the symbionts exhibited reduced fluorescence-based maximum quantum yield of photosystem II photochemistry (Fv/Fm) and increased cellular concentrations of sulphoquinovosyldiacylglycerol (SQDG), responses indicative of P-starvation (Wiedenmann *et al.*, 2013). Despite the initial increase to their symbiont densities these corals were found to have increased susceptibility to bleaching under light and/or thermal stress (Wiedenmann *et al.*, 2013). Follow-up studies using *Euphyllia paradivisa* indicated that exposure to high nitrate: low phosphate (HNLP) conditions produced a coral phenotype similar to that observed under severe nutrient limitation (low nitrate: low phosphate, LNLP), specifically bleaching occurred even under ambient temperature and light conditions and was associated with significantly reduced polyp size (Rosset, D'Angelo and Wiedenmann, 2015; Rosset *et al.*, 2017). Meanwhile, corals exposed to nutrient replete conditions (high nitrate: high phosphate, HNHP) or low nitrate: high phosphate (LNHP) conditions retained a healthy, unbleached appearance and polyp biomass was unaffected (Rosset, D'Angelo and Wiedenmann, 2015; Rosset *et al.*,

2017). The phenotype response of the coral polyp corresponded with the bleaching response, but at a cellular level the ultra-structure of the symbionts from each experimental treatment differed and importantly, zooxanthellae from the HNLP treatment showed signs of P-starvation (Rosset *et al.*, 2017). Impacts on the coral skeleton were not studied as part of these published experiments (Rosset, D'Angelo and Wiedenmann, 2015; Rosset *et al.*, 2017). However, a precise morphological correspondence between coral tissue and skeleton has previously been recorded in corals (Tambutté *et al.*, 2007), so it was hypothesised that modification of polyp size might have been recorded in the skeletal structure, specifically in the corallites.

Corallites are the parts of the coral skeleton deposited by a single polyp. The corallite is typically a tube-shaped structure that forms around and underneath the polyp and is enclosed by a wall known as a theca, from which plate-like vertically oriented structures called septa, radiate inwards towards the centre (Veron, 2000). In accordance with this basic framework, corallite shapes, wall structures and the presence and abundance of different skeletal elements vary between coral families, genera and species and these morphological differences provide one of the criteria upon which taxonomic classifications are commonly made (Veron, 2013; Madl, Schabetsberger and Lipovnik, 2014; Luzon *et al.*, 2017). But, at the species level corallite size, shape and the abundance of different skeletal elements may also vary when the polyp's ontogenetic development, plastic responses to environmental disturbance and/or seasonal cycles are recorded in the corallite structure. For example, asexual reproduction (by intra-tentacular budding) initiates in *Favia spp.* once the canalized ratio between the perimeter length and the surface area of the corallite exceeds a critical value (Gateño and Rinkevich, 2003). Another process recorded by the corallite is the cyclic formation of dissepiments which coincide with seasonal and lunar cycles (Peirano *et al.*, 2005; Dávalos-Dehullu, Hernández-Arana and Carricart-Ganivet, 2008; DeCarlo and Cohen, 2017) but can also be disrupted by thermal stress (DeCarlo and Cohen, 2017). Dissepiments are horizontally or vertically oriented plate-like skeletal structures which form either inside (endo-thecal) or outside (exo-thecal) the corallite wall. Endo-thecal dissepiments support the base of the polyp at the interface between occupied and vacant skeleton, and as the polyp grows upwards abandoned dissepiments are visible as ladder or wall-like structures in the vacated sections of the corallite (Budd and Stolarski, 2011; Madl, Schabetsberger and Lipovnik, 2014; Humblet, Hongo and Sugihara, 2015). The spacing between dissepiments in *Porites spp.* is reduced

both during winter and thermal-stress induced bleaching events, and at such times dissepiments may also fail to form; both responses contribute to the formation of high density bands in the skeleton at the level of the colony (DeCarlo and Cohen, 2017). High-density bands formed during thermal stress have also been associated with thickening of skeletal elements within, or peripheral to the corallite but some skeletal elements such as exo-thecal dissepiments, costae and theca are more prone to thickening than others e.g. septa, columella and endo-thecal dissepiments (Dávalos-Dehullu, Hernández-Arana and Carricart-Ganivet, 2008; Fouke, Trop and Sivaguru, 2021).

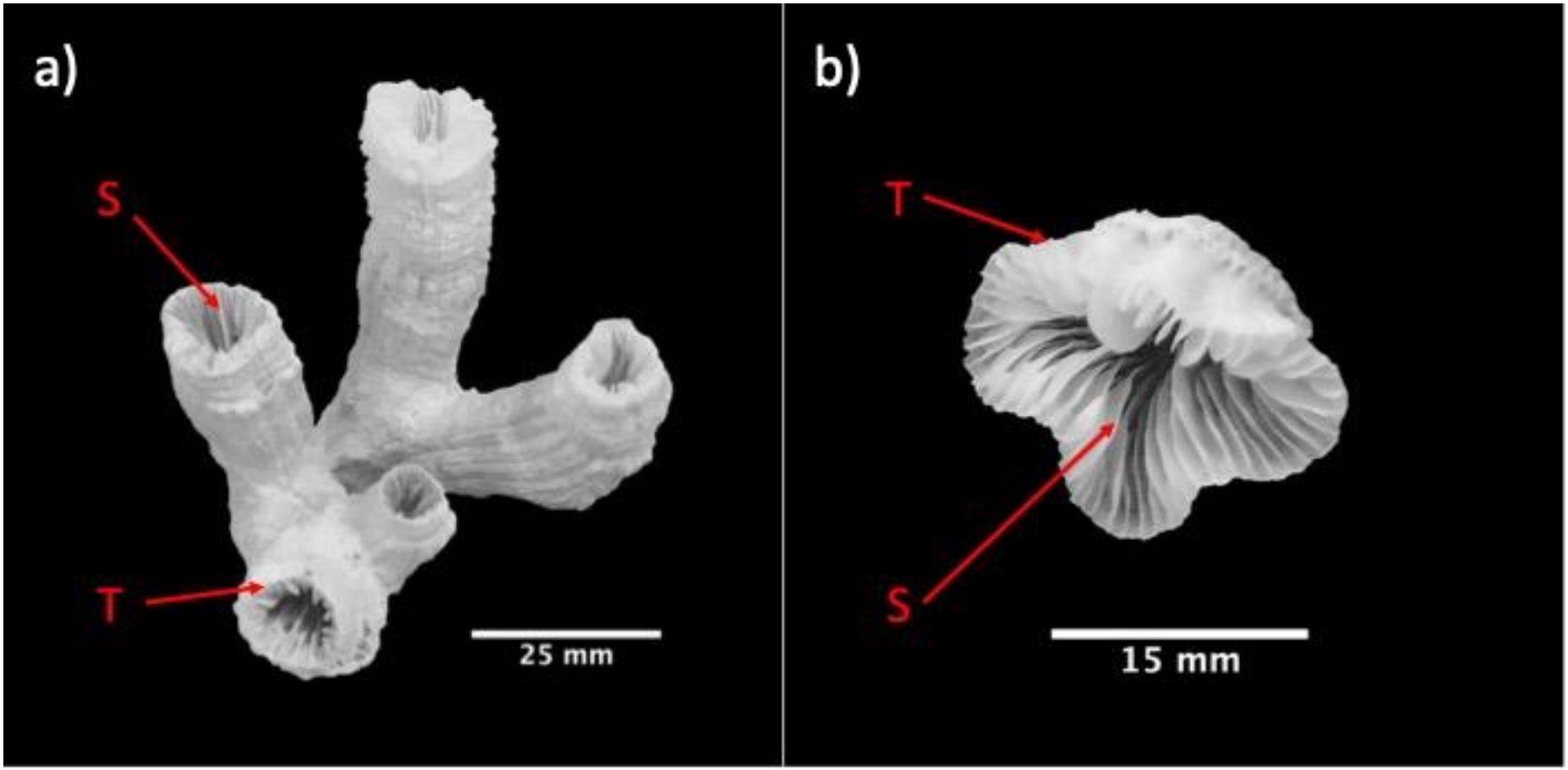

Figure 3.1. Photographs of the zooxanthellate coral, *E. paradivisa* at the level of fragment and an individual corallite. a) Digital photograph of a representative *E. paradivisa* fragment illustrating the phaceloid structure. This fragment hosts 5 corallites each of which is located at the terminus of its respective branch and is defined by its own distinct theca (T). Dichotomous branching points are identifiable as the points of asexual reproduction. Septa (S) are visible as plate-like structures which radiate inwards towards the centre of the calice from the inner surface of the theca. b) Digital photograph of a representative *E. paradivisa* corallite. The plate like septa (S) can be seen to radiate from the theca (T) inwards towards the centre of the calice where they plunge steeply into the corallite.

In this study, the corallites of *E. paradivisa* corals cultured during the aforementioned nutrient stress experiments (Rosset, D'Angelo and Wiedenmann, 2015; Rosset *et al.*, 2017) were analysed to investigate the impacts of nutrient limitation and skewed N:P ratios on corallite size and structure. *E. paradivisa* is an excellent species for use in such a study due to their phaceloid growth morphology. In this particular form of skeletal growth, the individual polyps are isolated at the tops of individual branches and are bound by their own theca (corallite wall). Corallites typically have a calice diameter > 10 mm and are characterised by non-exsert septa which radiate inwards from the theca and plunge steeply near the centre of the calice which lacks a columella (Madl, Schabetsberger and Lipovnik, 2014; Luzon *et al.*, 2017) (Figures 3.1a and b). Dichotomous branching points in the colony structure are readily identifiable as sites of asexual budding (Figure 3.1a). The supporting branches are effectively those parts of the skeleton which have been vacated by living tissue and track the upward growth of the corallites. Branches are characterised by the presence of additional internal skeletal elements – endo-thecal dissepiments. These form as walls oriented parallel to the theca and adjoin adjacent septa with, in many cases multiple dissepiments forming between two adjacent thecae. The large isolated corallites, and simple colonial structure facilitate analysis using both conventional and high-tech methods such as micro-computed tomography (μ-CT), and allow structural differences at macro- and micro-scales to be readily identified.

3.3. Methods

3.3.1. Coral husbandry

Colonies of *E. paradivisa* associated with *Cladocopium spp.* (formerly *Symbiodinium*, Clade C1) (Rosset, D'Angelo and Wiedenmann, 2015; Rosset *et al.*, 2017; LaJeunesse *et al.*, 2018) were exposed for at least six months to four different nutrient treatments in the experimental mesocosm of The Coral Reef Laboratory at The National Oceanography Centre, Southampton, UK. The mesocosm has previously been described in detail (D'Angelo and Wiedenmann, 2012) so a full description of the lighting, heating and filtration systems is not repeated here. The four nutrient treatments test the long-term impacts of the following four nutrient scenarios: - nutrient replete with respect to N and P (high nitrate: high phosphate, HNHP), severe limitation of both N and P (low nitrate: low

phosphate, LNLP), high nitrate: low phosphate (HNLP) and low nitrate: high phosphate (LNHP). The terms 'high' and 'low' are used merely to emphasize differences in the relative availability of N and P between treatments, and do not suggest that any of the treatments reflect the conditions found on a specific reef. More precisely, the long term dissolved inorganic nutrient conditions of each treatment can be summarised as HNHP = NO_3^- ~ 6.5 µM: PO_4^{3-} ~ 0.3 µM (N:P ratio ~ 22:1); HNLP = NO_3^- ~ 38 µM: PO_4^{3-} ~ 0.18 µM (N:P ratio ~211:1); LNHP = NO_3^- ~ 0.06 µM: PO_4^{3-} ~ 3.6 µM (N:P ratio ~1:60) and LNLP = NO_2^-/NO_3^- ~0.7, PO_4^{3-} ~0.006 µM (N:P ratio ~ 12:1) (Rosset, D'Angelo and Wiedenmann, 2015; Rosset *et al.*, 2017). Nutrient concentrations were maintained by the addition of sodium nitrate or -phosphate solutions via peristaltic pumps and/or the removal of nutrients via the addition of ethanols/ alcohols (D'Angelo and Wiedenmann, 2012). The relative proportions of dissolved inorganic nitrogen species in the mesocosm are typically NO_3^- ~90%, NO_2^- ~ 10% and NH^{4+}/NH_3 <0.7% (Rosset, D'Angelo and Wiedenmann, 2015). All corals remained unfed throughout the duration of the experimental period so the supplied doses of nitrate and phosphate are considered to be the primary sources of N and P available to the corals and that translocated carbohydrates from the zooxanthellae represented the primary source of nutrition. However, the mesocosm tanks are established ecosystems hosting a community of invertebrate animals, and algal growth on all tank walls is ubiquitous. It is likely that recycling of nutrients within the system, and the generation of particulate food by other organisms represented additional sources of sustenance. Nutrient concentrations were monitored as described in Rosset *et al.* (2017). Specifically, nitrate seawater indicator solution was prepared using the commercially available "NITRATE PRO REEF TEST KIT" (*Red Sea Fish Pharmaceuticals Limited, UK)* and subsequently analysed using a custom programmed colorimeter at 560 nm (DR900, HACH LANGE, UK) calibrated with nitrate standard solution in the range 0 to 20 mg l^{-1}. Seawater phosphate indicator solution was prepared using "Permachem® PhosVer® 3 (ascorbic acid method #8048, HACH LANGE) phosphate reagent" test kit (HACH LANGE, UK) and measured using the same colorimeter (DR900, HACH LANGE, UK). Corals were cultured in artificial seawater mixed using Tropic Marin Pro Reef Salt ® and temperature and salinity in all tanks were maintained at ~25 ℃ and ~35 p.s.u. respectively. All corals were subject to a 10/14-hour light/dark cycle at a photon flux of ~150 μmol m^{-1} s^{-2}, except in the case of those from the HNLP treatment which were temporarily acclimated at a lower photon flux (80 µmol m^{-1} s^{-2} for 4 months) to prevent

light-stress induced bleaching which is more likely under HNLP conditions (Wiedenmann *et al.*, 2013; Rosset *et al.*, 2017). The positions of individual corals were regularly alternated within tanks to minimise the impact of small-scale water flow/ light intensity differences. At the end of the culture phase, coral fragments were prepared by removing animal tissue from the coral skeletons using a Waterpick®. In total, corals were exposed to HNLP and LNHP conditions for > 6 months and to HNHP and LNLP conditions for > 1.5 years.

3.3.2. Measurement of corallite size and macro-scale morphological features

An overhead 'bird's eye-view' digital photograph of the calice of each corallite (n = 12 for HNHP, 24 for HNLP, 16 for LNHP and 25 for LNLP) was taken using an Olympus TG-4 Tough digital camera mounted on a tripod from a fixed height of 10 cm. The JPEG images were then scaled and analysed using the open source software package ImageJ (Fiji) version 2.0.0. The freehand draw tool was used to trace the perimeter of the outer edge of the theca. The traced shape was then measured using the built in 'Measure' tool to determine corallite area, theca length and the shape of the corallite. Shape was defined using circularity, a unitless property defined as Circ = 4π x $\frac{Area}{Perimeter\text{^}2}$; a value of 1.0 indicates a perfect circle and as the value approaches zero it indicates an increasingly elongated shape (Schneider, Rasband and Eliceiri, 2012). The number of septa present at the surface of the calice were counted with the aid of the 'multi-point' tool. The lengths and widths of septa vary greatly both between and within corallites, thus no minimum length or width was defined to determine whether an inward protrusion from the theca constituted a septa. Instead, all noticeable inward protrusions from the inner surface of the theca towards the centre were deemed to be septa. All measurements were taken by a single observer to ensure consistency.

3.3.3. Micro-computed tomography

A subset of representative corallites were selected from each treatment (n = 6) for analysis using micro-computed tomography (μ-CT) and removed from the supporting fragments using a slow speed saw. Prior to scanning, the skeletons were cleaned of any residual organic matter by repeatedly soaking in 10% NaClO solution 3 times for 30 minutes with

the solution being discarded after each soak. The skeletons were then further soaked in MilliQ water (18.2 M ohm cm^{-2}) twice (for 2 and 24 hours) before being oven dried at 50 ℃. µ-CT scanning was conducted at The Natural History Museum, London, UK (NHM) using a Nikon Metrology HMX ST225 (Nikon Metrology, Tring, UK). Fragments were analysed using a beam with voltage of 100 kV. A current of 70, 100 or 150 µA (details for each scan available upon request) was generated with a Tungsten reflection target and a 0.5 mm aluminium filter. Projections were obtained for each sample during a single 360° rotation and each set of radial projections was subsequently reconstructed into a 3-dimensional matrix of isotropic voxels at a resolution of ~12.5 µm using CT Pro 3D v5. Two fragments from each treatment were also selected for scanning at a lower resolution (~ 33 µm) to analyse the skeletal structure at and around the sites of asexual budding.

3.3.4. Analysis of skeletal thickness and abundance of dissepiments

All analyses of µ-CT files were conducted using the open source software ImageJ (Fiji) version 2.0.0. Profiles of mean skeletal element thickness were determined using the 'Thickness' function of the BoneJ plug-in (Doube *et al.*, 2010) to measure 1-voxel slices oriented perpendicular to the direction of growth at 1 mm intervals. The analysis of thickness profiles was limited to the top 6 mm of corallites due to the shallow nature of the LNLP corallites which, in most cases did not extend beyond this depth. Three primary skeletal elements which comprise the corallite structure were identified, these being theca, septa and dissepiments. Elements to be excluded from measurements were removed from the image prior to measurement using the freehand 'selection' tool. The theca was defined as the thick outer wall that bounds the extremities of the corallite. Septa were defined as vertically oriented plate-like elements radiating inwards from the inner surface of the theca towards the centre of the corallite. Dissepiments were defined as vertical walls oriented roughly parallel to the theca and which formed between adjoining septae (Budd and Stolarski, 2011; Madl, Schabetsberger and Lipovnik, 2014). Profiles of the dissepiment: septa ratio were determined by counting these skeletal elements with the aid of the 'multi-point' tool at depth intervals of 1 mm. Due to the irregular shapes of the corallites, and difficulties in orienting the 3D reconstructions to account for these irregularities it was common for portions of the corallite skeleton to be missing from the slices being analysed. In these instances, the portion of the skeleton that that was available for analysis within the

slice was assumed to be representative of the entire skeleton for the region of skeleton being assessed. The proportional abundance of dissepiments was consequently calculated using the equation $\frac{Dissepiments}{Dissepiments + septa}$. All dissepiment: septa analyses were conducted by a single observer to maintain consistency in the classification of skeletal elements.

3.3.5. Analysis of branch and corallite shape at branching sites

Changes to the shape (circularity) of branches above and below branching points were determined through comparison of the branch shape at 10 mm below the branching point, immediately below and immediately above the branching points.

3.3.6. Statistical analysis

All statistical analyses were conducted using R (version 4.0.3). Differences in corallite area, theca length, extension rate, circularity, the number of septa and the mean thickness of septa and dissepiments were determined using one-way ANOVA followed up by Tukey's Honestly Significant Difference tests. Where the underlying assumptions of the ANOVA were deemed to have been violated, the non-parametric Kruskal-Wallis test was preferred, followed up by Dunn's tests ('dunn.test' package using the Bonferroni correction). Multi-level linear regression models were constructed and subsequent regression analysis conducted to determine how the different nutrient treatments impacted the relationships between corallite size, shape, skeletal element thickness and the abundance of internal skeletal structures (septa and dissepiments). Changes to the shape (circularity) of branches above and below branching points were determined using two-tailed, paired t-tests.

3.4. Results

3.4.1. Macro-scale impacts on corallite size, shape and number of septa

Differences in the size, shape and structure of corallites between treatments were evident from a basic visual inspection and confirmed by analysis of digital photographs using image analysis software. HNHP corallites were significantly larger than those from the other treatments whether measured by calice area *(Kruskal-Wallis, chi-squared = 43.6, p <*

0.001) or theca length *(ANOVA, $F_{3,73} = 18.6$, $p < 0.001$)* and typically had high circularity (Figures 3.2a, b and c). Long-term exposure to LNHP conditions produced corallites with a less circular shape *(Kruskal-Wallis, chi-squared = 14.0, p = 0.003)* (Figure 3.2c), while corallites from the HNLP treatment were smaller than those from the other treatments and had significantly fewer septa at the surface of the calice *(ANOVA, $F_{3,73} = 23.6$, $p < 0.001$)* (Figure 3.2d).

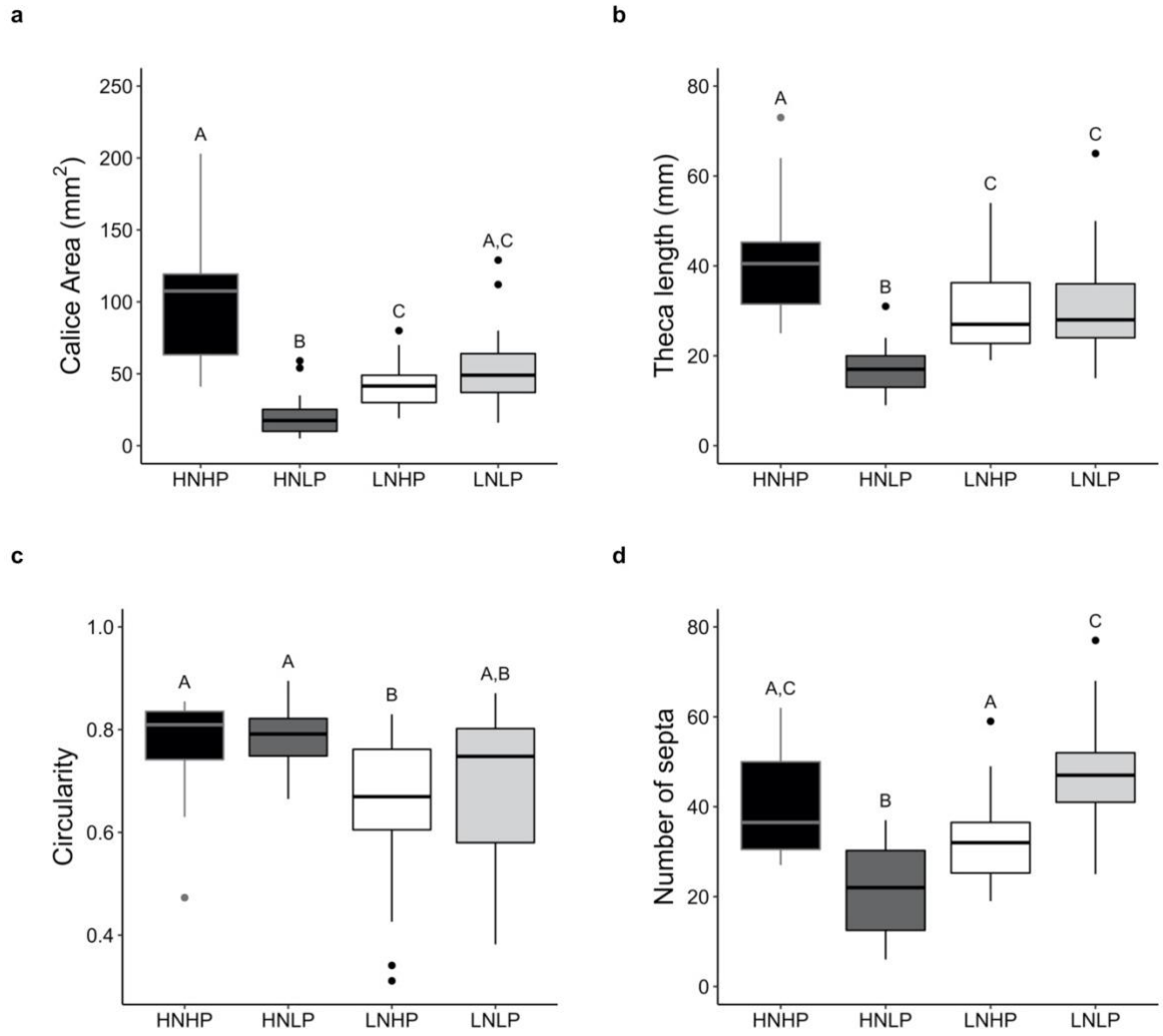

Figure 3.2. Quantitative analysis of the impacts of long-term exposure (≥ 6 months) to four different nutrient treatments on the size and structure of *E. paradivisa* corallites. a) calice area *(Kruskal-Wallis, chi-squared = 43.6, p < 0.001)*, b) theca length *(ANOVA, $F_{3,73} = 18.6$, $p < 0.001$)*, c) circularity *(Kruskal-Wallis, chi-squared = 14.0, p = 0.003)*and d) the number of septa present at the surface of the calice *(ANOVA, $F_{3,73} = 23.6$, $p < 0.001$*. HNHP = high nitrate: high phosphate (n =12), HNLP = high nitrate: low phosphate (n = 24), LNHP = low nitrate: high phosphate (n = 16) and LNLP = low nitrate: low phosphate (n = 25). Letters within each panel indicate statistically significant differences between treatments.

Differences in corallite size were associated with differences in the 3-dimensional shape of the corallites (Figure 3.3). In HNHP corals, corallites typically took the shape of an inverted irregular cone (similar to the end of a trumpet), such that the theca length increased with proximity to the surface of the calice (Figure 3.3a). The majority of corallites from the HNLP treatment (21 from 24 specimens) exhibited a characteristic not observed in corals from the other treatments. In these fragments, a well-defined structural discontinuity between the supporting branch and the base of the corallite defined an abrupt reduction in the size of the skeleton, such that the corallite was smaller in circumference than the supporting branch. The appearance of these discontinuities gave the impression that the old skeletal structure had been suddenly vacated by the polyp in favour of forming a new and smaller corallite. The internal skeletal structure (and in particular, the septa) of the branch immediately below this discontinuity was visible at the base of the corallites (Figure 3.3b). The profiles of corallites from the LNHP treatment took two forms; an irregular inverted conical/trumpet shape similar to that described for HNHP corals, but with a base which was reduced in size relative to the supporting branch (Figure 3.3c) or a columnar shape. In both cases, the length of the theca at the surface of the calice remained unchanged when compared to the perimeter of the supporting branch. Corallites from the LNLP treatment were easily distinguished from the other treatments and narrowed towards the surface of the calice, resulting a corallite with a theca that was smaller than the perimeter of the supporting branch (Figure 3.3d).

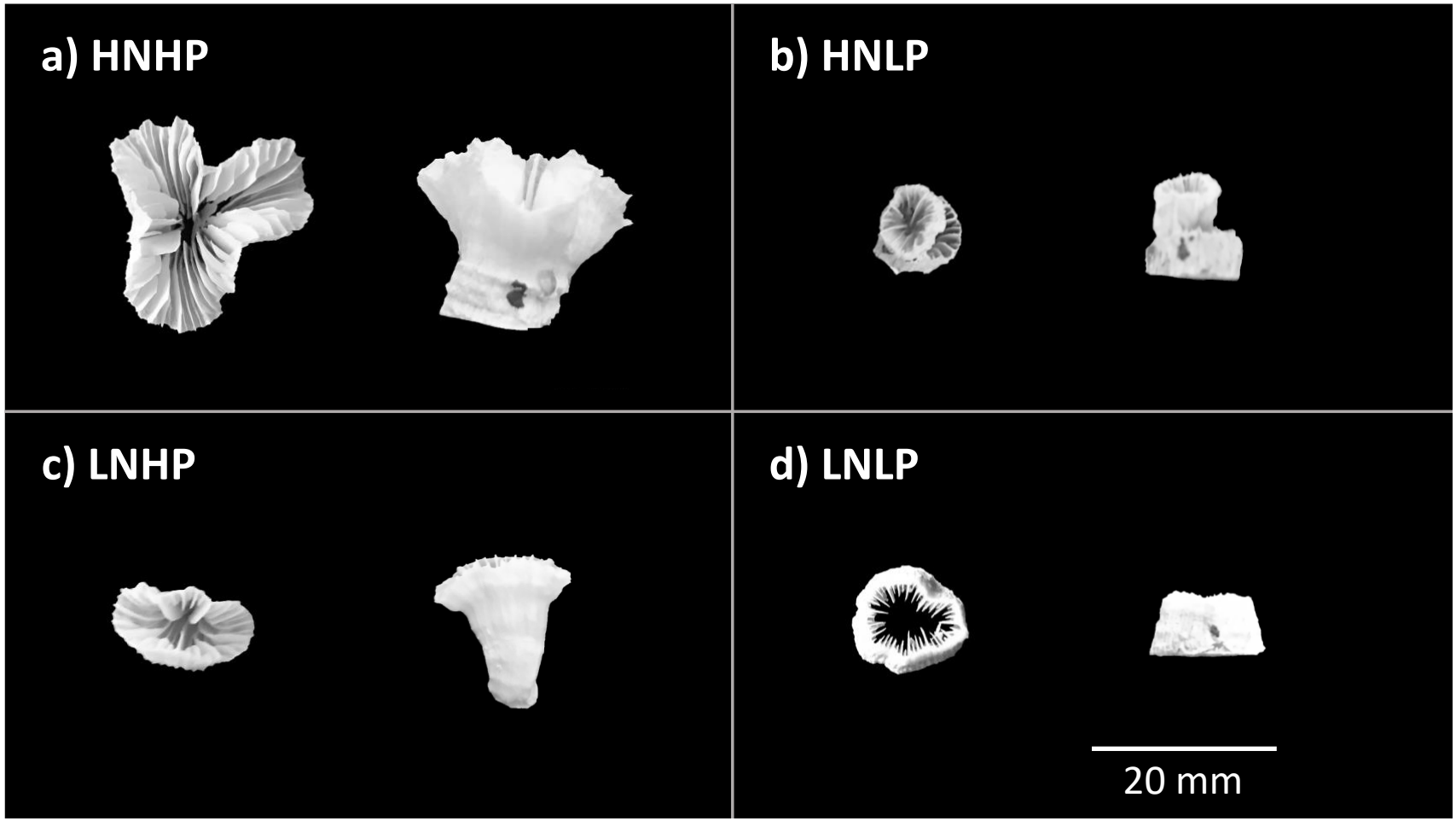

Figure 3.3. Digital photographs of *E. paradivisa* corallites after exposure to four different nutrient treatments for ≥ 6 months. a) HNHP = high nitrate: high phosphate, b) HNLP = high nitrate: low phosphate, c) LNHP = low nitrate: high phosphate and d) LNLP = low nitrate: low phosphate. Each panel shows an aerial view (left) and side profile (right) of the same representative corallite from each treatment. The scale shown in panel d) applies to all panels.

A linear model considering the effect of nutrient treatment identified a strong, negative relationship between corallite circularity and theca length *($F_{7,69} = 35.8$, $r^2 = 0.78$, $p < 0.001$).* Within the model, this relationship was preserved among corallites from the HNHP, LNHP and LNLP treatments but the slopes constructed for the LNHP and LNLP treatments were found to be statistically different to that of the HNHP treatment *($p < 0.05$).* In both cases, limitation of N or N+P was associated with corallites of a given size having a less circular shape than those from the HNHP treatment (Figure 3.4a). Corallites cultured under HNLP conditions were significantly smaller than those from the other treatments and no significant relationship between corallite size and shape was evident *($r^2 = 0.03$, $p = 0.43$).*

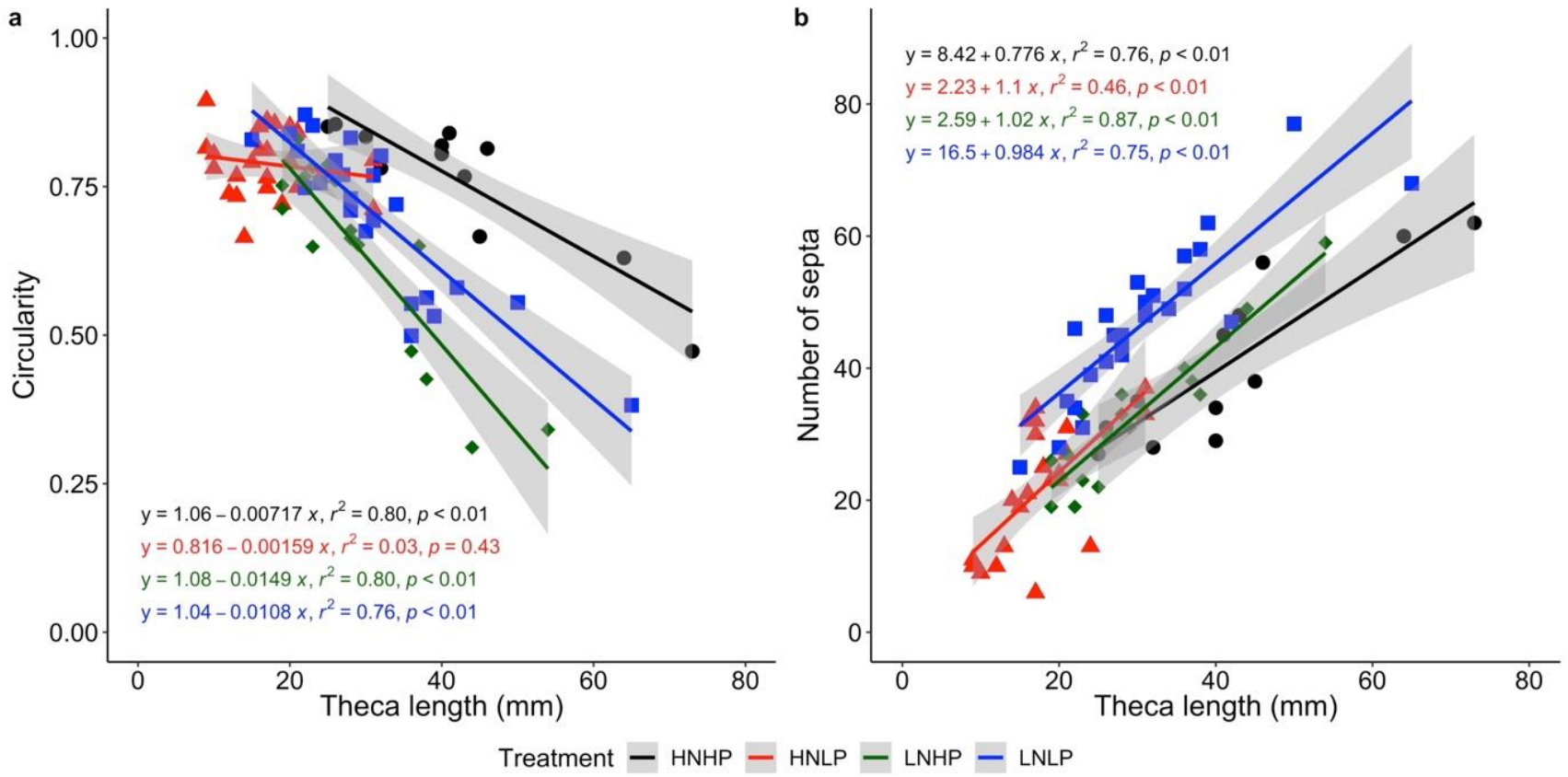

Figure 3.4. Impacts on the macro-structure of corallites of *E. paradivisa* following exposure to four different nutrient treatments for ≥ 6 months. Linear regressions showing a) the relationship between the theca length and circularity of the corallite at the surface of the calice for each of four treatments and, b) the relationship between the theca length and the number of septa at the surface of the calice for each of four treatments. The equation and r^2 value for the regression describing the relationship for each treatment is displayed in the respective panel, while data relating to the overall fit for each model is provided in the main text. Grey shading indicates the respective 95% confidence intervals for each regression. HNHP (black) = high nitrate: high phosphate, HNLP (red) = high nitrate: low phosphate, LNHP (green) = low nitrate: high phosphate and LNLP (blue) = low nitrate: low phosphate.

A linear model considering the effect of nutrient treatment indicated there was a strong, positive relationship between corallite size and the number of septa present at the surface of the calice *($F_{4,72} = 98.2$, $r^2 = 0.85$, $p < 0.001$).* Within this model, the slopes constructed for each nutrient treatment did not differ significantly *($p > 0.05$)* (Figure 3.4b) although the y-intercept estimated for the LNLP treatment was found to be greater than that of the HNHP treatment *($p < 0.001$).* The model explained the majority of observed variance in the HNHP, LNHP and LNLP corallites *($r^2 > 0.75$ in all cases)* and a large proportion of the variance in corallites from the HNLP treatment *($r^2 = 0.46$).* This positive correlation between corallite size and number of septa agreed well with the observed differences in the number of septa for corallites from each nutrient treatment (Figure 3.2d).

3.4.2. Impacts on skeletal element thickness

In all treatments the relative thicknesses of the three skeletal elements measured were the same:- theca > septa > dissepiments. Exposure to the LNHP and LNLP treatments caused significant thickening of both the theca *(ANOVA, $F_{3,20} = 70.8$, $p < 0.001$)* and septa *(ANOVA, $F_{3,20} = 48.1$, $p < 0.001$)* (Figures 3.5a and b). Dissepiments of corallites cultured under LNHP conditions were also significantly thicker than those of corallites cultured in the HNLP treatment *(Kruskal-Wallis, chi-squared = 11.1, $p = 0.01$)* but were not significantly different to those from the HNHP or LNLP treatments (Figure 3.5c). However, the observed differences between dissepiment thickness should be treated with caution because the HNHP and LNHP corals had very low numbers of dissepiments in the uppermost 6 mm of their corallites, potentially biasing this comparison.

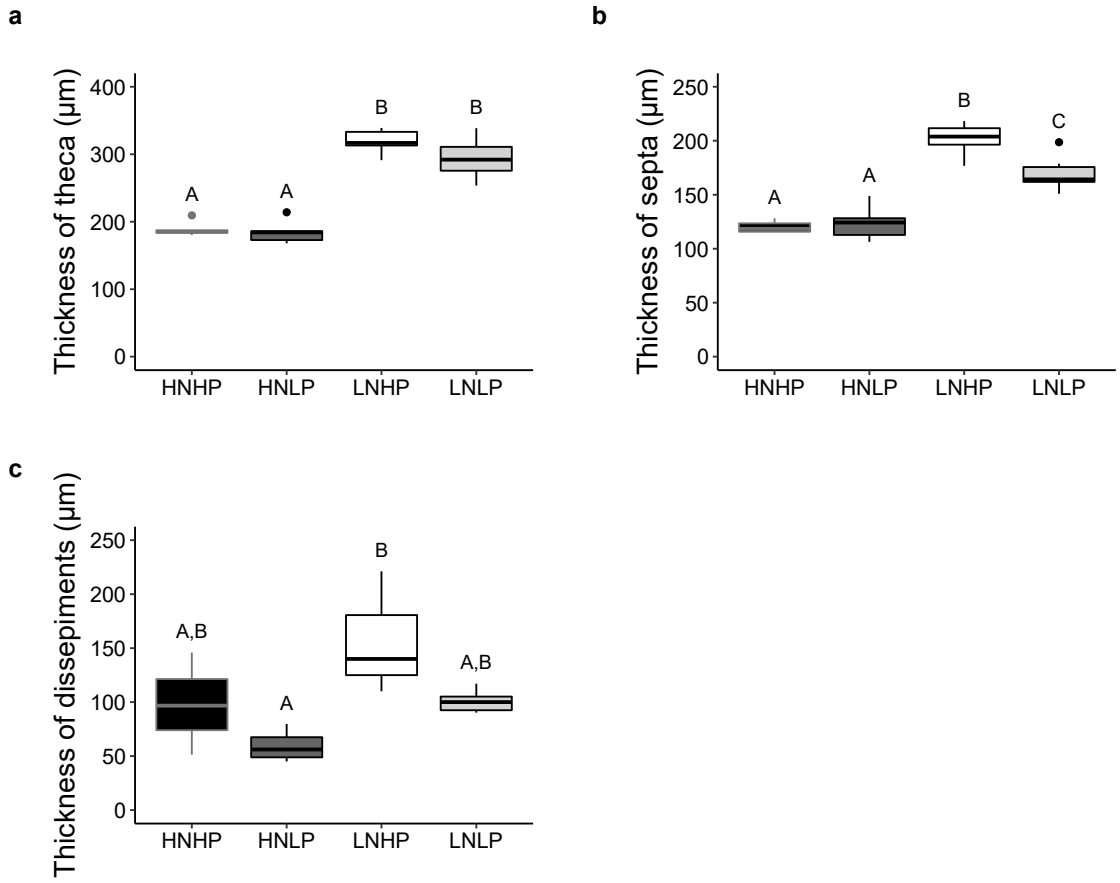

Figure 3.5. Quantitative analysis of skeletal element thickness in corallites of *E. paradivisa* after exposure to four different nutrient environments for ≥ 6 months. Mean skeletal element thickness of a) theca *(ANOVA, $F_{3,20}$ = 70.8, $p < 0.001$),* b) septa *(ANOVA, $F_{3,20}$ = 48.1, $p < 0.001$)* and, c) dissepiments *(Kruskal-Wallis, chi-squared = 11.1, $p = 0.01$)*. Mean skeletal element thickness was measured by µ-CT and relates to measurements of mean thickness in the top 6 mm of the corallite. HNHP = high nitrate: high phosphate, HNLP = high nitrate: low phosphate and LNLP = low nitrate: low phosphate (*n = 6* for each treatment). Letters within each panel indicate statistically significant differences between treatments.

Linear regression models considering the effect of the different nutrient treatments were constructed to determine whether skeletal element thickness was related to distance from the surface of the calice (corallite depth). These models indicated that the thicknesses of theca *($F_{7,136} = 80.9$, $r^2 = 0.81$, $p < 0.001$)* and septa *($F_{7,136} = 78.4$, $r^2 = 0.80$, $p < 0.001$)* were strongly and positively correlated with corallite depth. A similar regression model indicated that although there were differences in dissepiment thickness between the HNLP and LNLP treatments, no statistically significant relationship was detectable between the thickness of dissepiments and corallite depth *(ANOVA, $p = 0.18$).* Subsequent regression analyses revealed that the relationships between theca and septa thickness and corallite

depth were sensitive to the different nutrient treatments (Figures 3.6a and b). In corals exposed to the HNLP treatment, the relationships between theca and septa thickness and corallite depth were non-significant *($p > 0.05$ in both cases),* while exposure to the LNLP treatment altered the thickness profile of the theca such that the relationship with corallite depth was no longer significant *($p = 0.45$).* Strikingly, the skeletal element thickness of corals exposed to the LNHP treatments was strongly impacted, and both theca and septa thickened more rapidly with depth than was observed for corals from the HNHP treatment (*$p < 0.001$ in both cases*).

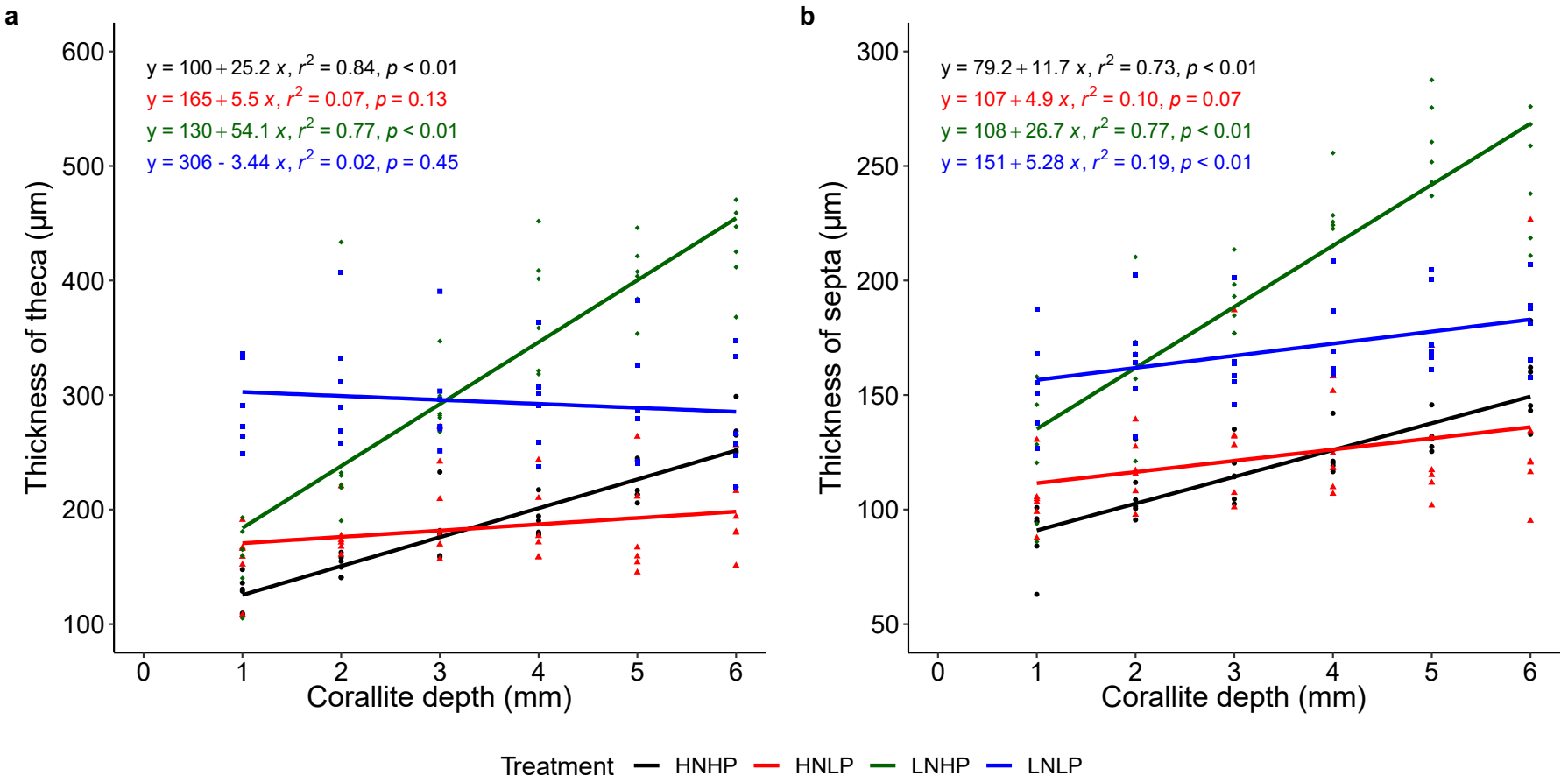

Figure 3.6. Profiles of mean skeletal element thickness against corallite depth for corallites of *E. paradivisa* after exposure to four different nutrient treatments for ≥ 6 months. a) Theca and b) Septa. Mean skeletal element thickness was determined by µ-CT and measurements were taken at 1 mm intervals throughout the top 6 mm of the corallite. Grey shading indicates the 95% confidence intervals of the fitted models. The coefficients of the respective regressions along with the associated r^2 and p-values are shown in each panel. HNHP = high nitrate: high phosphate, HNLP = high nitrate: low phosphate and LNLP = low nitrate: low phosphate. (n = 6 for each treatment).

3.4.3. Impacts on the formation of dissepiments

Changes to the internal structure of corallites were assessed by determining how the ratio of dissepiments: septa changed with depth within corallites. A linear model considering the effect of the different nutrient treatments indicated that the ratio of dissepiments: septa increased with corallite depth *($F_{7,136} = 88.6$, $r^2 = 0.82$, $p < 0.001$)*. But dissepiments were, for the most part absent from the uppermost 6 mm of corallites cultured in the HNHP and LNHP treatments, while being abundant throughout the uppermost 6 mm of corallites from the HNLP and LNLP treatments (Figure 3.7). Subsequent regression analysis confirmed that this difference in the relative abundance of dissepiments was statistically significant *($p < 0.001$)* and was clearly evident from a visual comparison of µ-CT cross-sections taken at 6 mm depth (Figure 3.8). The rate of increase in dissepiment: septa ratio with corallite depth in HNLP and LNLP corals was very similar, but the absolute value was consistently higher in HNLP corals indicating more dissepiments were present at shallower depths (Figure 3.7).

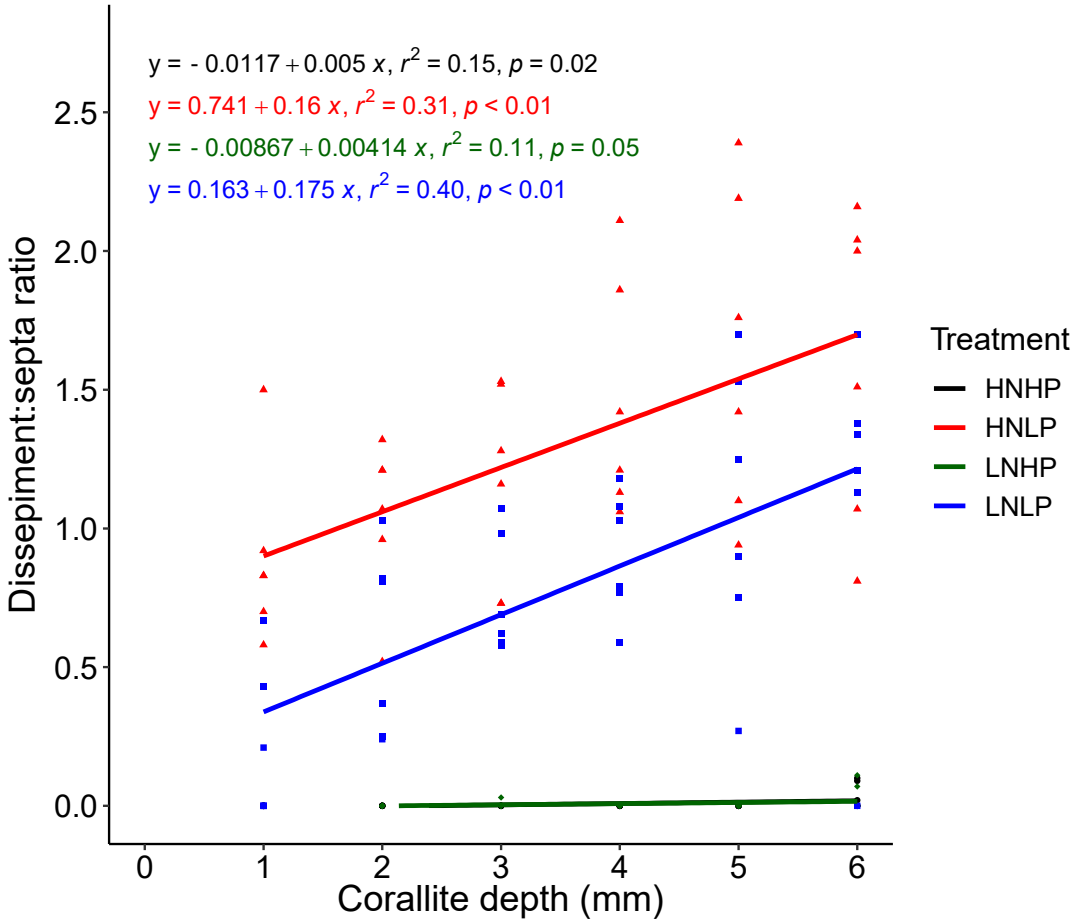

Figure 3.7. Profiles of the dissepiment: septa ratio with corallite depth in corallites of *E. paradivisa* after exposure to four different nutrient treatments for ≥ 6 months. The ratio was determined using analysis of μ-CT images with counts being taken at intervals of 1 mm in the uppermost 6 mm of corallites. Grey shading indicates the 95% confidence intervals of the fitted models. The coefficients of the respective regressions along with the associated r^2 and p-values are shown in each panel. HNHP = high nitrate: high phosphate, HNLP = high nitrate: low phosphate and LNLP = low nitrate: low phosphate. (n = 6 for all treatments). N.B. The regression for the HNHP treatment overlies the regression for the LNHP treatment.

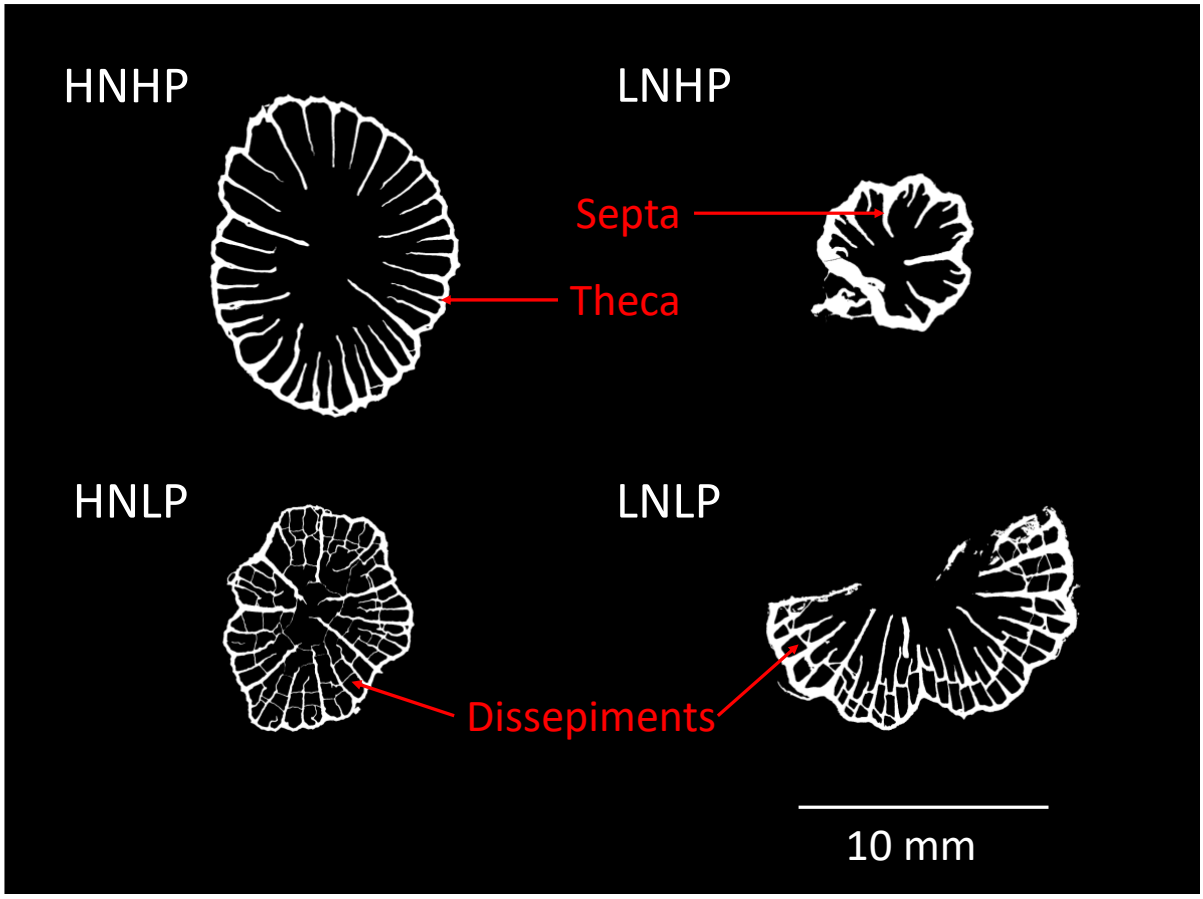

Figure 3.8. Cross sectional µ-CT images of *E. paradivisa* corallites after exposure to four different nutrient treatments for ≥ 6 months. Each cross-sectional image is a 1-voxel slice with a resolution of ~12.5 µm oriented perpendicular to the direction of linear extension and located 6 mm below the surface of the calice. Septa are present in all specimens and radiate inwards towards the centre of the corallite from the inner wall of the theca. HNHP = high nitrate: high phosphate, HNLP = high nitrate: low phosphate and LNLP = low nitrate: low phosphate. Dissepiments are only visible in the HNLP and LNLP corallites and are identifiable as the structures oriented roughly parallel to the theca and that join adjacent septa. The incomplete image shown for the LNLP corallite is a consequence of the irregular shape of the corallite and the angle at which it was mounted during scanning, this was a common effect in corals from all treatments and led to the quantification of dissepiment: septa ratios that were used for quantitative analysis (which is detailed in the main text).

3.4.4. Skeletal profiles of branching sites

Analysis of lower resolution scans (~33 µm) of coral fragments provided an insight into the skeletal structure of the at sites of asexual budding. Dichotomous branching sites indicative of asexual budding were commonplace among coral fragments from all of the nutrient treatments, having formed both before and during the experiment. Our analysis of branching points which formed prior to exposure to the experimental conditions indicated that under our control conditions (the HNHP treatment) there is a significant decrease

(paired t-test, $t_7 = 5.8$, p-value < 0.001) in branch circularity from ~0.7 at 10 mm below the branching point to 0.37 ± 0.02 at the budding site. Above the branching point, the circularity of the divergent branches is typically > 0.6 and not less than 0.5, this being not statistically different to that of the branch at 10 mm below the branching point *(paired t-test, $t_7 = 1.1$, $p = 0.3$).*

3.5. Discussion

In the skeletons of zooxanthellate corals, bands of alternating high- to low-density form seasonally, reflecting changes in SST and/or nutrient availability, whilst high-density 'stress bands' may also form as a consequence of thermal-stress induced bleaching (Peirano *et al.*, 2005; Barkley and Cohen, 2016; DeCarlo and Cohen, 2017; Barkley *et al.*, 2018). This phenomenon is best studied in massive corals, for which skeletal thickening in regions of high density has been observed in skeletal elements associated with, and peripheral to the corallite (Dávalos-Dehullu, Hernández-Arana and Carricart-Ganivet, 2008; DeCarlo and Cohen, 2017; Fouke, Trop and Sivaguru, 2021). It was recently demonstrated that chronic nutrient limitation, or nutrient-starvation arising from skewed N:P ratios can also cause temperature-independent bleaching, skeletal thickening and reduced skeletal porosity in *Acroporids* (Buckingham *et al.*, 2022). Meanwhile, two previous studies showed that exposure to the same conditions led to bleaching and reduced polyp sizes in *E. paradivisa* (Rosset, D'Angelo and Wiedenmann, 2015; Rosset *et al.*, 2017). But it was unclear how the corallite - the part of the skeleton that forms in contact with the polyp - might be impacted. Therefore, the skeletons of *E. paradivisa* cultured during those previous nutrient-stress experiments (Rosset, D'Angelo and Wiedenmann, 2015; Rosset *et al.*, 2017) were used to investigate the impacts of chronic nutrient limitation and skewed N:P ratios on corallite size, shape and structure. Macro-scale features were measured using digital photographs and image analysis software, while micro-scale features were analysed using micro-computed tomography (μ-CT). To our knowledge, this is the first study to examine the impacts of chronic nutrient stress and nutrient starvation on coral skeletons at the scale of the corallite and associated skeletal elements.

E. paradivisa exposed to the HNLP and LNLP treatments were bleached, and had significantly smaller polyps than the unbleached corals of the HNHP and LNHP treatments

(Rosset, D'Angelo and Wiedenmann, 2015; Rosset *et al.*, 2017). These impacts on polyp size were broadly replicated by measurements of corallite size following removal of the corals from culture (this study). Corals exposed to chronic nutrient limitation (LNLP) or skewed N:P ratios (HNLP and LNHP treatments) had smaller corallite areas and/or theca lengths than those cultured under nutrient replete (HNHP) conditions. Corallites from the HNLP treatment were the smallest, and the drastic reduction in corallite size was associated with a distinctive discontinuity between the base of the corallite and the supporting branch. The LNHP and LNLP treatments had a less pronounced impact on corallite size, and corals from these treatments did not exhibit the same discontinuity within their skeletons. Morphological characteristics of the epithelial tissue are precisely recorded at all scales in coral skeletons, such that the size and shape of the corallite is indicative of the size and shape of the basal portion of the polyp (Tambutté *et al.*, 2007). Reduced photosynthesis following bleaching is associated with decreased host lipid, carbohydrate and protein contents and loss of tissue biomass (Rodrigues and Grottoli, 2007). In this study, losses of polyp biomass occurred in those corals that bleached and this was recorded in the skeletons by reductions in corallite sizes. As such, the modifications to the corallite can be considered to be indicative of the coral's nutritional status.

There are several examples from the field that potentially link corallite size and host nutritional status. Foster (1979) reported increases in corallite diameter for *Montastraea annularis* and *Siderastrea siderea* following transplantation from a sand channel to a lagoon which had apparently higher levels of zooplankton, bacteria and dissolved organic matter indicative of higher food and nutrient availability. Also, *Montrastraea cavernosa* from mesophotic environments have smaller corallites than those found at shallower depths, and differences in zooxanthellae densities and chlorophyll concentrations suggest that light limitation might restrict carbon fixation and translocation to the host in corals from the lower-light environment (Studivan, Milstein and Voss, 2019). Corallite diameter has been observed to vary for a number of species of different genera based on geographic distribution throughout the Red Sea (Sadek *et al.*, 2018) suggesting that corallite size may be - at least in part - a plastic response to environmental conditions that is common among zooxanthellate corals. Importantly though, a recent study showed that polyp size (and correspondingly, corallite size) may be a less reliable indicator of tissue biomass than live tissue depth (Precoda *et al.*, 2020), and numerous studies have noted a positively correlated relationship between tissue thickness and nutritional status (Meyer and Schultz, 1985a;

Barnes and Lough, 1992; Cohen *et al.*, 2004; Barkley *et al.*, 2018; Qin *et al.*, 2020). Dissepiments form at the base of the polyp, at the interface between occupied and vacant skeleton (Barnes and Lough, 1992; DeCarlo and Cohen, 2017) so dissepiment depth can be used as a proxy for tissue thickness (Barnes and Lough, 1999; Barkley *et al.*, 2018). In our replicates, dissepiments were practically absent at depths ≤ 6mm among the unbleached HNHP and LNHP corals, indicating a tissue thickness of at least 6 mm when cultured under nutrient replete or very low N:P conditions. Contrastingly, in the bleached corals exposed to very high N:P ratios (HNLP treatment) or severely limiting nutrient concentrations (LNLP treatment), dissepiments were abundant at 1 mm, indicating a tissue depth of ≤ 1 mm. Furthermore, a greater abundance of shallow dissepiments in HNLP corallites suggested that tissue depth was even shallower in these corals, and when considered alongside the greater reduction in corallite size (calice area and theca length), this suggests that impacts on polyp biomass were most severe in those corals which had P-starved zooxanthellae (Wiedenmann *et al.*, 2013; Rosset *et al.*, 2017).

The different nutrient treatments impacted skeletal element thickness in two ways. Firstly, the mean thickness of theca and septa was greater for corallites exposed to the LNHP and LNLP treatments. Secondly, the positive relationship between skeletal element thickness and corallite depth for theca and septa was absent among HNLP and LNLP corals. Calcification occurs throughout the depth of the tissue layer (Barnes and Lough, 2001), so the longer the skeleton and calcifying cells of the ectoderm are in contact, the thicker the skeleton becomes. The duration that skeleton and tissue are in contact relies on a combination of skeletal extension rate, live tissue depth and periodic retraction or stretching of the live tissue (Barnes and Lough, 1992, 2001; Lough and Barnes, 1992; Mendes and Woodley, 2002; Cohen *et al.*, 2004; Dávalos-Dehullu, Hernández-Arana and Carricart-Ganivet, 2008; DeCarlo and Cohen, 2017; Barkley *et al.*, 2018), all of which impact the rate at which skeleton at the base of the polyp is vacated. For example, skeletal extension results in the polyp migrating upwards into newly formed skeleton and vacating the skeleton at its base, thus rapid extension rates limit the duration of contact between tissue and skeleton. Periodic retraction and stretching of the live tissue layer associated with lunar cycles leads to the formation of discrete dissepiments (Barnes and Lough, 2001; Dávalos-Dehullu, Hernández-Arana and Carricart-Ganivet, 2008; DeCarlo and Cohen, 2017) but since dissepiments in *E. paradivisa* form as continuous, wall-like structures this process can be disregarded for the purpose of this study. As previously discussed, the live

tissue layer in HNHP and LNHP corals was ≥ 6 mm, while in HNLP and LNLP corals it was ≤ 1 mm. We did not measure skeletal extension or calcification rates during this experiment. But, we can consider the impacts of the different nutrient treatments on the physiology of *E. paradivisa* (Rosset, D'Angelo and Wiedenmann, 2015; Rosset *et al.*, 2017) and on the skeletal extension and calcification rates of *Acropora polystoma* (Buckingham *et al.*, 2022) to aid our interpretation.

Polyps of *E. paradivisa* exposed to HNHP and LNHP treatments shared the same phenotype:- large polyps with an unbleached appearance associated with high densities of healthy zooxanthellae (Rosset *et al.*, 2017). The similarities of corallites from these two treatments – namely, the absence of shallow dissepiments and positive correlations between skeletal element thickness and corallite depth - further support this observation. A positive relationship between skeletal element thickness and distance from the apex of the calice, as is observed in HNHP and LNHP corallites, is exactly what we would expect if calcification rate and live tissue thickness remain constant, and skeletal thickening occurs throughout the depth of skeleton that is occupied by live tissue (Barnes and Lough, 2001). This relationship arises simply because the skeleton at increasing depths has been in contact with the live tissue for longer, and has therefore had more time to thicken. Theca and septa in LNHP corallites are thicker than those from HNHP corallites and this can be explained by either a) higher calcification rates, resulting in increased skeletal deposition per unit of time or, b) reduced extension rates, which prolong contact between tissue and skeleton, thereby increasing the duration and extent of skeletal thickening. Increased calcification rate as a consequence of N-limitation is unlikely, but *A. polystoma* had a linear extension rate ~3 times higher under HNHP conditions than in the LNHP treatment (Buckingham *et al.*, 2022). Therefore, the most likely explanation is that linear extension in LNHP corallites is reduced while calcification rate is maintained or relatively less impacted, resulting in prolonged contact between tissue and skeleton and enhanced thickening of the skeletal elements. In HNLP and LNLP corallites, the thickness of theca and septa is more homogenous within the uppermost 6 mm of the corallite. The most parsimonious explanation is that the reduction in live tissue depth results in a shortened period of contact between skeleton and tissue in deeper parts of the corallites, thereby reducing skeletal thickening. If, as observed for *A. polystoma* (Buckingham *et al.*, 2022), HNLP and LNLP conditions cause linear extension to be reduced in *E. paradivisa*, then newer skeleton near the apex of the calice may have undergone a relatively prolonged

period of thickening. The expected effect of reduced thickening at depth, and enhanced thickening near the surface of the calice would be homogenisation of the skeletal element thickness profile, and this is precisely what is seen in the profiles of corals from the HNLP and LNLP treatments. The thinner skeletal elements of the HNLP corallites when compared to the LNLP treatment likely reflect a severe impact on calcification rate when exposed to this treatment, as was observed for *A. polystoma* (Buckingham *et al.*, 2022). Whether the thickness of dissepiments is impacted by the different nutrient treatments remains unclear, due to the small sample size of dissepiments in HNHP and LNHP corallites, and the difference between HNLP and LNLP corallites being statistically non-significant.

A negative correlation was observed between corallite size and circularity in all treatments except under HNLP conditions, for which only very small corallites (theca length < 30 mm) were available for analysis. LNHP corallites of a given size were less circular than those from the other treatments, and a possible explanation is that exposure to low N:P ratios promotes budding in smaller polyps. This would make sense theoretically for organisms living in conditions where tissue growth is suppressed by N-limitation, but where carbohydrates and phosphorus - which are required for energy and the production of ATP and DNA – are replete. Changes to the shape of branches perpendicular to the direction of extension can be considered as past changes to the shape of the calice during upward extension of the corallite. In *E. paradivisa,* reductions in branch circularity were associated with sites of asexual budding/ branching, and under non-experimental conditions budding appears to initiate when calice circularity decreased to 0.37 ± 0.02. In a previous study, asexual (intra-tentacular) budding in massive *Favia spp.* was observed to initiate when the canalised ratio of two morphometric properties, determined from the polyp's area and theca length exceeded a critical value of 1.14, rather than when the polyp reached a particular size (Gateño and Rinkevich, 2003). The measurement of circularity used in this study utilises the same two morphometric properties (calice area and theca length), and circularity is inversely proportional to the morphometric ratio used by Gateño and Rinkevich (2003). The circularity value associated with budding in *E. paradivisa* of 0.37 is equivalent to a value of 1.65 used by Gateño and Rinkevich (2003). This implies that *E. paradivisa* polyps become more elongated than those of *Favia spp.* before asexual budding occurs. This difference could arise due to crowding on the flat surfaces of *Favia spp.*, where lateral extension might be limited by the presence of neighbouring polyps but

is not an issue for the spatially isolated polyps of *E. paradivisa*. Differential impacts on growth and asexual reproduction have previously been reported in cnidarians subject to malnourishment. When starved, the polyps of the zooxanthellate coral *Cladocora caespitosa* had decreased polyp growth rates but asexual budding was maintained, albeit at reduced rates (Rodolfo-Metalpa *et al.*, 2008). Similar responses have also been observed in anemones. In a starvation experiment, all starved individuals of the azooxanthellate *Nematostella vectensis* lost biomass but some still reproduced asexually, even up to 110 days after their last feed (Hand and Uhlinger, 1995). Meanwhile, starvation of the zooxanthellate anemone, *Exaiptasia diaphana* restricted host growth without a loss of biomass but dramatically increased asexual budding when compared to fed anemones which rapidly increased in size but had slower reproductive rates (Bedgood *et al.*, 2020). These studies show that malnourished cnidarians may continue to reproduce asexually even when malnourished and that, in some cases this may lead to budding at smaller polyp sizes (Hand and Uhlinger, 1995; Rodolfo-Metalpa *et al.*, 2008; Bedgood *et al.*, 2020). However, these previous studies do not relate to the specific nutrient conditions considered in this study. It is also important to note that under nutrient replete conditions, corallites reached larger sizes before comparable reductions in circularity were observed. This suggests that, if development towards asexual budding was the cause of the reduction in circularity then it likely represents an adaption to sub-optimal conditions.

The number of septa present at the surface of the calice was strongly related to theca length, and this relationship was preserved in corallites from all treatments. Furthermore, there was no difference between treatments in the rate at which new septa formed as theca length increased. However, LNLP corallites had more septa for a given corallite size and the most likely explanation can be ascertained from the distinctive profiles of their corallites. In LNLP corallites, corallite size decreased with proximity to the surface of the calice and it is likely that the higher-than-expected numbers of septa observed are relics, reflecting the fact that polyps shrunk within corallites that retained their pre-existing skeletal elements. In contrast, the inverted conical and columnar profiles observed in HNHP and LNHP corallites, and the drastic reduction in corallite size observed in HNLP corallites provide mechanisms by which the septa/theca length relationship can be maintained as corallite size is modified. Resistance to change in the rate of septal formation under nutrient stress is an important observation. The ordering, cycling and morphological characteristics of septa are widely used to aid taxonomic classifications in

Scleractinian corals (Tan *et al.*, 2011; Veron, 2013; Madl, Schabetsberger and Lipovnik, 2014; Humblet, Hongo and Sugihara, 2015) and the conservation of processes underpinning septal formation even when exposed to chronic stress vindicates such methods.

This study has advanced our understanding of the impacts that skewed N:P ratios and chronic nutrient limitation can have on the health of coral symbioses. While HNLP and LNLP conditions both lead to bleaching and loss of polyp biomass, the impacts on the coral-zooxanthellae symbiosis are most profound under high N:P ratios (the HNLP treatment), which are associated with malfunctioning photosynthesis in the residual P-starved symbionts (Wiedenmann *et al.*, 2013; Rosset *et al.*, 2017). The corallite is testament to these impacts. In HNLP corals, the full extent of biomass loss can be inferred from drastically reduced corallite size - which manifests itself as a discontinuity at the base of the corallite - and the formation of endo-thecal dissepiments at shallower depths within the corallite. Both features are indicative of greater polyp biomass loss than is observed under LNLP conditions. Furthermore, thinner skeletal elements indicate that calcification rates are probably more severely impacted under HNLP conditions. Contrastingly, very low N:P ratios (the LNHP treatment) appear to result in reduced linear extension rates but with relatively little, or no reduction to calcification rates or polyp biomass. It should be noted that exposure to HNLP conditions was for a shorter time period ($\geq$ 6 months) than for LNLP conditions ($\geq$ 18 months) so the difference between treatments in the severity of the impacts is if anything, somewhat muted. Samples exposed to the experimental conditions for the same length of time were unavailable for comparison, but this finding indicates that polyp biomass loss occurs more rapidly in P-starved (HNLP) corals than those exposed to chronic nutrient limitation (the LNLP treatment). Furthermore, previous studies have demonstrated that in corals exposed to HNLP conditions the translocation of carbon to the host is reduced, requiring greater utilisation of the coral's storage lipids to support host metabolism (Ezzat *et al.*, 2015; Tanaka *et al.*, 2017). Exactly why the impact of HNLP conditions is more severe than for LNLP conditions remains unclear. However, one possible explanation is linked to the enhanced susceptibility of zooxanthellate corals to bleaching under high N:P stoichiometries (Wiedenmann *et al.*, 2013; D'Angelo and Wiedenmann, 2014). Bleaching in corals arises due to increased production of harmful reactive oxygen species (ROS) by the zooxanthellae, and in bleached corals both host and

symbionts have been found to have cellular damage consistent with known responses to elevated levels of ROS (Lesser, 1997; Lesser and Farrell, 2004; Tchernov *et al.*, 2011). Transfer of ROS from algal symbionts to the host has not been directly verified but extracellular production of ROS by isolated *Symbiodinum* exposed to light and thermal stress has been observed (Rehman *et al.*, 2016). The more severe impact on host polyp volume and calcification rates may be indicative of increased catabolism of host energetic reserves to repair damaged cells and upregulate production of antioxidants capable of detoxifying ROS (Wooldridge, 2010).

The modification of septal thickness as a stress response is a previously unreported observation in zooxanthellate corals. However, the thickening of theca and other skeletal elements is known to contribute towards the formation of bands of high-density in coral skeletons, which can be used to infer seasonal environmental conditions and/or thermal bleaching events (Dávalos-Dehullu, Hernández-Arana and Carricart-Ganivet, 2008; Fouke, Trop and Sivaguru, 2021). However, bleaching events resulting in reduced extension and calcification rates that lead to the thickening of skeletal elements may not be unequivocally attributable to thermal stress, but have also been reported as a consequence of chronic nutrient stress in *Acropora polystoma* (Buckingham *et al.*, 2022). In the present study, skeletal thickening as a consequence of nutrient stress has been observed in a second, taxonomically and morphologically distinct species. This is potentially a key finding for paleoclimatology; if skeletal element thickening is a nutrient-stress response common among zooxanthellate corals, it may have implications for the reliable proxy use of skeletal high-density bands to reconstruct the thermal stress histories of coral communities. Alternatively, the findings of this study may provide an opportunity. In HNLP and LNLP corals, bleaching was associated with the loss of tissue thickness and homogenisation of theca thickness v depth profiles. Meanwhile, in the unbleached LNHP corals the undersupply of P limited polyp growth but tissue thickness was preserved, and skeletal thickening retained the normal theca thickness v depth profile. This may provide the basis for a more empirical method of distinguishing between ‘stress bands’ caused by bleaching and seasonally occurring high-density bands that occur due to restricted coral growth under conditions of limited nutrients and/or light. At present such distinctions are made rather arbitrarily. For example, DeCarlo and Cohen (2017) defined a ‘stress band’ as a band that is anomalous to the previous 7-year period with respect to dissepiment spacing and bulk calcification rate. Barkley *et al.* (2018) cited a similarly arbitrary definition by considering

a ‘stress band’ to be a widespread band throughout the full extent of a colony within which the density anomaly exceeds 2 standard deviations of the seasonal signal. It is possible that differences between theca thickness v depth profiles can be used to distinguish between periods of growth limitation and episodes of coral bleaching, but further experimental studies will be required to verify this.

The N:P ratios (>200:1) reported here, and which are so detrimental to coral health are much higher than those found even on anthropogenically disturbed reefs, partially due to the magnification that occurs when P values approach zero. But N:P ratios of > 70:1 have been reported from reef waters in the field and are associated with the decline of zooxanthellate corals (Spencer Davies, 1990; Lapointe, 1997; Szmant, 2002; Lapointe, Tewfik and Phillips, 2021). Furthermore, even a modest increase from ~10:1 to ~27:1 has been linked to coral reef decline (Lapointe *et al.*, 2019) suggesting that acclimation to ambient conditions may also influence the sensitivity of corals to changes in N:P stoichiometries. Finally, it should also be noted that the impacts of skewed N:P ratios are less pronounced at lower nitrate (< 0.7 μM) or higher phosphate concentrations (> 0.3 μM) (Rosset *et al.*, 2017) demonstrating that both N:P stoichiometries and absolute concentrations must be considered if the potential impacts of nutrient pollution are to be properly assessed and managed. Nutrient pollution is one of the primary threats to the persistence of coral reef ecosystems (GCRMN, 2020) and our findings demonstrate that if nutrification results in chronic exposure to high N:P ratios, it may have direct impacts on the nutritional status of corals that are recorded in the size, shape and skeletal structure of corallites. Local practitioners responsible for managing and mitigating anthropogenic disturbances on reefs must take a holistic approach to assessing the impacts of nutrient pollution by considering both nutrient concentrations and resultant seawater N:P stoichiometries.

Chapter 4 - Imbalanced nutrient enrichment and severe nutrient limitation alter stable isotope ratios and trace element contents in the skeletons of *Acropora polystoma* and *Euphyllia paradivisa*

4.1. Abstract

Nutrient stress caused by skewed seawater nitrogen (N): phosphorus (P) ratios or strongly limiting N and P concentrations causes temperature-independent bleaching in zooxanthellate corals, and can impact skeletal growth and microstructural properties. The stable isotope and trace element (TE) contents of coral skeletons are widely used as environmental proxies, and also to investigate coral physiology. However, the impacts of nutrient stress on these geochemical markers have not yet been characterised. To determine the impacts on coral geochemistry replicates of *Acropora polystoma* and *Euphyllia paradivisa* were cultured under four different nutrient treatments: - high nitrate: high phosphate (HNHP), high nitrate: low phosphate (HNLP), low nitrate: high phosphate (LNHP) and low nitrate: low phosphate (LNLP). Skeletal $\delta^{13}C$ and $\delta^{18}O$ ratios were determined using isotope ratio mass spectrometry (IRMS) while Li/Ca, Mg/Ca, Sr/Ca and B/Ca ratios were measured using laser ablated inductively coupled plasma mass spectrometry (ICP-MS). The geochemical responses to the HNHP, HNLP and LNLP treatments were broadly similar in both species. Large differences in skeletal Li/Ca, Mg/Ca, Sr/Ca and $\delta^{18}O$ values attributable to the treatment effects led to erroneously large proxy-derived estimations of temperature difference between treatment tanks. In contrast, the Li/Mg paleothermometer was less susceptible to disruption by nutrient stress. Li/Ca and Mg/Ca ratios were largely controlled by Rayleigh fractionation and potentially by differences in the isolation of the calcifying fluid. Correlations between skeletal $\delta^{13}C$ and Sr/Ca, B/Ca and $\delta^{18}O$ values were consistent with the carbonate chemistry of the calcifying fluid being modified by reduced photosynthesis in bleached corals. Differences in the geochemistry of HNLP and LNLP corals suggest that P-starvation of the symbionts exerts an additional influence on carbonate chemistry that impacts the skeletal incorporation of TE's and stable isotopes. Nutrient-stress mediated bleaching impacts coral skeletal geochemistry and may complicate the use of stable isotope and trace element ratios as environmental proxies.

4.2. Introduction

The geochemistry of coral skeletons provides useful tools to investigate paleo-, historic and contemporary changes to environmental and oceanographic conditions (Montaggioni *et al.*, 2006; Swart *et al.*, 2010; Barkley *et al.*, 2018). For example, trace element to calcium (TE/Ca) ratios such as Li/Ca, Mg/Ca and Sr/Ca and the stable isotope ratio ^{18}O:^{16}O have all been identified as potential paleo-thermometers (Weber and Woodhead, 1972; Beck *et al.*, 1992; Mitsuguchi *et al.*, 1996; Marriott, Henderson, Belshaw, *et al.*, 2004; Marriott, Henderson, Crompton, *et al.*, 2004), while B/Ca (in tandem with $\delta^{11}B$) can be used to constrain carbonate chemistry of the external seawater (D'Olivo *et al.*, 2019) and internal calcifying fluid (Holcomb *et al.*, 2016; McCulloch *et al.*, 2017; Decarlo, Holcomb and McCulloch, 2018). Knowledge of the processes governing coral geochemistry can also help when investigating the physiology of corals. For instance, skeletal $\delta^{13}C$ values can be used as proxies for symbiont photosynthesis (Swart, 1983; McConnaughey, 1989a, 1989b; Reynaud-Vaganay *et al.*, 2001; Frankowiak, Wang, *et al.*, 2016), while the relationships between TE/Ca ratios can indicate the degree to which the calcifying fluid is isolated from the external medium (Ram and Erez, 2021). As such, coral geochemical proxies are increasingly being used to investigate the impacts and extent of bleaching episodes on coral reefs (D'Olivo and McCulloch, 2017; Barkley *et al.*, 2018; Schoepf *et al.*, 2021), particularly because mass bleaching events are becoming so frequent and widespread that continuous monitoring of reef conditions is now impractical at all affected sites. Repeated mass bleaching events caused by thermal stress pose an immediate threat to the long-term survival of coral reef ecosystems globally (Hughes *et al.*, 2017a; Lough, Anderson and Hughes, 2018; GCRMN, 2020; Pörtner et. al., 2022). It is therefore crucial that the limitations and reliability of geochemical proxies are fully understood to best inform knowledge-based strategies for preserving these vital ecosystems. However, recent studies have demonstrated that bleaching may also be caused by temperature-independent nutrient stress, arising from imbalanced nitrate enrichment that results in high seawater nitrogen: phosphorus (N:P) ratios (Wiedenmann *et al.*, 2013; D'Angelo and Wiedenmann, 2014; Rosset *et al.*, 2017). These conditions also impact skeletal growth and structural properties such as skeletal element thickness and porosity (Buckingham *et al.*, 2022, Chapter 3). Previous studies have identified that both linear extension and calcification rates may influence TE/Ca ratios (Inoue *et al.*, 2007; Gabitov *et al.*, 2008, 2011). However, the impacts of skewed N:P stoichiometries on skeletal geochemistry have

not yet been thoroughly investigated, and the sensitivities of trace element and isotopic ratios to different forms of nutrient stress are unclear.

Coral skeletons are precipitated from a semi-isolated calcifying fluid (cf) composed of modified seawater, enclosed in a sub-micrometre space between the calicoblastic cells of the coral ectoderm and the existing skeleton/ substrate (reviewed in Tambutté *et al.*, 2011). In seawater, ions of calcium (Ca^{2+}) and dissolved inorganic carbon (DIC) which constitute the primary ingredients of coral skeletons are abundant. But, to induce precipitation of a calcium carbonate ($CaCO_3$) skeleton the coral must elevate $[Ca^{2+}]_{cf}$ and/or $[CO_3^{2-}]_{cf}$ to increase the saturation state of the calcifying fluid (Ω_{cf}) (Holcomb *et al.*, 2009). $[Ca^{2+}]_{cf}$ is elevated by the active transport of Ca^{2+} ions into the calcifying space by Ca-ATPase, which also elevates pH_{cf} by transporting H^+ ions in the opposite direction (Al-Horani, Al-Moghrabi and De Beer, 2003b). The upregulation of pH_{cf} causes re-speciation of DIC which increases $[CO_3^{2-}]_{cf}$, a process that is aided by the presence of carbonic anhydrase (Al-Horani, Al-Moghrabi and De Beer, 2003a). It has also been suggested that bicarbonate (HCO_3^-) transporters provide an additional source of DIC that serves to further increase $[CO_3^{2-}]_{cf}$ (Zoccola *et al.*, 2015). Ca-ATPase activity requires energy, and increases when photosynthesis rates are high, alongside respiration and ATP production (Al-Horani, Al-Moghrabi and De Beer, 2003a, 2003b), and such conditions are associated with rapid calcification rates (reviewed in Gattuso, Allemand and Frankignoulle, 1999). These conditions are also associated with an increased supply of DIC to the calcifying fluid. This is due to enhanced production of metabolic CO_2, which diffuses into the calcifying fluid down a concentration gradient created by the high pH_{cf}, and which provides the majority of carbon incorporated into the coral skeleton (Furla *et al.*, 2000; Al-Horani, Al-Moghrabi and De Beer, 2003b).

Paracellular leakage of unmodified seawater into the calcifying fluid has been demonstrated by the skeletal incorporation of cell impermeant molecules such as Calcein® and rare earth element tracers (E. Tambutté *et al.*, 2011; Gagnon, Adkins and Erez, 2012; Venn *et al.*, 2020), and represents the initial source of calcifying fluid which is subsequently modified by the coral. This leakage results in a supply of trace elements (TE) to the calcifying fluid at the same concentrations as they are found in the surrounding seawater, and these elements subsequently become incorporated into the skeleton at different rates. Skeletal TE incorporation rates are determined by 1) 'kinetic' effects which

control precipitation rates through thermodynamics and/or the saturation state of the calcifying fluid (Ω_{cf}), and 2) 'metabolic' effects that are biologically mediated by the coral and/or its symbionts. The rate at which a particular TE is incorporated into the coral skeleton is given by its distribution coefficient ($D_{El/Ca}$), with the coral skeleton being enriched relative to seawater with elements for which the $D_{El/Ca} > 1$, and depleted relative to seawater with elements for which $D_{El/Ca} < 1$. However, the environment can impact $D_{El/Ca}$. As an example, the respective $D_{El/Ca}$ values for skeletal Li/Ca, Mg/Ca and Sr/Ca, are all temperature dependent (Marriott, Henderson, Belshaw, *et al.*, 2004; Marriott, Henderson, Crompton, *et al.*, 2004; Gaetani and Cohen, 2006) and this is what distinguishes them as potential paleothermometers. However, skeletal Li/Ca and Mg/Ca ratios are also positively correlated with precipitation rate (Gabitov *et al.*, 2008, 2011) which is controlled by the saturation state of the calcifying fluid. Although Ω_{cf} itself is partly controlled by temperature, it is primarily a function of $[Ca^{2+}]_{cf}$ and $[CO_3^{2-}]_{cf}$, which as previously discussed are both biologically mediated by the coral (Furla *et al.*, 2000; Al-Horani, Al-Moghrabi and De Beer, 2003b, 2003a). This means that precipitation rate can change without any change to the ambient temperature and can result in a biological signal that overrides or overprints the thermodynamic signal, a phenomenon known as a 'vital effect' (Pérez-Huerta *et al.*, 2010). In the case of Li/Ca and Mg/Ca ratios, this complication has been overcome by the recognition that skeletal Li/Mg ratios are relatively insensitive to 'vital effects" and are now considered a more reliable paleothermometer (Case *et al.*, 2010; Raddatz *et al.*, 2013; Montagna *et al.*, 2014; Marchitto *et al.*, 2018). Skeletal Sr/Ca ratios have also been widely employed as a paleo-thermometer (Beck *et al.*, 1992; Reynaud *et al.*, 2007; Chen *et al.*, 2015; Kuffner *et al.*, 2017; Ross, DeCarlo and McCulloch, 2019) but can also vary between and within coral skeletons as a consequence of 'vital effects' (Holcomb *et al.*, 2009; Brahmi *et al.*, 2012). The nature and causes of the 'vital effects' impacting skeletal Sr/Ca remain poorly understood and differ from those affecting Li/Ca and Mg/Ca (Holcomb *et al.*, 2009; Brahmi *et al.*, 2012). However, it has been noted that thermal-stress mediated bleaching impacts skeletal Sr/Ca ratios and it is possible this may in some way be linked to changes to $[DIC]_{cf}$ (Allison and Finch, 2010b; Schoepf *et al.*, 2021). Despite the problems that 'vital effects' can cause, TE/Ca ratios remain in use as proxies and improved knowledge of the multiple controls on skeletal Li/Ca, Mg/Ca and Sr/Ca ratios has led to their use in investigating physiological processes, such as those which control the spatial heterogeneity of skeletal geochemistry or the impacts of bleaching (Holcomb *et al.*, 2009; Rollion-Bard and Blamart, 2015; D'Olivo and

McCulloch, 2017; Schoepf *et al.*, 2021). Often the interpretation of these proxies is complemented by measurements of skeletal B/Ca which is controlled by the ratio between borate and carbonate ions in the calcifying fluid ($[B(OH)_4^-]/[CO_3^{2-}]_{cf}$) and can be used in conjunction with skeletal $\delta^{11}B$ values to fully constrain carbonate chemistry of the calcifying fluid (Holcomb *et al.*, 2016; McCulloch *et al.*, 2017; Decarlo, Holcomb and McCulloch, 2018).

The stable isotope contents of coral skeletons are also governed by 'kinetic' and 'metabolic' effects (Swart, 1983; McConnaughey, 1989a, 1989b; Adkins *et al.*, 2003). The fractionation of oxygen (^{16}O and ^{18}O) isotopes between $CaCO_3$ and H_2O is temperature dependent (Urey, 1947; McCrea, 1950), leading to the recognition that $\delta^{18}O$ values in biological carbonates can be used as paleothermometers (Epstein and Mayeda, 1953). However, oxygen isotopes are also differentially fractionated between DIC species as a result of seawater pH (Usdowski and Hoefs, 1993). Because calcification in corals occurs too rapidly for equilibration to be attained between DIC species, the $\delta^{18}O$ of coral skeletons typically reflects the pH_{cf} to some extent (Adkins *et al.*, 2003; Rollion-Bard, Chaussidon and France-Lanord, 2003; Devriendt, Watkins and McGregor, 2017). However, there are several pathways by which DIC enters the calcifying space: - paracellular transport of all DIC species, metabolic CO_2 diffusion and active bicarbonate transport (Furla *et al.*, 2000; Al-Horani, Al-Moghrabi and De Beer, 2003b; Allison and Finch, 2010a; Zoccola *et al.*, 2015). Differences in the degrees to which these DIC species have already equilibrated with their previous environments and to which they subsequently equilibrate with each other in the calcifying space prior to calcification can also impact $\delta^{18}O$ values (Rollion-Bard, Chaussidon and France-Lanord, 2003; Allison and Finch, 2010a). Indeed, Rollion-Bard, Chaussidon and France-Lanord (2003) concluded that pH_{cf} is responsible for the 'vital effect" that disrupts the temperature signal of coral skeletal $\delta^{18}O$ values but that this also reflects the kinetics of isotopic equilibration with water before calcification. $\delta^{11}B$ is widely recognised as a more reliable proxy for pH_{cf} (Holcomb *et al.*, 2016; McCulloch *et al.*, 2017; Decarlo, Holcomb and McCulloch, 2018).

The skeletal $\delta^{18}O$ and $\delta^{13}C$ values of deep sea (azooxanthellate) corals form a linear relationship that passes through seawater equilibrium, indicating that temperature and pH affect the fractionation of both isotopes between DIC species in the calcifying fluid in a

similar manner (McConnaughey, 1989b, 2003; Adkins *et al.*, 2003). But the skeletons of zooxanthellate corals are relatively enriched in $\delta^{13}C$ when compared to deep sea corals (McConnaughey, 1989a, 1989b). This occurs because the zooxanthellae preferentially utilise $^{12}CO_2$ during photosynthesis, thereby enriching the surrounding tissue with $^{13}CO_2$ (Swart, 1983). Metabolic CO_2 diffusion from the coral tissue into the calcifying space provides about 70-75 % of C incorporated into the skeleton so this results in the skeleton becoming enriched in $\delta^{13}C$ (Swart, 1983; Furla *et al.*, 2000). In summary, this means that skeletal $\delta^{18}O$ and $\delta^{13}C$ values are subject to 'kinetic' fractionation but that the conditions governing kinetics are biologically mediated, and that metabolic processes related to photosynthesis may cause an additional 'vital effect' that overprints the temperature and/or pH signals (McConnaughey, 1989a, 1989b; Adkins *et al.*, 2003; Rollion-Bard, Chaussidon and France-Lanord, 2003).

Because the calcifying fluid from which the skeleton is precipitated is present as a semi-isolated reservoir between the calicoblastic cells and the skeleton, Rayleigh fractionation may also affect the skeletal TE content in corals (Gagnon *et al.*, 2007; Gaetani *et al.*, 2011). Trace elements within the calcifying fluid with distribution coefficients ($D_{El/Ca}$) > 1 (such as Sr) are preferentially incorporated into the skeleton relative to Ca, so that as calcification proceeds, the proportion of the element remaining in the fluid decreases. This means that at subsequent steps in the calcification process, the skeleton that forms from this Sr-depleted fluid is also relatively depleted in Sr relative to Ca. Conversely, elements with $D_{El/Ca} < 1$ (e.g. Li, Mg and B) are discriminated against, so that as calcification proceeds the element becomes enriched in the residual fluid. Skeleton that subsequently forms from the element-enriched fluid is consequently also enriched relative to Ca. This means that TE/Ca ratios can be used to calculate the proportion of Ca remaining in the fluid (F_{Ca}) at the time of calcification, and trends between two TE/Ca ratios which have different distribution coefficients can be diagnostic of the process (Stewart, Anagnostou and Foster, 2016). The semi-isolated nature of the calcifying fluid has been demonstrated by measuring the incorporation rates of Calcein®, a cell impermeant dye that is incorporated into the skeleton, and this supports the assertion that paracellular pathways provide a source of unmodified seawater to the calcifying fluid (S. Tambutté *et al.*, 2011; Venn *et al.*, 2020). Infiltration of unmodified water can replenish concentrations of depleted elements in the calcifying fluid or dilute those that are enriched so F_{Ca} can be

considered an indicator of the degree to which the calcifying fluid is isolated (Ram and Erez, 2021). The rate of paracellular seawater transport to the calcifying fluid is sensitive to environmental disturbance and a recent study on *Stylophora pistillata* demonstrated that changes to both seawater pH and temperature can alter paracellular transport rates (Venn *et al.*, 2020). Heat stress-mediated bleaching may also cause the F_{Ca} to increase, indicating a loss of 'precipitation efficiency' that could reflect reduced isolation of the calcifying fluid and/or decreased precipitation rate, and results in skeletal Li/Ca and Sr/Ca values being decreased and increased respectively (D'Olivo and McCulloch, 2017). Furthermore, the degree to which the calcifying fluid is isolated from the external medium differs between genera (Ram and Erez, 2021), potentially offering an explanation for different TE/Ca values being reported between species exposed to the same environmental conditions.

Spatial heterogeneity in the ultrastructure of coral skeletons is also associated with spatial variability in TE/Ca ratios (Holcomb *et al.*, 2009; Case *et al.*, 2010; Montagna *et al.*, 2014). In particular, amorphous granular crystals that form at 'centres of calcification' (COCs) are enriched in Li and Mg (indicative of rapid calcification) while the elongated fibrous crystals that form away from these regions have lower Li/Ca and Mg/Ca ratios (Holcomb *et al.*, 2009; Case *et al.*, 2010; Montagna *et al.*, 2014). The ordering of the crystalline structure is believed to be controlled by the synthesis of an organic matrix by the coral which is composed of excreted proteins, lipids and sugars (reviewed in Dubinsky and Stambler, 2011; S. Tambutté *et al.*, 2011). It has been proposed that the formation of COCs is promoted by magnesium- and sulfate-bearing compounds within this organic matrix which form binding points where calcification occurs fastest (Cuif *et al.*, 2003; Meibom *et al.*, 2004). This results in correspondence between organic matter content, the relative abundance of COCs and TE/Ca ratios (Cuif *et al.*, 2003; Sinclair, 2005; Sinclair, Williams and Risk, 2006). Given that the abundance and spacing between the different forms of crystal structure can vary within corals skeletons this provides another mechanism by which the bulk trace element composition of coral skeletons can be affected (Sinclair, 2005; Sinclair, Williams and Risk, 2006).

The dinoflagellate endosymbionts of the family *Symbiodinium* (LaJeunesse *et al.*, 2018) that reside in the gastrodermis of corals (commonly referred to as zooxanthellae) may supply >90% of the coral's energetic requirements through the translocation of excess carbohydrates, and also provide access to dissolved inorganic nutrients which would

otherwise be unavailable to the animal host (Falkowski *et al.*, 1984, 1993; Davy, Allemand and Weis, 2012; Rädecker *et al.*, 2015; Ferrier-Pagès *et al.*, 2016). Thermal stress-mediated bleaching involves the loss of zooxanthellae and the nutritional benefits they provide. If a coral fails to replace its symbiont population rapidly this may prove fatal, a phenomenon that is driving the rapid decline of coral reef ecosystems globally in response to anthropogenic climate change (Lesser, 1997; Hughes *et al.*, 2017a; Lough, Anderson and Hughes, 2018). Thermal-stress mediated bleaching reduces $[DIC]_{cf}$ and $[CO_3^{2-}]_{cf}$ (Schoepf *et al.*, 2021) and this modification of carbonate chemistry has the potential to alter skeletal TE/Ca and isotopic ratios. But, bleaching can also occur due to nutrient stress, whether arising from imbalanced nutrient enrichment that causes skewed N:P ratios or through severe nutrient limitation, and this can affect the growth and structure of coral skeletons (Wiedenmann *et al.*, 2013; D'Angelo and Wiedenmann, 2014; Rosset *et al.*, 2017; Buckingham *et al.*, 2022; Chapter 3). In particular, high N:P ratios cause P-starvation of the symbionts which is evident from altered symbiont lipid membranes and reduced photochemical efficiency (Fv/Fm) (Parkhill, Maillet and Cullen, 2001; Wiedenmann *et al.*, 2013; D'Angelo and Wiedenmann, 2014; Rosset *et al.*, 2017). The impact on coral skeletal structures of bleaching under high N:P ratios can be very similar to those that occur under severely limiting nutrient conditions, e.g. thickening of skeletal elements and reduced skeletal porosity in the branching *Acropora polystoma* (Buckingham *et al.*, 2022). But in *Euphyllia paradivisa,* the formation of dissepiments at shallower depths in the corallite under high N:P ratios indicates greater biomass loss, and therefore suggests a more severe impact on host energetic reserves when the symbionts are P-starved (Chapter 3). This observation is consistent with previous findings that P-starvation of the symbionts reduces carbon translocation to the host and requires greater utilisation of storage lipids to support host metabolism (Ezzat *et al.*, 2015; Tanaka *et al.*, 2017). Such an observation hints that energy requiring processes such as Ca-ATPase activity may be impacted, and this could have implications for skeletal TE/Ca and isotopic ratios. It is evident that nutrient-stress mediated bleaching impacts coral skeletal structures (Buckingham *et al.*, 2022, Chapter 3) but it remains unclear to what extent skeletal geochemistry is impacted or whether any effects are similar to, or different from those observed under thermal-stress bleaching. Therefore, we analysed the skeletal stable isotope and TE/Ca ratios for two coral species exposed to a suite of nutrient treatments during previous studies to investigate the impacts of skewed N:P ratios, nutrient replete and severely limiting nutrient conditions.

4.3. Methods

4.3.1. Coral husbandry

The impacts of nutrient enrichment, skewed N:P stoichiometries and severe nutrient limitation on the physiology and skeletal structure of zooxanthellate corals have previously been reported for *E. paradivisa* (Rosset, D'Angelo and Wiedenmann, 2015; Rosset *et al.*, 2017, Chapter 3) and *A. polystoma* (Buckingham *et al.*, 2022). In this study, the chemical composition of the skeletons of those same corals were analysed to determine whether these different nutrient conditions also impact skeletal geochemistry. Detailed descriptions of the mesocosm set-up (D'Angelo and Wiedenmann, 2012), husbandry and methods for controlling nutrient conditions can be found within the respective publications (Rosset, D'Angelo and Wiedenmann, 2015; Rosset *et al.*, 2017; Buckingham *et al.*, 2022), and only brief summaries are included here.

This series of experiments have investigated the impacts of four different nutrient treatments: - high nitrate: high phosphate (HNHP), low nitrate: low phosphate (LNLP), high nitrate: low phosphate (HNLP) and low nitrate: high phosphate (LNHP). In describing these nutrient treatments, the terms 'high' and 'low' are used only to describe the relative concentrations of N and P within each treatment, and there is no attempt to recreate the conditions found on a particular reef ecosystem. Fragments of *A. polystoma* were cultured under each nutrient treatment for 100 days, during which the mean concentrations of nitrate and phosphate for each treatment were:- HNHP = NO^{3-} ~ 4.5 μM, PO_4^{3-} ~ 0.6 μM, N:P ~8:1; HNLP = NO^{3-} ~0.073 mM, PO_4^{3-} not detectable (method detection limit = 0.21 μM); LNHP = NO^{3-} ~0.06 μM, PO_4^{3-} ~5.7 μM, N:P ~0.01 and LNLP = NO^{3-} not detectable, PO_4^{3-} not detectable. Light (~125 μmol m^{-2} s^{-1}, 12-hour light/dark cycle), temperature (~27 ℃) and salinity (~33 p.s.u.) were maintained at constant levels throughout (Buckingham *et al.*, 2022). Fragments of *E. paradivisa* were subject to long-term exposure (1.5 years for HNHP and LNLP corals and 6 months for HNLP and LNHP corals) to the same four nutrient treatments, albeit that the mean concentrations differed to a minor degree; HNHP = NO_3^- ~ 6.5 µM: PO_4^{3-} ~ 0.3 µM (N:P ratio ~ 22:1); HNLP = NO_3^- ~ 38 µM: PO_4^{3-} ~ 0.18 µM (N:P ratio ~211:1); LNHP = NO_3^- ~ 0.06 µM: PO_4^{3-} ~ 3.6 µM (N:P ratio ~1:60 and LNLP = NO_2^-/NO_3^- ~0.7, PO_4^{3-} ~0.006 µM (N:P ratio ~ 12:1). Conditions of light (150 μmol m^{-1} s^{-2}, 10/14 hour light/dark cycle), temperature (~25 ℃)

and salinity (~35 p.s.u.) also differed slightly from those used to culture *A. polystoma* but were consistent between treatments (Rosset, D'Angelo and Wiedenmann, 2015; Rosset *et al.*, 2017). The corals of both species were cultured in artificial seawater (Tropic Marin Pro Reef Salt ®) which was subject to weekly partial water changes. All corals remained unfed throughout the respective experiments and, because the relative proportions of dissolved inorganic nitrogen species are typically constant at NO_3^- ~90 %, NO_2^- ~ 10 % and NH^{4+}/NH_3 <0.7 % (Rosset, D'Angelo and Wiedenmann, 2015), it is considered that the experimental addition of nitrate and phosphate constituted the primary sources of nutrition available to the corals of each treatment.

4.3.2. Sample preparation for stable isotope analysis

At the conclusion of the culture phase, all coral skeletons were cleaned of animal tissue using a Waterpick®. Residual organic matter was then removed by repeatedly soaking the skeletons in 10 % NaClO solution (3 times for 30 minutes), followed by further soaks in MilliQ water (18.2 M ohm cm^{-2}) (twice for 2 and 24 hours). The skeletons were then oven dried at 50 ℃ for 24 hours. Powdered samples of coral skeleton (~ 0.1 to ~0.2 g) for stable isotope analysis were micro-milled from the fragments using a Dremel® hand drill. The microstructure of *A. polystoma* is too small to permit the targeting of specific skeletal elements using this technique so samples were obtained from the tip of the axial corallite, providing material from the most recently extended part of the skeleton. Corallites of *E. paradivisa* have larger and more open structures than those of *A. polystoma*, allowing targeted samples to be obtained from distinct skeletal elements. The septa was selected as the site of study because it has previously been shown that septa are the skeletal elements associated with tissue with the highest rates of gross photosynthesis (Al-Horani *et al.*, 2005); accordingly it was surmised that septa geochemistry was most likely to reflect impacts of the coral-zooxanthellae symbiosis on skeletal composition. Milled samples were obtained from the apexes of septa using the same method, providing material from the most recently deposited parts of the skeletons.

4.3.3. Sample preparation for trace element analysis

Fragments of *A. polystoma* and *E. paradivisa* were mounted in 25.4 mm moulds using MetPrep Ltd EPO-FLO low viscosity impregnating resin. Fragments of *A. polystoma* were cut at the base to create a flat surface for mounting upright inside the mould. The base of each coral was then glued to a glass coverslip to ensure they remained upright in the moulds when pouring the resin. In the case of *E. paradivisa*, the top of each coral was glued face down to a glass coverslip to hold them upright in the moulds when pouring the resin. Each mould was filled with resin to above the height of the coral sample before being placed into a vacuum chamber to evacuate any air and impregnate the sample. The samples were then cured at 70 ℃ overnight in an oven. After curing, the samples were removed from the moulds and labelled. Each sample was ground on a 125 µm metal bonded diamond disc using a rotary grinder until the tip was barely exposed. The samples were then lapped using 9.5 µm silicon carbide slurry on a glass plate until all scratches were removed. Finally, the samples were lightly polished on a 30 µm resin bonded diamond disc on a rotary grinder to assist in targeting on the LA-ICPMS.

4.3.4. Stable isotope analysis of coral samples

Isotopic analysis was performed in the Ocean and Earth Science department's stable isotope laboratory at the University of Southampton (National Oceanography Centre), UK. Coral samples were analysed using a Thermo Finnigan Kiel-IV Carbonate Device coupled to a Thermo Finnigan MAT253 isotope ratio mass spectrometer (IRMS). Powdered samples of coral (~ 40 µg) were weighed into borosilicate glass vials and reacted with 106.2 % phosphoric acid in the carbonate device, before the purified CO_2 was analysed using the MAT253 IRMS. Carbon and oxygen stable isotope ratios were normalised using a two-point calibration with NBS-19 and NBS-18 (International Atomic Energy Agency, Vienna, Austria) (Kim, Coplen and Horita, 2015). The reference material JCp-1 (Ed C Hathorne *et al.*, 2013) was used as an independent quality control, with an overall accuracy of 0.06 and 0.05 ‰ for $\delta^{13}C$ and $\delta^{18}O$ respectively, relative to Vienna Pee Dee Belemnite (VPDB). The long-term instrument precision of the device used is 0.03‰ for $\delta^{13}C$ and 0.06‰ for $\delta^{18}O$.

4.3.5. Trace element analysis of coral samples

Laser ablation trace element analysis was conducted in the geochemistry laboratory at The University of Southampton (National Oceanography Centre), UK using an Agilent 8900 ICP-MS Triple Quad ICP mass spectrometer coupled to an Elemental Scientific Lasers (Bozeman, MT, USA) NWR193 excimer laser ablation system with a TwoVol2 ablation chamber. Normalisation of raw trace element values was conducted using bracketed analyses of carbonate reference material JCp-1 and values specified in Hathorne *et al.* (2013). Prior to data collection, all standards and samples were ablated to remove surface contaminants and an on-peak gas blank subtraction was performed using the mean of bracketing gas blank analyses. An internal reference material (deep-sea coral reference PS69/318-1) (Foster *et al.*, 2013) was used as a consistency standard. The accuracy and reproducibility (defined by 2 standard deviations) of the measured skeletal Li/Ca, Mg/Ca and Sr/Ca ratios were both found to be better than $\pm$6.0 %. Li/Mg ratios were calculated using the measured Li/Ca and Mg/Ca values, and therefore the accuracy and precision values for Li/Mg are the sum of the respective values for Li/Ca and Mg/Ca. The accuracy and precision of the measured B/Ca ratios were both found to be better than $\pm$15 % and better than $\pm$3 %, respectively. Due to difficulties in resolving the micro-scale skeletal lattice structure of *A. polystoma* from the polished surfaces of the mounted samples, specific skeletal elements (such as septa or theca) could not be targeted within the skeletons. Instead, three 50 µm-wide ablation tracks were ablated from each sample at points where the skeletal surface available for ablation was wider than the width of the chosen ablation track. For *E. paradivisa*, the identification and targeting of specific skeletal elements was more straightforward and ablation tracks (50 µm wide) were taken from three different septa of each sampled corallite. The data for all samples was screened, and any cycles greater than 3 standard deviations from the mean were removed. A mean value for each TE/Ca content was then calculated for each coral using the three measurements. The representative uncertainties (expressed as 2σ) for each TE/Ca ratio that are presented in the figures of the results sections are the sum of the %age accuracy and %age precision (2 x standard deviations) values that were determined from repeated measures of the deep-sea reference material (PS69/318-1).

4.3.6. Normalisation of skeletal TE/Ca to culture medium TE/Ca concentrations

Dissolved trace element concentrations of the culture mediums were determined using quadrupole inductively coupled plasma–mass spectrometry (ICP-MS; Thermo Scientific X-Series). Standards and samples were prepared using 3% HNO_3 spiked with 5 ppb In, 5 ppb Re, and 20 ppb Be, which act as an internal calibration to monitor drift, and correct for mass bias in the absence of full bracketing standard procedure. The samples were then run against a multielement solution, gravimetrically determined and diluted to bracketing concentrations. The accuracy and precision of measurements were monitored by repeated measures of the internal consistency standards and the Mediterranean seawater standard IAEA-B1(Gonfiantini *et al.*, 2003; Tonarini *et al.*, 2003). The representative uncertainties (expressed as 2σ) for each TE/Ca ratio that are presented in the figures of the results sections are the sum of the %age accuracy and %age precision (2 x standard deviations) are Li/Ca = $\pm$23.2 %, Mg/Ca = $\pm$4.4 %, Sr/Ca = $\pm$4.6 % and B/Ca = $\pm$3.9 %. Trace element concentrations varied between the different nutrient treatment culture mediums so, to allow meaningful comparison between treatments the measured skeletal TE/Ca ratios were normalised against published TE seawater concentrations using the equation: $TE/Ca_{SkeletonNormalised} = TE/Ca_{Skeleton} * (TE/Ca_{CultureMedium}/ TE/Ca_{Seawater})$. The following values for seawater TE/Ca ratios were used $[Ca^{2+}]$ = 10.3 mmol kg^{-1}, $[Mg^{2+}]$ = 52.8 mmol kg^{-1}, $[Sr^{2+}]$ = 90.7 µmol kg^{-1} (Millero *et al.*, 2008) and $[Li^{+}]$ = 25.9 µmol kg^{-1} (Li, 1991).

4.3.7. Rayleigh fractionation models

The two coral species were not cultured alongside each other so individual Rayleigh fractionation models were constructed for each species and nutrient treatment. Models were constructed assuming the non-normalised values of the respective culture mediums to be the same as the starting composition of the calcifying fluid (FCa = 1.0), and using the following partition coefficients:- $K_d^{Li/Ca}$ = 0.00104 (Montagna *et al.*, 2014), $K_d^{Mg/Ca}$ = 0.000235, $K_d^{B/Ca}$ = 0.0037 (Stewart, Anagnostou and Foster, 2016) and $K_d^{Sr/Ca}$ = 1.13 (Gaetani and Cohen, 2006). The values plotted against these models (and which have been used to aid visualisation of the impact of Rayleigh fractionation) are the non-normalised TE/Ca values from each of the laser ablated tracks. This allowed for a greater number of data points than if the averaged values referred to in the main data analysis had been used.

Finally, the models were run using the R script from Stewart, Anagnostou and Foster (2016).

4.3.8. Statistical analysis

All statistical analyses were conducted using R (version 4.0.3). Differences between treatments in the contents of multiple trace elements (Li/Ca, B/Ca, Mg/Ca and Sr/Ca) were assessed using a robust MANOVA (non-parametric) approach following the method described in Munzel and Brunner, (2000) and implemented using the *mulrank()* function (Wilcox, 2005). The robust MANOVA was followed up by discriminant function analysis (DFA) to describe the functions (variates) responsible for the variance between treatments. Post-hoc two-way ANOVA tests were used to determine differences between species and treatments and to identify any significant interaction between treatment and species (which in this case indicates a difference in the response between species). Relationships between stable isotopes and/or trace elements have been described using both simple regression and multiple linear regression (MLR) models. Where MLR models have been presented, they were first compared to the best fitted simple regression model that could be constructed using just one predictor variable. The MLR model was only preferred when it was found to be both significantly different (ANOVA, $p < 0.05$) and a better fit than the simple regression, as indicated by having a lower Akaike Information Criterion (AIC) score.

4.4. Results

4.4.1. Impacts on skeletal $\delta^{13}C$ and $\delta^{18}O$

Two-way ANOVA confirmed significant species, treatment and interaction effects on skeletal $\delta^{13}C$ *($p < 0.001$ in all cases),* with values being significantly higher in *A. polystoma ($p < 0.001$)*. The significant interaction between treatment and species indicated that the nutrient treatments impacted skeletal $\delta^{13}C$ differently in the two species. This was particularly evident from the depletion of skeletal $\delta^{13}C$ under LNLP conditions, which was more substantial in *E. paradivisa*. HNHP and LNLP treatments were typically associated with higher and lower skeletal $\delta^{13}C$ values, respectively, for both species, but this difference was only statistically significant in *E. paradivisa* (Figure 4.1a). Skeletal $\delta^{18}O$ values were higher in *A. polystoma (Two-way ANOVA, $p < 0.001$)* and were also

significantly impacted by nutrient treatment *($p < 0.001$)*. A significant interaction between species and treatment *($p = 0.002$)* indicated that the effects of the nutrient treatments differed for the two species. Specifically, the HNLP treatment was associated with reduced skeletal $\delta^{18}O$ in both species but $\delta^{18}O$ was more strongly enriched in *A. polystoma* relative to *E. paradivisa* when cultured under LNHP conditions (Figure 4.1b).

A linear regression was fitted to assess the relationship between skeletal $\delta^{13}C$ and $\delta^{18}O$ for both species. In *A. polystoma,* a negative correlation between skeletal $\delta^{13}C$ and $\delta^{18}O$ ($r^2 = 0.52, p = 0.02$) was detected, but only after the exclusion of two anomalously low $\delta^{13}C$ values in HNLP corals (Figure 4.2a). In contrast, a very strong and negative relationship ($r^2 = 0.92, p < 0.001$) between skeletal $\delta^{13}C$ and $\delta^{18}O$ was observed in *E. paradivisa* (Figure 4.2b), suggesting tighter coupling between calcifying fluid $\delta^{13}C$ and $\delta^{18}O$.

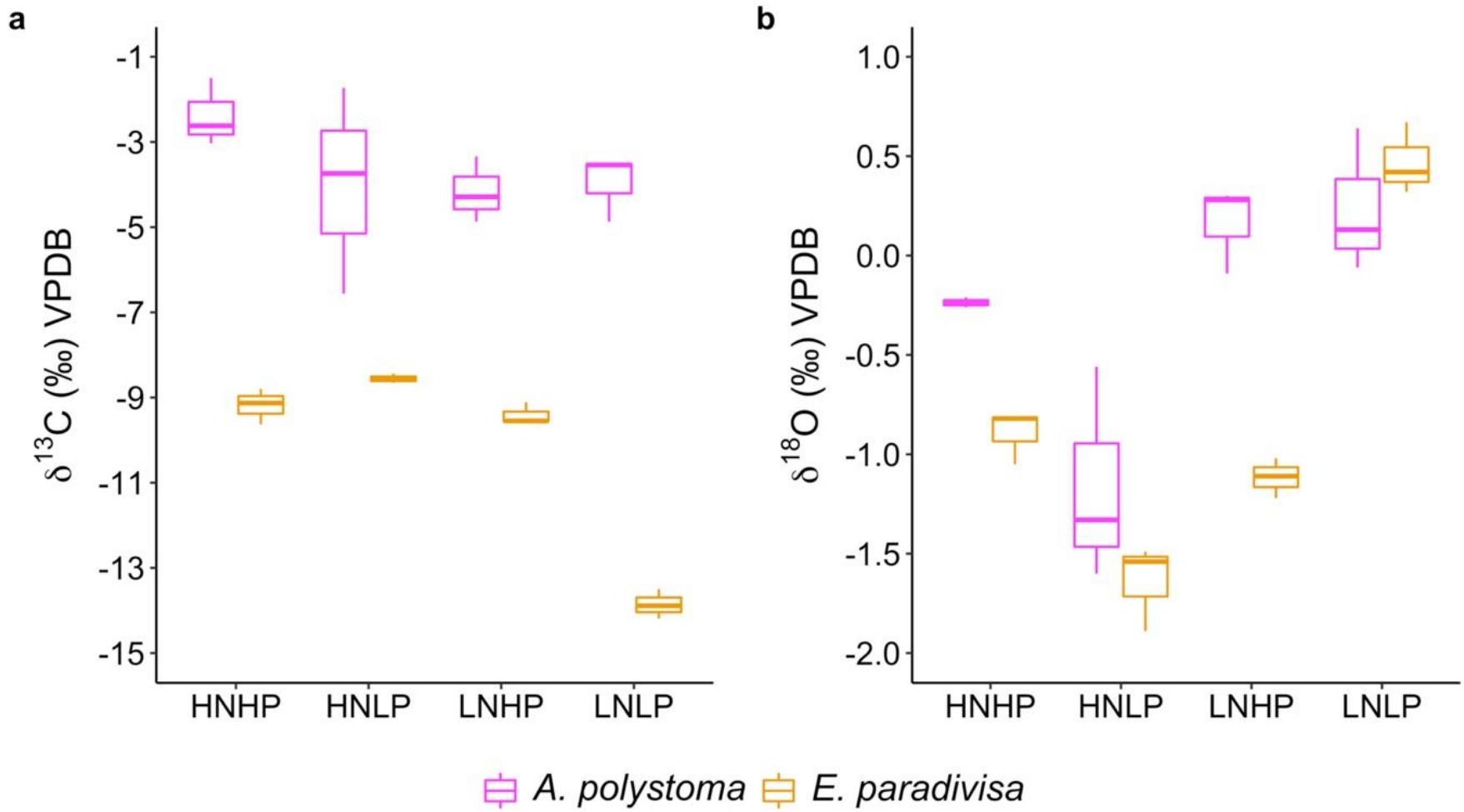

Figure 4.1. Skeletal stable isotope contents ($\delta^{13}C$ and $\delta^{18}O$) for *A. polystoma* and *E. paradivisa* after exposure to four different nutrient treatments. a) Skeletal $\delta^{13}C$ and b) skeletal $\delta^{18}O$. Stable isotope values were measured using IRMS with samples being obtained from the most recently extended portion of the skeleton. HNHP = high nitrate: high phosphate, HNLP = high nitrate: low phosphate, LNHP = low nitrate: high phosphate and LNLP = low nitrate: low phosphate. *(n = 3).*

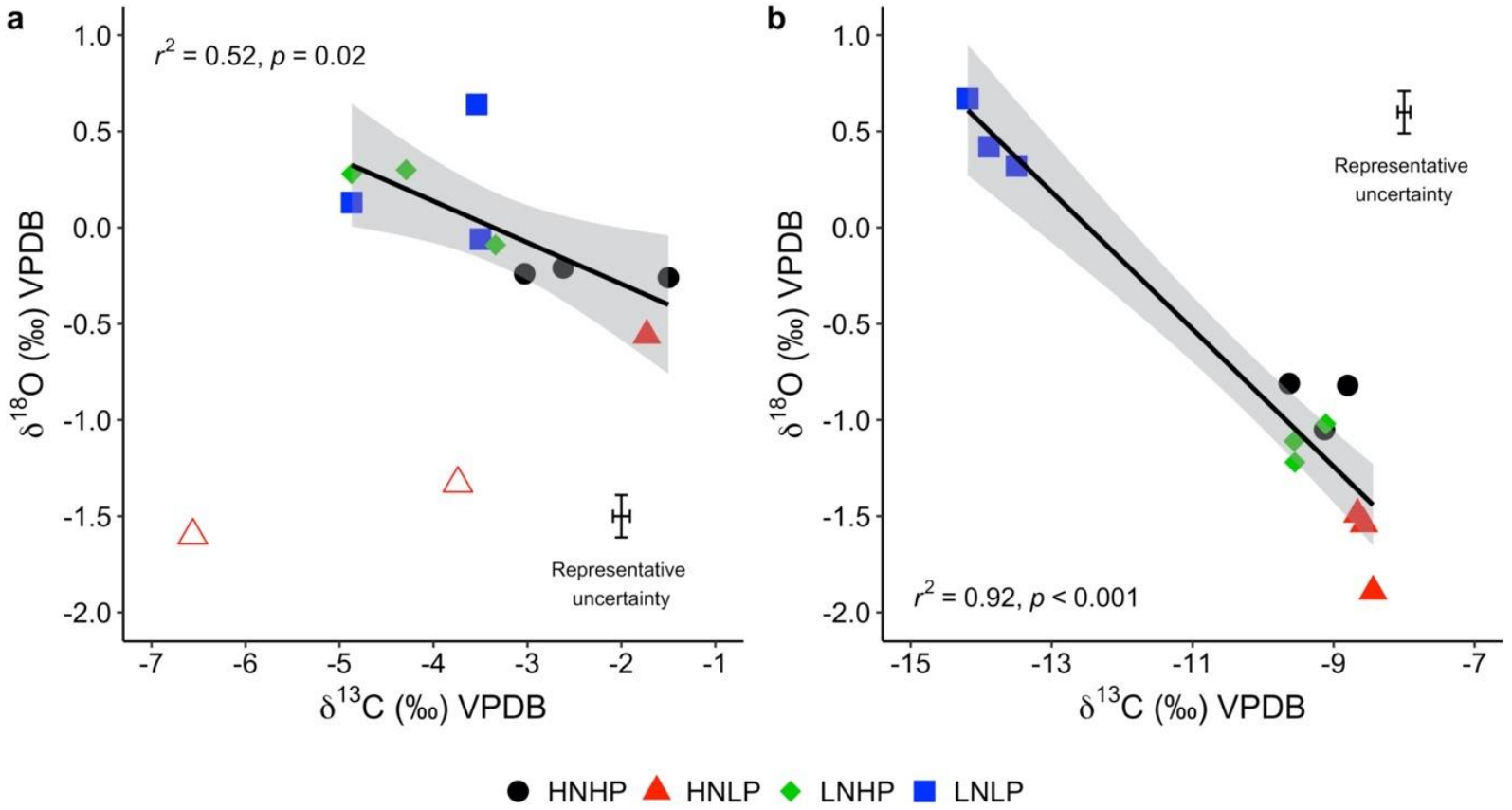

Figure 4.2. The relationship between skeletal δ^{13}C and δ^{18}O in a) *A. polystoma*, and b) *E. paradivisa* after exposure to four different nutrient treatments. In Figure A, the unfilled triangles for HNLP corals have been excluded from the fitted model (see main text). Each data point represents a single coral fragment in the case of *A. polystoma* and a single corallite in the case of *E. paradivisa*. All samples were obtained from most recently extended section of the respective fragment or corallite. Grey shading indicates the 95% confidence interval of the fitted model while the representative uncertainties for both isotopes are equal to 2σ (as determined by repeated measures of a standard reference material). HNHP = high nitrate: high phosphate, HNLP = high nitrate: low phosphate, LNHP = low nitrate: high phosphate and LNLP = low nitrate: low phosphate.

4.4.2. Impacts on Li/Ca, B/Ca, Mg/Ca and Sr/Ca

The skeletal concentrations of Li, B, Mg and Sr (expressed as TE/Ca) for both species are shown in Figure 4.3. A multivariate approach was used to assess differences in the TE/Ca contents between treatments for both species, thus reducing the likelihood of incorrectly failing to reject a null hypothesis (type II error). Structuring of the data frames for the two species in the same format allowed for direct comparison between the two species by considering the normalised skeletal values of Li/Ca, B/Ca, Mg/Ca and Sr/Ca. The robust MANOVA tests identified a significant effect of nutrient treatment on the trace element composition of *A. polystoma* ($F = 3.67$, $p = 0.006$) and *E. paradivisa* ($F = 11.3$, $p < 0.001$).

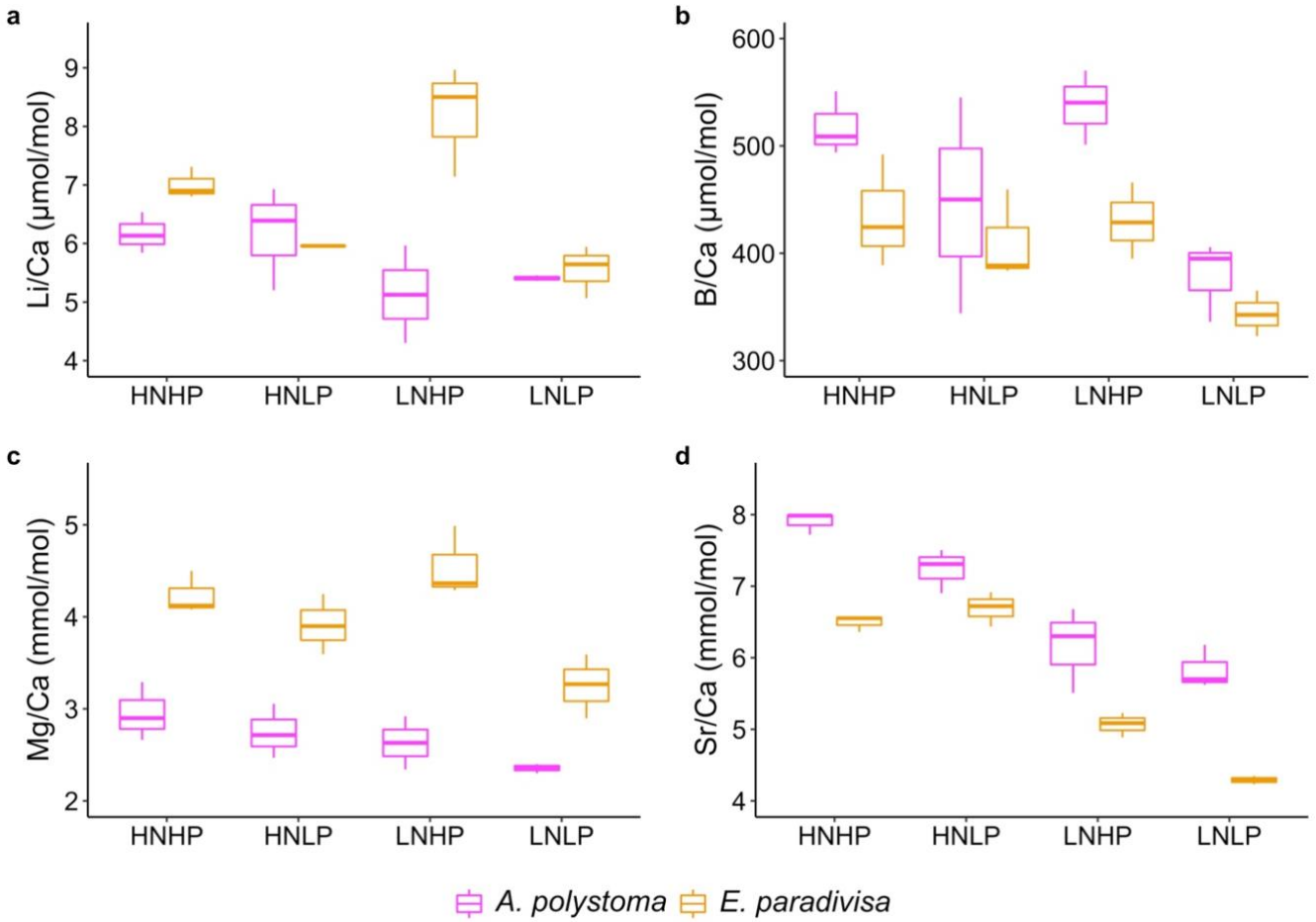

Figure 4.3. Selected skeletal TE/Ca contents of *A. polystoma* and *E. paradivisa* after exposure to four different nutrient treatments. a) Li/Ca, b) B/Ca, c) Mg/Ca and d) Sr/Ca. All TE/Ca contents were obtained from samples of the most recently extended section of the fragment/ corallite and measured using LA-ICP-MS. HNHP = high nitrate: high phosphate, HNLP = high nitrate: low phosphate, LNHP = low nitrate: high phosphate and LNLP = low nitrate: low phosphate *(n = 3).*

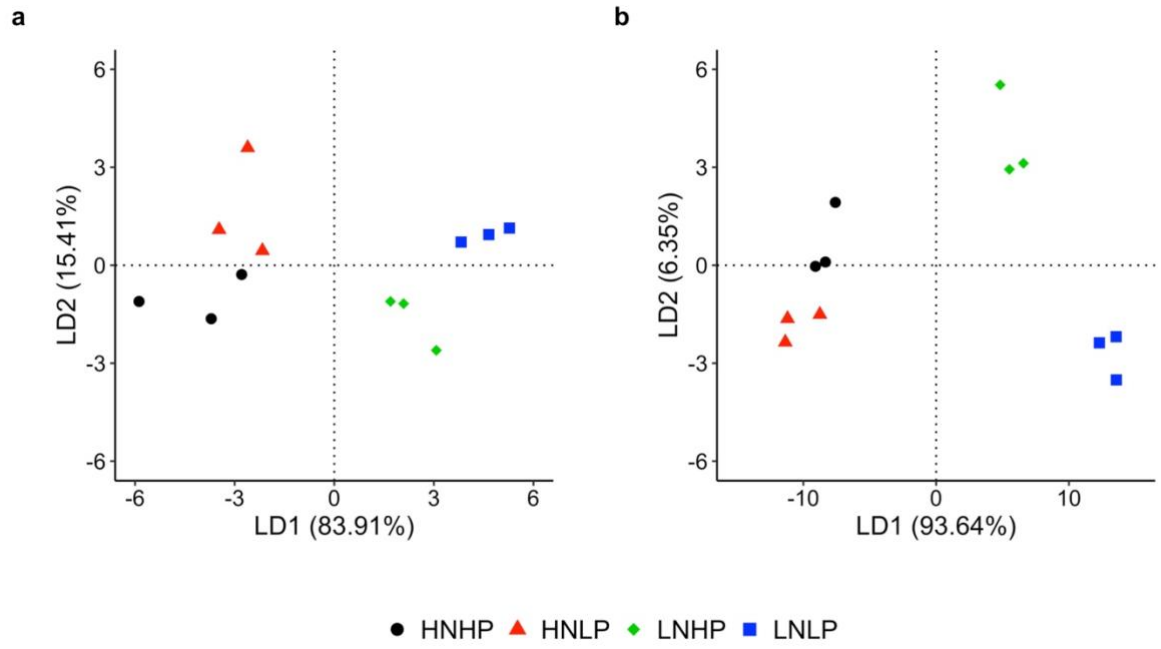

Figure 4.4. Discriminant function analyses relating to the skeletal TE/Ca contents of Li, B, Mg and Sr in a) *A. polystoma* and b) *E. paradivisa* after exposure to four different nutrient treatments. LD1 and LD2 refer to the to the two linear discriminant functions responsible for describing the majority of the variance between the treatments. Bracketed values indicate the percentage of the total variance described by each linear discriminant function. Each data point relates to a single coral fragment (*A. polystoma*) or corallite (*E. paradivisa*). The dashed lines through zero on each axis have been inserted to aid the visual interpretation of each plot. HNHP = high nitrate: high phosphate, HNLP = high nitrate: low phosphate, LNHP = low nitrate: high phosphate and LNLP = low nitrate: low phosphate.

The nature of the differences between treatments for both species were subsequently investigated using discriminant function analysis (DFA). In both cases, two linear discriminant (LD) functions were found to account for > 99% of the variance between treatments, and were sufficient to distinguish the coral skeletons of the different treatments in the same manner; LD1 differentiated HNHP and HNLP corals from those cultured in the LNHP and LNLP treatments, while LD2 differentiated HNHP and LNHP corals from HNLP and LNLP corals (Figure 4.4).

When interpreting the output of DFA, the values of coefficients represent the relative contribution of each variable to each linear discriminant function (variate), while the sign of the coefficient (+/-) indicates whether the relationship between the variable and the respective variate is positive or negative. The output for each DFA is shown in Table 4.1. For *A. polystoma*, the first discriminant function explained 83.91% of the variance and

differentiated the effect on Li/Ca from the other trace elements. Mg/Ca and Sr/Ca were the variables that contributed to the greatest difference between treatments. The second discriminant function (accounting for 15.47% of the variance) differentiated Li/Ca and Sr/Ca from B/Ca and Mg/Ca. For both variates, Mg/Ca was the variable that made the greatest relative contribution to the differences between treatments. For *E. paradivisa*, a greater proportion of the variance was described by the first discriminant function (93.64%). This function was different than for *A. polystoma* in that it did not differentiate the effect on Li/Ca from Mg/Ca and Sr/Ca. Furthermore, a much greater relative contribution to the variance described by LD1 was made by Sr/Ca than for *A. polystoma*. The second discriminant function was very similar to that of *A. polystoma*, except that it again affected Li/Ca differently and was of less importance to the overall variance between treatments. In summary, the DFA's indicated that the nature of TE/Ca variance due to the nutrient treatments was broadly similar for both species and that the most noteworthy difference was primarily with respect to the impacts on Li/Ca. In *A. polystoma*, differences in the treatment effect were driven by Mg/Ca and Sr/Ca while in *E. paradivisa*, differences between treatments were dominated by variance in Sr/Ca.

Table 4.1. Discriminant function analyses relating to the skeletal TE/Ca contents of Li, B, Mg and Sr in *A. polystoma* and *E. paradivisa* after exposure to four different nutrient treatments. For each analysis, the percentage of the total variance between treatments described by each linear discriminant function (LD) is indicated by the bracketed values. The values in columns 2 and 3 are the coefficients of the respective trace elements within each LD. The values of the coefficients indicate the relative importance of each variable within the respective variate, while the +/- signs indicate whether variables are positively or negatively correlated to the respective linear discriminant function.

A. polystoma	LD1 (83.91%)	LD2 (15.47%)
Li/Ca	0.497	-2.53
B/Ca	-0.002	0.016
Mg/Ca	-3.36	4.87
Sr/Ca	-2.88	-0.777
E. paradivisa	LD1 (93.64%)	LD2 (6.35%)
Li/Ca	-0.394	1.11
B/Ca	0.028	0.021
Mg/Ca	-0.643	1.94
Sr/Ca	-10.4	-0.959

Two-way ANOVA's were subsequently conducted to further aid the comparison between species. Li/Ca, B/Ca, Mg/Ca and Sr/Ca were all significantly impacted by nutrient

treatment *($p \leq 0.005$ in all cases)*. Li/Ca *($p < 0.001$)* and Mg/Ca *($p < 0.001$)* were significantly higher in *E. paradivisa*, and significant interactions between species and treatment confirmed that the nutrient treatments affected the incorporation of Li and Mg differently in the two species *($p < 0.05$ in both cases)*. B/Ca was higher in *A. polystoma* *($p = 0.005$)* and a significant effect of nutrient treatment was observed *($p = 0.002$,)* but there was no interaction between species and treatment *($p = 0.52$)*, suggesting that the B/Ca contents of both species were impacted in the same way by the nutrient treatments. Sr/Ca was higher in *A. polystoma* *($p < 0.001$)* and was significantly impacted by nutrient treatment *($p < 0.001$)*. A significant interaction between species and treatment *($p = 0.04$)* indicated that the nutrient treatments affected the skeletal incorporation of Sr differently in the two species. Two-way ANOVA was also conducted on Li/Mg content for both species (Figure 4.5). Li/Mg was significantly higher in *A. polystoma* *($p < 0.001$)* but was not affected by nutrient treatment in either species *($p = 0.19$)* and there was no interaction effect *($p = 0.08$)*.

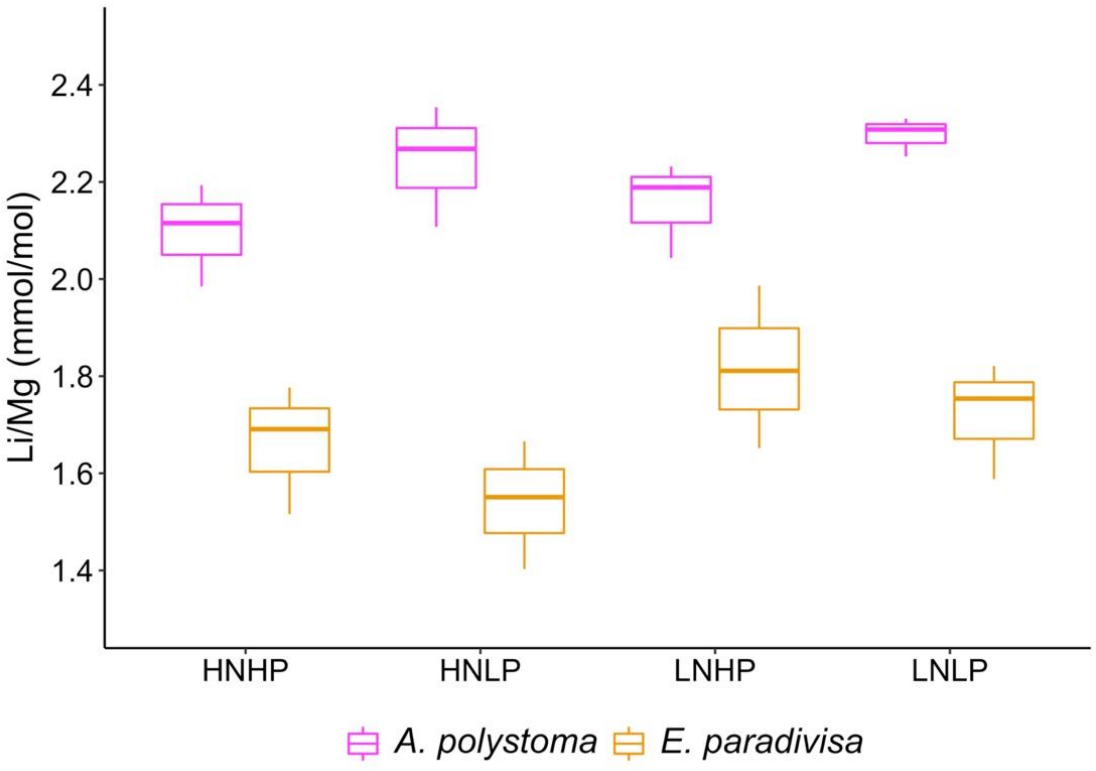

Figure 4.5. Skeletal Li/Mg ratios of *A. polystoma* and *E. paradivisa* after exposure to four different nutrient treatments. Li/Mg contents relate to the most recently extended section of the skeleton and measured using LA-ICP-MS. HNHP = high nitrate: high phosphate, HNLP = high nitrate: low phosphate, LNHP = low nitrate: high phosphate and LNLP = low nitrate: low phosphate *($n = 3$)*.

4.4.3. Evidence of Rayleigh fractionation affecting TE/Ca contents

Where the starting TE concentrations of the calcifying fluid are known, and when the $D_{El/Ca}$ values are available, the skeletal TE/Ca ratios can be modelled for the full range (from 0% to 100%) of values of calcium that remains in fluid (F_{Ca}) at the time of precipitation. Plotting the measured TE/Ca values for two TE's against their modelled values allows a qualitative assessment of whether Rayleigh fractionation plays an important role in controlling TE incorporation into the skeleton. If Rayleigh fractionation is responsible for determining the measured TE/Ca ratios then there should be good correspondence between the modelled and measured values throughout the possible range of F_{Ca} values. The Rayleigh models for Li/Ca v Mg/Ca indicated that Rayleigh fractionation likely plays a major role in controlling Li and Mg incorporation into the skeletons of both species, as indicated by the good correspondence between measured and predicted values (Figures 4.6a and c). Skeletal Li/Ca values were close to the predicted values of the respective Rayleigh models for both species (Figures 4.6a and c). The plotting of skeletal Li/Ca v Sr/Ca ratios against the respective Rayleigh model for *A. polystoma* showed that the trend of the measured values for the HNLP and LNHP treatments corresponded with the predicted trend of the modelled values (albeit with an offset to higher than expected Sr/Ca values), but that the trend was overprinted for the HNHP and LNLP treatments (Figure 4.6b). This indicated that Rayleigh fractionation is one of multiple factors that determine skeletal Sr/Ca in *A. polystoma* but that its influence is subject to change under the different nutrient treatments. In *E. paradivisa*, the trend for the measured Sr/Ca and Li/Ca values did follow the Rayleigh curves for all treatments but the values of Sr/Ca were higher than predicted, resulting in a uniformly off-set distribution of data points from the Rayleigh curves (Figure 4.6d). This suggests that in *E. paradivisa,* Rayleigh fractionation plays a role in determining skeletal Sr incorporation but that at least one other factor is important and serves to increase Sr/Ca values. Rayleigh models constructed with respect to B/Ca did not reveal any correlation with the other TE/Ca contents that could be attributed to Rayleigh fractionation.

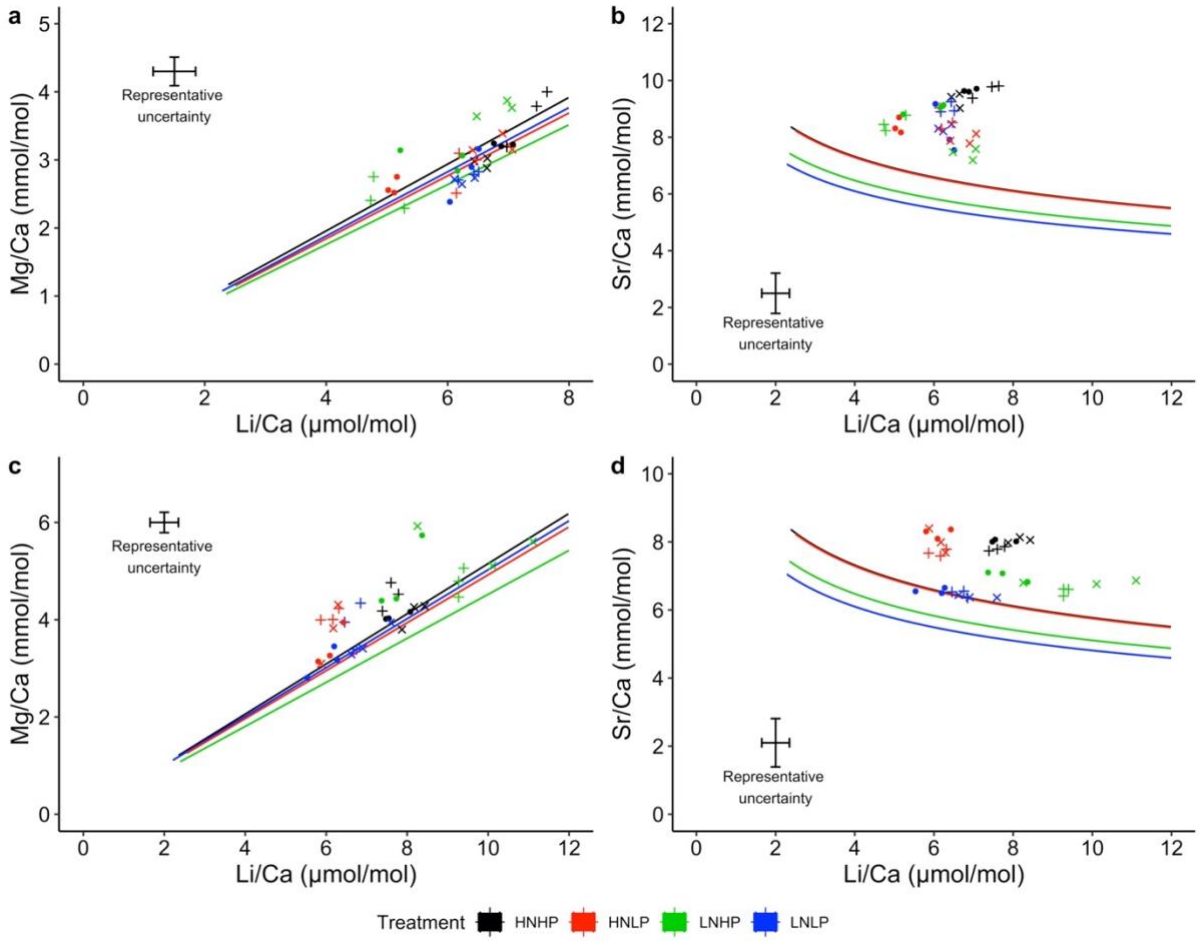

Figure 4.6. Rayleigh fractionation models showing the relationships between skeletal TE/Ca ratios for *A. polystoma* and *E. paradivisa* after exposure to four different nutrient treatments. The relationships between a) Li/Ca and Mg/Ca in *A. polystoma*, b) Li/Ca and Sr/Ca in *A. polystoma*, c) Li/Ca and Mg/Ca in *E. paradivisa* and d) Li/Ca and Sr/Ca in *E. paradivisa*. In each panel, a separate Rayleigh model has been constructed for each nutrient treatment. Three samples were taken from each fragment/ corallite and data points sharing the same symbol and colour within a plot were taken from the same coral. The representative uncertainties for both trace elements are equal to 2σ (as determined by repeated measures of a standard reference material). HNHP = high nitrate: high phosphate, HNLP = high nitrate: low phosphate, LNHP = low nitrate: high phosphate and LNLP = low nitrate: low phosphate. Note that in panel b, the Rayleigh curves for the HNHP and HNLP treatments are overlain.

4.4.4. Impacts on the degree of isolation of the calcifying fluid

Rayleigh fractionation should theoretically impact all TE/Ca ratios such that a good correspondence between the trends of measured and predicted values is observable in all plots. The absence of such an observation dictated that a more careful analysis be conducted to investigate the controls on the TE/Ca ratios under study. Li/Ca was the only skeletal elemental ratio found not to be partially influenced by a relationship with either either $\delta^{13}C$ or $\delta^{18}O$ in either species. It was therefore the TE/Ca ratio that was most strongly

influenced by Rayleigh fractionation, without any additional significant effect of factors that controlled for skeletal $\delta^{18}O$ or $\delta^{13}C$. The mean proportions of calcium remaining in the calcifying fluid (F_{Ca}) for each species and treatment were determined by identifying the numerical step in each respective Rayleigh model that corresponded with the measured skeletal Li/Ca ratios (n = 3) (Figure 4.7). Two-way ANOVA showed that F_{Ca} was higher in *A. polystoma (p = 0.001),* indicating a more open (less isolated) calcifying space than in *E. paradivisa.* F_{Ca} was also significantly impacted by nutrient treatment *(p = 0.001)* with HNLP corals having a higher F_{Ca} than the other treatments. There was a significant interaction between species and nutrient treatment *(p = 0.01*), confirming that the F_{Ca} of the two species were impacted differently by the nutrient treatments.

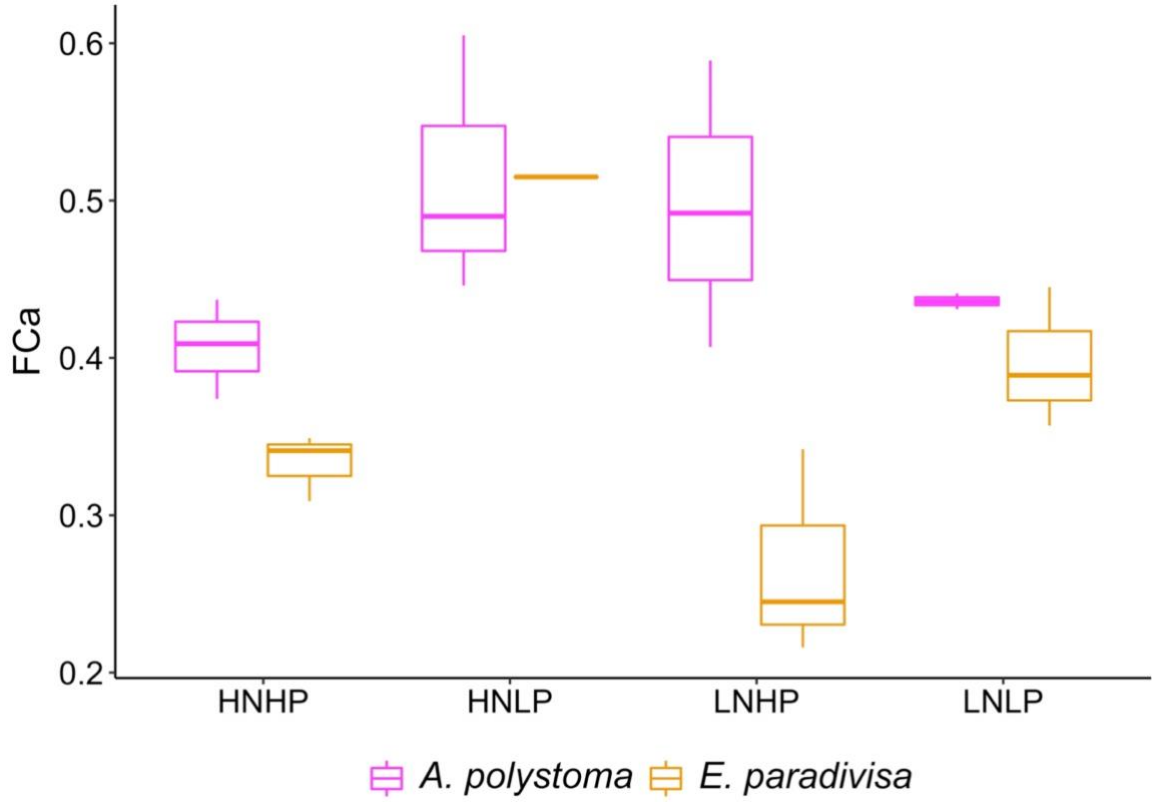

Figure 4.7. The calculated fraction of calcium remaining in the calcifying fluid (F_{Ca}) in the skeletons of *A. polystoma* and *E. paradivisa* at the time of calcification of sampled portions of skeleton. F_{Ca} values were calculated from the Li/Ca of each skeleton as determined from LA-ICP-MS. Corals were cultured in four different nutrient treatments: HNHP = high nitrate: high phosphate, HNLP = high nitrate: low phosphate, LNHP = low nitrate: high phosphate and LNLP = low nitrate: low phosphate *(n = 3).*

4.4.5. Relationship between skeletal TE/Ca contents and skeletal $\delta^{13}C$ and $\delta^{18}O$

No relationship between Li/Ca and skeletal $\delta^{13}C$ or $\delta^{18}O$ was found in either species. Rather, Li/Ca was strongly related to Mg/Ca in *A. polystoma* ($r^2 = 0.85$, $p < 0.001$) and *E. paradivisa* ($r^2 = 0.67$, $p = 0.001$), lending further support to the inference that Rayleigh fractionation likely plays a major role in controlling Li and Mg incorporation into the coral skeletons. No relationship was found between Mg/Ca and skeletal $\delta^{13}C$ or $\delta^{18}O$ in *A. polystoma* (Figures 4.8a and b), but for *E. paradivisa* Mg/Ca was correlated with both skeletal $\delta^{13}C$ and $\delta^{18}O$ (Figures 4.8c and d). However, the strength of these relationships was considerably weaker than the relationship between Li/Ca and Mg/Ca which has already been discussed. Accordingly, multiple linear regression models were constructed to determine whether skeletal Mg/Ca in *E. paradivisa* could be better described by Li/Ca and the additional predictors of skeletal $\delta^{13}C$ and/or $\delta^{18}O$ (Table 4.2). In *E. paradivisa*, Mg/Ca was best described by an MLR model incorporating the effects of Li/Ca and $\delta^{13}C$, and indicated that skeletal Mg/Ca and $\delta^{13}C$ were positively correlated. The standardised β-values indicated that the impact on Mg/Ca was greater for changes to Li/Ca than for changes to skeletal $\delta^{13}C$. This suggests that the regression associated with skeletal $\delta^{13}C$ should be imprinted on the dominant regression associated with Li/Ca, and this is evident in Figure 4.6c where data points for LNLP corals (which had lower $\delta^{13}C$ values) have skeletal Mg/Ca values that are less offset from their respective Rayleigh model than the data points for the other treatments.

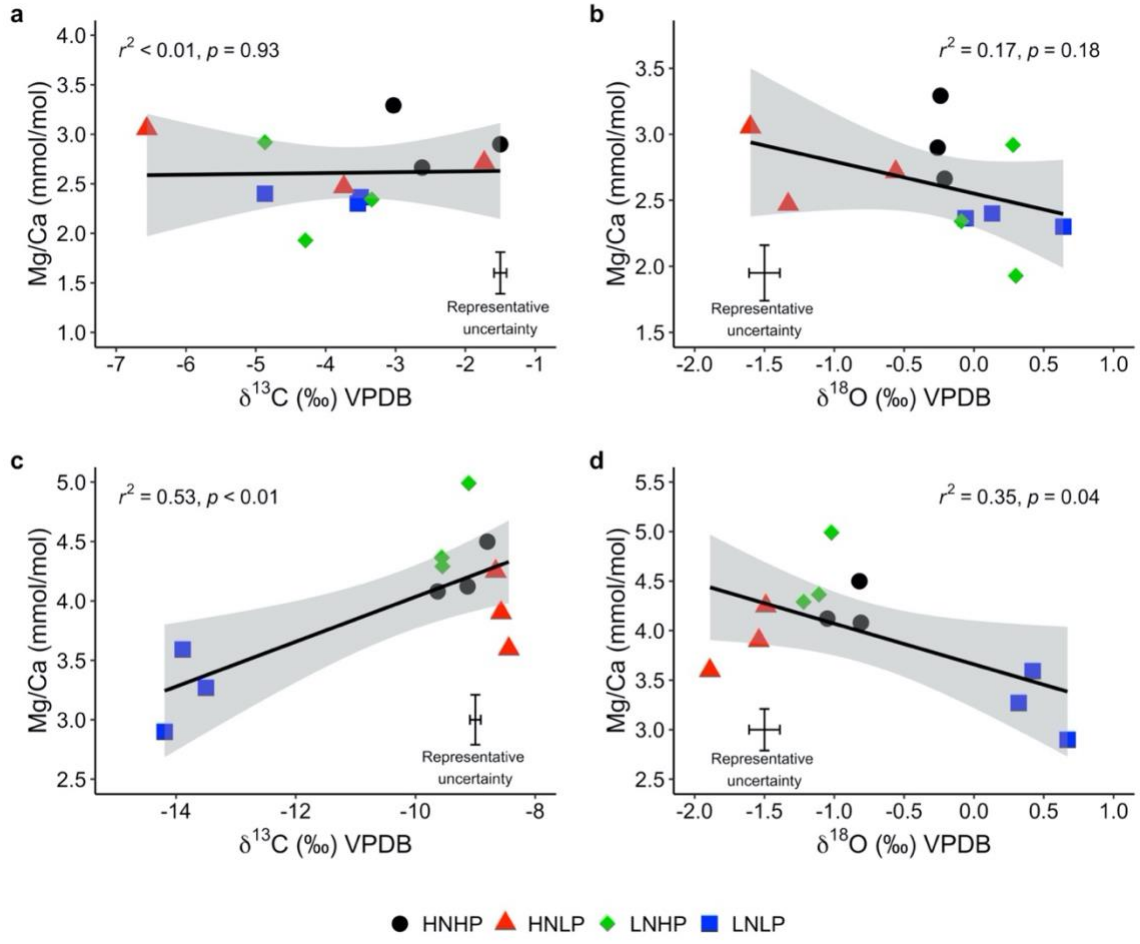

Figure 4.8. The relationship between skeletal stable isotope contents (δ^{13}C and δ^{18}O) and Mg/Ca content in the skeletons of *A. polystoma* and *E. paradivisa* after exposure to four different nutrient conditions. a) The relationship between skeletal δ^{13}C and Mg/Ca in *A. polystoma*, b) the relationship between skeletal δ^{18}O and Mg/Ca in *A. polystoma*, c) the relationship between skeletal δ^{13}C and Mg/Ca in *E. paradivisa* and d) the relationship between skeletal δ^{18}O and Mg/Ca in *E. paradivisa.* Each data point represents a single coral fragment in the case of *A. polystoma* and a single corallite in the case of *E. paradivisa*. All samples were obtained from most recently extended section of the respective fragment or corallite. Grey shading indicates the 95% confidence interval of the fitted model while the representative uncertainties for both isotopes are equal to 2σ (as determined by repeated measures of a standard reference material). HNHP = high nitrate: high phosphate, HNLP = high nitrate: low phosphate, LNHP = low nitrate: high phosphate and LNLP = low nitrate: low phosphate.

Table 4.2. Outputs of simple and multiple linear regression (MLR) models using skeletal Mg/Ca in *A. polystoma* and *E. paradivisa* as a dependent variable and skeletal Li/Ca, $\delta^{13}C$ and $\delta^{18}O$ values as predictor variables. r^2/R^2 = r-squared value of the fitted (simple/ multiple regression model, *b* = coefficient of the y-intercept (constant) or specified variable, *SE b* = the standard error of the coefficient, β = Pearsons' correlation coefficient in simple regression models or the standardised beta value of the specified variable in multiple regression models, and *p* = the p-value. In both cases, step 1 shows the best simple linear regression model. Where a 2nd step is shown, the MLR model was both a better fit (as determined by having a lower AIC) than the simple regression and also significantly different from the model used in step 1 *(ANOVA, $p < 0.05$)*.

	r^2/R^2	*b*	*SE b*	β	*p*
A. polystoma - step 1	0.85				< 0.001
Constant		-0.18	0.37		0.64
Li/Ca		0.49	0.07	0.92	< 0.001
E. paradivisa - step 1	0.67				0.001
Constant		1.30	0.60		0.06
Li/Ca		0.40	0.09	0.82	0.001
E. paradivisa – step 2	0.81				< 0.001
Constant		3.13	0.86		0.005
Li/Ca		0.30	0.08	0.61	0.005
$\delta^{13}C$		0.11	0.04	0.43	0.03

Simple linear regressions indicated there were positive correlations between skeletal Sr/Ca and $\delta^{13}C$ in both species (this being much stronger in *E. paradivisa*) (Figures 4.9a and c), and a negative relationship between Sr/Ca and $\delta^{18}O$ in *E. paradivisa* (Figure 4.9d). For both species, Sr/Ca was best described by an MLR model, albeit that the predictive variables for each species differed (Table 4.3). For *A. polystoma*, skeletal Sr/Ca was best described by the interaction of the processes controlling skeletal $\delta^{13}C$ and $\delta^{18}O$ which had opposite effects on Sr/Ca values. The standardised β-values indicated that the influence of the process controlling for skeletal $\delta^{13}C$ had a slightly stronger influence than that which controlled for skeletal $\delta^{18}O$. For *E. paradivisa*, Sr/Ca was best described by the interaction between the processes controlling for $\delta^{13}C$ and Li/Ca, with the process controlling for skeletal $\delta^{13}C$ (and with which Sr/Ca was positively correlated) being the dominant control. This suggests that the regression for Sr/Ca v Li/Ca should produce an identifiable trend with Sr/Ca values being higher than predicted by a Rayleigh model due to the positive relationship with skeletal $\delta^{13}C$, and this is shown in the respective Rayleigh model (Figure 4.6d). Both the Rayleigh model (Figure 4.6b) and the MLR indicate that in *A. polystoma*,

the influence of Rayleigh fractionation on skeletal Sr/Ca is overprinted by the processes controlling for skeletal $\delta^{13}C$ and/or $\delta^{18}O$ (particularly in corals from the HNHP and LNLP treatments). As before, third step MLR's were tested to assess whether the use of Li/Ca, $\delta^{13}C$ and $\delta^{18}O$ as predictor variables could better explain skeletal Sr/Ca. But in both cases, the step 3 MLR's failed to significantly improve upon the fit of the 2-step MLR's.

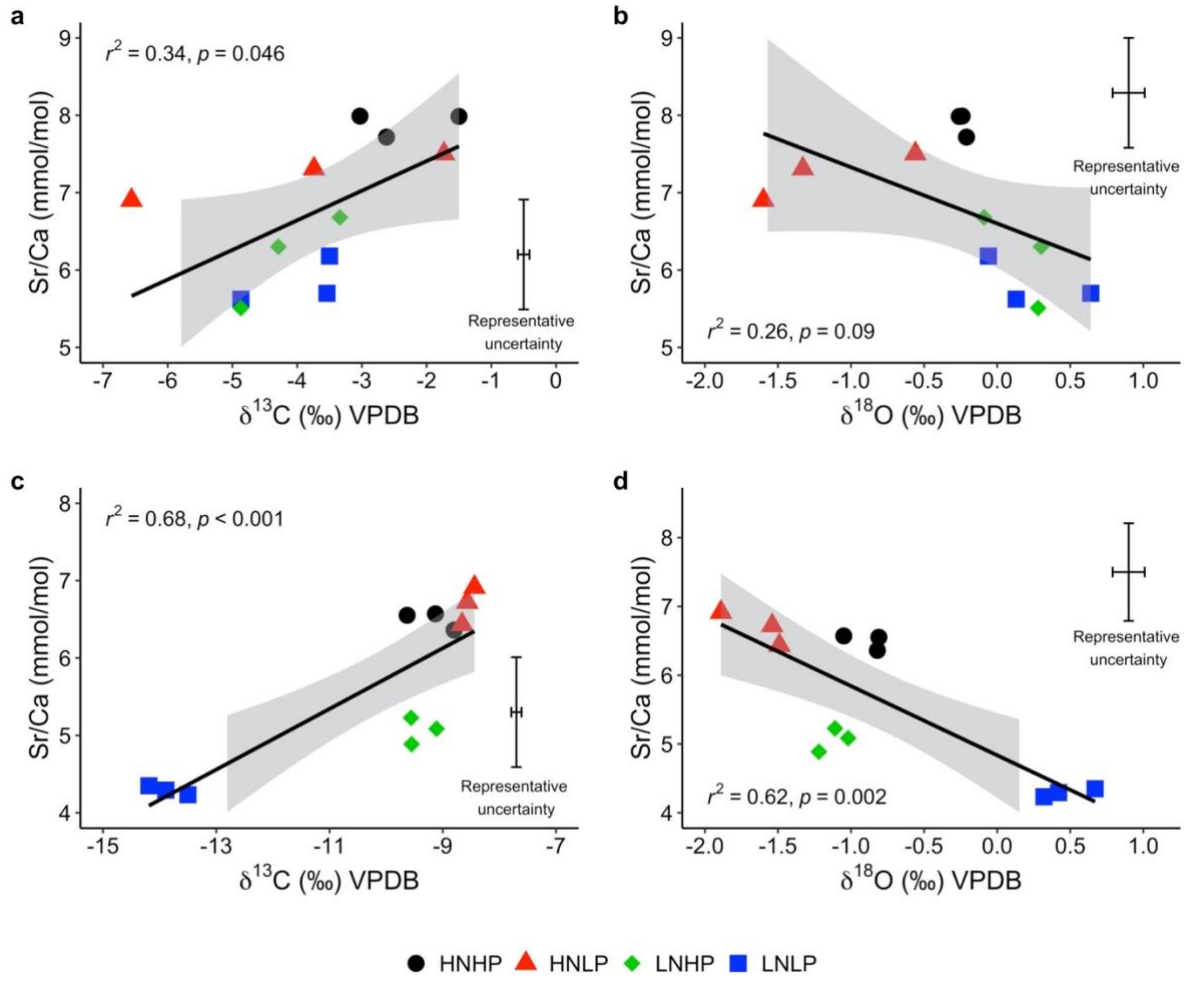

Figure 4.9. The relationship between skeletal stable isotope contents ($\delta^{13}C$ and $\delta^{18}O$) and Sr/Ca in the skeletons of *A. polystoma* and *E. paradivisa* after exposure to four different nutrient conditions. a) The relationship between skeletal $\delta^{13}C$ and Sr/Ca in *A. polystoma*, b) the relationship between skeletal $\delta^{18}O$ and Sr/Ca in *A. polystoma*, c) the relationship between skeletal $\delta^{13}C$ and Sr/Ca in *E. paradivisa* and d) the relationship between skeletal $\delta^{18}O$ and Sr/Ca in *E. paradivisa.* Each data point represents a single coral fragment in the case of *A. polystoma* and a single corallite in the case of *E. paradivisa*. All samples were obtained from most recently extended section of the respective fragment or corallite. Grey shading indicates the 95% confidence interval of the fitted model while the representative uncertainties for both isotopes are equal to 2σ (as determined by repeated measures of a standard reference material). HNHP = high nitrate: high phosphate, HNLP = high nitrate: low phosphate, LNHP = low nitrate: high phosphate and LNLP = low nitrate: low phosphate.

Table 4.3. Outputs of simple and multiple linear regression (MLR) models using skeletal Sr/Ca in *A. polystoma* and *E. paradivisa* as a dependent variable and skeletal Li/Ca, $\delta^{13}C$ and $\delta^{18}O$ values as predictor variables. r^2/R^2 = r-squared value of the fitted (simple/ multiple regression model, *b* = coefficient of the y-intercept (constant) or specified variable, *SE b* = the standard error of the coefficient, β = Pearsons' correlation coefficient in simple regression models or the standardised beta value of the specified variable in multiple regression models, and *p* = the p-value. In both cases, step 1 shows the best simple linear regression model. Where a 2nd step is shown, the MLR model was both a better fit (as determined by having a lower AIC) than the simple regression and also significantly different from the model used in step 1 *(ANOVA, $p < 0.05$)*.

	r^2/R^2	*b*	*SE b*	β	*p*
A. polystoma – step 1	0.34				0.046
Constant		8.17	0.65		< 0.001
$\delta^{13}C$		0.38	0.17	0.58	0.046
A. polystoma – step 2	0.77				0.001
Constant		8.28	0.41		< 0.001
$\delta^{13}C$		0.48	0.11	0.73	0.002
$\delta^{18}O$		-0.95	0.23	-0.67	0.003
E. paradivisa - step 1	0.68				< 0.001
Constant		9.66	0.88		< 0.001
$\delta^{13}C$		0.39	0.08	0.83	< 0.001
E. paradivisa - step 2	0.88				< 0.001
Constant		13.97	1.25		< 0.001
$\delta^{13}C$		0.51	0.06	1.08	< 0.001
Li/Ca		-0.46	0.12	-0.51	0.004

For B/Ca any signal attributable to the influence of Rayleigh fractionation had been completely overwhelmed in both species, and skeletal B/Ca was best described by a simple linear regression with $\delta^{13}C$ in both *A. polystoma* ($r^2 = 0.35$, $p = 0.04$) and *E. paradivisa* ($r^2 = 0.46$, $p = 0.01$) (Figures 4.10a and b). MLR models that were tested which incorporated the effects of other variables failed to provide better fits to the data.

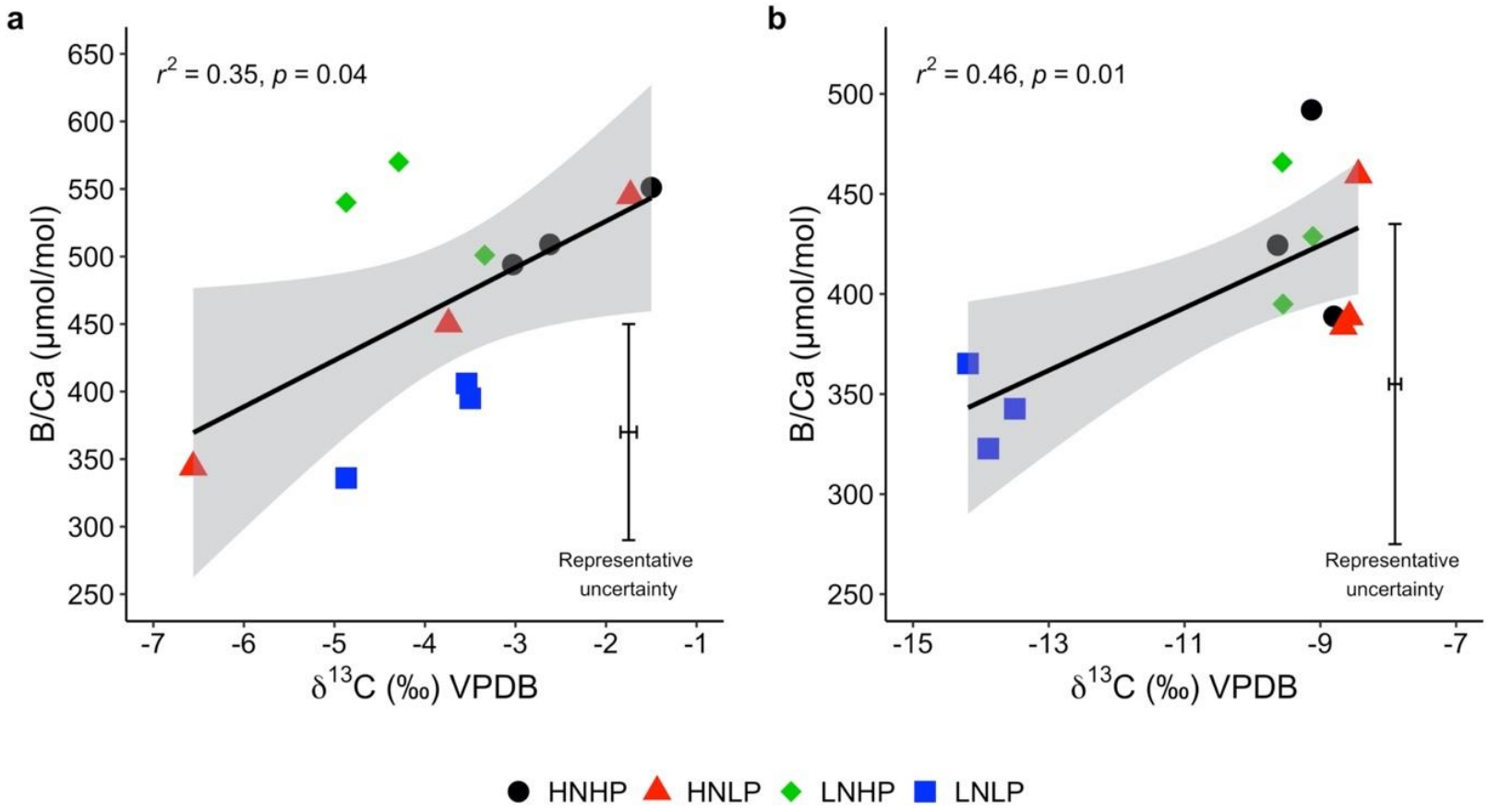

Figure 4.10. The relationship between skeletal δ^{13}C and B/Ca in a) *A. polystoma* and b) *E. paradivisa* after exposure to four different nutrient conditions. Each data point represents a single coral fragment in the case of *A. polystoma* and a single corallite in the case of *E. paradivisa*. All samples were obtained from most recently extended section of the respective fragment or corallite. Grey shading indicates the 95% confidence interval of the fitted model while the representative uncertainties for both isotopes are equal to 2σ (as determined by repeated measures of a standard reference material). HNHP = high nitrate: high phosphate, HNLP = high nitrate: low phosphate, LNHP = low nitrate: high phosphate and LNLP = low nitrate: low phosphate.

4.5. Discussion

Recent studies have shown that nutrient stress, caused by severe nutrient limitation or skewed seawater N:P stoichiometries can have detrimental impacts on the coral-zooxanthellae symbiosis, leading to enhanced bleaching susceptibility and the loss of polyp biomass (Wiedenmann *et al.*, 2013; Rosset, D'Angelo and Wiedenmann, 2015; Rosset *et al.*, 2017). Experimental studies on two morphologically and taxonomically distinct coral species have demonstrated that these conditions can also impact skeletal growth and structure. In *A. polystoma*, linear extension and calcification rates were differentially affected under nutrient-stress conditions, resulting in modifications to both skeletal element thickness and skeletal porosity (Buckingham *et al.*, 2022). In *E. paradivisa*, corallite size and skeletal element thickness were modified, and in those corals exposed to HNLP and LNLP conditions shallower dissepiments formed to support the shrunken polyps (Chapter 3). Such responses - particularly those relating to skeletal growth - suggest that calcification rates are disrupted by exposure to nutrient stress. Calcification rates are primarily controlled by the carbonate chemistry of the calcifying fluid, modifications of which have the potential to impact skeletal isotopic and TE ratios (McConnaughey, 1989a; Adkins *et al.*, 2003; Gabitov *et al.*, 2008, 2011). However, no previous studies had specifically investigated the impacts of nutrient stress caused by imbalanced nutrient enrichment or severe nutrient limitation on coral geochemistry. In this study it is shown that exposure to different forms of nutrient-stress impacts multiple skeletal isotopic and TE ratios, and does so in a broadly similar manner for two taxonomically distinct coral species.

4.5.1. Comparison of the impacts on skeletal $\delta^{13}C$ and $\delta^{18}O$ between species

Both species exhibited broadly similar isotopic responses to the different nutrient treatments, although these responses were typically more muted for *A. polystoma*. For both species, LNLP corals were enriched in skeletal $\delta^{18}O$, while in HNLP corals skeletal $\delta^{18}O$ was depleted. Across treatments there was a negative correlation between skeletal $\delta^{13}C$ and $\delta^{18}O$ values for both species. The HNLP and LNLP treatments caused bleaching in all corals of both species, but the isotopic signatures associated with these different forms of nutrient stress were distinct. This shows that bleaching caused by high N:P stoichiometries has a different impact on skeletal $\delta^{18}O$ values than bleaching due to severe nutrient

limitation, and that this difference in response was observed in both species. Astriking difference between species in their isotopic responses to the different nutrient treatments related to those corals cultured under LNHP conditions. In *A. polystoma,* 2 of the 3 LNHP corals which were analysed had bleached (whereas 3 out of 6 of the full dataset bleached) and the isotopic composition of their skeletons closely matched those of bleached corals from the LNLP treatment. Contrastingly for *E. paradivisa,* culture in the LNHP treatment did not cause bleaching in any corals and the skeletal isotopic compositions closely matched those of unbleached HNHP corals. This is a further indication that nutrient-stress mediated bleaching impacts the isotopic composition of coral skeletons. A probable explanation is that the coral's carbonate chemistry is modified.

This interpretation is drawn primarily through comparison of the isotopic compositions of LNLP and HNHP (nutrient replete) corals. Rates of respiration, calcification and Ca-ATPase activity are all higher when photosynthesis rates are high, resulting in higher pH_{cf} and Ω_{cf} (Al-Horani, Al-Moghrabi and De Beer, 2003b). Photosynthesis enriches skeletal $\delta^{13}C$ due to the preferential uptake of $^{12}CO_2$ by the symbionts which leaves the residual carbon pool enriched in $^{13}CO_2$ (Swart, 1983; McConnaughey, 1989a). As such, the depletion of skeletal $\delta^{13}C$ in bleached LNLP corals with low zooxanthellae densities probably reflects lower rates of photosynthesis, and possibly reduced rates of metabolically-derived DIC flux into the calcifying fluid. Meanwhile, the fractionation of oxygen isotopes in seawater (sw) is partially controlled by pH, resulting in lower $\delta^{18}O_{sw}$ values at higher pH_{sw} (Usdowski and Hoefs, 1993). Therefore, the enrichment of skeletal $\delta^{18}O$ in LNLP corals could possibly be explained by reduced pH_{cf}, which is known to occur when rates of photosynthesis and respiration are reduced (Al-Horani, Al-Moghrabi and De Beer, 2003b). If this is the case, then the depletion of skeletal $\delta^{18}O$ in HNLP corals may indicate elevated pH_{cf}. However, the link between $\delta^{18}O_{cf}$ and pH_{cf} is complicated and skeletal $\delta^{18}O$ values are also dependent on temperature, salinity, Ω_{cf}, the residence time of DIC in the calcifying fluid, and the activity of carbonic anhydrase (Weber and Woodhead, 1972; Rollion-Bard, Chaussidon and France-Lanord, 2003; Devriendt, Watkins and McGregor, 2017). This means that any interpretation of modifications to carbonate chemistry must be made cautiously and can only be reliably verified by measurement of skeletal $\delta^{11}B$, which is a less problematic proxy for pH_{cf} (Holcomb *et al.*, 2016) (this means of analysis could not be conducted during this study due to time constraints).

Studies using skeletal B/Ca ratios and $\delta^{11}B$ values have revealed that thermal-stress mediated bleaching impacts calcifying fluid chemistry primarily by decreasing $[DIC]_{cf}$ and $[CO_3^{2-}]_{cf}$, with associated reductions in pH_{cf} being either non-significant or more muted (McCulloch *et al.*, 2017; Schoepf *et al.*, 2021). Such a response would be consistent with the isotopic responses of *A. polystoma* and *E. paradivisa* to the LNLP treatment, but suggests that culture under HNLP conditions might have elicited a previously unreported impact of bleaching on carbonate chemistry.

4.5.2. Comparison of the impacts on skeletal TE/Ca between species

The TE/Ca ratios analysed were impacted in a broadly similar manner by the different nutrient treatments for both species. The most striking and consistent effect was that Sr/Ca ratios were high in HNHP and HNLP corals, and low in LNHP and LNLP corals for both species. The results of the DFA indicated that this was the single most important variate contributing to differences between the different nutrient treatments. B/Ca ratios were also impacted in a similar manner for both species, being higher in HNHP and LNHP corals, although this effect was more muted in *A. polystoma*. The most notable difference between the two species was that Li/Ca and Mg/Ca ratios were impacted differently by the LNHP treatment, possibly attributable to differences in the bleaching responses or changes to the isolation of the calcifying fluid. However, setting this difference aside, it can be said that there was remarkable consistency in the geochemical responses of both species to the HNHP, HNLP and LNLP treatments, and that each nutrient treatment elicited a distinct geochemical response. This finding should be considered alongside the fact that a number of coral species have been observed to respond to these three nutrient treatments in the same way. Under HNHP conditions corals retain high zooxanthellae densities and growth rates. Contrastingly, under both HNLP and LNLP conditions corals bleach; but HNLP and LNLP corals can be easily differentiated because P-starvation of the zooxanthellae (evident from reduced Fv/Fm) only occurs in HNLP corals (Wiedenmann *et al.*, 2013; Rosset *et al.*, 2017; Buckingham *et al.*, 2022). This suggests that coral skeletal geochemistry can be used to some extent to infer the status of the coral-zooxanthellae symbiosis because it is impacted by nutrient-stress mediated bleaching and an additional biological influence related to P-starvation of the symbionts. These biological influences on coral skeletal geochemistry also have implications for the use of associated climate proxies.

4.5.3. Implications for the use of geochemical climate proxies

4.5.3.1. $\delta^{18}O$

Two recent studies have collated the skeletal $\delta^{18}O$-thermal sensitivities for a number of different coral species. Xiao *et al.* (2014) began their study by collecting published thermal sensitivities of coral skeletal $\delta^{18}O$ from the existing literature, and also revisited the data from similar studies for which this particular calculation had not been made. In total they considered 12 publications and found that published values ranged between -0.138 and -0.34 ‰ /℃, a range that incorporated their own experimentally-derived value of -0.143 ‰ /℃ (Xiao *et al.*, 2014). Amongst this sample of the literature, the values calculated for *Acropora spp.* ranged between -0.143 and -0.34 ‰ /℃, while no studies related to corals from the genus *Euphyllia* (Xiao *et al.*, 2014). Similarly, Brenner, Linsley and Potts (2017) used the data from 17 different publications to identify a published thermal sensitivity range of -0.13 to -0.23 ‰ /℃, which was in good agreement with their own experimentally determined values of -0.184 and -0.123 ‰ /℃. The data presented by Brenner, Linsley and Potts (2017) did not include any assessments of the thermal sensitivities for the genera *Acropora* or *Euphyllia*.

In the present study, temperature was controlled for during both sets of experiments, and was not originally considered to be a factor likely to impact geochemical signals. However, when the mean skeletal $\delta^{18}O$ values of *A. polystoma* were analysed it was found that the difference between the highest (LNLP) and lowest (HNLP) mean values was 1.40 ‰. Using the full range of thermal sensitivities collated by Xiao *et al.* (2014) and Brenner, Linsley and Potts (2017) it can be seen that this equates to a proxy-derived temperature difference between the nutrient treatment tanks of 4.1 to 11.4 ℃, with the highest average temperature being that of the HNLP tank. Using just the published thermal sensitivities relating to *Acropora spp.,* this range was restricted to 4.1 to 9.8 ℃. From these calculations, even the smallest estimated temperature difference (determined using a thermal-sensitivity derived from *Acropora spp.)* between tanks was substantially larger than should have been expected, given that temperature conditions had been tightly controlled for. This observation prompted a re-analysis of the raw temperature data from the culture of the *A. polystoma* fragments, and it was shown that there was in fact a significant difference in temperature between the tanks *(ANOVA, $F_{3,44} = 8.1$, $p = 0.0002$)*.

However, the difference between the warmest tank (LNLP) and the coldest (HNLP) tank was only 1.1 ℃. This reanalysis of the raw temperature data therefore confirmed that the δ^{18}O-derived estimates of temperature difference between the tanks were incorrect. Not only was the magnitude of temperature difference overestimated but, perhaps more importantly the warmest tank was incorrectly identified as having been the coldest. When the mean δ^{18}O values of *E. paradivisa* corals were analysed the difference between the highest (LNLP) and lowest (HNLP) mean values was 2.11 ‰. This equates to an even larger temperature difference between tanks of 6.2 to 17.2 ℃, with temperature being highest in the HNLP tank. Unfortunately, the raw temperature data relating to the culture of *E. paradivisa* was not available from the original studies (Rosset, D'Angelo and Wiedenmann, 2015; Rosset *et al.*, 2017) to allow reanalysis. Therefore, it must be assumed that – as stated by the authors - there was no difference in temperature between the nutrient treatment tanks. Indeed, it should be noted that the mesocosm facility used during both sets of experiments is well established and stable, and the environmental conditions of all systems are monitored on a daily basis (D'Angelo and Wiedenmann, 2012). It seems implausible that temperature differences ≥ 4.1 ℃ between treatment tanks could have gone unnoticed or unaddressed for periods of 100 days or longer. In both species, culture in the HNLP treatment resulted in depletion of skeletal δ^{18}O when compared to corals cultured in nutrient enriched (HNHP) conditions, and this has the potential to lead to overestimations of SST. Conversely, in LNLP corals skeletal δ^{18}O was enriched and likely to result in proxy-derived underestimations of SST. Unfortunately, the isotopic compositions of the culture mediums were not measured during the original studies. Therefore, it cannot be entirely ruled out that differences in the isotopic composition of the culture mediums was a factor. It should also be noted that the thermal sensitivity of skeletal δ^{18}O is relatively poorly characterised in *Acropora spp.* while no studies have been conducted with species from the genus, *Euphyllia*. It is therefore possible that the thermal sensitivities of both species lie well outside the known range of thermal sensitivities for tropical corals. The thermal sensitivities of these two coral species could easily be resolved through a series of temperature calibration cultures, considering differences in the oxygen isotope composition of the different culture mediums. Meanwhile, the subsequent analysis of skeletal δ^{11}B would allow the influence of pH_{cf} on skeletal δ^{18}O to be properly characterised.

4.5.3.2. Sr/Ca

Reynaud *et al.* (2007) compiled a list of published thermal sensitivities for coral skeletal Sr/Ca that ranged between -0.033 and -0.33 mmol/mol / ℃ (from 17 publications dated between 1979 and 2003). This list was updated in the study conducted by Brenner, Linsley and Potts (2017) who collated 19 studies, including 6 that had been included in the study by Reynaud *et al.* (2007). Brenner, Linsley and Potts (2017) discarded the anomalously oversensitive value of -0.33 mmol/mol / ℃ which had been collected by Reynaud *et al.* (2007), and in doing so published a smaller range of between -0.042 and -0.140 mmol/mol / ℃ which encapsulated their own experimentally determined values of -0.061 and -0.047 mmol/mol / ℃. Amongst the range of values collated by these two sets of authors only one reliable value was attributable to *Acropora spp.*, this being a thermal sensitivity of -0.048 mmol/mol / ℃ (Sadler *et al.*, 2016). None of the thermal sensitivity published values related to corals from the genus, *Euphyllia*.

In the present study, for *A. polystoma* the difference between the highest (HNHP) and lowest (LNLP) mean skeletal Sr/Ca ratios was 2.07 mmol/mol. Using the more conservative range of thermal sensitivities collated by Brenner, Linsley and Potts (2017) this equates to a temperature difference between the treatment tanks of 14.8 to 49.3 ℃. Using the previously published value relating to *Acropora* (Sadler *et al.*, 2016) it equates to a temperature difference of 43.1 ℃. Even using the anomalously oversensitive value of -0.33 mmol/mol / ℃ collected by Reynaud *et al.* (2007) provides a proxy-derived estimate of temperature difference of 6.3 ℃. As with the δ^{18}O-derived estimates, these very large differences in Sr/Ca ratios between treatments are completely incompatible with the experimental conditions if temperature is the sole or dominant control on skeletal Sr/Ca values. For *E. paradivisa*, there was a similarly large difference in skeletal Sr/Ca ratios between the treatments with the highest (HNLP) and lowest (LNLP) mean values, this being 2.40 mmol/ mol. Using the range of thermal sensitivity values collated by Brenner, Linsley and Potts (2017) this equates to a temperature difference between tanks of 17.1 to 57.1 ℃. Even using the anomalously oversensitive value of -0.33 mmol/mol / ℃ listed in the Reynaud *et al.* (2007) paper provides a proxy-derived estimate of temperature difference of 7.3 ℃. The smallest Sr/Ca-derived estimates of temperature difference between tanks are too large to have gone unnoticed during either set of experiments, whilst the largest estimations of temperature difference exceed the full range of seawater

temperatures in the global oceans. The skeletal TE/Ca values presented in this study were normalised to account for differences in the TE composition of the culture mediums so differences in culture medium chemistry cannot explain these results. The results of this study suggest that the coral skeletal Sr/Ca paleothermometer is subject to 'vital effects' during periods of nutrient stress and that these 'vital effects' manifest differently dependent on the concentrations and/or stoichiometries of N and P.

4.5.3.3. Mg/Ca

In collating 4 previous studies, Reynaud *et al.* (2007) identified that published thermal sensitivities for Mg/Ca ranged between 0.088 and 0.129 ℃ / mmol/ mol, while their own experimentally derived value for *Acropora spp.* was slightly higher at 0.138 ℃ / mmol/ mol. In their subsequent study, Xiao *et al.* (2014) collated a further 7 publications and found that the published values had a slightly wider range of 0.088 to 0.28 mmol/ mol, while their own experimentally-derived value (also for *Acropora spp.*) was slightly lower at 0.0497 mmol/ mol. None of the studies collated related to corals from the *Euphyllia* genus.

For the present study, in *A. polystoma* the difference between the highest (HNHP) and lowest (LNLP) values for mean skeletal Mg/Ca was 0.60 mmol/mol. Using the full range of thermal sensitivities collated by Reynaud *et al.* (2007) and Xiao *et al.* (2014) this equates to a temperature difference between treatments of 2.1 to 12.1 ℃. The lower end of this temperature range does not represent a very large deviation from the true temperature difference. However, it should be noted that the higher value of 12.1 ℃ uses a thermal sensitivity derived from *Acropora spp.* (Xiao *et al.*, 2014) and that the other available value for *Acropora spp.* (Reynaud *et al.*, 2007) returns a temperature difference of 4.3 ℃. This suggests that values towards the higher end of this range might be more applicable for *Acropora spp.* For *E. paradivisa*, the difference between the highest (LNHP) and lowest (LNLP) mean skeletal Mg/Ca ratios was 1.30 mmol/ mol, giving a Mg/Ca-derived temperature difference between tanks of 4.6 to 14.8 ℃.

4.5.3.4. Li/Ca

The thermal sensitivity of Li/Ca in coral skeletons has been less extensively collated in the literature. However, Hathorne *et al.* (2013) derived values of -0.123 and -0.277 µmol/ mol / ℃ from examination of *Porites spp.* samples recovered from Japan and Tahiti, respectively.

In this study, for *A. polystoma* the difference between the highest (HNHP) and lowest (LNHP) mean skeletal Li/Ca values was 1.04 µmol/ mol. Using the values derived by Hathorne *et al.* (2013) this is equivalent to a temperature difference between tanks of 3.8 to 8.5 ℃. For *E. paradivisa*, the difference between the highest (LNHP) and lowest (LNLP) mean skeletal Li/Ca values was 2.65 µmol/ mol which equates to a temperature difference of 9.6 to 21.5 ℃. Li/Ca and Mg/Ca values have previously been shown to be correlated to calcification rate (Gabitov *et al.*, 2008, 2011) which, itself is controlled by Ω_{cf} (Zeebe, 2001). In corals, Ω_{cf} is determined by Ca-ATPase activity, the supply of metabolic CO_2 and the active transport of HCO_3^- ions (Furla *et al.*, 2000; Al-Horani, Al-Moghrabi and De Beer, 2003b; Zoccola *et al.*, 2015), meaning that both Li/Ca and Mg/Ca ratios are susceptible to biologically mediated 'vital effects'. Furthermore, skeletal Mg/Ca has been shown to be more strongly correlated to annual extension rates than to temperature (Inoue *et al.*, 2007). This has led to the notion that Li/Mg ratios provide a more reliable paleothermometer because they are relatively insensitive to biological influences (Raddatz *et al.*, 2013; Montagna *et al.*, 2014; Marchitto *et al.*, 2018).

4.5.3.5. Li/Mg

Of the five geochemical paleothermometers considered in this study ($\delta^{18}O$, Li/Ca, Mg/Ca, Sr/Ca and Li/Mg), Li/Mg was the only one that was not significantly impacted by the treatment effect in either species. Despite this, the small non-significant differences between treatments were analysed for both species to determine to what extent the Li/Mg paleothermometer might have been impacted. Li/Mg thermal sensitivity in coral aragonite has been subject to several studies. Hathorne *et al.* (2013) determined values of -0.0478 and -0.0604 mmol/ mol / ℃ for *Porites spp.* from different regions of the Pacific Ocean. Meanwhile, Ross, DeCarlo and McCulloch (2019) derived values of -0.06 and -0.09 mmol/ mol / ℃ for *Pocillipora spp.* and *Acropora spp.,* respectively. These values are

substantially lower than those calculated for cold water corals and reflect the fact that the relationship between Li/Mg and temperature is non-linear, albeit that this relationship is not necessarily evident unless large (~20 ℃) temperature ranges are considered (Hathorne *et al.*, 2013; Rollion-Bard and Blamart, 2015; Marchitto *et al.*, 2018; Ross, DeCarlo and McCulloch, 2019). Using the thermal sensitivity value for *Acropora spp.* which was determined from 4 species by Ross, DeCarlo and McCulloch (2019) it was found that the Li/Mg-derived temperature difference between the different nutrient treatment tanks for *A. polystoma* was equivalent to ~2.2 ℃. For *E. paradivisa*, using the full range of thermal sensitivities obtained for tropical corals, a temperature difference of ~3.1 to ~4.7 ℃ could be similarly derived. Therefore, for both species the geochemical paleothermometer least affected by exposure to the nutrient treatments was that of Li/Mg. Not only were the differences in Li/Mg ratios between treatments deemed non-significant, they also translated into the smallest proxy-derived estimations of temperature difference between the different nutrient treatment tanks. This is consistent with the view that it is the coral geochemical proxy least sensitive to the complications of 'vital effects' (Raddatz *et al.*, 2013; Montagna *et al.*, 2014; Marchitto *et al.*, 2018).

The impacts of the different nutrient treatments on coral skeletal $\delta^{18}O$, Sr/Ca, Li/Ca and Mg/Ca values suggest that the impacts of nutrient stress may pose serious complications for the interpretation of these established paleothermometers. However, it should be noted that spatial variability within the crystal structure of coral skeletons has the potential to imply erroneous temperature differences > 10 ℃ in deep-sea corals if 'bulk' samples are used to calibrate the paleothermometer (Robinson *et al.*, 2014). This has led to increased efforts to target regions of skeleton with corresponding crystal structures when assessing TE/Ca and isotopic proxies and this method is gaining favour on more recent studies (Holcomb *et al.*, 2009; Frankowiak, Kret, *et al.*, 2016; Kuffner *et al.*, 2017). The measurements obtained during this study relate to 'bulk' samples conducted at the microstructural, rather than the ultrastructural scale and it is possible that a more targeted approach could resolve some of the erroneous proxy-derived estimations of temperature difference between culture tanks.

4.5.4. Impacts on other geochemical proxies

4.5.4.1 $\delta^{13}C$

Skeletal $\delta^{13}C$ is enriched in symbiotic corals due to the favoured uptake of $^{12}CO_2$ by their symbionts, which results in ^{13}C-enrichment of the residual DIC pool and skeleton (Swart, 1983; McConnaughey, 1989a). $\delta^{13}C$ and $\delta^{18}O$ values are positively correlated in asymbiotic corals and this relationship typically follows a linear trend that passes through seawater equilibrium (McConnaughey, 1989a; Adkins *et al.*, 2003; Frankowiak, Wang, *et al.*, 2016). This means that when the $\delta^{13}C$ and $\delta^{18}O$ values of symbiotic and asymbiotic corals are plotted on the same graph, the values for symbiotic corals should be easily identifiable because they fall below the equilibrium line along which the values for asymbiotic corals are plotted (McConnaughey, 1989a; Adkins *et al.*, 2003; Frankowiak, Wang, *et al.*, 2016). The impact of bleaching under LNLP conditions is to reduce skeletal $\delta^{13}C$, such that the isotopic composition of the skeleton more closely resembles those of asymbiotic corals. This is entirely as one should expect, given that bleaching typically relates to loss of the zooxanthellae (Rosset, D'Angelo and Wiedenmann, 2015; Rosset *et al.*, 2017; Buckingham *et al.*, 2022). This effect is more modest in *A. polystoma*, but in *E. paradivisa* the extent to which $\delta^{13}C$ is reduced is of a similar magnitude to the difference between symbiotic and non-symbiotic species reported by McConnaughey (1989a). Such a response could be problematic for those researchers seeking to distinguish prehistoric asymbiotic from symbiotic corals (Frankowiak, Wang, *et al.*, 2016). Coral skeletal $\delta^{13}C$ is also gaining recognition as a useful proxy for measuring atmospheric $\delta^{13}C$, which in turn is used as a proxy for tracking emissions of anthropogenic CO_2 - the so called 'Suess effect' (Swart *et al.*, 2010; Dean, Leng and Mackay, 2014). The mean skeletal $\delta^{13}C$ of Atlantic corals has decreased by about 1.4 ‰ since c.1800, and since atmospheric observations at Mauna Loa commenced these values closely track atmospheric $^{13}CO_2$ measurements (Swart *et al.*, 2010). This is a similar value to the decrease in skeletal $\delta^{13}C$ observed in bleached *A. polystoma*, while for *E. paradivisa* the decrease in skeletal $\delta^{13}C$ in bleached LNLP corals was more than double this. This observation stresses the need for corals being used to aid atmospheric reconstructions to be sourced from reefs far from the influence of sources of anthropogenic disturbance that may impact geochemical proxies.

4.5.4.2 B/Ca

The full significance of the impact on skeletal B/Ca ratios is difficult to assess in the absence of skeletal $\delta^{11}B$ data which provides a proxy for pH_{cf}. This is because B/Ca is controlled by the ratio between borate and carbonate ions in the calcifying fluid $[B(OH)_4^-]/[CO_3^{2-}]_{cf}$ (Holcomb *et al.*, 2016) and $[CO_3^{2-}]_{cf}$ is a product of both $[DIC]_{cf}$ and pH_{cf}. Therefore, knowledge of one must precede the other. In *A. polystoma*, the decrease in B/Ca following exposure to LNLP conditions was ~100 µmol/ mol, indicating a substantial modification of either pH_{cf} or $[CO_3^{2-}]_{cf}$, or both. The possibility that nutrient-stress mediated bleaching modifies the carbonate chemistry of zooxanthellate corals is further implied by the impacts on skeletal $\delta^{13}C$ and $\delta^{18}O$ values, but cannot be properly investigated without first obtaining measurements of skeletal $\delta^{11}B$. In this sense, the impacts on B/Ca should be considered differently to the impacts on the other geochemical signals because, rather than representing a potential complication to the use of geochemical proxies it represents an opportunity to improve our understanding of the impacts of bleaching on coral carbonate chemistry.

4.5.5. Potential controls on TE/Ca ratios

Setting aside the variable impact of the LNHP treatment on Li/Ca and Mg/Ca values, it can be seen that the TE/Ca ratios of both species were impacted very similarly by the different nutrient treatments. However, this should not be taken to mean that the same physical and chemical factors are important for determining each of the TE/Ca ratios. This is evident when considering the role played by Rayleigh fractionation. Co-variance in Li/Ca and Mg/Ca ratios in both species was largely attributable to a dominant role of Rayleigh fractionation in determining the relative abundance of Li and Mg. But this was not the case for Sr or B. Instead, for both Sr/Ca and B/Ca positive correlations with skeletal $\delta^{13}C$ suggest that the influence of photosynthesis might be an important factor impacting Sr and B incorporation. This resulted in the Rayleigh fractionation signal being overprinted for Sr/Ca and overwhelmed for B/Ca. Photosynthesis is important for carbonate chemistry because high rates of photosynthesis provide the required energy to support high rates of respiration and Ca-ATPase activity, which in turn lead to higher rates of DIC flux to the calcifying fluid, higher $[CO_3^{2-}]_{cf}$, pH_{cf} and Ω_{cf}, and elevated calcification rates (Al-Horani, Al-Moghrabi and De Beer, 2003b; D'Olivo and McCulloch, 2017; Schoepf *et al.*, 2021).

Therefore, changes to the rates of photosynthesis can modify carbonate chemistry through multiple pathways which can alter $[DIC]_{cf}$ and pH_{cf} and this has the potential to impact Sr/Ca and B/Ca ratios, albeit not necessarily in the same way. The relationship between coral skeletal Sr/Ca, $[DIC]_{cf}$ and pH_{cf} is not fully understood, but it has been demonstrated that wide ranges of pH_{cf} or $[DIC]_{cf}$ values can produce similar Sr/Ca ratios, and that similar pH_{cf} and $[DIC]_{cf}$ values can produce wide ranges of Sr/Ca ratios, dependent on the specific balance between pH_{cf} and $[DIC]_{cf}$ (Allison and Finch, 2010b). Similarly, skeletal B/Ca is determined by both $[DIC]_{cf}$ and pH_{cf}, which can vary independently of each other in the calcifying fluid of corals (Holcomb *et al.*, 2016). In both species, HNLP and LNLP corals bleached as a consequence of nutrient stress. In *A. polystoma*, the skeletal $\delta^{13}C$ of HNLP and LNLP corals decreased, this being consistent with reduced photosynthesis. In *E. paradivisa* a similar impact on skeletal $\delta^{13}C$ was observed in LNLP, but not for HNLP corals. In both species Sr/Ca was elevated in HNLP corals. Higher skeletal Sr/Ca values may occur under conditions of increased pH_{cf} and decreased $[DIC]_{cf}$ (Allison and Finch, 2010b). Skeletal $\delta^{18}O$ is influenced by a negative relationship with pH_{cf} (Usdowski and Hoefs, 1993) and the negative relationship between skeletal $\delta^{18}O$ and Sr/Ca (which was stronger in *E. paradivisa*) and high Sr/ca and low $\delta^{18}O$ of the HNLP corals indicate a) that in both species pH_{cf} may have been elevated in HNLP corals (see further discussion in section 4.5.6) but that b) this effect was more influential on Sr/Ca in *E. paradivisa*. This could possibly be because this species retained fewer zooxanthellae than *A. polsytoma* and therefore had lower respiration rates resulting in lower $[DIC]_{cf}$. (Allison and Finch, 2010b) previously modelled such a relationship between pH_{cf}, $[DIC]_{cf}$ and skeletal Sr/Ca. Unfortunately, without measurements of skeletal $\delta^{11}B$ it is not possible to further characterise the nature of any potential impacts on carbonate chemistry that may have occurred during this study.

The degree to which the calcifying fluid is isolated from the external medium also impacts TE/Ca ratios because it alters the extent to which Rayleigh fractionation occurs. Seawater leakage into the calcifying space via paracellular channels increases F_{Ca} and returns calcifying fluid TE concentrations to values that are closer to that of unmodified seawater (E. Tambutté *et al.*, 2011; Venn *et al.*, 2020). This dilution of the precipitating medium means that for Li, Mg and B which have $D_{El/Ca} < 1$, TE/Ca ratios should be lower in more open systems, whilst Sr/Ca ($D_{Sr/Ca} > 1$) ratios should be higher. In this study F_{Ca} was higher

under HNLP conditions, indicating a less isolated calcifying fluid (more open system). For LNHP corals, F_{Ca} increased in *A. polystoma* but decreased in *E. paradivisa.* For both species, the measured values of Li/Ca and Mg/Ca were broadly consistent with the expected responses for the observed differences in F_{Ca} and this accounts for the only major difference in TE response between species to the different nutrient treatments. Contrastingly, the observed differences in skeletal Sr/Ca and B/Ca between nutrient treatments did not consistently correspond with the expected differences for the observed changes to F_{Ca}. This meant that although both high (HNLP) and low (LNHP) N:P stoichiometries caused changes to the degree of isolation of the calcifying fluid, this may have impacted Li/Ca and Mg/Ca ratios but was unlikely to have contributed towards differences in skeletal Sr/Ca or B/Ca.

Differences in the skeletal ultrastructure or organic matter content may also have contributed towards differences in skeletal TE/Ca ratios. Coral skeletons are characterised by two different crystal structures, these being granular Li- & Mg-enriched crystals associated with rapid calcification in COCs, and fibrous Li- & Mg-depleted crystals which form more slowly away from COCs and are associated with thickening and extension (Sinclair, Williams and Risk, 2006; Holcomb *et al.*, 2009; Case *et al.*, 2010; Montagna *et al.*, 2014). COCs coincide with regions of high organic content (Cuif *et al.*, 2003) and although Mg-enrichment in these regions might be partially attributable to the presence of Mg-bearing biomolecules (Gagnon *et al.*, 2007; Dubinsky and Stambler, 2011; S. Tambutté *et al.*, 2011) the degree of Mg-enrichment in these regions of the skeleton exceeds that which can be explained by organic matter alone (Sinclair, Williams and Risk, 2006). Furthermore, when synthetic aragonite precipitates from seawater two different crystal structures form; under high pH and/or Ω conditions crystals rapidly form as amorphous structures that are enriched in Li and Mg, while under lower pH and/or Ω conditions fibrous Li- /Mg-depleted crystals form more slowly (Gabitov *et al.*, 2008, 2011; Holcomb *et al.*, 2009). When considered alongside the results of Chapters 2 (Buckingham *et al.*, 2022) and 3 it can be seen that the differences in Li/Ca and Mg/Ca between treatments reported in this study could potentially be explained by differences in the relative abundance of granular and fibrous crystal structures. In both species, culture in the LNLP treatment resulted in significant skeletal thickening and lower Li/Ca and Mg/Ca values. This is consistent with a greater relative abundance of fibrous, Li-/ Mg-depleted crystals being present, this being particularly relevant because fibrous crystals are

associated with skeletal thickening (Holcomb *et al.*, 2009; Case *et al.*, 2010; Montagna *et al.*, 2014) Contrastingly, in *A. polystoma,* the thinnest skeletal elements were observed in HNHP corals and were associated with the highest Li/Ca and Mg/Ca values, which is consistent with a greater relative abundance of granular Li-/ Mg-enriched crystals (Sinclair, Williams and Risk, 2006; Holcomb *et al.*, 2009; Case *et al.*, 2010; Montagna *et al.*, 2014). For *E. paradivisa*, the same pattern was observed except for the fact that Li/Ca and Mg/Ca values were anomalously high in the thickened skeletons of LNHP corals, an effect potentially attributable to the low F_{Ca} (as previously discussed).

However, the role of the organic matrix should also not be forgotten. COCs coincide with regions of high organic content (Cuif *et al.*, 2003). It has been suggested that Mg-bearing molecules with high Ca-binding capacity are excreted by the coral at COCs to promote calcification, and that higher concentrations of Mg are subsequently incorporated into these regions of the skeletal structure (Gagnon *et al.*, 2007; Dubinsky and Stambler, 2011; S. Tambutté *et al.*, 2011). The organic matrix pervades the entire coral skeleton and is composed of excreted proteins, lipids and sugars (reviewed in Dubinsky and Stambler, 2011 and S. Tambutté *et al.*, 2011). It is excreted by the calicoblastic cells and its formation is considered to be a prerequisite for skeletal growth because it provides nucleation sites and a structural template around which the aragonite structure can form (reviewed in Dubinsky and Stambler, 2011 and S. Tambutté *et al.*, 2011). Because the organic matrix is comprised of proteins, lipids and sugars a continuous supply of nutrients, particularly N, P and C is required to sustain organic matrix formation and consequently the growth of new skeleton. It is possible that nutrient limitation/starvation under HNLP, LNHP and LNLP treatments inhibits organic matrix formation, and the formation of new COCs which may have restricted linear extension in *A. polystoma*. In such a situation the formation of Li- and Mg-depleted fibrous crystals around the existing skeletal structures may have been favoured, resulting in a thickened skeleton that is depleted in Li and Mg. This scenario is consistent with the findings of Inoue *et al.* (2007) who observed that skeletal Mg/Ca ratios are positively correlated to linear extension rates. Any potential modifications to the carbonate chemistry have the potential to promote feedback processes. For example, if pH_{cf} and/or Ω_{cf} were reduced under low nutrient conditions, slower precipitation rates could further reduce Li/Ca and Mg/Ca ratios (Gabitov *et al.*, 2008, 2011; Holcomb *et al.*, 2009). Conversely, if carbonate chemistry was simultaneously modified such that pH_{cf} and/or Ω_{cf} increased under high nutrient availability, any

enrichment of Li and Mg may have been more strongly enhanced by more rapid calcification rates. It is therefore interesting to note that in *E. paradivisa* variability in Mg/Ca was best described by an MLR that incorporated a positive correlation with skeletal $\delta^{13}C$. This indicates that Mg/Ca was potentially correlated to the rate of photosynthesis, which itself is known to be positively correlated to calcification rate (Al-Horani, Al-Moghrabi and De Beer, 2003b). Analysis of the skeletal ultrastructure using scanning electron microscope (SEM) and complemented with more targeted analysis of crystal geochemistry could potentially resolve some of these potential explanations for differences in skeletal geochemistry.

4.5.6. Potential impacts on carbonate chemistry

As previously discussed, there is good reason to suspect that carbonate chemistry was modified by exposure to the different forms of nutrient stress considered in this study. In the bleached LNLP corals of both species, skeletal $\delta^{13}C$ values were depleted, indicative of reduced photosynthetic activity due to the loss of zooxanthellae. Reduced photosynthetic activity limits respiration rate, (Al-Horani, Al-Moghrabi and De Beer, 2003b, 2003a) and therefore the production of metabolically derived CO_2 which provides the majority of DIC incorporated into the coral skeleton (Furla *et al.*, 2000). Schoepf *et al.* (2021) recently demonstrated that thermal-stress mediated bleaching resulting from loss of zooxanthellae causes $[DIC]_{cf}$ and $[CO_3^{2-}]_{cf}$ to decrease with no significant impact on pH_{cf}. This modification to carbonate chemistry was associated with decreases in skeletal Li/Ca and Mg/Ca ratios and increases in skeletal Sr/Ca and B/Ca ratios (Schoepf *et al.*, 2021). For Li/Ca and Mg/Ca which are correlated with precipitation/ extension rate (Inoue *et al.*, 2007; Gabitov *et al.*, 2008, 2011) this pattern of response was largely replicated in both species during this study. This indicates that pH_{cf} and/or Ω_{cf} may have been reduced by bleaching. Schoepf *et al.* (2021) also observed that bleaching caused skeletal B/Ca ratios to increase, potentially in response to reduced $[DIC]_{cf}$ and $[CO_3^{2-}]_{cf}$. However, for the HNLP and LNLP corals that bleached in this study the opposite response, a decrease in B/Ca was observed. Furthermore, skeletal Sr/Ca decreased in bleached LNLP corals but not in bleached HNLP corals. Both Sr/Ca and B/Ca skeletal ratios have a more complex relationship with carbonate chemistry than Li/Ca and Mg/Ca ratios (Allison and Finch, 2010b; Holcomb *et al.*, 2016) and it is possible that simultaneous changes to Ca-ATPase pumping and metabolic CO_2 flux may have established novel $[DIC]_{cf}$ and pH_{cf} conditions

which influenced TE incorporation. As previously discussed, skeletal $\delta^{18}O$ values offer a very tentative indication of pH_{cf} conditions and suggest that pH_{cf} may have increased in HNLP corals and decreased in LNLP corals. For bleached LNLP corals, this makes sense because reduced Ca-ATPase pumping (because of reduced photosynthesis) is likely to result in reduced H^+ ion export from the calcifying fluid and result in decreased pH (Al-Horani, Al-Moghrabi and De Beer, 2003b, 2003a). However, for HNLP corals increased pH_{cf} in response to bleaching would be a novel observation that was seen in both *A. polystoma* and *E. paradivisa*. Furthermore, it suggests a strong modification of carbonate chemistry because the calcifying fluids of both species became less isolated under HNLP conditions which likely decreased pH_{cf}.

A possible explanation for the anomalously low skeletal $\delta^{18}O$ values of HNLP corals can be derived from the results of previous studies and Chapters 2 and 3, particularly if the $\delta^{18}O$ values are assumed to be influenced by pH_{cf}. P-starvation of the zooxanthellae is a common response in symbiotic corals during chronic exposure to high N:P ratios (Wiedenmann *et al.*, 2013; D'Angelo and Wiedenmann, 2014; Rosset *et al.*, 2017; Buckingham *et al.*, 2022). P-starvation is identifiable from the substitution of thylakoid membrane phospholipids for sulpholipids, malfunctioning of photosynthetic apparatus and reduced Fv/Fm (Parkhill, Maillet and Cullen, 2001; Wiedenmann *et al.*, 2013; D'Angelo and Wiedenmann, 2014; Rosset *et al.*, 2017). Such modifications of thylakoid membrane composition lead to the increased generation of harmful reactive oxygen species (ROS) such as singlet oxygen $^1O_2$ or hydrogen peroxide (H_2O_2) which damage the photosynthetic apparatus of the symbionts and reduce Fv/Fm (Lesser, 1997; Tchernov *et al.*, 2004, 2011; Rehman *et al.*, 2016). Translocation of ROS to host cells could consequently occur (Tchernov *et al.*, 2011; Rehman *et al.*, 2016). H_2O_2 promotes lipid peroxidation which can cause host lipid membranes to become 'leaky' to Ca^{2+} ion invasion, potentially necessitating the enhanced upregulation of Ca-ATPase activity to maintain safe Ca concentrations within the host cells (Sandeman, 2008). Ca-ATPase activity could therefore theoretically increase as a consequence of oxidative stress in the host, resulting in enhanced Ca^{2+} /H^+ ion pumping and leading to elevated pH_{cf} and decreased skeletal $\delta^{18}O$ values (Al-Horani, Al-Moghrabi and De Beer, 2003a, 2003b). Furthermore, it has been suggested that during oxidative stress corals may need to expend additional energy to repair damaged cells and upregulate the production of antioxidants to detoxify ROS

(Wooldridge, 2010). It is therefore interesting to note that the impacts on corallite size and dissepiment formation observed in *E. paradivisa* suggest that polyp biomass loss was greatest under HNLP conditions, indicating that P-starvation of the symbionts potentially exerts additional physiological pressures on the coral host which result in greater use of energetic reserves (Chapter 3). It is possible that impacts such as oxidative stress and/or increased energetic expenditure are somehow responsible for the unique geochemical response associated with HNLP conditions, and that such a response arises due to modification of the calcifying fluid carbonate chemistry, possibly enhanced upregulation of pH_{cf}. However, as repeatedly stressed throughout this chapter, any potential modifications to the carbonate chemistry of the corals studied here cannot be properly characterised without first measuring skeletal $\delta^{11}B$.

4.5.7. Conclusions

In symbiotic corals, characteristic patterns in skeletal stable isotope and TE/Ca ratios arise in response to bleaching caused by different forms of nutrient stress. The paleo-thermometers Li/Ca, Mg/Ca, Sr/Ca and $\delta^{18}O$ are all impacted, and consideration of bulk measurements from nutrient-stressed corals leads to erroneous proxy-derived estimations of SST. Rayleigh fractionation and the extent of the calcifying fluid's isolation from the external medium are likely to be important for determining Li/Ca and Mg/Ca ratios, whereas skeletal Sr/Ca, B/Ca and $\delta^{18}O$ values are potentially impacted by modifications to the carbonate chemistry of the calcifying fluid caused by reduced photosynthetic rates. The geochemical response to bleaching under high seawater N:P stoichiometries differs from that observed under nutrient limiting conditions, suggesting that P-starvation of the symbionts exerts an additional influence on carbonate chemistry that may be indicative of increased energetic expenditure and/or oxidative stress in the host. The findings of this study highlight the need for researchers to consider the nutrient environment, and in particular N:P stoichiometries as a factor that can not only directly and negatively impact reef coral health but can also complicate the use of geochemical proxies.

Chapter 5 – Critique, synthesis and future directions

5.1. Chapter critiques

5.1.1. Critique of Chapter 2

The literature relating to the direct impacts of nutrient enrichment on skeletal growth and structure in zooxanthellate corals contains reports of divergent responses with regard to linear extension, calcification and skeletal density (Tomascik and Sander, 1985; Marubini and Davies, 1996; Koop *et al.*, 2001; Szmant, 2002; Fabricius, 2005; Dunn, Sammarco and LaFleur, 2012; Rocker *et al.*, 2017). This was an important problem to resolve as disagreement within the literature has the potential to undermine conservation efforts by making it harder to secure stakeholder support for such projects (Bell, Lapointe and Elmetri, 2007). A major strength of Chapter 2 lies in the fact that it includes a detailed re-evaluation of the published literature. This precedes the discussion of the paper's experimental findings, and provides a fresh insight into the contradictory results of previous studies. Furthermore, the paper's experimental results are entirely consistent with this re-evaluation of the literature. This strengthens the proposal that skewed N:P stoichiometries play a role in determining the responses of skeletal growth and structure to nutrient enrichment.

A meta-analysis of published studies had previously made good headway in identifying potential causes for the literature's seemingly contradictory results, by demonstrating that the impacts of nutrient enrichment on skeletal growth and structure are context-dependent (Shantz and Burkepile, 2014). It was found that N-enrichment enhances photosynthesis but reduces calcification, whilst P-enrichment has minimal impact on photosynthesis but increases calcification. Furthermore, nutrient enrichment derived from anthropogenic sources (including experimental enrichment) is more likely to have a negative impact on skeletal growth metrics than natural sources of nutrient enrichment, while some taxa (such as *Acroporids*) are more susceptible to negative impacts than others (Shantz and Burkepile, 2014). The authors of the meta-analysis also identified marginally significant effects of N:P stoichiometry on both linear extension and calcification. But, these findings were only mentioned in passing and the supporting figures were relegated to their supplementary material (Shantz and Burkepile, 2014). This was because the authors were concerned that

the literature analysed lacked any studies that considered nitrate enrichment (they only related to ammonium) and that the ammonium levels considered were very high. Therefore, the authors of the meta-analysis cautioned that the observed effect was equally likely to be attributable to either the species of DIN that had been enriched, or the enrichment level (Shantz and Burkepile, 2014).

Despite correctly identifying that N:P stoichiometry can determine whether the impacts on skeletal growth are positive or negative, Shantz and Burkepile (2014) failed to appreciate the significance of their finding. The literature review conducted as part of Chapter 2 identified additional studies which had been missed during the Shantz and Burkepile meta-analysis (Tanaka *et al.*, 2007; Dikou, 2009), and also benefitted from the inclusion of studies that post-dated it (Browne *et al.*, 2015; Tanaka *et al.*, 2017; Silbiger *et al.*, 2018; Savage, 2019). However, it should be noted that some other studies included in the meta-analysis of Shantz and Burkepile could not be sourced, these being primarily conference-related publications. An important observation from Chapter 2's evaluation of the literature was that high N:P ratios (> 35:1) are primarily associated with negative impacts on skeletal growth metrics and, more importantly that such high N:P ratios have only been reported from reef settings following anthropogenic nutrient enrichment (Spencer Davies, 1990; Lapointe, 1997; Szmant, 2002; Lapointe, Tewfik and Phillips, 2021). Thus, a potential explanation for the association between anthropogenic sources of nutrient enrichment and negative growth metrics was identified. Shantz and Burkepile (2014) had been unable to confidently make this link with the data available to them. This relationship was then tested using a model species from the genera *Acropora* (which both studies had identified as being particularly sensitive) through the enrichment of nitrate. Statistically significant results were obtained. Therefore, in combination with the findings of the literature review and the previous meta-analysis (Shantz and Burkepile, 2014), the results of Chapter 2 demonstrated that the resultant N:P stoichiometry of seawater is a factor that can have negative impacts on coral skeletal growth, and that this can occur following enrichment of nitrate as well as ammonium. This is an important step forward, despite only being a small advance on the progress made by Shantz and Burkepile (2014). It is also consistent with the observations that short-term positive impacts on metrics of photobiology (such as increased zooxanthellae density) following N-enrichment can ultimately have negative impacts coral health (Wiedenmann *et al.*, 2013) and skeletal growth (Shantz and Burkepile, 2014).

At the time of submission, Chapter 2 is the only chapter within this thesis that has been published, this being online in the journal *Coral Reefs* on 20th April 2022 (DOI: 10.1007/s00338-022-02223-0). Despite this piece of work's successful navigation through the peer-review process, there are several deficiencies in the methods used during both the culturing phase, and the post-culture analysis using μ-CT. Whilst these shortcomings do not render the published results invalid, they did require that certain (otherwise unnecessary) assumptions were made when interpreting the data, and could be considered minor weaknesses of the study.

The best-practice method for measuring the calcification rate of corals during culture is by using repeated measures made using the buoyant weight method. This method has two advantages over the one used in this study (wet weight measured after a defined drip-off period). These are 1) it prevents differential rates of water drainage from coral skeletons to alter measurements of coral weight and, 2) it removes a potential source of stress which can be placed on corals when they are repeatedly removed from the seawater/ culture medium (Jokiel, Maragos and Franzisket, 1978). Since the buoyant weight method was not used, it cannot be explicitly ruled out that the drainage of the coral skeletons differed, either between samples or during different stages of the experiment. Therefore, some level of unmeasured uncertainty is attributable to these measurements. Fortunately, the results obtained for linear extension and calcification do not suggest that this methodological deficiency was a major issue. The observed patterns between linear extension and calcification that were derived from these measurements were in complete agreement with the observed responses that affected the skeletal microstructure (skeletal element thickness and porosity). In fact, these measurements provided the only feasible explanation for the observed modifications to the coral skeletons, namely that thickening occurred when linear extension ceased but calcification continued. As such, the measurements of calcification provided information that was vital for a robust interpretation of the data obtained through μ-CT analysis. In this sense, the fact that calcification was measured during the culture phase (albeit not using the best-practice method) should be considered a strength of the study's methodology.

The analysis conducted using μ-CT could have been more complete. The open source software programme ImageJ that was used for image analysis was adequate for the tasks undertaken, but has limited functionality. Its use during this project was unavoidable due to

limitations placed on the availability of more suitable hardware and software resources during the COVID-19 pandemic. These computational limitations dictated that the analysis of individual coral fragments was restricted to two regions of interest (ROIs) per sample, and that more widespread variability within fragments could not be mapped or analysed. It is not considered that these analytical shortcomings undermine the findings of this chapter, but they do represent a missed opportunity to exploit the full potential of the dataset. For example, it would have been useful to compare the skeletal element thickness profiles of corals from each of the different nutrient treatments to that of an *Acropora pulchra* from a natural setting which had been previously imaged at the same facility (Roche *et al.*, 2011). This would have allowed a more robust evaluation of this study's relevance to real-world settings.

5.1.2. Critique of Chapter 3

The corals described in Chapter 3 are the subjects of two previously published papers which describe the broad phenological responses of *Euphyllia paradivisa* corals when cultured under four different nutrient treatments, and the impacts of these treatments on their algal symbionts (Rosset, D'Angelo and Wiedenmann, 2015; Rosset *et al.*, 2017). Because the original studies were concerned with determining the impacts on the coral-zooxanthellae symbiosis, linear extension and calcification were not measured. As such, the impacts on skeletal growth rates cannot be quantified, and discussion of the treatment effects is restricted to relative differences between the treatments. Fortunately, because these experiments involved exposure to the experimental conditions for $\geq$ 6 months, and the size differences between treatments were very large, these differences could confidently be assigned to the treatment effect.

The choice of species used for this experiment could be considered both a strength and a weakness of this study. *E. paradivisa* has a phaceloid colonial structure, meaning that polyps are isolated from each other at the ends of individual branches (Madl, Schabetsberger and Lipovnik, 2014; Luzon *et al.*, 2017). Therefore, *E. paradivisa* polyps are able to develop without the spatial constraints that are placed on polyps of branching or mounding species by neighbouring polyps. This allows the full potential of the treatment effects on corallite growth to be assessed, while analysis of the corallite structure is made easier by the large and open nature of the *E. paradivisa* corallite (Madl, Schabetsberger

and Lipovnik, 2014; Luzon *et al.*, 2017). However, *E. paradivisa* - which is predominantly found at mesophotic depths - is highly adaptable even to high-light conditions, and is typically only excluded from shallower depths due to competitive exclusion (Sinniger *et al.*, 2016; Eyal *et al.*, 2019). Furthermore, *E. paradivisa* can survive periods of complete darkness (Eyal *et al.*, 2019) or heterotrophic starvation (Rosset *et al.*, 2017) that last for ≥ 1 year, demonstrating a strong capacity to rely on alternative sources of nutrition when growth conditions are unfavourable. As such, a weakness of this study is that *E. paradivisa* could potentially be regarded as an exceptionally hardy and adaptable species. This calls into doubt the suitability of *E. paradivisa* as a 'model species', and the relevance of these results for other species and genera could potentially be questioned.

With regards to the methods, the primary weakness of this paper relates to the fact that corallite size (calice area and theca length) and shape (circularity) were determined from the analysis of digital photographs. The use of 2-dimensional images to measure the size and shape of a 3-dimensional structure is prone to error. This is because the dimensions of uneven surfaces inevitably become distorted when translated into 2 dimensions, resulting in erroneous measurements from the 2-dimensional image. The magnitude of this effect is difficult to assess and equally hard to correct for, and no attempt to do so has been made. Consequently, the measurements of corallite area, theca length and circularity all have an unquantified level of uncertainty attributable to them, the significance of which has not been properly assessed. However, it should be noted that the differences in size between treatments were typically large and strikingly evident, even from a casual visual inspection.

In Chapter 3's discussion, it is posited that the impact of the HNLP treatment is more detrimental to *E. paradivisa* than that of the LNLP treatment. This conclusion was reached based on two considerations. Firstly, there was no significant difference in polyp size, zooxanthellae density (Rosset *et al.*, 2017) or tissue depth (determined from dissepiment depth) between the two treatments, despite HNLP corals being exposed to experimental conditions for a much shorter length of time (Rosset, D'Angelo and Wiedenmann, 2015; Rosset *et al.*, 2017). This suggest a much more rapid loss of polyp biomass and zooxanthellae density in HNLP corals. Secondly, in HNLP corals the symbionts showed symptoms of P-starvation (Rosset *et al.*, 2017). P-starvation of the zooxanthellae lowers the thermal threshold for bleaching (Wiedenmann *et al.*, 2013) and may lead to the

extracellular production of ROS by the symbionts (Rehman *et al.*, 2016). It has been proposed that under such circumstances, the host must expend additional energy to produce protective antioxidants (Wooldridge, 2010). Such a response could explain the greater rate of biomass loss observed in HNLP corals. While this tantalising conclusion is reasonable it must remain purely speculative. With hindsight, measurements of photosynthesis, respiration and calcification rates during the culture phase would have allowed for a much more robust assessment of the impacts on coral physiology, and a better understanding of how this impacts skeletal growth. Failing to take these measurements is a weakness of this study.

5.1.3. Critique of Chapter 4

A major weakness of Chapter 4 derives from the fact that the water chemistry of the treatment tanks was not measured during the culture phases to determine $\delta^{18}O$ and $\delta^{13}C$ values. Consequently, it cannot be ruled out that differences in skeletal isotope values arose due to differences in the isotopic compositions of the culture mediums. The frustrating aspect of this is that both coral species exhibited broadly similar patterns in their isotopic responses to the different nutrient treatments. This suggests that exposure to different forms of skewed N:P ratios, or severe nutrient limitation elicits characteristic responses that are replicated across genera. This interpretation is supported by a similar pattern of responses when the TE/Ca values are considered. Unfortunately, because the culture medium $\delta^{18}O$ and $\delta^{13}C$ values were not measured, it is unlikely that the results of the isotope analysis will be suitable for publication. This has important ramifications because coral skeletal $\delta^{18}O$ is still considered to be a reliable paleothermometer. However, its uniform response to the HNLP and LNLP treatments in both species indicates that previously unrecognised 'vital effects' may be expressed when corals are exposed to nutrient stress, and that they can impact the reliability of skeletal $\delta^{18}O$ as a climate proxy. Exclusion of the ^{13}C data limits discussion of the potential physiological impacts on the corals when exposed to the different nutrient treatments, and the impacts these can have on TE/Ca ratios. It is very likely that photosynthesis was reduced in the bleached corals of both species when exposed to the LNLP treatment, and that this is detectable from the reduced skeletal $\delta^{13}C$ values of these corals (Swart, 1983; McConnaughey, 1989a). However, without normalising to account for differences in isotopic composition between culture mediums, this data cannot be relied upon to support such an argument in a peer-

reviewed publication. This being said, the isotope data has been retained within Chapter 4 to allow the full impacts of the different nutrient treatments to be considered. However, it is duly recognised that uncertainty in the reliability of the isotope data constitutes a major weakness of the study.

A further weakness of this study relates to the acquisition of TE/Ca ratios. This data was derived in the form of 'bulk samples' which homogenise the spatial variability within skeletons that has been recorded for Li/Ca, Mg/Ca, Sr/Ca and B/Ca (Holcomb *et al.*, 2009; Allison and Finch, 2010b; Case *et al.*, 2010; Brahmi *et al.*, 2012; Montagna *et al.*, 2014; Chalk *et al.*, 2021). Such spatial variability in coral skeletons has been attributed to differences in localised calcifying conditions, potentially brought about by spatial variability in any or all of the following:- pH_{cf}, Ω_{cf}, organic content and crystal structure (Meibom *et al.*, 2004; Holcomb *et al.*, 2009; Allison and Finch, 2010b; Case *et al.*, 2010; Brahmi *et al.*, 2012; Montagna *et al.*, 2014; Chalk *et al.*, 2021). Although comparison of these 'bulk' TE/Ca ratios between treatments can be very informative it has been shown that the use of such samples can potentially lead to the erroneous interpretation of climate proxies (Robinson *et al.*, 2014). This has led to some researchers preferring to target regions of skeleton with corresponding crystal structures when assessing TE/Ca and isotopic proxies (Holcomb *et al.*, 2009; Frankowiak, Kret, *et al.*, 2016; Kuffner *et al.*, 2017). The untargeted approach used in this study does not invalidate its results, and it should be noted that both coral species showed broadly similar geochemical responses to the different forms of nutrient stress. This suggests that the different forms of nutrient stress prompt characteristic physiological responses that are manifested in skeletal TE/Ca ratios. These physiological responses likely affect any or all of the following :-pH_{cf}, Ω_{cf}, organic matrix content or distribution of different crystal structures (Meibom *et al.*, 2004; Holcomb *et al.*, 2009; Allison and Finch, 2010b; Case *et al.*, 2010; Brahmi *et al.*, 2012; Montagna *et al.*, 2014; Chalk *et al.*, 2021). Therefore, the main problem arising from the use of an untargeted sampling method is that it prevents the causes of these TE/Ca differences between treatments being more thoroughly investigated.

It was initially intended that skeletal $\delta^{11}B$ would also be measured. Where $\delta^{11}B$ of the culture medium and the skeleton is known pH_{cf} can be quantified, and subsequently B/Ca can be used to calculate $[DIC]_{cf}$ (Holcomb *et al.*, 2016; McCulloch *et al.*, 2017; Decarlo,

Holcomb and McCulloch, 2018). Photosynthesis, respiration, ATP production and calcification have been found to be positively correlated in zooxanthellate corals (Al-Horani, Al-Moghrabi and De Beer, 2003b). For corals that bleached during this study, it is suspected that DIC supply to the calcifying space decreased as a consequence of reduced photosynthesis and respiration. This is hinted at by the depleted $\delta^{13}C$ values of the LNLP corals, but cannot be confirmed without the missing $\delta^{11}B$ data. It is hoped that this outstanding element of the work can be completed at a later date.

A strength of this paper is that - unlike most geochemical studies - the impacts on TE/Ca ratios were assessed using multivariate methods, namely robust MANOVA and linear discriminant analysis (LDA). Multivariate methods reduce the likelihood of making type II errors, this being the erroneous failure to reject a null hypothesis. The MANOVA was able to identify that some differences in TE/Ca ratios which would have been deemed non-significant using a univariate approach, actually contributed towards a statistically significant geochemical difference between treatments. Furthermore, by structuring the data frames for both species in exactly the same format, the LDA's demonstrated that both species responded in a broadly similar geochemical manner to the different nutrient treatments. As such, the use of multivariate analytical methods allowed for a more complete understanding of the impacts of skewed N:P ratios and nutrient imitation on coral geochemistry, than may have been possible using an univariate approach.

5.2. The contribution of this thesis to the field of study

Previous research into the effects of skewed N:P ratios on zooxanthellate corals has primarily focussed on the impacts that such conditions have on coral bleaching sensitivity and the biochemistry and ultrastructure of *Symbiodinium* cells (Wiedenmann *et al.*, 2013; Rosset, D'Angelo and Wiedenmann, 2015; Rosset *et al.*, 2017). Such research was prompted by the observation that increased levels of DIN on the Great Barrier Reef correlated with an increased likelihood of corals to bleach during periods of thermal stress (Wooldridge, 2009). Changes to the biochemical composition of symbiont-bound lipids that occur in response to imbalanced N-enrichment can lead to increased symbiont production of ROS (Tchernov *et al.*, 2004; Wiedenmann *et al.*, 2013). Elevated levels of ROS may cause oxidative stress in zooxanthellate corals and have long been considered a

trigger for bleaching (Lesser, 1996, 1997). The work of Wiedenmann *et al.* (2013) established a mechanism that explains how the imbalanced enrichment of DIN increases the bleaching susceptibility of zooxanthellate corals. This work was followed up by the studies of Rosset et al. which demonstrated that, in addition to modifying the biochemistry and ultra-structure of zooxanthellae cells, exposure to skewed N:P ratios also negatively impacts coral polyp biomass (Rosset, D'Angelo and Wiedenmann, 2015; Rosset *et al.*, 2017). In the meantime, Shantz and Burkepile (2014) had very cautiously identified a potential link between seawater N:P stoichiometry and the coral skeletal growth response to nutrient enrichment. Their work had been motivated by the fact that divergent responses had been reported in the published literature for linear extension, calcification and skeletal density following nutrient enrichment (Tomascik and Sander, 1985; Koop *et al.*, 2001; Szmant, 2002; Fabricius, 2005; Dunn, Sammarco and LaFleur, 2012). Shantz and Burkepile had re-assessed the literature using meta-analysis, but the available data was not sufficient to allow any firm conclusions to be made regarding the impact of skewed N:P ratios on skeletal growth. Instead, they had little alternative but to conclude that the species of enriched DIN or level of enrichment could be more or equally as important (Shantz and Burkepile, 2014), and much of the data relating to the influence of N:P stoichiometry was confined to their paper's supplementary material.

The work described in Chapter 2 brought together these different avenues of research to show that - in addition to impacting coral and zooxanthellae physiology - skewed N:P stoichiometries can impact skeletal growth and structure. Furthermore, these impacts are entirely consistent with the published data, which until now had not been assessed along these lines to this extent. Misinterpretation of the published literature has, in the past led to incorrect management policies being implemented by marine managers charged with protecting reef ecosystems (Bell, Lapointe and Elmetri, 2007). Chapter 2 has added to a growing body of evidence that suggests changes to the N:P stoichiometry of seawater, that can occur following imbalanced nutrient enrichment negatively impact the health and skeletal growth of zooxanthellate corals (Spencer Davies, 1990; Shantz and Burkepile, 2014; Lapointe *et al.*, 2019; Lapointe, Tewfik and Phillips, 2021). Furthermore, the literature review component of Chapter 2 revealed that amongst all published studies involving N:P ratios >35:1, the source of nutrient enrichment was either from pollution or through the experimental manipulation of culture medium/seawater conditions. This is an important observation because it implies that harmfully high seawater N:P ratios on coral

reefs can be avoided through the strict management of polluting activities alone. Coral reefs are in rapid decline throughout their global range and, although this is primarily due to global climate change, the land-based input of nutrients has also been identified as an important local stressor that contributes towards reef degradation (GCRMN, 2020). By providing an improved degree of clarity to this aspect of reef ecology, the findings of Chapter 2 should be considered a useful contribution to the urgent research underpinning conservation efforts.

In Chapter 2 it was shown that the micro-structure of coral skeletons can be modified when linear extension and calcification are differentially impacted by nutrient conditions. In particular, under HNHP conditions fragments of *Acropora polystoma* had rates of linear extension that increased at a disproportionately fast rate when compared to the rate of calcification, resulting in thinning of skeletal elements and increased skeletal porosity. Conversely, under HNLP and LNLP conditions linear extension ceased but calcification continued, resulting in thickening of skeletal elements and reduced skeletal porosity. Chapter 3 built on this work but the analysis was focussed on the impact on the corallites. It was shown that nutrient-stress mediated modifications to the skeletal structure are not necessarily limited to skeletal element thickness and its associated impact on skeletal porosity. For *E. paradivisa*, the size and internal structure of corallites were additionally impacted by nutrient stress, and the effects differed between the different nutrient treatments. In particular, it was demonstrated that the decreases in polyp biomass/volume that occurred in bleached (HNLP and LNLP) corals resulted in the formation of shallower endo-thecal dissepiments and homogenisation of skeletal element thickness throughout the depth of the corallite. This contrasted with the response of nutrient limited but unbleached (LNHP) corals, the skeletal elements of which thickened more uniformly and retained the inversely correlated relationship between skeletal element thickness and distance from the apex of the calice.

Thickening of skeletal elements can contribute to the formation of regions of high density in coral skeletons (Dávalos-Dehullu, Hernández-Arana and Carricart-Ganivet, 2008; Fouke, Trop and Sivaguru, 2021). When reconstructing the life histories of corals, researchers have previously identified high density regions as having formed when skeletal growth is either inhibited by unfavourable seasonal conditions (Peirano *et al.*, 2005; Dávalos-Dehullu, Hernández-Arana and Carricart-Ganivet, 2008; Fouke, Trop and

Sivaguru, 2021) or stunted during episodes of bleaching (DeCarlo and Cohen, 2017; Barkley *et al.*, 2018). Most studies of this type rely on counting the number of seasonally-formed density bands and/or monthly dissepiments and then correlating these features against records of extreme climatic conditions and/or the dates of known bleaching events. Different methods have been used to distinguish 'stress bands' from seasonal high-density bands, however these distinctions are typically arbitrarily defined. For example, a 'stress band' has been defined as being anomalous to the previous 7-year period with respect to dissepiment spacing and bulk calcification rate (DeCarlo and Cohen, 2017), or being a widespread band throughout the full extent of a colony within which the density anomaly exceeds 2 standard deviations of the seasonal signal (Barkley *et al.*, 2018).

The results presented in Chapter 3 could potentially provide an additional or alternative empirically-derived method for differentiating seasonal and stress-related high-density regions in coral skeletons, particularly when the full skeleton or climate record is unavailable. However, there are several considerations would need to be addressed beforehand. Firstly, the impacts of thermal-stress mediated bleaching on *E. paradivisa* corallites have not been assessed, so it is unclear whether homogenisation of skeletal thickness also occurs within corallites under such conditions. It is also unclear whether the characteristic modifications to corallite structure described for *E. paradivisa* are restricted to corals that share the same morphology or even to just this species. Finally, it is not known to what extent subsequent skeletal growth (following recovery) might further modify the skeleton, thus potentially deleting the characteristic signatures relating to skeletal thickness.

Whether or not Chapter 3's findings can be used to reliably identify signatures of bleaching in coral skeletons remains to be determined. However, it should be noted that this is the first study to examine the impacts of nutrient stress on the structure of zooxanthellate coral skeletons at the level of the corallite, so these findings do constitute an original contribution of knowledge to the field of study. Furthermore, Chapter 3's results lend support to the assertion that dissepiment depth can be used as a proxy for determining polyp tissue depth and/or biomass (Barnes and Lough, 1992; Barkley *et al.*, 2018; Precoda *et al.*, 2020). This could prove useful for those researchers seeking to investigate the impacts of environmental disturbance on coral physiology.

The use of coral skeletal trace element and stable isotope ratios as climate proxies is far more established than that of modifications to the skeletal microstructure. But, the careful use of geochemical proxies is made more difficult by the fact that various biological signals may overprint or override climatic signals, a phenomenon collectively referred to as 'vital effects' (Gagnon *et al.*, 2007; Pérez-Huerta *et al.*, 2010; Juillet-Leclerc *et al.*, 2014; Robinson *et al.*, 2014). The influence of 'vital effects' on geochemical proxies can be minimised by either targeting specific crystal structures within a coral skeleton (Holcomb *et al.*, 2009; Frankowiak, Kret, *et al.*, 2016; Kuffner *et al.*, 2017) or through careful species-specific calibrations (Montagna *et al.*, 2014; Ross, DeCarlo and McCulloch, 2019). However, such work requires a good working knowledge of all the environmental factors that are liable to induce such 'vital effects', and the extent to which they may affect the relevant climate proxy. Given that the impact of skewed N:P stoichiometries on the skeletal growth response of corals had not been previously appreciated, it was not surprising to observe that no work had yet been undertaken to assess the impacts on skeletal geochemistry.

Chapter 4 assesses the impact of four different nutrient treatments on multiple TE/Ca and stable isotope ratios, all of which have previously been used as proxies to investigate the environmental or physiological conditions under which coral skeletons formed (Weber and Woodhead, 1972; Swart, 1983; Beck *et al.*, 1992; Mitsuguchi *et al.*, 1996; Marriott, Henderson, Belshaw, *et al.*, 2004; Holcomb *et al.*, 2016). The results of Chapter 4 demonstrated that each of the different nutrient treatments elicited a characteristic geochemical response, and that these responses were broadly similar in two morphologically and taxonomically distinct coral species. It was then established that the magnitude of the observed differences in skeletal Li/Ca, Mg/Ca, Sr/Ca and $\delta^{18}O$ values between treatments were large enough to produce erroneous proxy-derived estimates of temperature difference between the culture tanks. It should be noted that (similar to temperature) anthropogenic impacts on water quality can follow seasonal patterns (Caccia and Boyer, 2005; Browne *et al.*, 2015) and at least one study has previously noted an impact of increased phosphorus availability on the reliability of the Sr/Ca SST proxy (de Villiers, Shen and Nelson, 1994). Therefore, the main implication of Chapter 4 is that it identifies variability in nutrient concentrations and/or N:P stoichiometries as a potential factor that complicates the proxy use of TE/Ca and stable isotope ratios. This is a novel finding that should be considered by researchers seeking to use coral-derived geochemical

proxies, particularly those investigating reefs impacted by the anthropogenic input of inorganic nutrients.

To summarise, the papers comprising Chapters 2-4 of this thesis have individually and collectively, made a substantial contribution to knowledge in the field of coral ecology. In Chapter 2, apparently contradictory reports from the published literature relating to coral skeletal growth responses to nutrient enrichment were resolved by a careful re-assessment of the existing literature. Support for the newly established link between seawater N:P stoichiometry and the nature of the skeletal growth response was then provided by new experimental findings. In Chapter 3, it was established that the impacts of nutrient-stress on skeletal growth can extend to modification of the size, shape and the internal architecture of corallites, reflecting changes to the polyp biomass. Finally, in Chapter 4 it was shown that exposure to different forms of skewed N:P ratios and/or severe nutrient limitation results in the modification of skeletal geochemistry, and that similar responses to the different forms of nutrient stress may be shared by taxonomically distinct coral species.

5.3. Potential directions for future research

As with many research projects, the findings presented within this body of work pose a number of questions which could direct future research. Some of these questions arise due to limitations of the present study and require additional work to be conducted on the samples to hand. But there is also further research that could be conducted to establish the full extent to which coral reefs are exposed to the impacts of skewed N:P stoichiometries.

Firstly, there is more work that can be conducted to investigate the micro-structure of the coral skeletons that have been analysed here. As previously discussed, the 3-dimensional image files relating to *A. polystoma* could not be mapped in their entirety due to computational limitations. It would be useful for this to be done, particularly with respect to latitudinal mapping of skeletal element thickness and skeletal porosity. Of particular interest is the extent to which infilling (skeletal thickening) is 'sacrificed' throughout different regions of the skeleton to support enhanced linear extension when nutrient conditions are replete. *Acroporids* have high fragmentation potential - especially when wave energy is high such as during storms (Bright *et al.*, 2016; Puotinen *et al.*, 2020) - and

breakage is most likely to occur in the regions of the skeleton which are most porous (Chamberlain, 1978). Theoretically, if modification of the thickness profile causes regions of high porosity to extend further down a branch, it could potentially increase the size of fragments that detach when wave energy is high. However, it is also possible that a highly porous large fragment would then more rapidly break into smaller pieces during subsequent impacts with the sea floor and debris. Small detached fragments are more likely to be displaced far from their parent colony, so are more likely to settle in unfavourable sites and die (Lirman, 2000). Contrastingly, large fragments are less likely to be displaced large distances so are more likely to settle on live colonies of the same species; this improves their survival prospects because they can then fuse to the corals beneath (Lirman, 2000). This means that modifications to coral skeletal thickness (and therefore mechanical strength) have the potential to impact the resilience of coral ecosystems to storm damage. This is important because the frequency of the strongest storms is predicted to increase as global warming intensifies in the coming years (Gleixner *et al.*, 2014). As such, further work is required to understand of the full implications of modifications to skeletal properties that occur following nutrient enrichment, and how this may impact *Acroporid*-dominated coral reef ecosystems in the future. In particular, analysis of modifications to the 3-dimensional microstructure (using μ-CT) could be complemented by experiments that test the impacts of such modifications on the mechanical strength of coral skeletons.

Another direction for future research would be to extend the analysis of the skeletons to an examination of the skeletal ultrastructure. It is unclear whether differences in skeletal TE/Ca ratios arise due to uniform enrichment/ depletion throughout coral skeletons, or whether they arise as a consequence of changes to the relative abundance of different crystal structures (which have different TE/Ca ratios) (Holcomb *et al.*, 2009; Case *et al.*, 2010; Montagna *et al.*, 2014). The former might indicate a uniform modification of carbonate chemistry throughout the coral skeleton, whilst the latter might be indicative of differences in the relative abundance of 'centres of calcification' and organic matrix. As discussed in Chapter 4, there is good reason to suspect that both carbonate chemistry and the production rate of 'organic matrix' could be impacted by the different forms of nutrient-stress tested during this project. More detailed analysis of the skeletons using a scanning electron microscope (SEM) complemented with targeted chemical analysis - such as nanoscale secondary ion mass spectrometry (nano-SIMS) - could determine whether

there are differences between treatments in a) the ratio of fibrous to granular crystals and b) the TE/Ca ratios of corresponding crystal structures. The former might indicate that that the observed geochemical differences arise due to re-ordering of crystal structures, a phenomenon that could reflect differences in organic matrix synthesis (reviewed in Dubinsky and Stambler, 2011 and S. Tambutté *et al.*, 2011). Alternatively, the latter might suggest a more widespread impact on carbonate chemistry, that is shared throughout the entire coral colony. Nano-scale analysis of the chemical composition of the skeleton should be extended to include that of skeletal $\delta^{18}O$ and $\delta^{13}C$ to allow the relationships between TE/Ca and isotopes to be investigated further.

Of course, either observation would require further work before any such conclusions could be made, and this might include work to isolate and quantify the organic matter content. Such further studies of the skeletal ultrastructure and spatially correlated variability in geochemistry could aid in resolving some of the uncertainties regarding several different aspects of coral biology and geochemistry. This includes the processes underpinning the formation of skeletal structures, the impacts of 'vital effects' on geochemical proxies and the impacts of bleaching on coral carbonate chemistry. These are all lines of research being actively worked on at the time of writing.

The impacts of the different nutrient treatments on carbonate chemistry can only be properly assessed by extending the chemical analysis of the skeletons to include that of $\delta^{11}B$. This would allow quantification of the differences in both pH_{cf} and $[DIC]_{cf}$ between the different treatments. The $\delta^{13}C$ data presented in Chapter 4 suggests that photosynthesis (and therefore DIC supply) was likely to have been reduced in bleached corals subjected to severe nutrient limitation (the LNLP treatment), while the somewhat unreliable pH-proxy of $\delta^{18}O$ suggests that pH_{cf} may have also decreased. This response is consistent with the positive correlations that have been observed in zooxanthellate corals between photosynthesis, respiration, calcification and pH_{cf} (Al-Horani, Al-Moghrabi and De Beer, 2003b, 2003a). Conversely, in HNLP corals the problematic $\delta^{18}O$-proxy suggested that pH_{cf} might have increased following bleaching. This potential response differs both from the observed response to LNLP conditions and the response to thermal-stress mediated bleaching (McCulloch *et al.*, 2017; Schoepf *et al.*, 2021). If it is confirmed that pH_{cf} does increase under HNLP conditions this would constitute a novel response, potentially related

to P-starvation of the symbionts. However, such an effect cannot be properly investigated without first properly constraining calcifying fluid chemistry, and this can only be done conclusively by measuring skeletal $\delta^{11}B$.

In Chapter 2 it was highlighted that amongst studies relating to the impacts of nutrient enrichment on coral skeletal growth, N:P ratios > 35:1 have only been reported in those studies for which nutrient pollution or experimental addition of nutrients was the cause of enrichment. Excessively high N:P ratios on polluted coral reefs (in some cases as high as 74:1) have been reported in Barbados (Spencer Davies, 1990), Jamaica (Lapointe, 1997) Brazil (Szmant, 2002) and Florida, USA (Lapointe, Tewfik and Phillips, 2021) and in all cases were linked to coral reef decline. However, the true extent of the problem of exposure to skewed N:P stoichiometries on reefs is not known. Wooldridge (2009) identified a link between terrestrially sourced DIN-enrichment of coral reefs and spatial variation in coral bleaching susceptibility along a large section of the Great Barrier Reef, Australia (GBR). However, Rocker *et al.* (2017) found that in the Burdekin region of the GBR, *Acropora tenuis* at nearshore sites with relatively high concentrations of nutrients had higher extension rates than their counterparts found on offshore reefs with lower nutrient concentrations. Of the sites considered by Rocker *et al.* (2017), the one with the highest nutrient concentrations (and highest extension rates in *A. tenuis*) was at Magnetic Island, which had a seawater N:P ratio (considering both organic and inorganic forms of N and P) of ~25:1. Their observations are consistent with the experimental findings presented in Chapter 2, specifically those relating to high linear extension rates in *Acroporids* following balanced N and P enrichment (Buckingham *et al.*, 2022). When the Wooldridge paper is revisited it is apparent that Magnetic Island lies within the only small section (~50 km) of a ~500 km stretch of coastline which does not have high bleaching susceptibility (Wooldridge, 2009). It is possible that differences in N:P stoichiometry, rather than absolute DIN-concentrations might have been responsible for some of the bleaching patterns observed by Wooldridge (2009). Obviously, this cannot be investigated in retrospect, but several studies have already linked coral reef decline to sustained increases in average seawater N:P ratios (Lapointe *et al.*, 2019; Lapointe, Tewfik and Phillips, 2021). Such observations point to a need for increased research effort to be placed on determining the spatial and temporal variability in seawater N:P ratios, especially on coral reefs impacted by anthropogenic nutrient enrichment. Furthermore, future field-study based publications should endeavour to report the seawater concentrations of all species of

organic and inorganic nutrients whenever possible, thereby allowing inorganic and absolute N:P ratios to be calculated retrospectively by other researchers if necessary. If universally adopted, such a practice would allow for better comparison between the findings of field and laboratory studies. This is especially important given that the nitrogen uptake potential of the coral host varies for different forms of DIN and DON (Grover *et al.*, 2002, 2003, 2006, 2008).

5.4. Concluding thoughts

Global warming caused by anthropogenic emissions of CO_2 from fossil fuel use has been identified as the primary threat to the survival of coral reefs around the world, but this threat is exacerbated by more localised stressors such as coastal development, input of land-based pollution and overfishing (GCRMN, 2020). A recent 'blueprint for coral reef survival' identified that if coral reefs are to avoid becoming 'extremely diminished' over the next 20-30 years, a coordinated and comprehensive response involving global leaders, coral scientists, conservation NGO's and local communities around the world must be implemented immediately (Kleypas *et al.*, 2021). For such a response to be successful there must be a degree of consensus on relevant scientific advice, otherwise incorrect policy decisions will be made and important stakeholder support may be withheld from conservation and/or management projects (Bell, Lapointe and Elmetri, 2007). This thesis has resolved some apparent contradictions in the scientific literature pertaining to the impacts of nutrient pollution on skeletal growth, and has also provided new information regarding the potential reliability of structural and geochemical climate proxies under such conditions. It is hoped that this small contribution of knowledge to the field of study can help to improve scientific consensus and refine the use of established methods of study with the aim of conserving our coral reefs for future generations.

Appendices

Appendix 1.

Supplementary materials

1) Supplementary Tables

Supplementary Table 1: Summary of analysed studies relating to the effects of nutrient enrichment on *Acropora spp.* The Plus symbol (+) represents a statistically significant increase in the designated metric as reported by the authors, zero (0) represents no significant effect and the minus symbol (–) represents a significant decrease. NA: Not applicable. HNHP = high nitrogen: high phosphorus, HNLP = high nitrogen: low phosphorus and LNHP = low nitrogen: high phosphorus. The list of analysed studies is given under "Supplementary References".

Reference	Species	Study type/ Location	Linear Extension	Calcification	Skeletal Density	[N] by species	[P] by species	[DIN] (μM)	[DIP] (μM)	N:P ratio	Stoichiometry class
Bongiorni et al (2003)	*Acropora eurystoma*	Field adj to fish farm/ Eilat	+	+	NA	NO_3^- = 0.385 μM NO_2^- = 0.095 μM NH_4^+ & NH_3 = 1.016 μM	PO_4^{3-} = 0.123 μM	1.496	0.123	12.2	HNHP
Dunn et al (2012)	*Acropora muricata*	Laboratory	+	NA	-	NO_3^- = 0.11 mg/l	PO_4^{3-} = 0.2mg/l	1.77	2.11	0.8	HNHP
Dunn et al (2012)	*Acropora muricata*	Laboratory	+	NA	-	NO_3^- = 0.13 mg/l NO_2^- = 0.09 mg/l	PO_4^{3-} = 0.5 mg/l	3.54	5.26	0.7	HNHP
Savage (2019)	*Acropora formosa*	Field-undisturbed /Fiji	+	NA	NA	NO_3^- = 11.543 μM NH_4^+ & NH_3 = 1.172 μM	PO_4^{3-} = 0.391 μM	12.715	0.391	32.5	HNHP
Rocker et al (2017)	*Acropora tenuis*	Field - Anthrop./ Australia	+	NA	-	DIN = 0.36 μM DON = 5.53 μM	DOP = 0.15 μM PO_4^{3-} = 0.09 μM	5.89	0.24	24.5	HNHP

Fabricius et al (2013)	*Acropora millepora*	Laboratory	NA	0	NA	NO_3^- = 0.26 μM NH_4^+ & NH_3 = 0.22 μM DON = 3.63 μM	DOP = 0.058 μM PO_4^{3-} = 0.83 μM	0.48	0.83	0.58	HNHP
Fabricius et al (2013)	*Acropora millepora*	Laboratory	NA	0	NA	NO_3^- = 0.24 μM NH_4^+ & NH_3 = 0.21 μM DON = 7.82 μM	DOP = 0.115 μM PO_4^{3-} = 1.12 μM	0.45	1.12	0.40	LNHP
Fabricius et al (2013)	*Acropora millepora*	Laboratory	NA	0	NA	NO_3^- = 0.12 μM NH_4^+ & NH_3 = 0.21 μM DON = 7.79 μM	DOP = 0.073 μM PO_4^{3-} = 0.93 μM	0.33	0.93	0.35	LNHP
Renegar & Riegl (2005)	*Acropora cervicornis*	Laboratory	NA	0	NA	NO_3^- = 5.13 μM	PO_4^{3-} = 0.07 μM	5.13	0.07	73.3	HNLP
Renegar & Riegl (2005)	*Acropora cervicornis*	Laboratory	NA	0	NA	NO_3^- = 0.45 μM	PO_4^{3-} = 2.15 μM	0.45	2.15	0.2	LNHP
Renegar & Riegl (2005)	*Acropora cervicornis*	Laboratory	NA	-	NA	NO_3^- = 4.98 μM	PO_4^{3-} = 2.09 μM	4.98	2.09	2.4	HNHP
Renegar & Riegl (2005)	*Acropora cervicornis*	Laboratory	NA	-	NA	NO_3^- = 9.93 μM	PO_4^{3-} = 0.07 μM	9.93	0.07	142	HNLP
Renegar & Riegl (2005)	*Acropora cervicornis*	Laboratory	NA	-	NA	NO_3^- = 0. 73 μM	PO_4^{3-} = 4.14 μM	0.73	4.14	0.18	LNHP
Renegar & Riegl (2005)	*Acropora cervicornis*	Laboratory	NA	-	NA	NO_3^- = 10.01 μM	PO_4^{3-} = 4.06 μM	10.01	4.06	2.5	HNHP

Tanaka et al (2007)	*Acropora pulchra*	Laboratory	NA	+	NA	NO_3^- = 5.0 μM	PO_4^{3-} = 0.3 μM	5.0	0.3	16.7	HNHP
Koop et al (2001)	*Acropora longicyathus*	Field - experiment Australia	0	0	NA	NO_3^- = 2.94 μM NH_4^+ / NH_3 = 11.45 μM	PO_4^{3-} = 0.2 μM	14.39	0.2	72	HNLP
Koop et al (2001)	*Acropora longicyathus*	Field - experiment Australia	-	+	+	NO_3^- = 2.94 μM NH_4^+ / NH_3 = 36.2 μM	PO_4^{3-} = 0.16 μM	39.14	0.16	245	HNLP
Koop et al (2001)	*Acropora longicyathus*	Field - experiment Australia	0	0	NA	NO_3^- = 2.94 μM NH_4^+ / NH_3 = 0.65 μM	PO_4^{3-} = 2.34 μM	3.59	2.34	1.5	HNHP
Koop et al (2001)	*Acropora longicyathus*	Field - experiment Australia	+	+	-	NO_3^- = 2.94 μM NH_4^+ / NH_3 = 0.65 μM	PO_4^{3-} = 5.14 μM	3.59	5.14	0.7	HNHP
Koop et al (2001)	*Acropora longicyathus*	Field - experiment Australia	0	0	NA	NO_3^- = 2.94 μM NH_4^+ / NH_3 = 11.45 μM	PO_4^{3-} = 2.34 μM	14.39	2.34	6.1	HNHP
Koop et al (2001)	*Acropora longicyathus*	Field - experiment Australia	+	+	NA	NO_3^- = 2.94 μM NH_4^+ / NH_3 = 36.2 μM	PO_4^{3-} = 5.14 μM	39.14	5.14	7.6	HNHP
Koop et al (2001)	*Acropora palifera*	Field - experiment Australia	0	NA	NA	NO_3^- = 2.94 μM NH_4^+ / NH_3 = 11.45 μM	PO_4^{3-} = 0.2 μM	14.39	0.2	72	HNLP
Koop et al (2001)	*Acropora palifera*	Field - experiment Australia	-	-	NA	NO_3^- = 2.94 μM NH_4^+ / NH_3 = 36.2 μM	PO_4^{3-} = 0.16 μM	39.14	0.16	245	HNLP
Koop et al (2001)	*Acropora palifera*	Field - experiment Australia	0	NA	NA	NO_3^- = 2.94 μM NH_4^+ / NH_3 = 0.65 μM	PO_4^{3-} = 2.34 μM	3.59	2.34	1.5	HNHP

Koop et al (2001)	*Acropora palifera*	Field - experiment Australia	+	+	NA	NO_3^- = 2.94 μM NH_4^+ / NH_3 = 0.65 μM	PO_4^{3-} = 5.14 μM	3.59	5.14	0.7	HNHP
Koop et al (2001)	*Acropora palifera*	Field - experiment Australia	0	NA	NA	NO_3^- = 2.94 μM NH_4^+ / NH_3 = 11.45 μM	PO_4^{3-} = 2.34 μM	14.39	2.34	6.1	HNHP
Koop et al (2001)	*Acropora palifera*	Field - experiment Australia	+	0	NA	NO_3^- = 2.94 μM NH_4^+ / NH_3 = 36.2 μM	PO_4^{3-} = 5.14 μM	39.14	5.14	7.6	HNHP
Koop et al (2001)	*Acropora aspera*	Field - experiment Australia	NA	NA	NA	NO_3^- = 2.94 μM NH_4^+ / NH_3 = 11.45 μM	PO_4^{3-} = 0.2 μM	14.39	0.2	72	HNLP
Koop et al (2001)	*Acropora aspera*	Field - experiment Australia	NA	0	NA	NO_3^- = 2.94 μM NH_4^+ / NH_3 = 36.2 μM	PO_4^{3-} = 0.16 μM	39.14	0.16	245	HNLP
Koop et al (2001)	*Acropora aspera*	Field - experiment Australia	NA	NA	NA	NO_3^- = 2.94 μM NH_4^+ / NH_3 = 0.65 μM	PO_4^{3-} = 2.34 μM	3.59	2.34	1.5	HNHP
Koop et al (2001)	*Acropora aspera*	Field - experiment Australia	NA	-	NA	NO_3^- = 2.94 μM NH_4^+ / NH_3 = 0.65 μM	PO_4^{3-} = 5.14 μM	3.59	5.14	0.7	HNHP
Koop et al (2001)	*Acropora aspera*	Field - experiment Australia	NA	NA	NA	NO_3^- = 2.94 μM NH_4^+ / NH_3 = 11.45 μM	PO_4^{3-} = 2.34 μM	14.39	2.34	6.1	HNHP
Koop et al (2001)	*Acropora aspera*	Field - experiment Australia	NA	0	NA	NO_3^- = 2.94 μM NH_4^+ / NH_3 = 36.2 μM	PO_4^{3-} = 5.14 μM	39.14	5.14	7.6	HNHP

Supplementary Table 2: Summary of reviewed studies relating to the effects of nutrient enrichment of species other than *Acropora* spp. Plus symbol (+) represents a statistically significant increase in the designated metric as reported by the authors, zero (0) represents no significant effect and the minus symbol (–) represents a significant decrease. NA: Not applicable. HNHP = high nitrogen: high phosphorus, HNLP = high nitrogen: low phosphorus and LNHP = low nitrogen: high phosphorus. The list of analysed studies is given under "Supplementary References".

Reference	Species	Study type/ Location	Linear Extension	Calcification	Skeletal Density	[N] by species	[P] by species	DIN (μM)	DIP (μM)	N:P ratio	Stoichiometry class
Bongiorni et al (2003)	*Stylophora pistillata*	Field close to fish farm/ Eilat	+	NA	NA	NO_3^- = 0.385 μM NO_2^- = 0.095 μM NH_4^+ & NH_3 = 1.016 μM	PO_4^{3-} = 0.123 μM	1.496	0.123	12.2	HNHP
Dikou (2009)	*Merulina ampliata*	Field – Natural/ Nutrient /sediment gradient	-	NA	NA	NO_3^- = 40 ppb	PO_4^{3-} = 15 ppb	0.65	0.16	4.1	HNHP
Edinger et al (2000)	*Porites lobata*	Field - Anthrop./ Indonesia	-	NA	NA	NO_3^- = 1.46 μM	PO_4^{3-} = 0.46 μM	1.46	0.46	3.2	HNHP
Elizalde-Rendon et al (2010)	*Porites astreoides*	Field - Anthrop./ Caribbean	-	-	-	NO_3^- = 14.65 μM	PO_4^{3-} = 2.8 μM	14.65	2.8	5.2	HNHP
Jompa & McCook (2002)	*Porites cylindrica*	Field - experiment Australia	0	NA	NA	NH_4^+ & NH_3 = 10 μM	PO_4^{3-} = 1.0 μM	10	1	10	HNHP
Marubini et al (1999)	*Porites porites*	Laboratory	-	-	NA	NO_3^- = 20.2 μM	PO_4^{3-} = 0.05 μM	20.2	0.05	404	HNLP

Marubini et al (1999)	*Porites porites*	Laboratory	-	-	NA	NH_4^+ & NH_3 = 20.2 μM	PO_4^{3-} = 0.05 μM	20.2	0.05	404	HNLP
Meyer & Schultz (1985)	*Poites furcata*	Field adj. to fish farm/ US Virgin I.	0	+	0	DON = 3.9 mmol m^2	PO_4^{3-} = 0.2 mmol m^2	3.9	0.2	19.5	HNHP
Stambler et al (1991)	*Pocillipora damicornis*	Laboratory	0	NA	NA	NH_4^+ & NH_3 = 2.0 μM	PO_4^{3-} = 2.0 μM	2.0	2.0	1	HNHP
Stambler et al (1991)	*Pocillipora damicornis*	Laboratory	0	NA	NA	NH_4^+ & NH_3 = 2.0 μM	PO_4^{3-} = 0.5 μM	2.0	0.5	4	HNHP
Stambler et al (1991)	*Pocillipora damicornis*	Laboratory	0	NA	NA	NH_4^+ & NH_3 = 7.0 μM	PO_4^{3-} = 0.1 μM	7.0	0.1	70	HNLP
Stambler et al (1991)	*Pocillipora damicornis*	Laboratory	-	NA	NA	NH_4^+ & NH_3 = 15 μM	PO_4^{3-} = 0.1 μM	15	0.1	150	HNLP
Stambler et al (1991)	*Pocillipora damicornis*	Laboratory	-	NA	NA	NH_4^+ & NH_3 = 15 μM	PO_4^{3-} = 0.5 μM	15	0.5	30	HNHP
Stambler et al (1991)	*Pocillipora damicornis*	Laboratory	-	NA	NA	NH_4^+ & NH_3 = 15 μM	PO_4^{3-} = 2.0 μM	15	2.0	7.5	HNHP
Tomascik & Sander (1985)	*Montastrea annularis*	Field – Anthrop./ Barbados	-	NA	NA	NO_2 & NO_3^- - N = 0.816 ug l NH_4^+ & NH_3 – N = 0.976 ug l	PO_4^{3-} - P = 0.103 ug l	0.128	0.0033	38.8	HNLP

Tomascik & Sander (1985)	*Montastrea annularis*	Field – Anthrop./ Barbados	-	NA	NA	NO_2 & NO_3^- - N = 4.424 ug l NH_4^+ & NH_3 – N = 2.695 ug l	PO_4^{3-} - P = 0.214 ug l	0.5085	0.0069	73.7	HNLP
Fabricius et al (2013)	*Montipora tuberculosa*	Laboratory	NA	0	NA	NO_3^- & NO_2^- = 0.26 μM NH_4^+ = 0.22 μM PON = 3.63 μM	SRP = 0.058 μM POP = 0.83 μM	0.48	0.83	0.58	HNHP
Fabricius et al (2013)	*Montipora tuberculosa*	Laboratory	NA	-	NA	NO_3^- & NO_2^- = 0.24 μM NH_4^+ = 0.21 μM PON = 7.79 μM	SRP = 0.115 μM POP = 1.12 μM	0.45	1.12	0.40	LNHP
Fabricius et al (2013)	*Montipora tuberculosa*	Laboratory	NA	0	NA	NO_3^- & NO_2^- = 0.12 μM NH_4^+ = 0.21 μM PON = 7.82 μM	SRP = 0.073 μM POP = 0.93 μM	0.33	0.93	0.35	LNHP
Ferrier-Pages et al (2000)	*Stylophora pistillata*	Laboratory	NA	-	NA	NH_4^+ & NH_3 = 9 μM	PO_4^{3-} = 0.2 μM	9	0.2	45	HNLP
Ferrier-Pages et al (2000)	*Stylophora pistillata*	Laboratory	NA	-	NA	NH_4^+ & NH_3 = 0.4 μM	PO_4^{3-} = 2.8 μM	0.4	2.8	0.1	LNHP
Ferrier-Pages et al (2000)	*Stylophora pistillata*	Laboratory	NA	-	NA	NH_4^+ & NH_3 = 8.5 μM	PO_4^{3-} = 2.4 μM	8.5	2.4	3.5	HNHP
Ferrier-Pages et al (2000)	*Stylophora pistillata*	Laboratory	NA	-	NA	NH_4^+ & NH_3 = 19.5 μM	PO_4^{3-} = 0.2 μM	19.5	0.2	97.5	HNLP

Ferrier-Pages et al (2000)	*Stylophora pistillata*	Laboratory	NA	-	NA	NH_4^+ & NH_3 = 0.4 μM	PO_4^{3-} = 2.8 μM	0.4	2.8	0.1	LNHP
Ferrier-Pages et al (2000)	*Stylophora pistillata*	Laboratory	NA	-	NA	NH_4^+ & NH_3 = 18.5 μM	PO_4^{3-} = 2.4 μM	18.5	2.4	7.7	HNHP
Ferrier-Pages et al (2001)	*Stylophora pistillata*	Laboratory	NA	-	NA	NO_3^- = 2.5 μM NH_4^+ & NH_3 = 0.4 μM	PO_4^{3-} = 0.2 μM	2.9	0.2	14.5	HNHP
Godinot et al (2011)	*Stylophora pistillata*	Laboratory	NA	0	NA	NO_3^- = 0.4 μM NH_4^+ & NH_3 = 0.5 μM	PO_4^{3-} = 0.5 μM	0.9	0.5	1.8	HNHP
Godinot et al (2011)	*Stylophora pistillata*	Laboratory	NA	+	NA	NO_3^- = 0.4 μM NH_4^+ & NH_3 = 0.5 μM	PO_4^{3-} = 0.5 μM	0.9	2.5	0.4	LNHP
Marubini & Davies (1996)	*Porites porites*	Laboratory	NA	-	NA	NO_3^- = 1.0 μM	PO_4^{3-} = 2.5 μM	1.0	0.05	20	HNHP
Marubini & Davies (1996)	*Porites porites*	Laboratory	NA	-	NA	NO_3^- = 5.0 μM	PO_4^{3-} = 0.5 μM	5.0	0.05	100	HNLP
Marubini & Davies (1996)	*Porites porites*	Laboratory	NA	-	NA	NO_3^- = 20 μM	PO_4^{3-} = 0.5 μM	20	0.05	400	HNLP
Marubini & Davies (1996)	*Montastrea annularis*	Laboratory	NA	-	NA	NO_3^- = 1.0 μM	PO_4^{3-} = 2.5 μM	1.0	0.05	20	HNHP
Marubini & Davies (1996)	*Montastrea annularis*	Laboratory	NA	-	NA	NO_3^- = 5.0 μM	PO_4^{3-} = 0.5 μM	5.0	0.05	100	HNLP

Marubini & Davies (1996)	*Montastrea annularis*	Laboratory	NA	-	NA	NO_3^- = 20 μM	PO_4^{3-} = 0.5 μM	20	0.05	400	HNLP
Marubini & Atkinson (1999)	*Porites compressa*	Laboratory	NA	0	NA	NO_3^- = 0.91 μM NH_4^+ & NH_3 = 0.41 μM	PO_4^{3-} = 0.13 μM	1.32	0.13	10.2	HNHP
Marubini & Atkinson (1999)	*Porites compressa*	Laboratory	NA	0	NA	NO_3^- = 1.48 μM NH_4^+ & NH_3 = 0.46 μM	PO_4^{3-} = 0.12 μM	1.94	0.12	16.2	HNHP
Marubini & Atkinson (1999)	*Porites compressa*	Laboratory	NA	0	NA	NO_3^- = 5.66 μM NH_4^+ & NH_3 = 0.42 μM	PO_4^{3-} = 0.11 μM	6.08	0.11	55	HNLP
Meyer et al (1983)	*Porites furcata*	Field-natural/US Virgin I.	NA	+	NA	DON = 3.9 mmol m^2	PO_4^{3-} = 0.2 mmol m^2	3.9	0.2	19.5	HNHP
Silbiger et al (2018)	*Porites compressa, Montipora capitata*	Laboratory	NA	-	NA	NO_3^- = 3.6 μM	PO_4^{3-} = 1.08 μM	3.6	1.08	3.3	HNHP
Silbiger et al (2018)	*Porites compressa, Montipora capitata*	Laboratory	NA	-	NA	NO_3^- = 7.61 μM	PO_4^{3-} = 2.6 μM	7.61	2.6	2.9	HNHP
Spencer Davies (1990)	Porites porites	Field-Anthrop./ Barbados	NA	0	NA	NO_3^- = 4.92 ug l	PO_4^{3-} = 0.17 ug l	0.0794	0.00179	44	HNLP
Spencer Davies (1990)	Montastrea annularis	Field-Anthrop./ Barbados	NA	-	NA	NO_3^- = 4.92 ug l	PO_4^{3-} = 0.17 ug l	0.0794	0.00179	44	HNLP

Tanaka et al (2017)	*Montipora digitata*	Laboratory	NA	0	NA	NO_3^- = 1.86 μM NO_2^- = 0.14 μM NH_4^+ & NH_3 = 0.02 μM	PO_4^{3-} = 0.02 μM	2.02	0.02	101	HNLP
Tanaka et al (2017)	*Montipora digitata*	Laboratory	NA	0	NA	NO_3^- = 1.37 μM NO_2^- = 0.11 μM NH_4^+ & NH_3 = 0.02 μM	PO_4^{3-} = 0.12 μM	1.50	0.12	12.5	HNHP
Tanaka et al (2017)	*Porites cylindrica*	Laboratory	NA	0	NA	NO_3^- = 1.73 μM NO_2^- = 0.14 μM NH_4^+ & NH_3 = 0.03 μM	PO_4^{3-} = 0.03 μM	1.90	0.03	63	HNLP
Tanaka et al (2017)	*Porites cylindrica*	Laboratory	NA	0	NA	NO_3^- = 1.46 μM NO_2^- = 0.12 μM NH_4^+ & NH_3 = 0.04 μM	PO_4^{3-} = 0.12 μM	1.62	0.12	13.5	HNHP
Koop et al (2001)	*Stylophora pistillata*	Field - experiment Australia	NA	NA	NA	NO_3^- = 2.94 μM NH_4^+ / NH_3 = 11.45 μM	PO_4^{3-} = 0.2 μM	14.39	0.2	72	HNLP
Koop et al (2001)	*Stylophora pistillata*	Field - experiment Australia	NA	-	NA	NO_3^- = 2.94 μM NH_4^+ / NH_3 = 36.2 μM	PO_4^{3-} = 0.16 μM	39.14	0.16	245	HNLP
Koop et al (2001)	*Stylophora pistillata*	Field - experiment Australia	NA	NA	NA	NO_3^- = 2.94 μM NH_4^+ / NH_3 = 0.65 μM	PO_4^{3-} = 2.34 μM	3.59	2.34	1.5	HNHP
Koop et al (2001)	*Stylophora pistillata*	Field - experiment Australia	NA	0	NA	NO_3^- = 2.94 μM NH_4^+ / NH_3 = 0.65 μM	PO_4^{3-} = 5.14 μM	3.59	5.14	0.7	HNHP
Koop et al (2001)	*Stylophora pistillata*	Field - experiment Australia	NA	NA	NA	NO_3^- = 2.94 μM NH_4^+ / NH_3 = 11.45 μM	PO_4^{3-} = 2.34 μM	14.39	2.34	6.1	HNHP

Koop et al (2001)	*Stylophora pistillata*	Field - experiment Australia	NA	0	NA	NO_3^- = 2.94 μM NH_4^+ / NH_3 = 36.2 μM	PO_4^{3-} = 5.14 μM	39.14	5.14	7.6	HNHP
Koop et al (2001)	*Pocillipora damicornis*	Field - experiment Australia	NA	0	NA	NO_3^- = 2.94 μM NH_4^+ / NH_3 = 11.45 μM	PO_4^{3-} = 0.2 μM	14.39	0.2	72	HNLP
Koop et al (2001)	*Pocillipora damicornis*	Field - experiment Australia	NA	-	NA	NO_3^- = 2.94 μM NH_4^+ / NH_3 = 36.2 μM	PO_4^{3-} = 0.16 μM	39.14	0.16	245	HNLP
Koop et al (2001)	*Pocillipora damicornis*	Field - experiment Australia	NA	0	NA	NO_3^- = 2.94 μM NH_4^+ / NH_3 = 0.65 μM	PO_4^{3-} = 2.34 μM	3.59	2.34	1.5	HNHP
Koop et al (2001)	*Pocillipora damicornis*	Field - experiment Australia	NA	0	NA	NO_3^- = 2.94 μM NH_4^+ / NH_3 = 0.65 μM	PO_4^{3-} = 5.14 μM	3.59	5.14	0.7	HNHP
Koop et al (2001)	*Pocillipora damicornis*	Field - experiment Australia	NA	0	NA	NO_3^- = 2.94 μM NH_4^+ / NH_3 = 11.45 μM	PO_4^{3-} = 2.34 μM	14.39	2.34	6.1	HNHP
Koop et al (2001)	*Pocillipora damicornis*	Field - experiment Australia	NA	-	NA	NO_3^- = 2.94 μM NH_4^+ / NH_3 = 36.2 μM	PO_4^{3-} = 5.14 μM	39.14	5.14	7.6	HNHP

2) **Supplementary Figure**

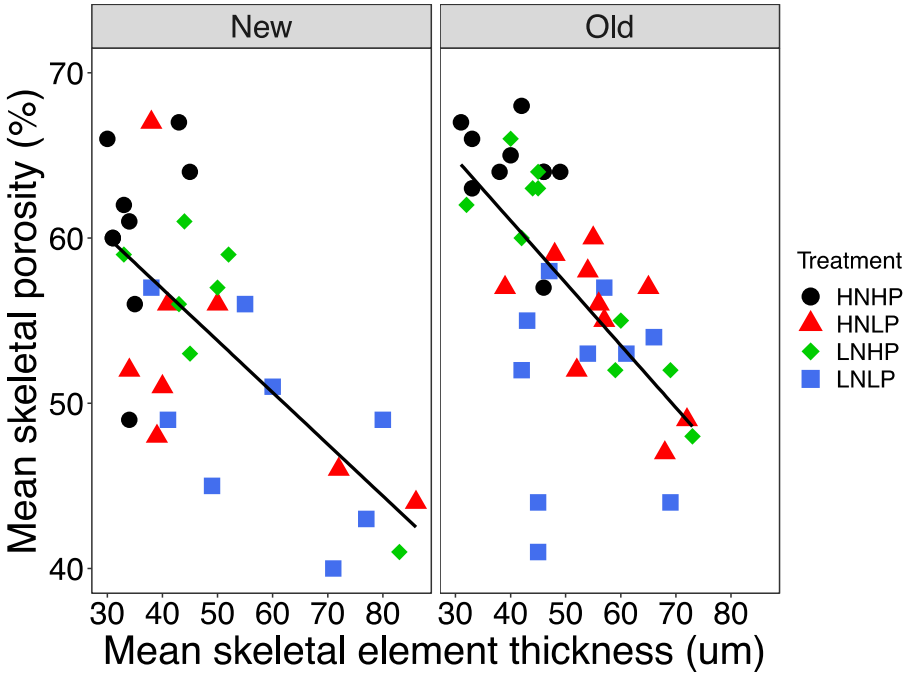

Supplementary Figure 1: The relationship between mean skeletal element thickness and mean skeletal porosity in *Acropora polystoma* for 'new' and 'old' skeleton when cultured under 4 different nutrient treatments for > 10 weeks. Each point represents a measurement within the region of interest (see main text) for a single coral fragment. Statistically significant correlations were found in both the 'new' (R^2 = 0.46, p << 0.001) and 'old' skeleton (R^2 = 0.39, p << 0.001). HNHP = high nitrate: high phosphate, HNLP = high nitrate: low phosphate, LNHP = low nitrate: high phosphate and LNLP = low nitrate: low phosphate.

3) Supplementary Methods

Macro used in ImageJ for analysis of CT scan slices

The following Macro was utilized for all measurements relating to "skeletal element thickness" and "porosity". Prior to running the macro an individual slice within the region of interest was selected. The macro relies upon the BoneJ plug-in being installed.

```
run("3D Project...", "projection=[Brightest Point] axis=Y-Axis slice=1 initial=0 total=360 rotation=10 lower=1 upper=255 opacity=0 surface=100 interior=50");
setOption("BlackBackground", false);
run("Make Binary", "method=Intermodes background=Dark calculate");
run("Thickness", "thickness mask");
run("Volume Fraction", "algorithm=Voxel surface=6 use");
setOption("BlackBackground", false);
run("Dilate", "stack");
run("Dilate", "stack");
run("Dilate", "stack");
run("Dilate", "stack");
run("Dilate", "stack");
run("Fill Holes", "stack");
run("Erode", "stack");
run("Erode", "stack");
run("Erode", "stack");
run("Erode", "stack");
run("Erode", "stack");
run("Volume Fraction", "algorithm=Voxel surface=6 use");
String.copyResults();
String.copyResults();
```

4) Supplementary References

Bongiorni L, Shafir S, Angel D, Rinkevich B (2001) Survival, growth and gonad development of two hermatypic corals subjected to in situ fish-farm nutrient enrichment. Mar Ecol Prog Ser. 253:137–44.

Browne NK, Tay JKL, Low J, Larson O, Todd PA (2015) Fluctuations in coral health of four common inshore reef corals in response to seasonal and anthropogenic changes in water quality. Mar Environ Res 105:39–52.

Dikou A (2009) Skeletal linear extension rates of the foliose scleractinian coral Merulina ampliata (Ellis & Solander, 1786) in a turbid environment. Mar Ecol. 30:405–15.

Dunn JG, Sammarco PW, LaFleur G (2012) Effects of phosphate on growth and skeletal density in the scleractinian coral Acropora muricata: A controlled experimental approach. J Exp Mar Bio Ecol. 411:34–44.

Edinger EN, Limmon G V., Jompa J, Widjatmoko W, Heikoop JM, Risk MJ (2000) Normal Coral Growth Rates on Dying Reefs: Are Coral Growth Rates Good Indicators of Reef Health? Mar Pollut Bull. 40:404–25.

Elizalde-Rendón EM, Horta-Puga G, González-Diaz P, Carricart-Ganivet JP (2010) Growth characteristics of the reef-building coral Porites astreoides under different environmental conditions in the Western Atlantic. Coral Reefs. 29:607–14.

Fabricius KE, Cséke S, Humphrey C, De'ath G (2013) Does Trophic Status Enhance or Reduce the Thermal Tolerance of Scleractinian Corals? A Review, Experiment and Conceptual Framework. PLoS One. 8:1–12.

Ferrier-Pagès C, Schoelzke V, Jaubert J, Muscatine L, Hoegh-Guldberg O (2001) Response of a scleractinian coral, Stylophora pistillata, to iron and nitrate enrichment. J Exp Mar Bio Ecol. 259249–61.

Ferrier-Pagès C, Gattuso JP, Dallot S, Jaubert J (2000) Effect of nutrient enrichment on growth and photosynthesis of the zooxanthellate coral Stylophora pistillata. Coral Reefs. 19:103–13.

Godinot C, Ferrier-Pagès C, Montagna P, Grover R (2011) Tissue and skeletal changes in the scleractinian coral Stylophora pistillata Esper 1797 under phosphate enrichment. J Exp Mar Bio Ecol 409:200–7.

Jompa J, McCook LJ (2002) The effects of nutrients and herbivory on competition between a hard coral (Porites cylindrica) and a brown alga (Lobophora variegata). Limnol Oceanogr. 47:527–34.

Koop K, Booth D, Broadbent A, Brodie J, Bucher D, Capone D, Coll J, Dennison W, Erdmann M, Harrison P, Hoegh-Guldberg O, Hutchings P, Jones GB, Larkum AWD, O'Neil J, Steven A, Tentori E, Ward S, Williamson J, Yellowlees D (2001) ENCORE: The effect of nutrient enrichment on coral reefs. Synthesis of results and conclusions. Mar Pollut Bull 42:91–120

Marubini F, Atkinson MJ (1999) Effects of lowered pH and elevated nitrate on coral calcification. Mar Ecol Prog Ser. 188:117–21.

Marubini F, Davies PS (1996) Nitrate increases zooxanthellae population density and reduces skeletogenesis in corals. Mar Biol. 127:319–28.

Marubini F, Thake B, May P (1999) Bicarbonate Addition Promotes Coral Growth. Limnol Oceanogr. 44:716–20.

Meyer JL, Schultz ET (1985) Tissue Condition and Growth Rate of Corals Associated with Schooling Fish. Limnol Oceanogr. 30:157–66.

Meyer JL, Schultz ET, Helfman GS (1983) Fish Schools : An Asset to Corals. Science 220:1047–9.

Renegar DA, Riegl BM (2005) Effect of nutrient enrichment and elevated CO2 partial pressure on growth rate of Atlantic scleractinian coral Acropora cervicornis. Mar Ecol Prog Ser. 293:69–76.

Riegl B, Johnston M, Glynn PW, Keith I, Rivera F, Vera-Zambrano M, Banks, S, Feingold, J, Glynn, PJ (2019) Some environmental and biological determinants of coral richness, resilience and reef building in Galápagos (Ecuador). Sci Rep 9:1–16.

Rocker MM, Francis DS, Fabricius KE, Willis BL, Bay LK (2017) Variation in the health and biochemical condition of the coral Acropora tenuis along two water quality gradients on the Great Barrier Reef , Australia. Mar Pollut Bull 119:106–19.

Savage C (2019) Seabird nutrients are assimilated by corals and enhance coral growth rates. Sci Rep 9:4284.

Silbiger NJ, Nelson CE, Remple K, Sevilla JK, Quinlan ZA, Putnam HM, Fox MD, Donahue MJ (2018) Nutrient pollution disrupts key ecosystem functions on coral reefs. Proc R Soc B Biol Sci. 285:2–10.

Spencer Davies P (1990) A rapid method for assessing growth rates of corals in relation to water pollution. Mar Pollut Bull. 21:346–8.

Stambler N, Popper N, Dubinsky Z, Stimson J (1991) Effects of nutrient enrichment and water motion on the coral Pocillopora damicornis. Pacific Sci. 45:299–307.

Tanaka Y, Grottoli AG, Matsui Y, Suzuki A, Sakai K (2017) Effects of nitrate and phosphate availability on the tissues and carbonate skeleton of scleractinian corals. Mar Ecol Prog Ser. 570:101–12.

Tanaka Y, Miyajima T, Koike I, Hayashibara T, Ogawa H (2007) Imbalanced coral growth between organic tissue and carbonate skeleton caused by nutrient enrichment. Limnol Oceanogr. 521139–46.

Tomascik T (1990) Growth rates of two morphotypes of Montastrea annularis along a eutrophication gradient, Barbados, W.I. Mar Pollut Bull. 21:376–81.

Tomascik T, Sander F (1985) Effects of eutrophication on reef-building corals. Mar Biol. 87:143–55.

Appendix 2

The preparation of coral samples for isotopic analysis was conducted by obtaining powdered samples from the tips of each sampled corallite. This was achieved using a handheld Dremel® hand drill. Samples were simply drilled lightly causing a small quantity of skeleton at the apical tip of the sample to become powdered.

For trace element analysis it was necessary to mount the samples in cylindrical mould that could be mounted into the sampling stage of the mass spectrometer. Examples of *Acropora polsytoma* (Supplementary Figure 2) and *Euphyllia paradivisa* (Supplementary Figures 3 and 4) are shown below. The laser ablated samples were obtained from the exposed and polished surface that is shown facing the camera in the overhead views provided as illustrative examples in Supplementary figures 3 and 4.

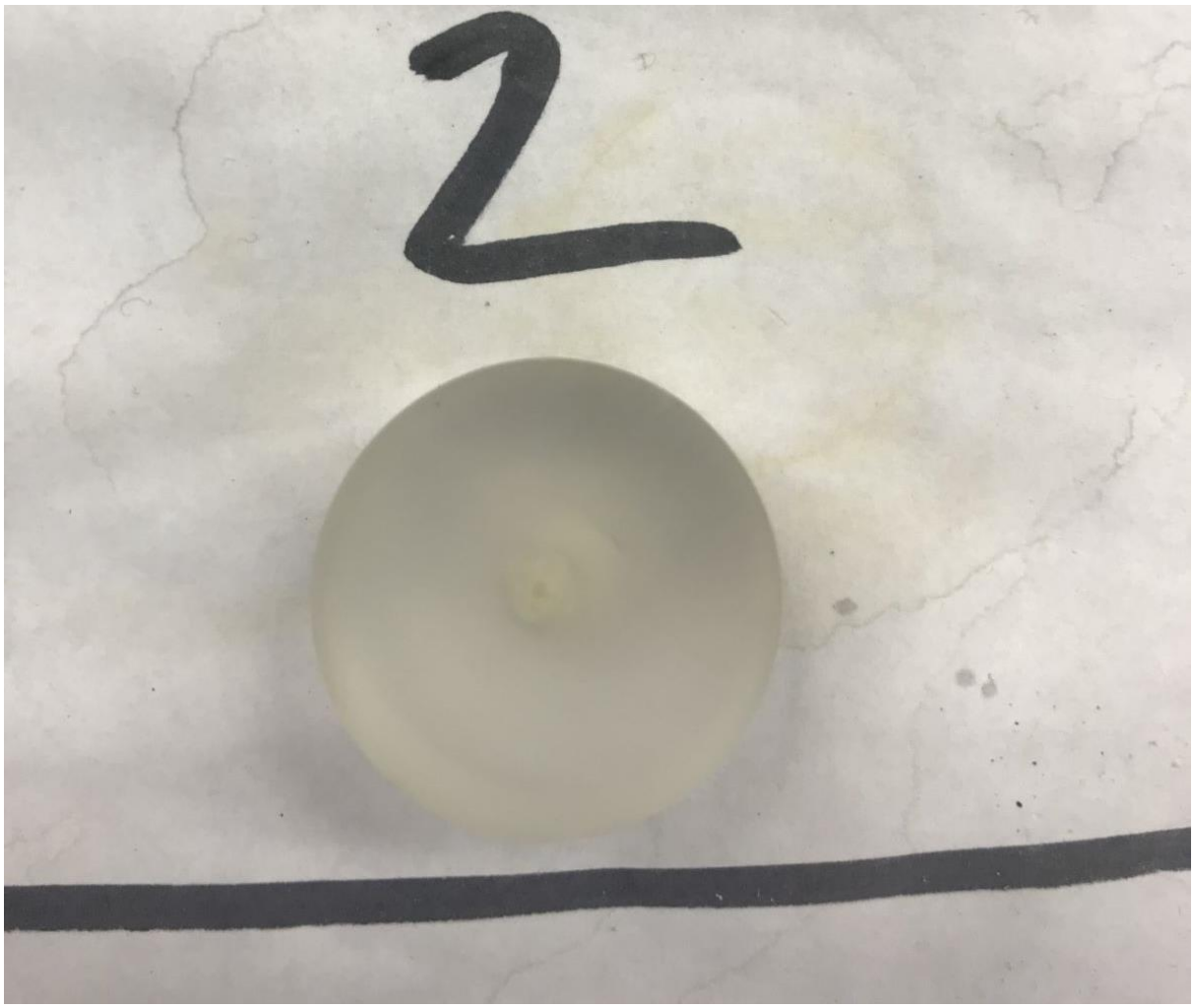

Supplementary Figure 2. Resin mounted corallite of *Acropora polystoma* (overhead view). The process by which the corallite is mounted is explained in section 4.3.3.

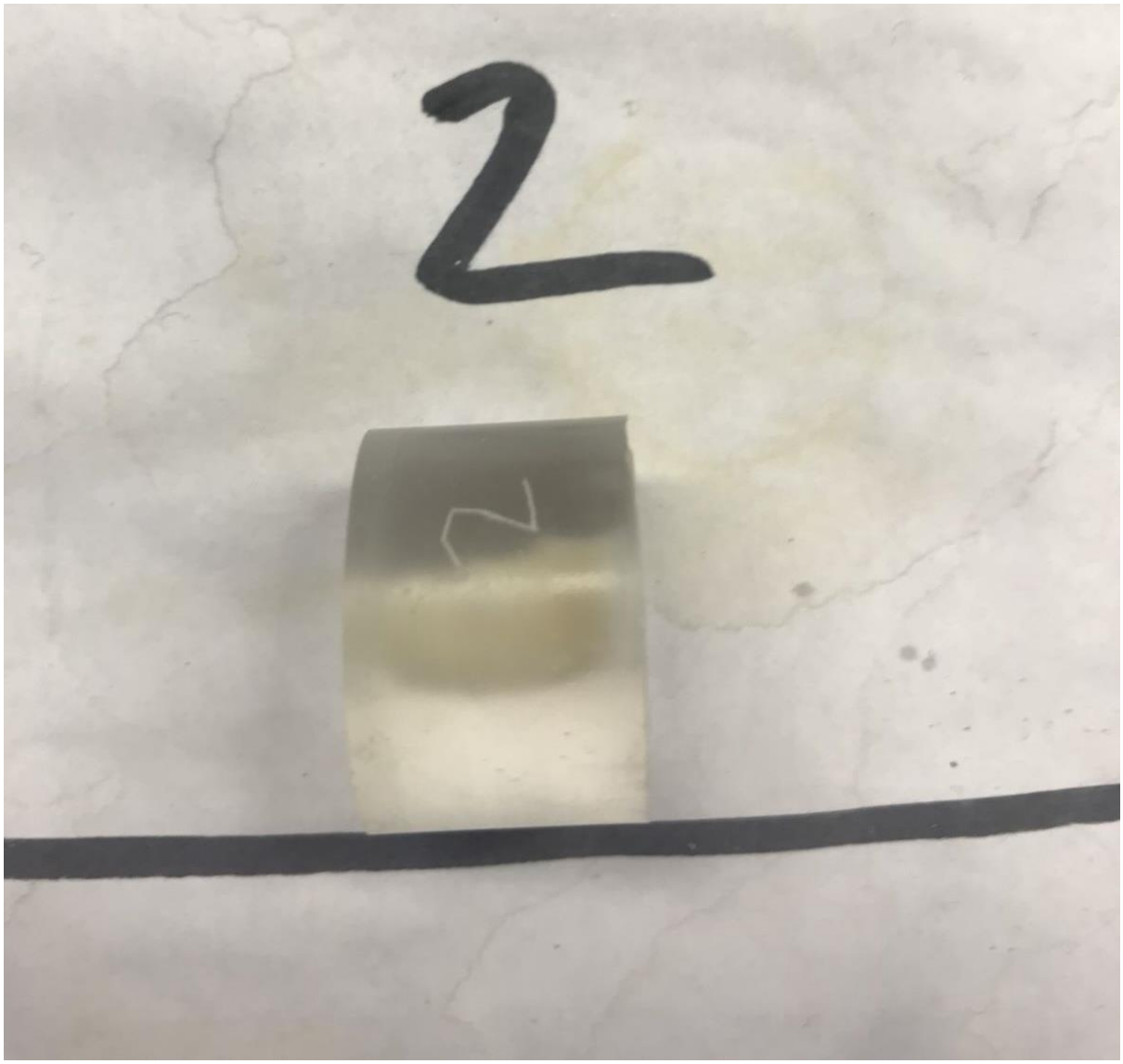

Supplementary Figure 3. Resin mounted corallite of *Acropora polystoma* (side view). The process by which the corallite is mounted is explained in section 4.3.3.

Supplementary Figure 4. Resin mounted corallite of *Euphyllia paradivisa* (overhead view). The process by which the corallite is mounted is explained in section 4.3.3.

References

Adkins, J. F. *et al.* (2003) 'Stable isotopes in deep-sea corals and a new mechanism for "vital effects"', *Geochimica et Cosmochimica Acta*, 67(6), pp. 1129–1143.

Al-Horani, F. A. *et al.* (2005) 'Spatial distribution of calcification and photosynthesis in the scleractinian coral Galaxea fascicularis', *Coral Reefs*, 24(1), pp. 173–180.

Al-Horani, F. A., Al-Moghrabi, S. M. and De Beer, D. (2003a) 'Microsensor study of photosynthesis and calcification in the scleractinian coral, Galaxea fascicularis: Active internal carbon cycle', *Journal of Experimental Marine Biology and Ecology*, 288(1), pp. 1–15.

Al-Horani, F. A., Al-Moghrabi, S. M. and De Beer, D. (2003b) 'The mechanism of calcification and its relation to photosynthesis and respiration in the scleractinian coral Galaxea fascicularis', *Marine Biology*, 142(3), pp. 419–426.

Allison, N. *et al.* (2011) 'Controls on Sr/Ca and Mg/Ca in scleractinian corals: The effects of Ca-ATPase and transcellular Ca channels on skeletal chemistry', *Geochimica et Cosmochimica Acta*, 75(21), pp. 6350–6360.

Allison, N. and Finch, A. A. (2010a) 'The potential origins and palaeoenvironmental implications of high temporal resolution δ18O heterogeneity in coral skeletons', *Geochimica et Cosmochimica Acta*, 74(19), pp. 5537–5548.

Allison, N. and Finch, A. A. (2010b) 'δ11B, Sr, Mg and B in a modern Porites coral: the relationship between calcification site pH and skeletal chemistry', *Geochimica et Cosmochimica Acta*, 74(6), pp. 1790–1800.

Annis, E. R. and Cook, C. B. (2002) 'Alkaline phosphatase activity in symbiotic dinoflagellates (zooxanthellae) as a biological indicator of environmental phosphate exposure', *Marine Ecology Progress Series*, 245, pp. 11–20.

Aston, E.A., Williams, G.J., Green, J.M., Davies, A.J., Wedding, L.M., Gove, J.M., Jouffray, J.B., Jones, T.T., Clark, J. (2019) 'Scale-dependent spatial patterns in benthic communities around a tropical island seascape', *Ecography*, 42, pp. 578-590

Baird, A. H. and Marshall, P. A. (2002) 'Mortality Growth and Reproduction Corals GBR', *Marine Ecology Progress Series*, 237, pp. 133–141.

Baker, A. C., Glynn, P. W. and Riegl, B. (2008) 'Climate change and coral reef bleaching: An ecological assessment of long-term impacts, recovery trends and future outlook', *Estuarine, Coastal and Shelf Science*, 80(4), pp. 435–471.

Baker, D. M. *et al.* (2018) 'Climate change promotes parasitism in a coral symbiosis',

ISME Journal, 12(3), pp. 921–930.

Baker, D. M., Webster, K. L. and Kim, K. (2010) 'Caribbean octocorals record changing carbon and nitrogen sources from 1862 to 2005', *Global Change Biology*, 16(10), pp. 2701–2710.

Barkley, H. C. *et al.* (2018) 'Repeat bleaching of a central Pacific coral reef over the past six decades (1960-2016)', *Nature Biology Communications*, 1(177), pp. 1–10.

Barkley, H. C. and Cohen, A. L. (2016) 'Skeletal records of community-level bleaching in Porites corals from Palau', *Coral Reefs*, 35(4), pp. 1407–1417.

Barnes, D. J. and Devereux, M. J. (1988) 'Variations in skeletal architecture associated with density banding in the hard coral Porites', *Journal of Experimental Marine Biology and Ecology*, 121(1), pp. 37–54.

Barnes, D. J. and Lough, J. M. (1992) 'Systematic variations in the depth of skeleton occupied by coral tissue in massive colonies of Porites from the Great barrier reef', *Journal of Experimental Marine Biology and Ecology*, 159(1), pp. 113–128.

Barnes, D. J. and Lough, J. M. (1999) 'Porites growth characteristics in a changed environment: Misima Island, Papua New Guinea', *Coral Reefs*, 18(3), pp. 213–218.

Barnes, D. J. and Lough, J. M. (2001) 'On the nature and causes of luminescent lines and bands in coral skeletons', *Coral Reefs*, 19(3), pp. 221–230.

Beck, J. W. *et al.* (1992) 'Sea-Surface Temperature from Coral Skeletal Strontium / Calcium Ratios', *Science*, 257, pp. 644–647.

Bedgood, S. A. *et al.* (2020) 'Nutritional drivers of adult locomotion and asexual reproduction in a symbiont-hosting sea anemone Exaiptasia diaphana', *Marine Biology*, 167(39), pp. 1–12.

Bednarz, V. N. *et al.* (2017) 'The assimilation of diazotroph-derived nitrogen by scleractinian corals depends on their Metabolic Status', *mBio*, 8(1), pp. 1–14.

Bell, P. R. F., Lapointe, B. E. and Elmetri, I. (2007) 'Reevaluation of ENCORE: Support for the eutrophication threshold model for coral reefs', *Ambio*, 36(5), pp. 416–424.

Benavides, M., Bednarz, V. N. and Ferrier-Pagès, C. (2017) 'Diazotrophs: Overlooked Key Players within the Coral Symbiosis and Tropical Reef Ecosystems?', *Frontiers in Marine Science*, 4, pp. 1–17.

Benson, B. E. *et al.* (2018) 'Apparent timing of density banding in the Caribbean coral Siderastrea siderea suggests complex role of key physiological variables', *Coral Reefs*, 38(1), pp. 165–176.

Bongiorni, L. *et al.* (2003) 'Survival, growth and gonad development of two

hermatypic corals subjected to in situ fish-farm nutrient enrichment', *Marine Ecology Progress Series*, 253(2001), pp. 137–144.

Brahmi, C. *et al.* (2012) 'Skeletal growth dynamics linked to trace-element composition in the scleractinian coral Pocillopora damicornis', *Geochimica et Cosmochimica Acta*, 99, pp. 146–158.

Brenner, L. D., Linsley, B. K. and Potts, D. C. (2017) 'A modern Sr/Ca-δ18O-sea surface temperature calibration for Isopora corals on the Great Barrier Reef', *Paleoceanography*, 32(2), pp. 182–194.

Bright, A. J. *et al.* (2016) 'Disease prevalence and snail predation associated with swell-generated damage on the threatened coral, Acropora palmata (Lamarck)', *Frontiers in Marine Science*, 3, p. Article 77.

Brodie, J. *et al.* (2005) 'Are increased nutrient inputs responsible for more outbreaks of crown-of-thorns starfish? An appraisal of the evidence', *Marine Pollution Bulletin*, 51(1–4), pp. 266–278.

Browne, N. K. *et al.* (2015) 'Fluctuations in coral health of four common inshore reef corals in response to seasonal and anthropogenic changes in water quality', *Marine Environmental Research*, 105, pp. 39–52.

Bucher, D. J., Harriott, V. J. and Roberts, L. G. (1998) 'Skeletal micro-density, porosity and bulk density of acroporid corals', *Journal of Experimental Marine Biology and Ecology*, 228(1), pp. 117–136.

Buckingham, M. C. *et al.* (2022) 'Impact of nitrogen (N) and phosphorus (P) enrichment and skewed N:P stoichiometry on the skeletal formation and microstructure of symbiotic reef corals', *Coral Reefs*,

Budd, A. F. and Stolarski, J. (2011) 'Corallite wall and septal microstructure in scleractinian reef corals: Comparison of molecular clades within the family Faviidae', *Journal of Morphology*, 272(1), pp. 66–88.

Buddemeier, R. W. and Maragos, J. E. (1974) 'Radiographic studies of reef coral exoskeletons: Rates and patterns of coral growth', *Journal of Experimental Marine Biology and Ecology*, 14, pp. 179–200.

Caccia, V. G. and Boyer, J. N. (2005) 'Spatial patterning of water quality in Biscayne Bay, Florida as a function of land use and water management', *Marine Pollution Bulletin*, 50(11), pp. 1416–1429.

Caroselli, E. *et al.* (2011) 'Environmental implications of skeletal micro-density and porosity variation in two scleractinian corals', *Zoology*, 114(5), pp. 255–264.

Case, D. H. *et al.* (2010) 'Environmental and biological controls on Mg and Li in deep-sea scleractinian corals', *Earth and Planetary Science Letters*, 300(3–4), pp. 215–225.

Chalk, T. B. *et al.* (2021) 'Mapping coral calcification strategies from in situ boron isotope and trace element measurements of the tropical coral Siderastrea siderea', *Scientific Reports*, 11(472), pp. 1–13.

Chamberlain, J. A. (1978) 'Mechanical Properties of Coral Skeleton : Compressive Strength and its Adaptive Significance', *Paleobiology*, 4(4), pp. 419–435.

Chen, T. *et al.* (2015) 'Testing coral paleothermometers (B/Ca, Mg/Ca, Sr/Ca, U/Ca and ∂18O) under impacts of large riverine runoff', *Acta oceol. Sin*, 34(8), pp. 20–26.

Chisholm, J. R. M. and Gattuso, J. P. (1991) 'Validation of the alkalinity anomaly technique for investigating calcification of photosynthesis in coral reef communities', *Limnology and Oceanography*, 36(6), pp. 1232–1239.

Cohen, A. L. *et al.* (2004) 'How brain corals record climate: an integration of skeletal structure, growth and chemistry of Diploria labyrinthiformis from Bermuda', *Marine Ecology Progress Series*, 271, pp. 147–158.

Cole, A. J., Pratchett, M. S. and Jones, G. P. (2008) 'Diversity and functional importance of coral-feeding fishes on tropical coral reefs', *Fish and Fisheries*, 9(3), pp. 286–307.

Cooper, T. F. *et al.* (2008) 'Temporal dynamics in coral bioindicators for water quality on coastal coral reefs of the Great Barrier Reef', *Marine and Freshwater Research*, 59(8), pp. 703–716.

Couce, E., Ridgwell, A. and Hendy, E. J. (2012) 'Environmental controls on the global distribution of shallow-water coral reefs', *Journal of Biogeography*, 39(8), pp. 1508–1523.

Couch, C. S. *et al.* (2017) 'Mass coral bleaching due to unprecedented marine heatwave in Papahānaumokuākea Marine National Monument (Northwestern Hawaiian Islands)', *PLoS ONE*, 12(9), pp. 1–27.

Cuif, J. P. *et al.* (2003) 'XANES mapping of organic sulfate in three scleractinian coral skeletons', *Geochimica et Cosmochimica Acta*, 67(1), pp. 75–83.

Cybulski, J. D. *et al.* (2020) 'Coral reef diversity losses in China' s Greater Bay Area were driven by regional stressors', *Science Advances*, 6(40), p. eabb1046.

D'Angelo, C. and Wiedenmann, J. (2012) 'An experimental mesocosm for long-term studies of reef corals', *Journal of the Marine Biological Association of the United Kingdom*, 92(4), pp. 769–775.

D'Angelo, C. and Wiedenmann, J. (2014) 'Impacts of nutrient enrichment on coral reefs: new perspectives and implications for coastal management and reef survival', *Current Opinion in Environmental Sustainability*, 7, pp. 82–93.

D'Olivo, J. P. *et al.* (2019) 'Deconvolving the long-term impacts of ocean acidification and warming on coral biomineralisation', *Earth and Planetary Science Letters*, 526.

D'Olivo, J. P. and McCulloch, M. T. (2017) 'Response of coral calcification and calcifying fluid composition to thermally induced bleaching stress', *Scientific Reports*, 7(1), pp. 1–15.

Dávalos-Dehullu, E., Hernández-Arana, H. and Carricart-Ganivet, J. P. (2008) 'On the causes of density banding in skeletons of corals of the genus Montastraea', *Journal of Experimental Marine Biology and Ecology*, 365(2), pp. 142–147.

Davies, P. S. (1989) 'Short-term growth measurements of corals using an accurate buoyant weighing technique', *Marine Biology*, 101, pp. 389–395.

Davy, S. K., Allemand, D. and Weis, V. M. (2012) 'Cell Biology of Cnidarian-Dinoflagellate Symbiosis', *Microbiology and Molecular Biology Reviews*, 76(2), pp. 229–261.

Dean, J. R., Leng, M. J. and Mackay, A. W. (2014) 'Is there an isotopic signature of the anthropocene?', *Anthropocene Review*, 1(3), pp. 276–287.

DeCarlo, T. M. and Cohen, A. L. (2017) 'Dissepiments, density bands and signatures of thermal stress in Porites skeletons', *Coral Reefs*, 36(3), pp. 749–761.

Decarlo, T. M., Holcomb, M. and McCulloch, M. T. (2018) 'Reviews and syntheses: Revisiting the boron systematics of aragonite and their application to coral calcification', *Biogeosciences*, 15(9), pp. 2819–2834.

Devriendt, L. S., Watkins, J. M. and McGregor, H. V. (2017) 'Oxygen isotope fractionation in the CaCO3-DIC-H2O system', *Geochimica et Cosmochimica Acta*, 214, pp. 115–142.

Dikou, A. (2009) 'Skeletal linear extension rates of the foliose scleractinian coral Merulina ampliata (Ellis & Solander, 1786) in a turbid environment', *Marine Ecology*, 30(4), pp. 405–415.

Doube, M. *et al.* (2010) 'BoneJ: Free and extensible bone image analysis in ImageJ', *Bone*, 47(6), pp. 1076–1079.

Dubinsky, Z. and Jokiel, P. (1994) 'Ratio of Energy and Nutrient Fluxes Regulates Symbiosis between Zooxanthellae and Corals', *Pacific Science*, 48(3), pp. 313–324.

Dubinsky, Z. and Stambler, N. (2011) *Coral Reefs: An ecosystem in transition*.

Dunn, J. G., Sammarco, P. W. and LaFleur, G. (2012) 'Effects of phosphate on growth and skeletal density in the scleractinian coral Acropora muricata: A controlled experimental approach', *Journal of Experimental Marine Biology and Ecology*, 411, pp. 34–44.

Duprey, N. N., Yasuhara, M. and Baker, D. M. (2016) 'Reefs of tomorrow: eutrophication reduces coral biodiversity in an urbanized seascape', *Global Change Biology*, 22(11), pp. 3550–3565.

Edinger, E. N. *et al.* (2000) 'Normal Coral Growth Rates on Dying Reefs: Are Coral Growth Rates Good Indicators of Reef Health?', *Marine Pollution Bulletin*, 40(5), pp. 404–425.

Elizalde-Rendón, E. M. *et al.* (2010) 'Growth characteristics of the reef-building coral Porites astreoides under different environmental conditions in the Western Atlantic', *Coral Reefs*, 29(3), pp. 607–614.

Enríquez, S., Méndez, E. R. and Iglesias-Prieto, R. (2005) 'Multiple Scattering on Coral Skeletons Enhances Light Absorption by Symbiotic Algae', *Limnology and Oceanography*, 50(4), pp. 1025–1032.

Epstein, S. and Mayeda, T. (1953) 'Variation of O18 content of waters from natural sources', *Geochemica et Cosmochimica Acta*, 4, pp. 213–224.

Eyal, G. *et al.* (2019) 'Photoacclimation and induction of light-enhanced calcification in the mesophotic coral Euphyllia paradivisa', *Royal Society Open Science*, 6(2).

Ezzat, L. *et al.* (2015) 'New insights into carbon acquisition and exchanges within the coral-dinoflagellate symbiosis under NH4+ and NO3- supply.', *Proceedings of the Royal Society B: Biological Sciences*, 282(1812), p. 20150610.

Fabricius, K. E. (2005) 'Effects of terrestrial runoff on the ecology of corals and coral reefs: Review and synthesis', *Marine Pollution Bulletin*, 50(2), pp. 125–146.

Fabricius, K. E. *et al.* (2013) 'Does Trophic Status Enhance or Reduce the Thermal Tolerance of Scleractinian Corals? A Review, Experiment and Conceptual Framework', *PLoS ONE*, 8(1), pp. 1–12.

Falkowski, P. G. *et al.* (1984) 'Light and the Bioenergetics of a Symbiotic Coral', *BioScience*, 34(11), pp. 705–709.

Falkowski, P. G. *et al.* (1993) 'Population Control in Symbiotic Corals', *BioScience*, 43(9), pp. 606–611.

Ferrier-Pagès, C. *et al.* (2016) 'Phosphorus metabolism of reef organisms with algal

symbionts', *Ecological Monographs*, 86(3), pp. 262–277.

Foster, A. B. (1979) 'Phenotypic plasticity in the reef corals Montastrea annularis (Ellis & Solander) and Siderastrea siderea (Ellis & Solander)', *Journal of Experimental Marine Biology and Ecology*, 39, pp. 25–54.

Foster, G. L. *et al.* (2013) 'Interlaboratory comparison of boron isotope analyses of boric acid, seawater and marine CaCO3 by MC-ICPMS and NTIMS', *Chemical Geology*, 358, pp. 1–14.

Fouke, K. W., Trop, J. M. and Sivaguru, M. (2021) 'Changes in Coral Skeleton Growth Recorded by Density Band Stratigraphy, Crystalline Structure, and Hiatuses', *Frontiers in Marine Science*, 8(December), pp. 1–16.

Fowell, S. E. *et al.* (2016) 'Intrareef variations in Li/Mg and Sr/Ca sea surface temperature proxies in the Caribbean reef-building coral Siderastrea siderea', *Paleoceanography*, 31(10), pp. 1315–1329.

Frankowiak, K., Kret, S., *et al.* (2016) 'Fine-scale skeletal banding can distinguish symbiotic from asymbiotic species among modern and fossil scleractinian corals', *PLoS ONE*, 11(1), pp. 1–21.

Frankowiak, K., Wang, X. T., *et al.* (2016) 'Photosymbiosis and the expansion of shallow-water corals', *Science Advances*, 2(11), pp. 1–8.

Frentzen, M. (2004) 'Phosphatidylglycerol and sulfoquinovosyldiacylglycerol: Anionic membrane lipids and phosphate regulation', *Current Opinion in Plant Biology*, 7(3), pp. 270–276.

Furla, P. *et al.* (2000) 'Sources and mechanisms of inorganic carbon transport for coral calcification and photosynthesis', *Journal of Experimental Biology*, 203(22), pp. 3445–3457.

Furla, P., Allemand, D. and Orsenigo, M. N. (2000) 'Involvement of H+-ATPase and carbonic anhydrase in inorganic carbon uptake for endosymbiont photosynthesis', *American Journal of Physiology - Regulatory Integrative and Comparative Physiology*, 278(4), pp. R870–R881.

Furnas, M. *et al.* (2005) 'In the other 90%: Phytoplankton responses to enhanced nutrient availability in the Great Barrier Reef Lagoon', *Marine Pollution Bulletin*, 51(1–4), pp. 253–265.

Gabitov, R. I. *et al.* (2008) 'Experimental determination of growth rate effect on U6+ and Mg2+ partitioning between aragonite and fluid at elevated U6+ concentration', *Geochimica et Cosmochimica Acta*, 72(16), pp. 4058–4068.

Gabitov, R. I. *et al.* (2011) 'In situ δ7Li, Li/Ca, and Mg/Ca analyses of synthetic aragonites', *Geochemistry, Geophysics, Geosystems*, 12(3).

Gaetani, G. A. *et al.* (2011) 'Rayleigh-based, multi-element coral thermometry: A biomineralization approach to developing climate proxies', *Geochimica et Cosmochimica Acta*, 75(7), pp. 1920–1932.

Gaetani, G. A. and Cohen, A. L. (2006) 'Element partitioning during precipitation of aragonite from seawater: A framework for understanding paleoproxies', *Geochimica et Cosmochimica Acta*, 70(18), pp. 4617–4634.

Gagnon, A. C. *et al.* (2007) 'Sr/Ca and Mg/Ca vital effects correlated with skeletal architecture in a scleractinian deep-sea coral and the role of Rayleigh fractionation', *Earth and Planetary Science Letters*, 261(1–2), pp. 280–295.

Gagnon, A. C., Adkins, J. F. and Erez, J. (2012) 'Seawater transport during coral biomineralization', *Earth and Planetary Science Letters*, 329–330, pp. 150–161.

Gateño, D. and Rinkevich, B. (2003) 'Coral polyp budding is probably promoted by a canalized ratio of two morphometric fields', *Marine Biology*, 142(5), pp. 971–973.

Gattuso, J. P., Allemand, D. and Frankignoulle, M. (1999) 'Photosynthesis and Calcification at Cellular , Organismal and Community Levels in Coral Reefs : A Review on Interactions and Control by Carbonate Chemistry', *American zoologist*, 39(1), pp. 160–183.

GCRMN (2020) 'Status of Coral Summary for Policymakers – Status of Coral Reefs of the World : 2020', p. 7. Available at: https://gcrmn.net/wp-content/uploads/2021/11/Status-of-Coral-Reefs-of-the-World-2020-Summary-for-Policymakers.pdf.[Accessed on 03/10/2022]

Gladfelter, E. H. (1982) 'Skeletal development in Acropora cervicornis: I. Patterns of calcium carbonate accretion in the axial corallite', *Coral Reefs*, 1, pp. 45–51.

Gladfelter, E. H. (2007) 'Skeletal development in Acropora palmata (Lamarck 1816): A scanning electron microscope (SEM) comparison demonstrating similar mechanisms of skeletal extension in axial versus encrusting growth', *Coral Reefs*, 26(4), pp. 883–892.

Gleixner, S. *et al.* (2014) 'An inter-hemispheric comparison of the tropical storm response to global warming', *Climate Dynamics*, 42, pp. 2147–2157.

Godinot, C., Ferrier-pagès, C. and Grover, R. (2009) 'Control of phosphate uptake by zooxanthellae and host cells in the scleractinian coral Stylophora pistillata', *Limnology and Oceanography*, 54(5), pp. 1627–1633.

Goldberg, W. M. (2018) *Coral Food, Feeding, Nutrition, and Secretion: A Review*, *Results and Problems in Cell Differentiation*.

Gonfiantini, R. *et al.* (2003) 'Intercomparison of boron isotope and concentration measurements. Part II: Evaluation of results', *Geostandards Newsletter*, 27(1), pp. 41–57.

Graham, N. A. J. and Nash, K. L. (2013) 'The importance of structural complexity in coral reef ecosystems', *Coral Reefs*, 32(2), pp. 315–326.

Grottoli, A. G., Rodrigues, L. J. and Palardy, J. E. (2006) 'Heterotrophic plasticity and resilience in bleached corals', *Nature*, 440(7088), pp. 1186–1189.

Grover, R. *et al.* (2002) 'Uptake of ammonium by the scleractinian coral Stylophora pistillata: Effect of feeding, light, and ammonium concentrations', *Limnology and Oceanography*, 47(3), pp. 782–790.

Grover, R. *et al.* (2003) 'Nitrate uptake in the scleractinian coral Stylophora pistillata', *Limnology and Oceanography*, 48(6), pp. 2266–2274.

Grover, R. *et al.* (2006) 'Urea uptake by the scleractinian coral Stylophora pistillata', *Journal of Experimental Marine Biology and Ecology*, 332(2), pp. 216–225.

Grover, R. *et al.* (2008) 'Uptake of dissolved free amino acids by the scleractinian coral Stylophora pistillata', *Journal of Experimental Biology*, 211(6), pp. 860–865.

Guan, Y., Hohn, S. and Merico, A. (2015) 'Suitable environmental ranges for potential Coral reef habitats in the tropical ocean', *PLoS ONE*, 10(6), pp. 1–17.

Guo, W. (2019) 'Seawater temperature and buffering capacity modulate coral calcifying pH', *Scientific Reports*, 9(1), pp. 1–13.

Haas, A. F. *et al.* (2010) 'Organic matter release by the dominant primary producers in a Caribbean reef lagoon: Implication for in situ O2 availability', *Marine Ecology Progress Series*, 409, pp. 27–39.

Hand, C. and Uhlinger, K. R. (1995) 'Asexual Reproduction by Transverse Fission and Some Anomalies in the Sea Anemone Nematostella vectensis', *Invertebrate Biology*, 114(1), pp. 9–18.

Harland, A. D. and Davies, P. S. (1995) 'Symbiont photosynthesis increases both respiration and photosynthesis in the symbiotic sea anemone Anemonia viridis', *Marine Biology*, 123(4), pp. 715–722.

Hathorne, Ed C *et al.* (2013) 'Interlaboratory study for coral Sr / Ca and other element / Ca ratio measurements', 14, pp. 3730–3750.

Hathorne, E. C. *et al.* (2013) 'Lithium in the aragonite skeletons of massive Porites corals: A new tool to reconstruct tropical sea surface temperatures', *Paleoceanography*, 28(1), pp. 143–152.

Hoegh-Guldberg, O. E. *et al.* (2007) 'Coral Reefs Under Rapid Climate Change and

Ocean Acidification', *Science*, 318, pp. 1737–1742.

Holcomb, M. *et al.* (2009) 'Compositional and morphological features of aragonite precipitated experimentally from seawater and biogenically by corals', *Geochimica et Cosmochimica Acta*, 73(14), pp. 4166–4179.

Holcomb, M. *et al.* (2016) 'Factors affecting B/Ca ratios in synthetic aragonite', *Chemical Geology*, 437, pp. 67–76.

Holcomb, M., Cohen, A. L. and McCorkle, D. C. (2013) 'An evaluation of staining techniques for marking daily growth in scleractinian corals', *Journal of Experimental Marine Biology and Ecology*, 440, pp. 126–131.

Houlbrèque, F. and Ferrier-Pagès, C. (2009) 'Heterotrophy in tropical scleractinian corals', *Biological Reviews*, 84(1), pp. 1–17.

Hughes, A. D. and Grottoli, A. G. (2013) 'Heterotrophic compensation: A possible mechanism for resilience of coral reefs to global warming or a sign of prolonged stress?', *PLoS ONE*, 8(11), pp. 1–10.

Hughes, T. P. *et al.* (2017) 'Coral reefs in the Anthropocene', *Nature*, 546(7656), pp. 82–90.

Hughes, T.P. *et al.* (2017a) 'Global warming and recurrent mass bleaching of corals', *Nature*, 543(7645), pp. 373–377.

Hughes, T. P., Kerry, J. T., *et al.* (2018) 'Global warming transforms coral reef assemblages', *Nature*, 556(7702), pp. 492–496.

Hughes, T. P., Anderson, K. D., *et al.* (2018) 'Spatial and temporal patterns of mass bleaching of corals in the Anthropocene', *Science*, 359(6371).

Humblet, M., Hongo, C. and Sugihara, K. (2015) 'An identification guide to some major Quaternary fossil reef-building coral genera (Acropora, Isopora, Montipora, and Porites)', *Island Arc*, 24(1), pp. 16–30.

Inoue, M. *et al.* (2007) 'Empirical assessment of coral Sr/Ca and Mg/Ca ratios as climate proxies using colonies grown at different temperatures', *Geophysical Research Letters*, 34(12), pp. 2002–2005.

Inoue, M. *et al.* (2018) 'A simple role of coral-algal symbiosis in coral calcification based on multiple geochemical tracers', *Geochimica et Cosmochimica Acta*, 235, pp. 76–88.

Jokiel, P. L., Maragos, J. E. and Franzisket, L. (1978) *Coral growth: buoyant weight technique*, *Stoddart, D.R., Johannes, R.E. (Eds.), Coral reef: research methods. Unesco, Paris*.

Jompa, J. and McCook, L. J. (2002) 'The effects of nutrients and herbivory on

competition between a hard coral (Porites cylindrica) and a brown alga (Lobophora variegata)', *Limnology and Oceanography*, 47(2), pp. 527–534.

Juillet-Leclerc, A. *et al.* (2014) 'Light is an active contributor to the vital effects of coral skeleton proxies', *Geochimica et Cosmochimica Acta*, 140, pp. 671–690.

Kim, S. T., Coplen, T. B. and Horita, J. (2015) 'Normalization of stable isotope data for carbonate minerals: Implementation of IUPAC guidelines', *Geochimica et Cosmochimica Acta*, 158, pp. 276–289.

Kinsey, D. W. and Davies, P. J. (1979) 'Effects of elevated nitrogen and phosphorus on coral reef growth', 24(5), pp. 935–940.

Kleypas, J. *et al.* (2021) 'Designing a blueprint for coral reef survival', *Biological Conservation*, 257, p. 109107.

Kleypas, J. A., Mcmanus, J. W. and Menez, L. A. B. (1999) 'Environmental Limits to Coral Reef Development : Where Do We Draw the Line ?', *American Zoology*, 39(1), pp. 146–159.

Koop, K. *et al.* (2001) 'ENCORE: The effect of nutrient enrichment on coral reefs. Synthesis of results and conclusions', *Marine Pollution Bulletin*, 42(2), pp. 91–120.

Kopp, C. *et al.* (2013) 'Highly Dynamic Cellular-Level Response of Symbiotic Coral to a sudden increase in environmental nitrogen', *The ISME Journal*, 4(3), pp. 1–9.

Kuffner, I. B. *et al.* (2017) 'Fidelity of the Sr/Ca proxy in recording ocean temperature in the western Atlantic coral Siderastrea siderea', *Geochemistry, Geophysics, Geosystems*, 18, pp. 178–188.

LaJeunesse, T. C. *et al.* (2018) 'Systematic Revision of Symbiodiniaceae Highlights the Antiquity and Diversity of Coral Endosymbionts', *Current Biology*, 28(16), pp. 2570-2580.e6.

Lange, I. D. and Perry, C. T. (2019) 'Bleaching impacts on carbonate production in the Chagos Archipelago: influence of functional coral groups on carbonate budget trajectories', *Coral Reefs*, 38(4), pp. 619–624.

Lange, I. D. and Perry, C. T. (2020) 'A quick, easy and non-invasive method to quantify coral growth rates using photogrammetry and 3D model comparisons', *Methods in Ecology and Evolution*, 11(6), pp. 714–726.

Lange, I. D., Perry, C. T. and Alvarez-Filip, L. (2020) 'Carbonate budgets as indicators of functional reef "health": A critical review of data underpinning census-based methods and current knowledge gaps', *Ecological Indicators*, 110.

Lapointe, B. E. (1997) 'Nutrient thresholds for bottom-up control of macroalgal

blooms on coral reefs in Jamaica and southeast Florida', *Limnology and Oceanography*, 42(5 II), pp. 1119–1131.

Lapointe, B. E. *et al.* (2019) 'Nitrogen enrichment, altered stoichiometry, and coral reef decline at Looe Key, Florida Keys, USA: a 3-decade study', *Marine Biology*, 166:108.

Lapointe, B. E., Tewfik, A. and Phillips, M. (2021) 'Macroalgae reveal nitrogen enrichment and elevated N:P ratios on the Belize Barrier Reef', *Marine Pollution Bulletin*, 171.

LaVigne, M. *et al.* (2010) 'Coral skeleton P/Ca proxy for seawater phosphate: Multi-colony calibration with a contemporaneous seawater phosphate record', *Geochimica et Cosmochimica Acta*, 74(4), pp. 1282–1293.

Lema, K. A., Willis, B. L. and Bourneb, D. G. (2012) 'Corals form characteristic associations with symbiotic nitrogen-fixing bacteria', *Applied and Environmental Microbiology*, 78(9), pp. 3136–3144.

Lesser, M. P. (1996) 'Elevated temperatures and ultraviolet radiation cause oxidative stress and inhibit photosynthesis in symbiotic dinoflagellates', *Limnology and Oceanography*, 41(2), pp. 271–283.

Lesser, M. P. (1997) 'Oxidative stress causes coral bleaching during exposure to elevated temperatures', *Coral Reefs*, 16(3), pp. 187–192.

Lesser, M. P. and Farrell, J. H. (2004) 'Exposure to solar radiation increases damage to both host tissues and algal symbionts of corals during thermal stress', *Coral Reefs*, 23(3), pp. 367–377.

Li, Y.H. (1991) 'Distribution patterns of the elements in the ocean: A synthesis', *Geochimica et Cosmochimica Acta*, 55(11), pp. 3223–3240.

Li, Y. *et al.* (2020) 'The 3D Reconstruction of Pocillopora Colony Sheds Light on the Growth Pattern of This Reef-Building Coral', *iScience*, 23(6).

Lirman, D. (2000) 'Fragmentation in the branching coral Acropora palmata (Lamarck): Growth, survivorship, and reproduction of colonies and fragments', *Journal of Experimental Marine Biology and Ecology*, 251(1), pp. 41–57.

Liu, G., Strong, A. E. and Skirving, W. (2003) 'Remote sensing of sea surface temperatures during 2002 barrier reef coral bleaching', *Eos*, 84(15), pp. 2002–2004.

Lough, J. M., Anderson, K. D. and Hughes, T. P. (2018) 'Increasing thermal stress for tropical coral reefs : 1871 – 2017', *Scientific Reports*, 8(6079), pp. 1–8.

Lough, J. M. and Barnes, D. J. (1992) 'Comparisons of skeletal density variations in Porites from the central Great Barrier Reef', *Journal of Experimental Marine Biology and*

Ecology, 155(1), pp. 1–25.

Luzon, K. S. *et al.* (2017) 'Resurrecting a subgenus to genus: Molecular phylogeny of Euphyllia and Fimbriaphyllia (order Scleractinia; family Euphyllidae; clade V)', *PeerJ*, 2017(12), pp. 1–38.

Madl, P., Schabetsberger, R. and Lipovnik, C. (2014) 'Scleractinian Coral Taxonomy', pp. 1–58. Available at: http://biophysics.sbg.ac.at/talk/coral-lecture.pdf.

Marchitto, T. M. *et al.* (2018) 'A simple biomineralization model to explain Li, Mg, and Sr incorporation into aragonitic foraminifera and corals', *Earth and Planetary Science Letters*, 481, pp. 20–29.

Marriott, C. S., Henderson, G. M., Crompton, R., *et al.* (2004) 'Effect of mineralogy, salinity, and temperature on Li/Ca and Li isotope composition of calcium carbonate', *Chemical Geology*, 212(1–2), pp. 5–15.

Marriott, C. S., Henderson, G. M., Belshaw, N. S., *et al.* (2004) 'Temperature dependence of δ7Li, δ44Ca and Li/Ca during growth of calcium carbonate', *Earth and Planetary Science Letters*, 222(2), pp. 615–624.

Marshall, P. A. (2000) 'Skeletal damage in reef corals: relating resistance to colony morphology', *Marine Ecology Progress Series*, 200, pp. 177–189.

Marshall, P. A. and Baird, A. H. (2000) 'Bleaching of corals on the Great Barrier Reef: Differential susceptibilities among taxa', *Coral Reefs*, 19(2), pp. 155–163.

Marubini, F. and Davies, P. S. (1996) 'Nitrate increases zooxanthellae population density and reduces skeletogenesis in corals', *Marine Biology*, 127(2), pp. 319–328.

McConnaughey, T. (1989a) '13C and 18O isotopic disequilibrium in biological carbonates: I. Patterns', *Geochimica et Cosmochimica Acta*, 53(1), pp. 151–162.

McConnaughey, T. (1989b) '13C and 18O isotopic disequilibrium in biological carbonates: II. In vitro simulation of kinetic isotope effects', *Geochimica et Cosmochimica Acta*, 53(1), pp. 163–171.

McConnaughey, T. A. (2003) 'Sub-equilibrium oxygen-18 and carbon-13 levels in biological carbonates: Carbonate and kinetic models', *Coral Reefs*, 22(4), pp. 316–327.

McCrea, J. M. (1950) 'On the isotopic chemistry of carbonates and a paleotemperature scale', *The Journal of Chemical Physics*, 18(6), pp. 849–857. d

McCulloch, M. *et al.* (2012) 'Coral resilience to ocean acidification and global warming through pH up-regulation', *Nature Climate Change*, 2(8), pp. 623–627.

McCulloch, M. T. *et al.* (2017) 'Coral calcification in a changing World and the interactive dynamics of pH and DIC upregulation', *Nature Communications*, (8), p. Article

15686.

McNally, S. P. *et al.* (2017) 'Multifaceted impacts of the stony coral Porites astreoides on picoplankton abundance and community composition', *Limnology and Oceanography*, 62(1), pp. 217–234.

Meibom, A. *et al.* (2004) 'Distribution of magnesium in coral skeleton', *Geophysical Research Letters*, 31(23), pp. 1–4.

Mendes, J. M. and Woodley, J. D. (2002) 'Effect of the 1995-1996 bleaching event on polyp tissue depth, growth, reproduction and skeletal band formation in Montastraea annularis', *Marine Ecology Progress Series*, 235, pp. 93–102.

Meyer, J. L. and Schultz, E. T. (1985) 'Migrating haemulid fishes as a source of nutrients and organic matter on coral reefs', *Limnology and Oceanography*, 30(1), pp. 146–156.

Meyer, J. L and Schultz, E. T. (1985a) 'Tissue Condition and Growth Rate of Corals Associated with Schooling Fish', *Limnology and Oceanography*, 30(1), pp. 157–166.

Meyer, J. L., Schultz, E. T. and Helfman, G. S. (1983) 'Fish Schools : An Asset to Corals', *Science*, 220(4601), pp. 1047–1049.

Miller, D. J. and Yellowlees, D. (1989) 'Inorganic Nitrogen Uptake by Symbiotic Marine Cnidarians : A Critical Review', *Proceedings of the Royal Society B: Biological Sciences*, 237(1286), pp. 109–125.

Millero, F. J. *et al.* (2008) 'The composition of Standard Seawater and the definition of the Reference-Composition Salinity Scale', *Deep-Sea Research Part I: Oceanographic Research Papers*, 55(1), pp. 50–72.

Mitsuguchi, T. *et al.* (1996) 'Mg / Ca Thermometry in Coral Skeletons', *Science*, 274(5289), pp. 961–963.

Moore, C.M. et al. (2003) 'Processes and patterns of oceanic nutrient limitation', *Nature Geoscience*, 6, pp 701-710.

Montaggioni, L. F. *et al.* (2006) 'Coral barium/calcium record of mid-Holocene upwelling activity in New Caledonia, South-West Pacific', *Palaeogeography, Palaeoclimatology, Palaeoecology*, 237(2–4), pp. 436–455.

Montagna, P. *et al.* (2014) 'Li/Mg systematics in scleractinian corals: Calibration of the thermometer', *Geochimica et Cosmochimica Acta*, 132, pp. 288–310.

Morgan, K. M. and Kench, P. S. (2012) 'Skeletal extension and calcification of reef-building corals in the central Indian Ocean', *Marine Environmental Research*, 81, pp. 78–82.

Munzel, U. and Brunner, E. (2000) 'Nonparametric tests in the unbalanced

multivariate one-way design', *Biometrical Journal*, 42(7), pp. 837–854.

Muscatine, L. *et al.* (1989) 'The Effect of External Nutrient Resources on the Population Dynamics of Zooxanthellae in a Reef Coral', *Proceedings of the Royal Society B: Biological Sciences*, 236(1284), pp. 311–324.

Muscatine, L., Pool, R. R. and Cernichiari, E. (1972) 'Some factors influencing selective release of soluble organic material by zooxanthellae from reef corals', *Marine Biology*, 13, pp. 298–308.

Muscatine, L., Tambutte, E. and Allemand, D. (1997) 'Morphology of coral desmocytes, cells that anchor the calicoblastic epithelium to the skeleton', *Coral Reefs*, 16(4), pp. 205–213.

O'Neil, J. M. and Capone, D. G. (2008) *Nitrogen Cycling in Coral Reef Environments*, *Nitrogen in the Marine Environment*.

Ohno, Y. *et al.* (2017) 'Calcification process dynamics in coral primary polyps as observed using a calcein incubation method', *Biochemistry and Biophysics Reports*, 9, pp. 289–294.

Parkhill, J. P., Maillet, G. and Cullen, J. J. (2001) 'Fluorescence-based maximal quantum yield for PSII as a diagnostic of nutrient stress', *Journal of Phycology*, 37(4), pp. 517–529.

Peirano, A. *et al.* (2005) 'Monthly variations in calix growth, polyp tissue, and density banding of the Mediterranean scleractinian Cladocora caespitosa (L.)', *Coral Reefs*, 24(3), pp. 404–409.

Pérez-Huerta, A. *et al.* (2010) 'Vital effects in the context of biomineralization', *Workshop on Biominerals and Biomineralization Processes*, (1), pp. 35–45. Available at: http://www.ehu.eus/sem/seminario_pdf/SEMINARIO_SEM_7_035.pdf.

Pernice, M. *et al.* (2012) 'A single-cell view of ammonium assimilation in coral-dinoflagellate symbiosis', *ISME Journal*, 6(7), pp. 1314–1324.

Perry, C. T. *et al.* (2020) 'Bleaching-driven reef community shifts drive pulses of increased reef sediment generation', *Royal Society Open Science*, 7(4), p. 192153.

Pörtner H. *et al*. (2022) *Climate Change 2022 - Impacts, Adaptation and Vulnerability - Summary for Policymakers*, *Ipcc*.

Precoda, K. *et al.* (2020) 'Tissue biomass trades off with growth but not reproduction in corals', *Coral Reefs*, 39(4), pp. 1027–1037.

Puotinen, M. *et al.* (2020) 'Towards modelling the future risk of cyclone wave damage to the world's coral reefs', *Global Change Biology*, 26(8), pp. 4302–4315.

Purkis, S. J., Graham, N. A. J. and Riegl, B. M. (2008) 'Predictability of reef fish diversity and abundance using remote sensing data in Diego Garcia (Chagos Archipelago)', *Coral Reefs*, 27(1), pp. 167–178.

Qin, Z. *et al.* (2019) 'Spatial and Intergeneric Variation in Physiological Indicators of Corals in the South China Sea: Insights Into Their Current State and Their Adaptability to Environmental Stress', *Journal of Geophysical Research: Oceans*, pp. 3317–3332.

Qin, Z. *et al.* (2020) 'Latitudinal variation in reef coral tissue thickness in the South China Sea: Potential linkage with coral tolerance to environmental stress', *Science of the Total Environment*, 711, p. 134610.

Raddatz, J. *et al.* (2013) 'Stable Sr-isotope, Sr/Ca, Mg/Ca, Li/Ca and Mg/Li ratios in the scleractinian cold-water coral Lophelia pertusa', *Chemical Geology*, 352, pp. 143–152.

Rädecker, N. *et al.* (2015) 'Nitrogen cycling in corals: the key to understanding holobiont functioning?', *Trends in Microbiology*, 23(8), pp. 490–497.

Rahav, O. *et al.* (1989) 'Ammonium metabolism in the zooxanthellate coral, Stylophora pistillata', *Proceedings of the Royal Society B: Biological Sciences*, 236, pp. 325–337.

Ram, S. and Erez, J. (2021) 'The Distribution Coefficients of Major and Minor Elements in Coral Skeletons Under Variable Calcium Seawater Concentrations', *Frontiers in Earth Science*, 9(May), pp. 1–14.

Rehman, A. U. *et al.* (2016) 'Symbiodinium sp. cells produce light-induced intra- and extracellular singlet oxygen, which mediates photodamage of the photosynthetic apparatus and has the potential to interact with the animal host in coral symbiosis', *New Phytologist*, 212, pp. 472–484.

Reshef, L. *et al.* (2006) 'The Coral Probiotic Hypothesis', *Environmental Microbiology*, 8(12), pp. 2068–2073.

Reynaud-Vaganay, S. *et al.* (2001) 'Effect of light on skeletal 13C and 18O, and interaction with photosynthesis, respiration and calcification in two zooxanthellate scleractinian corals', *Palaeogeography, Palaeoclimatology, Palaeoecology*, 175, pp. 393–404.

Reynaud, S. *et al.* (2007) 'Light and temperature effects on Sr/Ca and Mg/Ca ratios in the scleractinian coral Acropora sp.', *Geochimica et Cosmochimica Acta*, 71(2), pp. 354–362.

Rippe, J. P. *et al.* (2018) 'Corals sustain growth but not skeletal density across the Florida Keys Reef Tract despite ongoing warming', *Global Change Biology*, 24(11), pp. 5205–5217.

Robinson, L. F. *et al.* (2014) 'The geochemistry of deep-sea coral skeletons: A review of vital effects and applications for palaeoceanography', *Deep-Sea Research Part II: Topical Studies in Oceanography*, 99, pp. 184–198.

Roche, R. C. *et al.* (2010) 'Quantification of porosity in Acropora pulchra (Brook 1891) using X-ray micro-computed tomography techniques', *Journal of Experimental Marine Biology and Ecology*, 396(1), pp. 1–9.

Roche, R. C. *et al.* (2011) 'Spatial variation in porosity and skeletal element characteristics in apical tips of the branching coral Acropora pulchra (Brook 1891)', *Coral Reefs*, 30(1), pp. 195–201.

Rocker, M. M. *et al.* (2017) 'Variation in the health and biochemical condition of the coral Acropora tenuis along two water quality gradients on the Great Barrier Reef , Australia', *Marine Pollution Bulletin*, 119(2), pp. 106–119.

Rodolfo-Metalpa, R. *et al.* (2008) 'Effects of temperature, light and heterotrophy on the growth rate and budding of the temperate coral Cladocora caespitosa', *Coral Reefs*, 27(1), pp. 17–25.

Rodrigues, L. J. and Grottoli, A. G. (2006) 'Calcification rate and the stable carbon, oxygen, and nitrogen isotopes in the skeleton, host tissue, and zooxanthellae of bleached and recovering Hawaiian corals', *Geochimica et Cosmochimica Acta*, 70(11), pp. 2781–2789.

Rodrigues, L. J. and Grottoli, A. G. (2007) 'Energy reserves and metabolism as indicators of coral recovery from bleaching', *Limnology and Oceanography*, 52(5), pp. 1874–1882.

Rodrigues, L. J., Grottoli, A. G. and Pease, T. K. (2008) 'Lipid class composition of bleached and recovering Porites compressa Dana, 1846 and Montipora capitata Dana, 1846 corals from Hawaii', *Journal of Experimental Marine Biology and Ecology*, 358(2), pp. 136–143.

Rollion-Bard, C. and Blamart, D. (2015) 'Possible controls on Li, Na, and Mg incorporation into aragonite coral skeletons', *Chemical Geology*, 396, pp. 98–111.

Rollion-Bard, C., Chaussidon, M. and France-Lanord, C. (2003) 'pH control on oxygen isotopic composition of symbiotic corals', *Earth and Planetary Science Letters*, 215(1–2), pp. 275–288.

Ross, C. L. *et al.* (2018) 'Mechanisms and seasonal drivers of calcification in the temperate coral turbinaria reniformis at its latitudinal limits', *Proceedings of the Royal Society B: Biological Sciences*, 285(1879).

Ross, C. L., DeCarlo, T. M. and McCulloch, M. T. (2019) 'Calibration of Sr/Ca,

Li/Mg and Sr-U Paleothermometry in Branching and Foliose Corals', *Paleoceanography and Paleoclimatology*, 34(8), pp. 1271–1291.

Rosset, S. *et al.* (2017) 'Phosphate deficiency promotes coral bleaching and is reflected by the ultrastructure of symbiotic dinoflagellates', *Marine Pollution Bulletin*, 118(1–2), pp. 180–187.

Rosset, S., D'Angelo, C. and Wiedenmann, J. (2015) 'Ultrastructural Biomarkers in Symbiotic Algae Reflect the Availability of Dissolved Inorganic Nutrients and Particulate Food to the Reef Coral Holobiont', *Frontiers in Marine Science*, 2, pp. 1–10.

Roth, M. S. (2014) 'The engine of the reef: Photobiology of the coral-algal symbiosis', *Frontiers in Microbiology*, 5((Article 422)), pp. 1–22.

Ruppert, J. L. W. *et al.* (2013) 'Caught in the Middle: Combined Impacts of Shark Removal and Coral Loss on the Fish Communities of Coral Reefs', *PLoS ONE*, 8(9), pp. 1–9.

Sadek, M. A. *et al.* (2018) 'Comparative morphology on some sclerectanian corals in Arabian Gulf and the Egyptian Coast of the Red Sea', *Egyptian Journal of Aquatic Biology & Fisheries*, 22(3), pp. 13–24.

Sadler, J. *et al.* (2016) 'Acropora interbranch skeleton Sr/Ca ratios: Evaluation of a potential new high-resolution paleothermometer', *Paleoceanography*, 31(4), pp. 505–517.

Sandeman, I. M. (2008) 'Light driven lipid peroxidation of coral membranes and a suggested role in calcification', *Revista de Biologia Tropical*, 56, pp. 1–9.

Savage, C. (2019) 'Seabird nutrients are assimilated by corals and enhance coral growth rates', *Scientific Reports*, 9(1), p. 4284.

Schneider, C. A., Rasband, W. S. and Eliceiri, K. W. (2012) 'NIH Image to ImageJ: 25 years of image analysis', *Nature Methods*, 9(7), pp. 671–675.

Schoepf, V. *et al.* (2021) 'Heat stress differentially impacts key calcification mechanisms in reef-building corals', *Coral Reefs*. doi: 10.1007/s00338-020-02038-x.

Shantz, A. A. and Burkepile, D. E. (2014) 'Context-dependent effects of nutrient loading on the coral-algal mutualism', *Ecology*, 95(7), pp. 1995–2005.

Sheppard, C. *et al.* (2005) 'Coral mortality increases wave energy reaching shores protected by reef flats: Examples from the Seychelles', *Estuarine, Coastal and Shelf Science*, 64(2–3), pp. 223–234.

Shick, J. M. *et al.* (2011) 'Responses to iron limitation in two colonies of Stylophora pistillata exposed to high temperature: Implications for coral bleaching', *Limnology and Oceanography*, 56(3), pp. 813–828.

Shinn, E. A. (1976) 'Coral reef recovery in Florida and the Persian Gulf',

Environmental Geology, 1(4), pp. 241–254.

Siebeck, U. E. *et al.* (2006) 'Monitoring coral bleaching using a colour reference card', *Coral Reefs*, 25(3), pp. 453–460.

Silbiger, N. J. *et al.* (2018) 'Nutrient pollution disrupts key ecosystem functions on coral reefs', *Proceedings of the Royal Society B: Biological Sciences*, 285, p. 20172718.

Sinclair, D. J. (2005) 'Correlated trace element "vital effects" in tropical corals: A new geochemical tool for probing biomineralization', *Geochimica et Cosmochimica Acta*, 69(13), pp. 3265–3284.

Sinclair, D. J., Williams, B. and Risk, M. (2006) 'A biological origin for climate signals in corals - Trace element "vital effects" are ubiquitous in Scleractinian coral skeletons', *Geophysical Research Letters*, 33(17), pp. 1–5.

Sinniger, F. *et al.* (2016) 'Euphyllia paradivisa, a successful mesophotic coral in the northern Gulf of Eilat / Aqaba , Red Sea', *Coral Reefs*, 35(1), pp. 91–102.

Smith, A. *et al.* (2021) 'Field measurements of a massive Porites coral at Goolboodi (Orpheus Island), Great Barrier Reef', *Scientific Reports*, 11(1), pp. 1–6.

Spencer Davies, P. (1990) 'A rapid method for assessing growth rates of corals in relation to water pollution', *Marine Pollution Bulletin*, 21(7), pp. 346–348.

Sproles, A. E. *et al.* (2018) 'Phylogenetic characterization of transporter proteins in the cnidarian-dinoflagellate symbiosis', *Molecular Phylogenetics and Evolution*, 120, pp. 307–320.

Stambler, N. *et al.* (1991) 'Effects of nutrient enrichment and water motion on the coral Pocillopora damicornis', *Pacific Science*, 45(3), pp. 299–307.

Stewart, J. A., Anagnostou, E. and Foster, G. L. (2016) 'An improved boron isotope pH proxy calibration for the deep-sea coral Desmophyllum dianthus through sub-sampling of fibrous aragonite', *Chemical Geology*, 447, pp. 148–160.

Studivan, M. S., Milstein, G. and Voss, J. D. (2019) 'Montastraea cavernosa corallite structure demonstrates distinct morphotypes across shallow and mesophotic depth zones in the Gulf of Mexico', *PLoS ONE*, 14(3), pp. 1–21.

Sun, D. *et al.* (2008) 'Variability of skeletal growth and δ13C in massive corals from the South China Sea: Effects of photosynthesis, respiration and human activities', *Chemical Geology*, 255(3–4), pp. 414–425.

Sutton, D. C. and Hoegh-Guldberg, O. (1990) 'Host-Zooxanthella Interactions in Four Temperate Marine Invertebrate Symbioses: Assessment of Effect of Host Extracts on Symbionts', *The Biological Bulletin*, 178(2), pp. 175–186.

Swart, P. K. (1983) ‘Carbon and Oxygen Isotope Fractionation in Scleractinian Corals : a Review’, *Earth-Science Reviews*, 19, pp. 51–80.

Swart, P. K. *et al.* (2010) ‘The 13C Suess effect in scleractinian corals mirror changes in the anthropogenic CO2 inventory of the surface oceans’, *Geophysical Research Letters*, 37(5), pp. 1–5.

Szmant, A. M. (2002) ‘Nutrient enrichment on coral reefs: Is it a major cause of coral reef decline?’, *Estuaries*, 25(4), pp. 743–766.

Tambutté, E. *et al.* (2007) ‘Observations of the tissue-skeleton interface in the scleractinian coral Stylophora pistillata’, *Coral Reefs*, 26(3), pp. 517–529.

Tambutté, E. *et al.* (2011) ‘Calcein labelling and electrophysiology: Insights on coral tissue permeability and calcification’, *Proceedings of the Royal Society B: Biological Sciences*, 279(1726), pp. 19–27.

Tambutté, S. *et al.* (2011) ‘Coral biomineralization: From the gene to the environment’, *Journal of Experimental Marine Biology and Ecology*, 408(1–2), pp. 58–78.

Tan, S. H. *et al.* (2011) ‘Training Manual on Coral Taxonomy in Southeast Asia’, *Wildlife Research*, (June 2015), p. 122.

Tanaka, Y. *et al.* (2006) ‘Translocation and conservation of organic nitrogen within the coral-zooxanthella symbiotic system of Acropora pulchra, as demonstrated by dual isotope-labeling techniques’, *Journal of Experimental Marine Biology and Ecology*, 336(1), pp. 110–119.

Tanaka, Y. *et al.* (2007) ‘Imbalanced coral growth between organic tissue and carbonate skeleton caused by nutrient enrichment’, *Limnology and Oceanography*, 52(3), pp. 1139–1146.

Tanaka, Y. *et al.* (2015) ‘Partitioning of nitrogen sources to algal endosymbionts of corals with long-term ^{15}N-labelling and a mixing model’, *Ecological Modelling*, 309–310, pp. 163–169.

Tanaka, Y. *et al.* (2017) ‘Effects of nitrate and phosphate availability on the tissues and carbonate skeleton of scleractinian corals’, *Marine Ecology Progress Series*, 570(3), pp. 101–112.

Tchernov, D. *et al.* (2004) ‘Membrane lipids of symbiotic algae are diagnostic of sensitivity to thermal bleaching in corals’, *Proceedings of the National Academy of Sciences*, 101(37), pp. 13531–13535.

Tchernov, D. *et al.* (2011) ‘Apoptosis and the selective survival of host animals following thermal bleaching in zooxanthellate corals’, *Proceedings of the National Academy*

of Sciences, 108(24), pp. 9905–9909.

Thurber, R. L. V. *et al.* (2014) 'Chronic nutrient enrichment increases prevalence and severity of coral disease and bleaching', *Global Change Biology*, 20, pp. 544–554.

Titlyanov, E. A. *et al.* (1996) 'Degradation of zooxanthellae and regulation of their density in hermatypic corals', *Marine Ecology Progress Series*, 139, pp. 167–178.

Tomascik, T. and Sander, F. (1985) 'Effects of eutrophication on reef-building corals', *Marine Biology*, 87, pp. 143–155.

Tonarini, S. *et al.* (2003) 'Intercomparison of boron isotope and concentration measurements. Part I: Selection, preparation and homogeneity tests of the intercomparison materials', *Geostandards Newsletter*, 27(1), pp. 21–39.

Tyrrell, T. (1999) 'The relative influences of nitrogen and phosphorus on oceanic primary production', *Nature*, 400(6744), pp. 525–531.

Urey, H. C. (1947) 'The Thermodynamic Properties of Istotopic Substances', *Journal of the Chemical Society*, 0, pp. 562–581.

Usdowski, E. and Hoefs, J. (1993) 'Oxygen isotope exchange between carbonic acid, bicarbonate, carbonate, and water: A re-examination of the data of McCrea (1950) and an expression for the overall partitioning of oxygen isotopes between the carbonate species and water', *Geochimica et Cosmochimica Acta*, 57(15), pp. 3815–3818.

Uthicke, S., Furnas, M. and Lønborg, C. (2014) 'Coral reefs on the edge? Carbon chemistry on inshore reefs of the great barrier reef', *PLoS ONE*, 9(10).

Venn, A. A. *et al.* (2020) 'Paracellular transport to the coral calcifying medium: Effects of environmental parameters', *Journal of Experimental Biology*, 223(17).

Veron, J. (2013) 'Overview of the taxonomy of zooxanthellate Scleractinia', *Zoological Journal of the Linnean Society*, 169(3), pp. 485–508.

de Villiers, S., Shen, G. T. and Nelson, B. K. (1994) 'The Sr Ca-temperature relationship in coralline aragonite: Influence of variability in (Sr Ca)seawater and skeletal growth parameters', *Geochimica et Cosmochimica Acta*, 58(1), pp. 197–208.

Voss, J. D. and Richardson, L. L. (2006) 'Nutrient enrichment enhances black band disease progression in corals', *Coral Reefs*, 25(4), pp. 569–576.

Wall, C. B. *et al.* (2019) 'Spatial variation in the biochemical and isotopic composition of corals during bleaching and recovery', *Limnology and Oceanography*, 64(5), pp. 2011–2028.

Wallace, C. C. (1985) 'Reproduction, recruitment and fragmentation in nine sympatric species of the coral genus Acropora', *Marine Biology*, 88, pp. 217–233.

Ware, J. R., Smith, S. V. and Reaka-Kudla, M. L. (1992) 'Coral reefs: sources or sinks of atmospheric CO2?', *Coral Reefs*, 11(3), pp. 127–130.

Warner, M. E., Fittt, W. K. and Schmidt, G. W. (1999) 'Damage to Photosystem II in Symbiotic Dinoflagellates . A Determinant of Coral Bleaching', *Proceedings of the National Academy of Sciences, USA*, 96(14), pp. 8007–8012.

Weber, J. N. and Woodhead, P. M. J. (1972) 'Temperature dependence of oxygen-18 concentration in reef coral carbonates', *Journal of Geophysical Research*, 77(3), pp. 463–473.

Weis, V. M. (2008) 'Cellular mechanisms of Cnidarian bleaching: Stress causes the collapse of symbiosis', *Journal of Experimental Biology*, 211(19), pp. 3059–3066.

Wiedenmann, J. *et al.* (2013) 'Nutrient enrichment can increase the susceptibility of reef corals to bleaching', *Nature Climate Change*, 3(2), pp. 160–164.

Wijgerde, T. *et al.* (2011) 'Extracoelenteric zooplankton feeding is a key mechanism of nutrient acquisition for the scleractinian coral Galaxea fascicularis', *Journal of Experimental Biology*, 214(20), pp. 3351–3357.

Wooldridge, S. A. (2009) 'Water quality and coral bleaching thresholds: Formalising the linkage for the inshore reefs of the Great Barrier Reef, Australia', *Marine Pollution Bulletin*, 58(5), pp. 745–751.

Wooldridge, S. A. (2010) 'Is the coral-algae symbiosis really "mutually beneficial" for the partners?', *BioEssays*, 32(7), pp. 615–625.

Xiao, Y. K. *et al.* (2014) 'Correlation between δ18O, Sr/Ca and Mg/Ca of coral Acropora and seawater temperature from coral culture experiments', *Science China Earth Sciences*, 57(5), pp. 1048–1060.

Yellowlees, D., Rees, T. A. V. and Leggat, W. (2008) 'Metabolic interactions between algal symbionts and invertebrate hosts', *Plant, Cell and Environment*, 31(5), pp. 679–694.

Zoccola, D. *et al.* (2015) 'Bicarbonate transporters in corals point towards a key step in the evolution of cnidarian calcification', *Scientific Reports*, 5(Article 09983), pp. 1–11.

Bibliography (including web-based references)

EPA (United States Environmental Protection Agency) - https://www.epa.gov/coral-reefs/basic-information-about-coral-reefs [Accessed on 03/10/2022]

Faure, G., Mensing, T.M. (2005), *Isotopes, Principles and Applications*, 3rd Edition, Wiley, New Delhi

UNEP (United Nations Environment Programme) - https://www.unep.org/explore-topics/oceans-seas/what-we-do/protecting-coral-reefs [Accessed on 03/10/2022]

Veron (Corals of the world) - http://www.coralsoftheworld.org/page/home/ [Accessed on 03/10/2022]

WoRMS (World Register of Marine Species) - https://www.marinespecies.org [Accessed on 03/10/2022]

Zeebe, R.E., Wolf-Gladrow, D., (2001) CO_2 in Seawater: Equilibrium, Kinetics, Isotopes, 1st Edition, Elsevier